INVESTIGATING THE NEDD4-MEDIATED UBIQUITINATION OF PMEPA1, AND ITS POTENTIAL ROLE IN THE REGULATION OF THE ANDROGEN RECEPTOR AS PART OF THE STEROID RESPONSE PATHWAY IN PROSTATIC CANCER

HELEN MARGARET MARKS

School of Biological & Chemical Sciences,

Queen Mary, University of London

THESIS SUBMITTED TO THE UNIVERSITY OF LONDON FOR THE DEGREE OF DOCTOR OF PHILOSOPHY

DECLARATION BY CANDIDATE

I declare that the work presented in this thesis is my own and that the thesis presented is the one upon which I expect to be examined. Any quotation or paraphrase from the published or unpublished work of another person has been duly acknowledged in the work which I present for examination.

Signed (Candidate) ..... Date: .....

ABSTRACT

Ubiquitination is an extremely important post-translational modification, regulating a wide variety of cellular processes including proteasomal degradation, subcellular targeting, endocytosis and DNA repair. The HECT class of E3 ligases catalyse the final step of ubiquitin conjugation to the substrate; the Nedd4 family make up 9 members of this class in humans, and are implicated in pathologies ranging from congenital ion channel misregulation to cancer, via the TGF-ß signalling pathway. The Nedd4-like proteins contain WW substrate recognition domains, which recognise and bind proline–rich PY motifs. This work focuses on the interaction between Nedd4 and PMEPA1, a membrane protein showing altered expression in prostate cancer and a known Nedd4 substrate. PMEPA1 is recognised as important in several cancers, although its detailed function is not yet known; it is upregulated in prostate cancer and has been postulated to decrease cellular androgen receptor (AR) via a negative feedback loop involving Nedd4 in a ubiquitin-proteasome dependent process. Misregulation of the AR response to testosterone is associated with a more advanced form of prostatic cancer and poor patient prognosis, for which there are currently few treatment options available.

PMEPA1 contains two well-documented canonical (PPxY) PY motifs both required for interaction with Nedd4. This work details the identification and characterisation of a third motif with a variant PY (vPY) sequence, QPTY. Our findings indicate that the loss of this vPY motif leads to a significant reduction in Nedd4-dependent ubiquitination *in vitro*. In addition, the nature of the amino acid residues surrounding the vPY motif also appears to play a role in the functionality of the site. Alongside these experiments, immunodetection of protein levels in HeLa and LNCaP cell lysates was used in conjunction with confocal microscopy to shed light on the interactions between PMEPA1, Nedd4 and AR *in vitro* and *in vivo*. A possible non-proteasomal role for ubiquitination in the PMEPA1-AR interaction, as opposed to the simple ubiquitin-proteasome mediated degradation previously proposed, is discussed in the light of this new data. This work has expanded previous knowledge of the specificity of the PY-WW interaction, as well as providing a basis for further investigation, and possibly clinical targeting, of the role of PMEPA1 and AR in prostate cancer.

ACKNOWLEDGEMENTS

Thankyou to the Biotechnology & Biological Sciences Research Council for the funding to complete this project, and to Queen Mary, University of London for being home for the last four years.

I am hugely grateful to Dr. Jim Sullivan for giving me the opportunity to take on this project, and for his patience, support and expertise throughout. He has always made time for my questions, even the stupid ones, and his insight and depth of knowledge are inspiring. I hope one day to be able to put away that much red wine at lunchtime and still go back to work!

Dr. Tatiana Novoselova was an absolutely invaluable source of help and information and is much missed as a member of the group, not least for her incredible ability to keep even Jim's lab bench clean.

Thankyou especially to Dr. Ruth Rose, who has become a great friend as well as colleague over the last few years. Her ability to know exactly when to offer tea, advice and puppy cuddles, as well as her enormous internal database of protein biochemistry knowledge, has played a large role in getting me to this stage.

I am grateful to Dr. James Wilkinson of Nanotemper, Germany for his help in obtaining the microscale thermophoresis data, even allowing me to take over his kitchen at home to repeat some experiments, and to Dr. Robert Janes and Prof. Richard Pickersgill, who have both provided invaluable time, advice and equipment to assist my attempts at structural biology.

Mr. Mahesh Pancholi, Ms. Jen Armstrong-McKay, Ms. Sarah Tirrell and Ms. Alison Penfold have all given me the luxury of always having a London base, as well

as lots of laughs, advice, KFC, Nando's and wine. Thanks so much guys, I promise to start paying my way more now.

Mr. Jay Paul, Mr. Steve Pestaille, Dr. Raj Joseph and Dr. Michaela Egertova have all gone above & beyond the call of duty in helping with technical & administrative problems, lending out supplies as well as hands when I have been desperate.

My Mum and Dad have been incredibly trusting and patient throughout, despite my appalling failure to ever explain what it is I have actually been doing all these years instead of getting a job. I hope this goes some way towards a thankyou, and I hope to make you proud.

Finally, I couldn't have produced this labour of love without the financial & emotional support of Mr. Caspar Berry, who has been by my side and seen me at my highest and lowest, without flinching or letting me throw the laptop out of the window. Thankyou, now and every day.

CONTENTS

LIST OF FIGURES

1. Introduction

2. Materials & Methods

3.1. Investigating the interaction between Nedd4 and PMEPA1 in vitro

3.2. In vivo localisation of PMEPA1 and AR

6. Appendices

1. INTRODUCTION

1.1 Ubiquitin and ubiquitination

1.1.1 Ubiquitination in the context of post-translational modifications

Post-translational modification of proteins facilitates an extremely high level of variation and complexity in cellular proteins; from a genome containing a maximum of 25,000 genes (International Human Genome Sequencing Consortium, 2004), a proteome consisting of over a million functional and structural protein variants (Jensen, 2004). Over 200 PTMs have been identified (Walsh, 2006), including some which are reversible, and an additional level of diversity is made possible by multiple sequential modifications, with widely varying effects. These are assisted by a diverse selection of enzymes and cofactors, as well as non-proteins such as lipids and small non-organic molecules, including phosphate ions, which can be covalently bonded to alter the nature of the protein.

Ubiquitin, and an ever-increasing number of ubiquitin-like proteins (UBLs) such as SUMO and FAT10, are a family of structurally similar protein molecules which are covalently attached to proteins in an enzyme-mediated process. They serve diverse functional purposes which are summarised in figure 1.1, but are linked by a common secondary structure and a common multi-step cascade attachment mechanism. Ubiquitin and SUMO and the most relevant to this project and are covered in more detail below.

Name	Size (kDa)	First Discovered	Functions
Ubiquitin	8.5	1975	Proteasomal degradation, intracellular trafficking, endocytosis, regulation of inflammatory and stress response, DNA repair, viral budding, apoptosis, cell cycle control, neuronal morphogenesis and maintenance, transcription control via histone modification
SUMO	11.5	1997	Intracellular trafficking, transcriptional regulation, DNA repair, regulation of inflammatory response
NEDD8	9	1997	Regulation of cell cycle progression and cytoskeletal assembly, via regulation of ubiquitin conjugation machinery, embryogenesis and placental differentiation
FAT10	18.5	1996	Proteasomal degradation, mediation of apoptosis, dendritic cell maturation and differentiation
ISG15	17	1987	Innate immune response in higher Eukaryotes, tumorigenesis
UFM1	9	2004	As yet undefined; associated with endoplasmic reticulum homeostasis and
FUBI	9	1992	As yet undefined; associated with tumorigenesis
GABARAP	14	1999	Intracellular transport of GABA receptors, regulation of autophagy and apoptosis
GABARAPL1	14	2001	Intracellular trafficking of opioid receptors, formation and maturation of autophagosomal vesicles
ATP7	78	1999	Caspase-induced autophagy, selective mitochondrial destruction, cell cycle regulation, axonal maintenance and homeostasis
LC3	14	1994	Formation of autophagosomes
URM1	11	2005	Oxidative stress response, regulation of tRNA stability

Figure 1.1. Ubiquitin-like proteins in humans. Overview of Eukaryotic proteins sharing a common domain structure with ubiquitin, their sizes, historical discovery dates and their diverse functions

1.1.2 Ubiquitin discovery

Ubiquitin was first identified as a free polypeptide involved in differentiation of immunocytes in 1975 and provisionally designated ubiquitous immunopoietic polypeptide (UBIP) due to its being highly conserved in numerous yeast and mammalian tissue extracts (Goldstein et al, 1975). Shortly after, the full sequence of the renamed ubiquitin was published as an adenylate cyclase stimulating peptide, and shown to be so highly conserved that, at the time, it was thought to be universal in living cells (Schlesinger et al, 1975). In 1977, covalent attachment of an unidentified non-histone protein to a lysine residue in the histone H2a was observed (Goldknopf & Busch, 1977); this was soon revealed through sequence comparison to be ubiquitin (Hunt & Dayhoff, 1977).

At the time, a role for ubiquitin in proteasomal degradation was not suspected. The early observation that intracellular proteolysis in eukaryotic cells uses ATP (Simpson, 1953) was a biochemical curiosity that could not be explained by conventional ideas regarding protein turnover. In attempting to evaluate this phenomenon, reticulocyte extracts, lacking the lysosome which had been previously identified as having a proteolytic function (de Duve et al, 1953), was used. It was discovered that protein degradation in this extract required two fractions I and II; fraction I contained a small protein designated ATP-dependent proteolysis factor I (APF-1), and APF-1 formed covalently linked high molecular weight conjugates prior to degradation (Ciechanover et al, 1978). This was followed soon after by the observation that fraction II of the reticulocyte lysis contained as a high molecular weight species, APF-2, which was stabilised by ATP. Both fractions I and II were shown to be necessary for the proteolytic activity of the lysate (Hershko et al, 1980). It was rapidly established that the ATP-

dependent incorporation of APF-1 into high molecular weight conjugates was the first step of this proteolysis pathway (Ciechanover et al, 1980), that APF-1 binds to many different cellular proteins, and that the free APF-1 it is regenerated from these conjugates by amidases (Hershko et al, 1980). It is now clear that APF-2 is the 26S proteasome (Waxman et al, 1987), a multi-subunit catalytic complex which assembles in the presence of ATP (Orino et al, 1991) and specifically degrades ubiquitinated proteins (Ugai et al, 1993), and APF-1 is ubiquitin. This was later confirmed by sequential and functional analyses showing that the two proteins were in fact the same (Wilkinson et al, 1980).

1.1.3 Ubiquitin structure

The first primary structure of ubiquitin to be published was the bovine protein in 1975, using trypsin digestion and sequencing of the resulting peptides (Schlesinger et al, 1975); this identified a 74 amino acid peptide with a single chain. Further analysis showed that the physiologically active form of ubiquitin is in fact 76 residues in length, and the truncated version was most likely an *in vitro* proteolytic artefact (Wilkinson & Audhya, 1981). Human (Schlesinger & Goldstein, 1975), fish (Watson et al, 1978), insect (Gavilanes et al, 1982) and mouse (Finch et al, 1990) ubiquitin sequences followed, and by the mid-1980s it was clear that the protein was almost universally conserved among Eukaryotes. As recently as this year, the ubiquitin sequence of the parasitic fluke *Clonorchis sinensis* was published and shown to be "extraordinarily conserved" when compared to other species (Huang et al, 2013). Preliminary structural studies using circular dichroism and NMR predicted that ubiquitin is a globular protein with a tightly folded structure, mostly consisting of random coil with approximately 28%

helix and 12% β-sheet (Cary et al, 1980). More advanced structural resolution came in the mid-1980s, with a crystallographic analysis showing a much greater degree of ordered structure than previously indicated; one α-helix and four strands of β-sheet, as well as a large rigid turn stabilised by hydrogen bonding, encompassing around 90% of the primary sequence (see figure 1.2). In addition, a buried 'core' consisting of 16 hydrophobic residues, a hydrophobic 'pocket' on the surface of the molecule, and the protrusion, and mobile nature, of the carboxy-terminal Gly-Gly through which the molecule binds lysine residues, were identified (Vijay-Kumar et al, 1985). The specific pattern formed by four of the β-strands surrounding the α-helix became recognised as a signature fold, the β-grasp, common to ubiquitin-like proteins such as SUMO (Bayer et al, 1998), despite the lack of significant primary sequence similarity.

1.1.4 Types of ubiquitination and their functions

As well as the primary, secondary and tertiary structure of ubiquitin as a monomer, there is another aspect of its structure which plays a key role in ubiquitin-mediated signalling – its ability to form chains. Ubiquitin binds to proteins via an isopeptide bond linking the carboxyl group on its terminal glycine with the side chain amine on a lysine residue (Busch & Goldknopf, 1981) in a process known as ubiquitination, or ubiquitylation. The initial conjugation must necessarily be to a lysine on the substrate, but ubiquitin itself contains 7 lysine residues (K6, K11, K27, K29, K33, K48 and K63), as well as a terminal amine group, which can function as anchor points for additional isopeptide linkages. Proteins can be modified by a single ubiquitin molecule on a single

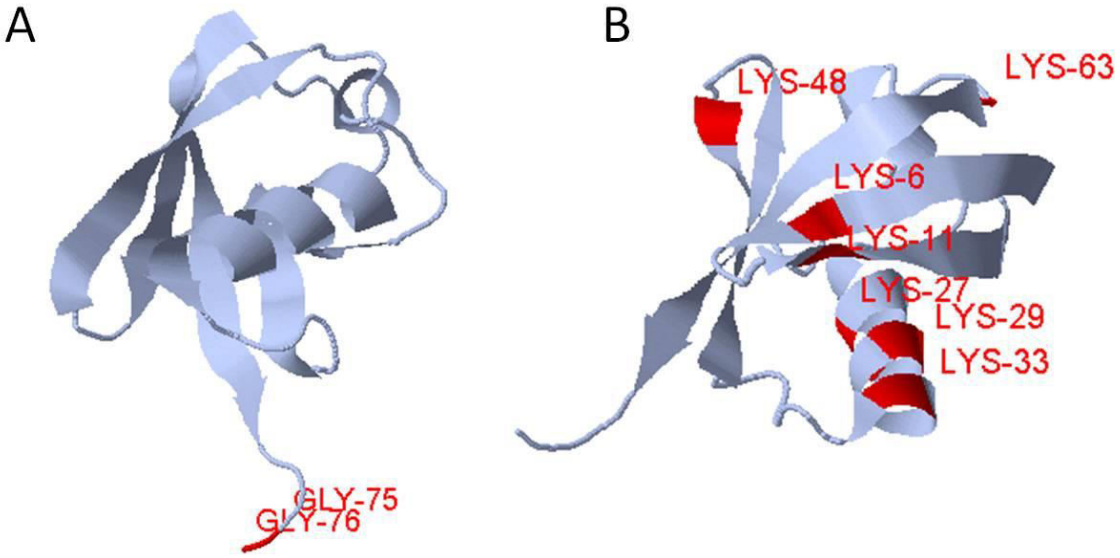

Figure 1.2. Crystallographic structures of ubiquitin at 1.8Ä resolution. The secondary structure is shown with β-sheet represented as flat arrows and α-helix represented as spiral arrows. The overall structure is shown in panel (A), with the four strands of the characteristic β-fold surrounding the single α-helix (foreground). The flexible Gly-Gly tail is visible as the end of the molecule on the bottom left. The positions of the 7 lysine residues are highlighted in panel (B). Images were rendered using Polyview-3D and JMol; RCSB PDB reference 1UBQ with original structure published by Vijay-Kumar et al, 2007.

lysine (monoubiquitination), single ubiquitin molecules on multiple lysines (multiubiquitination) or chain-linked ubiquitin molecules on one or more lysines (polyubiquitination) (see figure 1.3).

Monoubiquitination and multiubiquitination of proteins, along with the formation of very short 2- and 3-monomer ubiquitin chains, act as a signal for various non-proteasomal cellular processes. The first of these to be identified was histone regulation (Busch & Goldknopf, 1981); this is a conserved role, as part of the DNA damage response, which has been shown to be crucial for sporulation and growth in yeast (Robzyk et al, 2000) as well as gene regulation in *Drosophila* (Pham & Sauer, 2000). Constitutive monoubiquitination of histones complexed with DNA represses transcription of the DNA (Zhou et al, 2008) and also serves to initiate the DNA damage repair cascade by recruiting kinases to the site of strand breaks (Pan et al, 2011). Monoubiquitination is also required for viral budding (Patnaik et al, 2000) and is the major form of ubiquitination involved in the complicated regulation of endocytosis (Terrell et al, 1998). Endocytosis is an important mechanism by which cell surface proteins, such as receptor tyrosine kinases and permeases, are regulated. In both yeast (Shih et al, 2000) and mammalian cells (Nakatsu et al, 2000), monoubiquitination and multiubiquitination (Haglund et al, 2003) of the cytoplasmic region of surface proteins is sufficient both to trigger internalisation and sort the proteins into lysosomal degradation pathways. The default cellular pathway for internalised proteins is recycling back to the cell surface (Mayor et al. 1993), so sorting of proteins from the endosome to the multivesicular body (MVB) pathway, which is essential for their correct delivery to the lysosome or vacuole, requires a positive signal. If the lysine residues on endocytosed proteins, such as the yeast hydrolytic enzyme Cps1p, are removed by mutagenesis, they cannot progress into the MVB and instead accumulate at the vacuolar membrane

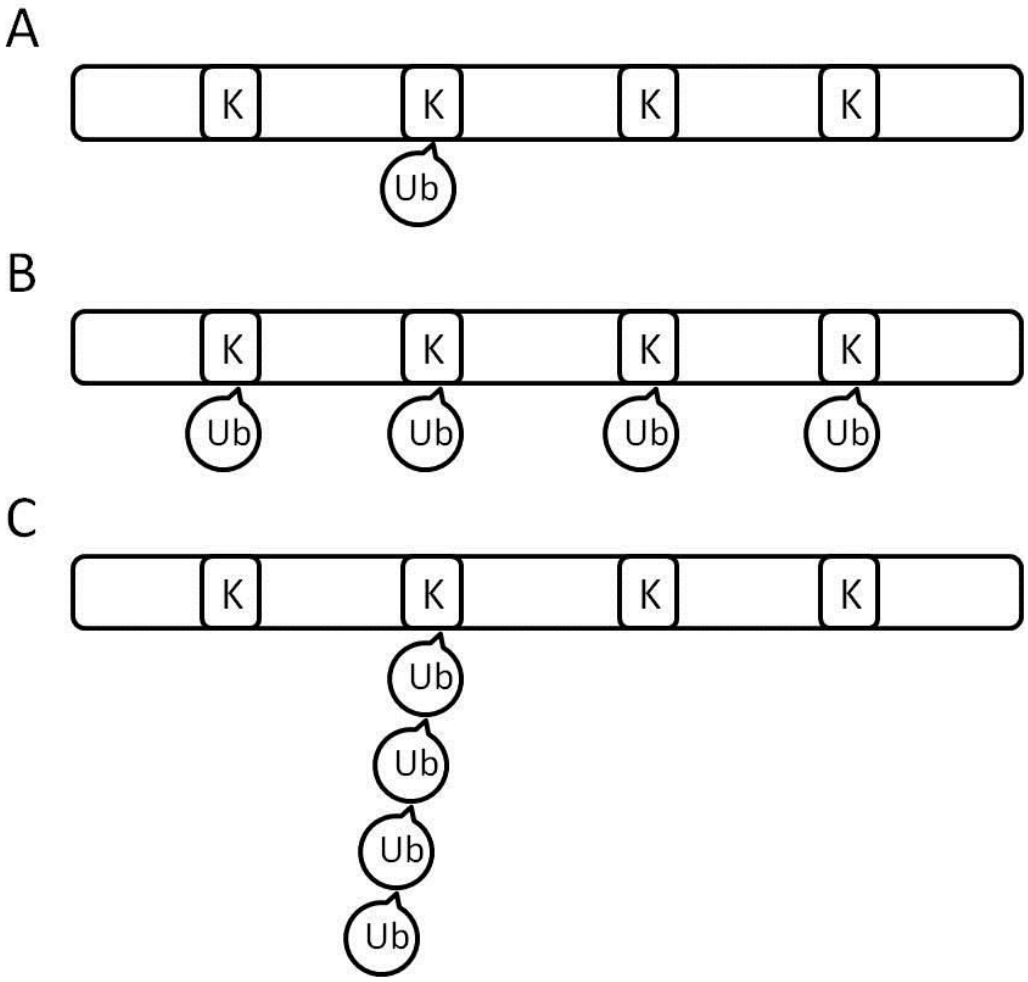

Figure 1.3. Schematic illustration of different forms of ubiquitination. An example protein is presented with four lysine residues (K) with the attachment of a single ubiquitin (Ub) moiety on a single lysine (**A**) – monoubiquitination, single ubiquitin moieties on multiple lysines (**B**) – multiubiquitination, and a ubiquitin chain (**C**) – polyubiquitination.

(Reggiori & Pelham, 2001). Another aspect of this sorting process is direct sorting from the trans-Golgi network to the lysosome, without diverting to the cell surface; this was first reported in yeast as a result of increased nitrogen availability, decreasing the amount of Gap1p amino acid permease at the plasma membrane (De Craene et al, 2001), and later found to be a result of GGA (Golgi-associated γ-adaptin homologues, Arf-binding) proteins binding to ubiquitin on the surface of the target protein (Scott et al, 2004). The Golgi compartment marker TMD-23 was recently found to translocate to the vacuole when conjugated to ubiquitin (Scheuring et al, 2012) in plant cells, indicating that the ubiquitination signal alone is sufficient to trigger endosomal trafficking of Golgi proteins. These single-moiety and short chain modifications cannot be recognised by the ubiquitin receptors on the 26S proteasome, so this form is not directly involved in the targeting of proteins to the proteasome (Thrower et al, 2000) – there is, however, an example of one of the proteasomal ubiquitin receptor subunits in yeast, Rpn10, being regulated by monoubiquitination, blocking the ubiquitin interacting motif and indirectly regulating proteasomal degradation (Isasa et al, 2010).

Polyubiquitination of substrate proteins can occur in various forms due to the multiple conjugation points on the ubiquitin chain described earlier. Each configuration has a specific structural character, with the different lysine linkages conferring varying degrees of flexibility and exposing different parts of the ubiquitin molecules. For example, linear chains, linked through K63 or the N-terminal methionine, adopt an open conformation, with no contact between ubiquitin monomers (apart from the single linkage point) and a high degree of flexibility (Komander et al, 2009). These linear chains are implicated in the NF-κB-mediated immune response pathway, via the ubiquitin-binding adapter NEMO; this binding is dependent on surface residues which are only exposed due to the stretched conformation of the ubiquitin, and hence is specific for the linear conformation

(Rahighi et al, 2009). In contrast, K48-linked chains, which are the principal signal for proteasomal targeting (Finley et al, 2004), adopt a more tightly packed, closed structure, with the hydrophobic surface residues sheltered in the space between the two moieties (Varadan et al, 2002). The less common K11-linked chains also adopt a close-packed conformation, but with the receptor-binding Ile44 residue exposed, and have, relatively recently, been identified as a cell cycle regulation signal (Bremm et al, 2010). The other lysine linkages have all been identified *in vitro* but their *in vivo* functions are less well defined; for example, K6-linked chains are tightly packed like K48 chains, but have an asymmetric structure unlike any other identified (Virdee et al, 2010). All non-linear types of chain play a role in protein degradation to some degree (Xu et al, 2009) and it may be that their roles are redundant, a reflection of the importance of the ubiquitin-mediated signalling in Eukaryotic cells.

Instances of mixed-linkage chains, in which more than one lysine linkage is present on a single protein, are increasingly being reported (Ben-Saaden et al, 2006; Kim et al, 2007; Goto et al, 2010). It is not currently clear what the role of these mixed linkages is; the RING ligase Ring1B autoubiquitinates, generating chains containing a mixture of K11, K48 and K63-linkages, and all three components are required to Ring1B to successfully ubiquitinate it's substrate, the histone H2A (Ben-Saaden et al, 2006). However, receptors which selectively bind single linkage types, such as Rap80, which has specific affinity for K63-linked chains, show no difference in binding affinity between mixed- and single-linkage chains (Nakasone et al, 2013), indicating that the topology within a mixed-linkage chain is no different to one containing a single linkage type.

1.1.5 Enzymes involved in the ubiquitination reaction

The key to the formation of different ubiquitin chains lies in the multi-step process of ubiquitin conjugation; ubiquitinating a protein involves a sequential cascade of 3 enzymes. This cascade is illustrated in figure 1.4; firstly, an E1 activating enzyme activates the ubiquitin, and then an E2 conjugating enzyme carries the activated ubiquitin via a thiol ester into position. Finally, an E3 ligase enzyme enables the transfer of the ubiquitin from the E2 to a lysine on the substrate (Scheffner et al, 1995). Each of these plays a fundamental role in the ubiquitination of proteins as well as substrate recognition and specificity of chain type.

Ubiquitin activating enzymes, referred to as E1 as they are the first enzyme involved in the conjugation reaction, are the least variable of the three. Originally thought to be a single protein (McGrath et al, 1991) designated Uba1, a small number of homologues have since been identified in yeast (Dohmen et al, 1995), wheat (Hatfield & Vierstra, 1992) and humans (Pelzer et al, 2007). The chemistry of the E1-catalysed reaction was resolved over 30 years ago, and relies on the generation of a ubiquitin-adenylate intermediate, still tightly bound to an ATP-binding domain on the E1; this leaves the terminal carboxyl group on the ubiquitin moiety open to attack by the catalytic cysteine, to create a high-energy thioester bond which is then targeted by the next enzyme in the cascade (Haas & Rose, 1982). The structural events that accompany this activation are unknown, but solved crystal structures of the ubiquitin-like protein SUMO in complex with its E1 enzyme (Olsen et al, 2010) indicate that a major reconfiguration of the region containing the active site cysteine occurs between adenylation of the protein and formation of the thioester conjugate to allow the formation of the high-energy bond.

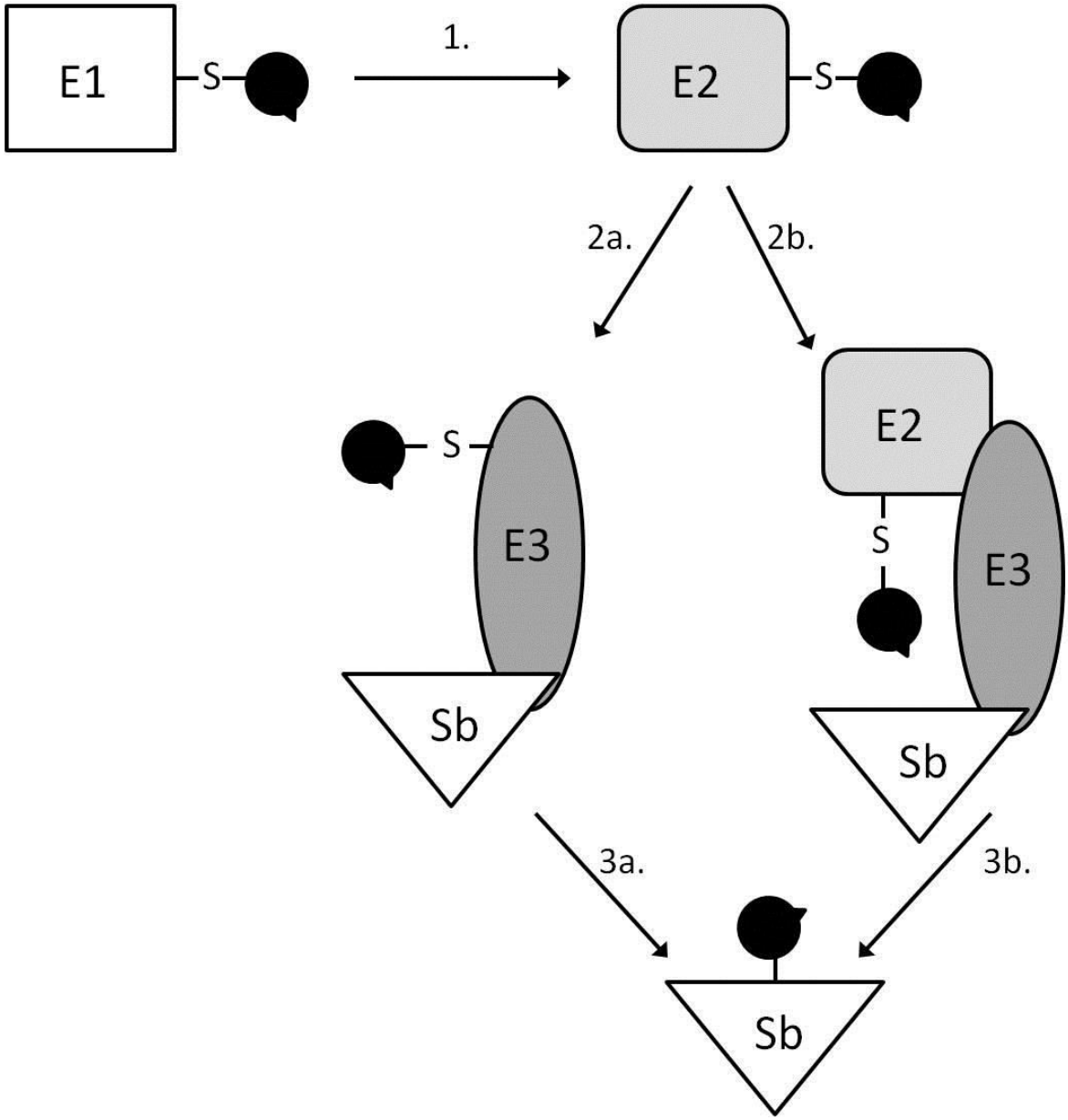

Figure 1.4. Schematic illustration of the stages of ubiquitin transfer. Free ubiquitin (black) binds to an activating enzyme E1 via a high-energy thioester bond. This activated ubiquitin is then transferred onto a ubiquitin conjugating enzyme, E2 (1). From there one of two routes to conjugation is followed; either a HECT type E3 ubiquitin ligase receives the ubiquitin onto itself (2a) and catalyses active transfer onto the substrate (3a), or a RING type E3 ubiquitin ligase binds both the ubiquitin-bound E2 and the substrate at separate sites (2b) and facilitates transfer from the E2 directly onto the substrate by acting as a scaffold (3b).

Ubiquitin conjugating enzymes, referred to as E2s, have a conserved structure and catalytic cysteine similar to that found on E1s. While in humans there are only 2 E1s, there are around 30 E2s (van Wijk & Timmers, 2010) which conjugate ubiquitin, each of which is associated with a specific downstream function. While there is necessarily a high degree of conservation, in order to retain E1- and ubiquitin-binding capability and catalytic activity, there is sufficient variability to allow selectivity of interaction with E3s, and therefore of function (Martinez-Noel et al, 2001). The E1-E2 binding event is triggered by ubiquitin binding to E1; binding between free E1 and E2 is weak (Hershko et al, 1983). This is because the E2 binding surface actually consists of a combination of domains on the E1 and ubiquitin itself (Olsen & Lima, 2013); once this association has occurred, the high-energy ubiquitin thioester bond is rapidly transferred from the E1 to the E2 active site (Pickart, 2001).

The final step in the ubiquitination cascade, the transfer of ubiquitin onto the substrate, is achieved by one of a huge group of E3s referred to as ubiquitin ligases. These are the most complex and diverse of all the enzymes involved, with over 600 distinct enzymes identified in humans alone (Li et al, 2008). There are two types of E3 which are very different structurally and in their method of catalysis; this subject is covered in more depth in section 1.2. Broadly speaking, the HECT-type ligases actively catalyse the transfer of the ubiquitin from the E2 onto a catalytic cysteine within themselves before transferring it onto the substrate, while the RING-type ligases act as a molecular ‘scaffold’ to bring the substrate and the E2 into close enough proximity that the ubiquitin can be transferred directly from the E2 to the substrate. It is the wide variety of E3s that confer specificity to the ubiquitination reaction; each has a specific substrate recognition domain which enables binding to the ubiquitination target, either by the E3 alone or in complex with the correct E2.

1.2 HECT type ligases and the Nedd4 family

1.2.1 Types of ubiquitin ligase enzymes

As mentioned above, there are two distinct classes of ubiquitin ligases, which have evolved completely distinct mechanisms to achieve the same goal; the transfer of ubiquitin from the E2 onto a substrate protein. First identified in the early 1990s as a cysteine-rich domain with similarities to zinc-binding proteins (Freemont et al, 1991), the RING finger ligases were named after initial database searches showed similarities to the newly identified Really Interesting New Gene 1 (RING1) and zinc finger domains (Stemberg, 1991). Their function as E3 ligases was only realised almost a decade later, as the role of the conserved zinc-coordinating residues in mediating ubiquitination and the E2-binding properties of the domains came to light (Kamura et al, 1999, Ohta et al, 1999, Lorick et al, 1999). The conserved zinc-binding cysteine and histidine residues form part of a cleft in the surface of the proteins to which E2s directly when loaded with ubiquitin (Zhen et al, 2000). A separate, spatially distant substrate binding site associates with the protein to be ubiquitinated and holds it in the correct position for direct transfer of ubiquitin from the E2 (Orlicky et al, 2003); this is sometimes facilitated by a conformational change on the E3 which can in turn be initiated by binding of ubiquitin-like proteins such as Nedd8 (Duda et al, 2008). The precise mechanism of ubiquitin transfer from the E2 to the substrate has not yet been elucidated, but the recently solved structure of the RING E3 RNF4 in complex with the E2 Ubc5Ha and ubiquitin showed that the RING domain acts to lock ubiquitin into the E2 active site and extend its conformation in such a way as to activate the thioester bond to attack a substrate lysine

(Plechanovova et al, 2012). Crucially, at no point is an E3-ubiquitin intermediate formed; the transfer occurs from the E2 directly onto the substrate.

This is in direct contrast to the other major type of E3 ligase, the HECT (Homologous to E6-AP Carboxyl Terminus) ligases, named for the first to be identified as functioning as a catalytic enzyme rather than a scaffold. These form a small minority of all the E3s in Eukaryotic systems; around 30 HECT ligases have been identified in mammals. Rather than acting as a scaffold to mediate a transfer of ubiquitin from the E2 onto the substrate, HECT family ligases have a conserved cysteine residue at the active site onto which the thioester ubiquitin bond is transferred from the E2, forming a stable E3-ubiquitin thioester intermediate prior to the ubiquitin being transferred onto the substrate (Scheffner et al, 1995). The HECT domain itself has two major features; the C-terminal ("C lobe") region, containing the catalytic cysteine, and the N-terminal lobe ("N lobe"), which binds the E2 (Huang et al, 1999). The residues in between the two lobes have been described as a "hinge" (Verdecia et al, 2003), allowing rotational flexibility to bring the two lobes into closer contact and facilitate thioester transfer from the active site on the E2 to that on the E3. The importance of this hinge is emphasised by the fact that mutations in E6-AP which cause the genetic disorder Angelman syndrome are located in this region (Kishino et al, 1997). While the overall structure of the HECT domain and the catalytic cysteine are universally conserved among these ligases, the N lobe is much more variable, conferring specificity for certain E2s (Jentsch et al, 1992). As well as specificity for E2s, HECT E3s are associated with specific ubiqutin chain types, for example the yeast ligase Rsp5p is associated with K63 linkage (Galan and Haguenauer-Tsapis, 1997), while the mammalian E3 KIAA0010 catalyses the formation of K29 and K48 chains (You & Pickart, 2001). The HECT domain is located at the C-terminus of the proteins, with the remainder of the protein determining subclassification into one of three

types; the HERC family, Nedd4 family, or other HECTs. The HERC family are distinguished by containing one or more RCC1-like domains (RLDs), multi-subunit protein binding domains, at their N-terminus. They have multiple functions which are still being elucidated, including regulation of intracellular membrane trafficking, but their ubiquitination substrates have not yet been identified (Garcia-Gonzalo & Rosa, 2005), although there is evidence for a role in the regulation of the HECT ligase E6AP, and therefore a role in Angelman syndrome (Harlalka et al, 2013). There are 6 members of the HERC family in humans, along with 13 that don't appear to follow any pattern, having only the C-terminal HECT in common alongside assorted protein-binding domains such as zinc fingers and even RING motifs. However, the best characterised in terms of their ubiquitination activity, and the most relevant to this project, are the Nedd4 family ligases, described in more detail in section 1.2.2.

There are some ligases which defy easy categorisation into either of the main designations; the IpaH proteins are secreted by some bacterial pathogens to modulate the host immune response (Aishida et al, 2007). When the structure of IpaH from the bacterium *Shigella flexneri* was solved in 2008, it was found to be an entirely novel class of E3 ubiquitin ligase, with a catalytic cysteine reminiscent of a HECT ligase but with different secondary structure around the catalytic site and no conservation of the C-terminal region of the HECT domain, working in the context of a mechanistically unique cascade involving non-covalent binding of the E2 to ubiquitin (Singer et al, 2008; Zhu et al, 2008). These are still relatively poorly studied, especially compared to the two major ligase groups, but recent work has revealed that IpaH0722 blocks the host immune response by promoting proteasomal degradation of the NF-κB pathway signalling molecule TRAF2 (Ashida et al, 2013). Finally, a hybrid class of ligases with aspects of both RING and HECT type enzymes has recently emerged as separate, having been

previously classified as a subtype of RING ligases. These are known as "RING-between-RING" (RBR) type, and include the ligase associated with familial Parkinson's disease, Parkin (Wendel et al, 2011). These RBR's bind E2 though a conventional RING domain, but have a conserved in-between RING (IBR) and second, noncanonical RING (RING2) domain, and form a thioester bond directly between a conserved cysteine on this RING2 and the ubiquitin, in a manner reminiscent of HECT-type ligases (Wendel et al, 2011). Once again, insights into this novel hybrid class are just starting to be presented, and at present little is known about them beyond the basics of their mechanism of transfer.

1.2.2 Structure of the Nedd4 family ligases

Nedd4 family ligases are linked by a common domain structure that includes a HECT domain at the C-terminus, a lipid-binding C2 domain at the N-terminus, and a number of substrate recognition 'WW' domains in between. The family are named for the first member to be identified, Neural precursor cell Expressed Developmentally Down-regulated protein 4 (Kumar et al, 1992), and are conserved across Eukaryotes, from a single member in yeast to 9 in humans (see figure 1.5). The C2 domain mediates plasma membrane binding via phospholipids, including endosomes, in a calcium-dependent manner (Dunn et al, 2004), and also plays an auto-inhibitory role, stabilising both the enzymes themselves and their substrates by interacting both intra- and intermolecularly with the C-terminal HECT domain (Wiesner et al, 2007).

The number and arrangement of WW domains is what distinguishes the Nedd4 family members from each other. These small, approximately 38-residue regions are defined by four conserved aromatic residues, including two conserved tryptophans which give them their name (Bork & Sudol, 1995). Their primary sequence homology is quite low, even

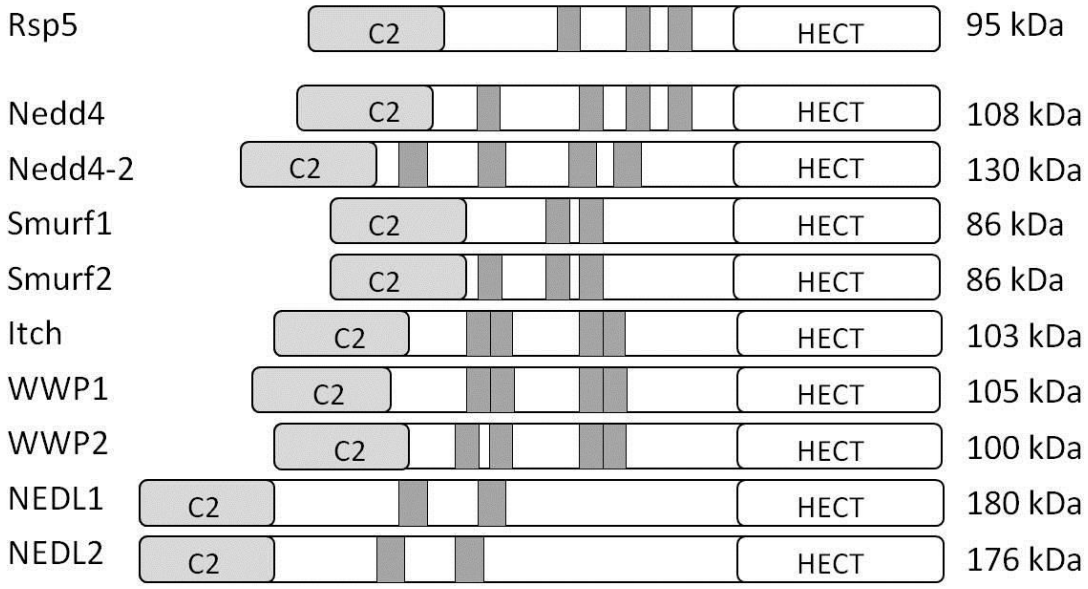

Figure 1.5. Comparative illustration of the domain structure of the Eukaryotic Nedd4 ubiquitin ligase family. The topmost diagram shows the single yeast Nedd4 family member, Rsp5p, in the context of the nine human Nedd4 ligases listed below. The C2 and HECT domains are conserved, with the number and arrangement of the WW domains (dark grey) providing variation in substrate specificity and function.

f

between WW domains on the same protein; WW2 on the oncogenic transcription factor YAP, for example, has a primary sequence closer to that of a WW domain on the yeast Nedd4 ligase Rsp5p than WW1 on YAP itself (Sudol et al, 1995). Early structural studies showed that specific WW domain resides, including the conserved tryptophans, form a hydrophobic surface that binds strongly to the sequence proline-proline-X-tyrosine (PPxY) (Macias et al, 1996). An example of a WW domain from *Drosphila* Nedd4 bound to a PY motif is shown in figure 1.6. However, not all WW domains have these "PY motifs" as their preferred targets, instead targeting phosphorylated serine side chains alongside proline residues (Verdecia et al, 2000), glycine- and methionine-rich motifs (Bedford et al, 1998) or longer proline-rich sequences (Bedford et al, 1997). Not all WW domains within a protein are equal; for example, WW3 of the canonical human Nedd4 protein binds the epithelial sodium channel ENaC, a well-studied Nedd4 substrate, 20-30 times more strongly than either WW2 or WW4, while WW1 shows no affinity for ENaC at all (Lott et al, 2002). The variation between the primary sequences of WW domains, and the different arrangements in different Nedd4 family members, allows each to retain distinct substrate specificity and functionality (Peng et al, 2007).

1.2.3 Members of the Nedd4 family and their functions

1.2.3.1 In the genus Saccharomyces

The Nedd4 ligases are highly conserved through Eukaryotic systems, varying in number from just a single member, Rsp5p, in yeast, to nine in humans. *Rsp5* is an essential gene in yeast (Hein et al, 1995), and has many functions, including regulation of transcription via RNA polymerase binding (Huibregtse et al, 1997), glucose-mediated activation of the plasma membrane H+ ATPase (de la Fuente et al, 1997) and regulation

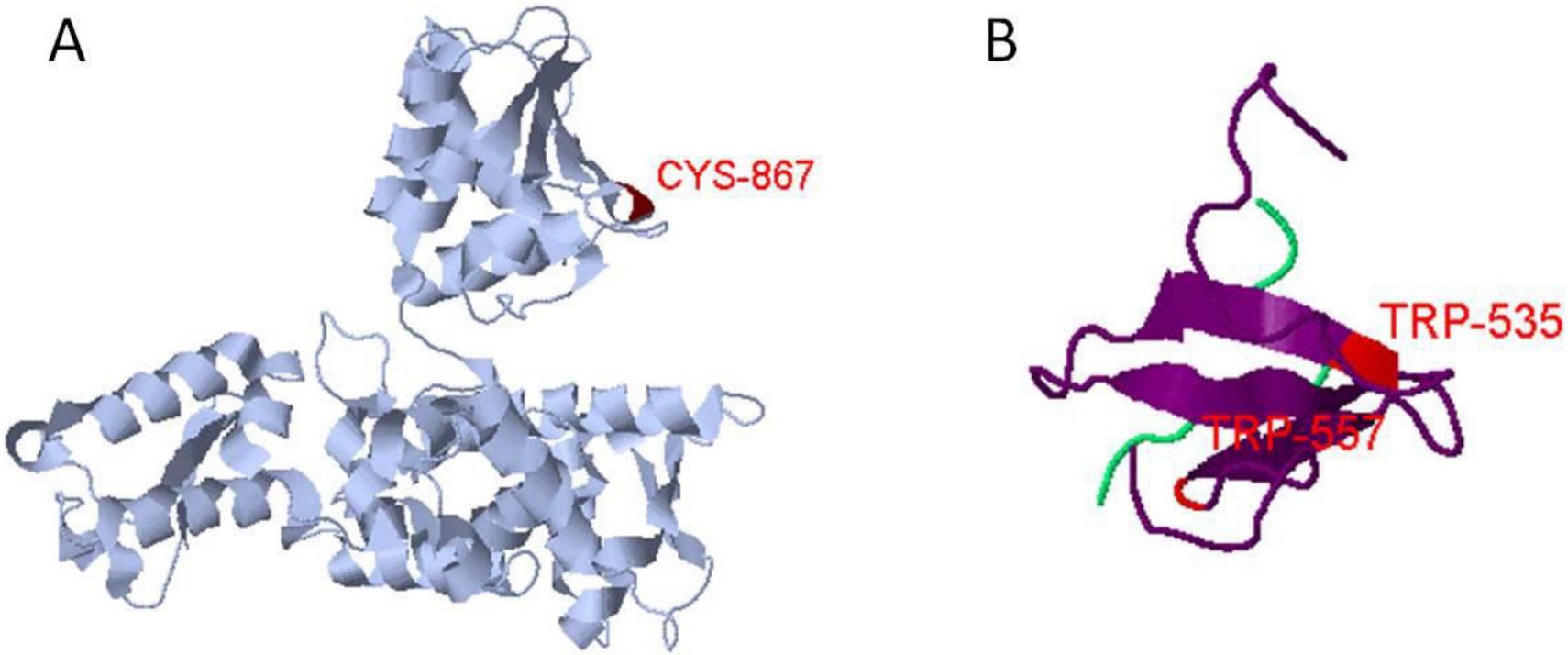

Figure 1.6. Structures of conserved domains of the Nedd4 ubiquitin ligase family. Crystallographic structure of the HECT domain from human Nedd4 at 2.5Ä resolution in grey with the conserved catalytic cysteine highlighted in red (**A**); RCSB PDB reference 2XBF with original structure published by Maspero et al, 2011. Lowest energy consensus solution NMR structure of the WW3 domain of *Drosophila* Nedd4 in complex with the LPXY motif of Commisureless (**B**), with the WW domain chain shown in purple with the ligand shown in green. The two conserved tryptophan residues of the WW domain are highlighted in red; RCSB PDB reference 2EZ5 with original structure published by Kanelis et al, 2006. Images were rendered using Polyview-3D and JMol.

of mitochondrial inheritance (Fisk & Yaffe, 1999). The best-studied role of Rsp5p is in the yeast endocytic pathway, mediating the regulation of plasma membrane proteins by internalisation and passage into the vacuolar degradation (which has a similar function to the mammalian lysosome). This is an extremely important pathway as yeast need to react quickly to changes in the environment to maintain internal homeostasis. There are many examples in the literature, including the amino acid permeases Fur4p (Galan et al, 1996) and Gap1p (Springael & André, 1998), the galactose transporter Gal2p (Horak & Wolf, 1996) and the ATP-binding cassette drug transporter Pdr5p (Egner et al, 1995) of membrane proteins which are ubiquitinated by Rsp5p, and subsequently internalised, in a process which is halted by inhibition of vacuolar proteases, but not of the proteasome. The ability of Rsp5p, as a single ligase, to recognise multiple targets is mediated by adaptor proteins, which act to mediate between the ligase and its substrate, especially if that substrate does not contain a direct recognition motif. The Rsp5p adaptor Bsd2 is an example of such a protein; it contains WW domain recognition motifs (PY motifs) which act as binding motifs for Rsp5p, and in turn binds transmembrane domain-containing proteins such as the metal ion transporter Smf1p (Liu & Culotta, 1999), and the ATPase Pma1p (Luo & Chang, 1997). This is an example of an adaptor with homologues in mammalian systems, the mouse proteins Ndfip1 & Ndfip2, which are essential for the interaction of the mammalian ligase WWP2 with the iron transporter DMT1 (Foot et al, 2008), as well as several other Nedd4 family ligase pathways (Mund & Pelham, 2010). However adaptors seem to be less prevalent in higher organisms, which was postulated by Novoselova et al (2012) to be because they have instead developed a wider range of more specific ligases.

1.2.3.2 In the genus Drosophila

The number of Nedd4 family ligases increases with increasing organism complexity, from the single yeast Rsp5p through three in *Drosophila;* dNedd4, which indirectly regulates axonal formation via Commisureless (Myat et al, 2002), Su(dx), which downregulates several genes associated with the Notch signalling pathway (Mazaleyrat et al, 2003) and dSmurf, which regulates embryonic organogenesis (Podos et al, 2001).

1.2.3.3. In mammals

Mammals have a total of nine Nedd4 ligases, with additional regulation and further complexity arising from alternative splicing arrangements (Flasza et al, 2002). The main functions are summarised in figure 1.7; the canonical member Nedd4, now also known as Nedd4-1, has been shown *in vivo* to regulate growth & development via the insulin response pathway (Cao et al, 2008), as well as to promote tumorigenesis by ubiquitinating & destabilising the tumour suppressor PTEN (Wang et al, 2007). In addition, Nedd4-1 is associated with neuronal development and differentiation (Persaud et al, 2011), ubiquitin-mediated sorting of newly synthesised proteins to the plasma membrane (Rougier et al, 2011) and clathrin-mediated endocytosis of cell surface receptors (Katz et al, 2002; Vina-Vilaseca et al, 2011). Nedd4-2 (previously known as Nedd4-like, NEDD4L) shares a high degree of homology with Nedd4-1, but has distinct substrate specificity (Persaud et al, 2009), and is particularly associated with the ubiquitination and regulation of the epithelial Na^+ channel ENaC, which is disrupted in the hereditary hypertensive disorder Liddle syndrome (Zhou et al, 2007). The Smad ubiquitin regulatory factors, Smurf1 and Smurf2, have a similarly high degree of sequence similarity, and were originally thought to be functionally redundant (Narimatsu

Protein name	Alternative designations	Primary functions
Nedd4	Nedd4-1	Regulation of growth & development, tumorigenesis, neuronal development & differentiation, protein sorting & endocytosis.
Nedd4-2	NEDD4L	Some overlap with Nedd4; regulation of ENaC in Liddle syndrome
Smurf1	SMAD-specific E3 ubiquitin-protein ligase 1	Cell growth and differentiation, protein kinase regulation, autophagy.
Smurf2	SMAD-specific E3 ubiquitin-protein ligase 2	Some overlap with Smurf1; cell cycle progression regulation, tumour suppression & senescence.
AIP4	Itch	Cytokine regulation, tumour suppression, regulation of NFκB & notch signalling pathways, regulation of inflammatory immune response.
WWP1	Tiul1, AIP5	Cell proliferation, highly expressed in prostate and breast cancer, virus proliferation.
WWP2	AIP2	Some overlap with WWP1; tumour prevention via stabilisation of TGF-β pathway components, metal transporter regulation
NEDL1	HECW-1	Associated with cytotoxic aggregates in familial neurodegenerative disease, p53-mediated apoptotic cell death
NEDL2		Some overlap with NEDL1; stabilization of p73-dependent transcriptional activation

Figure 1.7. Mammalian members of the Nedd4 ubiquitin ligase family. Summary of the nine members of the Nedd4 ligase family in mammals, their canonical designation, alternative names and their functions.

et al, 2009). However, they do have some distinct roles, for example Smurf1 lacks the C2 domain-mediated auto-inhibition observed in Smurf2, resulting in selective affinity for the GTPase RhoA (Lu et al, 2011), while Smurf2 depletion results in cell cycle irregularities that Smurf1 cannot compensate for (Osmundson et al, 2008). In the case of tissue separation during embryonic development, the two work antagonistically, with Smurf2 targeting the receptor ephrinB1 and Smurf1 acting as an inhibitor, binding to ephrinB1 in place of Smurf2 but not catalysing ubiquitination or degradation (Hwang et al, 2013). Atrophin-1 interacting protein 4 (AIP4), also known as Itch due to the multiple immunological phenotypes of knockout mice (Perry et al, 1998), is associated with lysosomal degradation of the melanosomal protein Melan-A (Lévy et al, 2005) and negative regulation of tumorigenic cytokines (Ahmed et al, 2011), as well as acting as part of a complex of proteins to regulate NFκB signalling (Shembade et al, 2008). WW domain-containing protein 1 (WWP1), also known as Tiul1 and AIP5, is highly expressed in androgen-independent prostate cancer (Gu et al, 2005) and promotes cell proliferation in prostate cancer tissues (Chen et al, 2007). WWP1 is also amplified in breast cancer (Chen et al, 2007), implying steroid hormone regulation. WWP2 shares some functional characteristics with WWP1; for example, both promote virion release in an ubiquitination-dependent process (Martin-Serrano et al, 2005), but retains its own distinct functionality, for example in the Ndfip-dependent regulation of the iron transporter DMT1 (Foot et al, 2008). The final two members of the family, the Nedd4-like ubiquitin ligases (NEDL) 1 & 2, are less well characterised. Both NEDL1, aka HECW-1, and NEDL2 are associated with p53-mediated apoptosis (Li et al, 2008; Miyazaki et al, 2003) and NEDL1 is also linked to innate behavioural characteristics in *C. elegans* (Chang et al, 2011)

While each member of the Nedd4 family has its own functions and substrates, there is sometimes a degree of redundancy and overlap between them; for example, both Itch and Nedd4-2 are associated with increased survival of neuronal tissue following transient ischaemia, but only in the case of Nedd4-2 is this mediated by the adaptor/activator Ndfip1 (Lackovic et al, 2012). However, Ndfip1 and Itch have been shown to interact in different tissue types (Oliver et al, 2006), indicating that this is not an exclusive mechanism.

1.3 PY motifs and PMEPA1

1.3.1 PY motifs as WW-domain interacting motifs

The term 'PY motif' was coined by Chen & Sudol (1995) with reference to the putative YAP ligands WBP (WW-domain binding proteins) -1 & 2. At that point, the WW domain was newly characterised as a 38 residue conserved region found in several unrelated proteins, including Rsp5p and Nedd4, which was postulated as being a protein-binding domain due to its similarity to protein-binding SH3 domains (Yu et al, 1994). Chen & Sudol isolated the shared sequence PPxY and reported that they bound the WW domain of YAP with high affinity & specificity (Chen & Sudol, 1995). Schild et al (1996) again referred to the 'PY motif', this time with the sequence PPPxY, with reference to such a conserved consensus sequence in the alpha, beta and gamma subunits of the epithelial sodium channel ENaC. While it had been previously observed that deletion of the C-terminus of any of the subunits resulted in Liddle syndrome, a hereditary hypertension (Shimkets et al, 1994; Schild et al, 1995), this was the first time the residues responsible for the disease had been isolated. Taking into account that

Nedd4 was known to bind ENaC via WW domains (Staub et al, 1996), this was the first link between Nedd4 family ligases and PY motifs (Schild et al, 1996). By 1999, WW domains had been delineated into three groups according to their binding affinity (Espanel & Sudol, 1999), with group I WW domains, including those of YAP and the Nedd4 family, being defined as those with the core interaction sequence PPxY, as opposed to separate groups which were associated with either proline-rich regions punctuated with lysines (Chan et al, 1996), or proline-glycine-methionine motifs (Bedford et al, 1998). While the structures of the different WW domain classes are broadly conserved, mutation of a single conserved leucine in a canonical group 1 WW domain from YAP was shown to be sufficient to induce a switch from PPxY to polyproline substrate specificity (Espanel & Sudol, 1999). The conformationally rigid, cyclic structure of the proline backbone means that proline-rich sequences form a left-handed helical structure known as a polyproline II (PPII) helix (Creamer, 1998), forming a very distinct recognition motif which require a unique 'groove' in the binding surface to accommodate it. Different classes of WW domains differ according to the number of these 'grooves' their surfaces form, which in turn is dictated by the number and position of the conserved aromatic residues (Zarrinpar & Lim, 2000). This groove, dubbed the 'X-P' binding groove, in group 1 WW domains such as those of Nedd4, is formed from the second conserved tryptophan, Trp_{487}, and a second conserved aromatic residue, Phe_{476} (Kanelis et al, 2001). Between the β-strands that form this X-P groove are two linking loops which essentially enclose both ends of the groove, and therefore determine the substrate specificity. Especially important and conserved in group I WW domains is loop II, which forms a hydrophobic 'pocket' that the tyrosine residue of the PY motif binds to. Loop I shows more variation between individual WW domains, for example in

having conserved proline and alanine residues in WW3 of Nedd4 which are not present in other WW domains (Henry et al, 2003), thereby contributing to substrate specificity.

1.3.2 Different permutations of PY motifs & the roles of multiple PY motifs

Following the initial reporting of PY motifs as PPxY and PPPxY, as described above, in the mid-nineties, several PY-containing proteins, particular cell surface receptors and ion channels, were identified and used in turn to identify novel WW-domain containing proteins (Pirozzi et al, 1997). The first indication that PY motifs may be more variable than previously thought came with a screen of bacteriophage M13, which identified the alternative consensus LxLPxY (Kasanov et al, 2001) as a specific Nedd4 family recognition sequence, and by 2004 this had been refined to LPxY (Fotia et al, 2004). Leucine and other large, branched residues had been identified previously as being acceptable substitutes for proline with regards to SH3-binding domains, which share an X-P groove structure with WW domains (Yu et al, 1994). The LPxY form of PY motif was recognised as common and classed as a canonical motif by 2008 (Bruce et al, 2008), having been identified in a variety of substrates including tight junction kinases, and the HECT domain of Nedd4 ligases themselves (Patrie, 2005; Bruce et al, 2008). It was later established that some WW domains, such as WW3 of Nedd4, bind LPxY motifs more efficiently than others, such as the WW domain of YAP (Kanelis et al, 2006). While occasional reports of Nedd4 WW domains binding to non-PY sequences, such as phosphorylated serine (Edwin et al, 2010) and extended motifs (Chong et al, 2006), the L/PPxY motif is still the most common and generally accepted Nedd4 WW domain binding motif.

The same paper that reported differences in binding affinity of WW domains to L/PPxY motifs also noted that the two motifs LPSY and PPCY, of the *Drosophila* protein Commisureless bound different WW domains of Nedd4, WW3 and WW4 respectively (Kanelis et al, 2006). The two motifs are only five residues apart on the substrate protein, making it spatially unlikely that simultaneous binding is occurring. The authors do not present any alternative hypothesis for the role of the two motifs. While there are many examples of a single PY motif being necessary and sufficient for Nedd4-mediated binding, for example the inositol phosphatise MTMR4 (Plant et al, 2009) and the kinase SGK1 (Wiemuth et al, 2010), other published interactions require more than one such sequence, for example the interaction of the Ndfip adaptors with Itch (Mund & Pelham, 2009). In addition, not all PY motifs in a protein may behave equally; Ndfip 2 contains three PY motifs, all of the PPxY type, but removing either PY2 or PY3 has a greater effect on its ability to bind to and activate Itch than PY1 (Mund & Pelham, 2009).

In 2007, a variant APSY motif was identified on the yeast Rsp5p adaptor Bsd2p, which was shown to be just as important for its activity as a second, canonical PY motif (Sullivan et al, 2007). This was important not only because it was the first time that a residue other than leucine or proline had been identified at position 1 of a functional PY motif, but because it revealed several interesting points about the interaction of Nedd4 ligases and their substrates. The variant PY motif was shown to have an indispensible role in Bsd2p-mediated ubiquitination of Cps1p *in vivo*, despite demonstrating only weak binding to Rsp5p WW domains *in vitro.* In addition, substituting the variant alanine for a proline eliminated the binding to Rsp5p, as did switching the positions of the two motifs, suggesting that multiple PY motifs binding to specific WW domains is important for activity. Finally, and importantly, this paper posited a model for the role of multiple PY motifs; one may bind transiently to the ligase to ensure correct orientation of the ligase

with respect to the adaptor, before being displaced, in this case by another adaptor with a stronger affinity for the WW domain. To date, this is the only published example of such a variant motif and the best-described model of multiple PY motif roles in the same protein.

1.3.3 Identification of PMEPA1 as a Nedd4 substrate, and the PY motifs in PMEPA1

PMEPA1 (prostate transmembrane protein, androgen induced 1) was first identified as one of a number of androgen-induced genes present in the LNCaP prostate cancer cell line and called TMEPA1 (transmembrane, prostate androgen induced RNA 1) (Xu et al, 2000). It was put forward at the time as a potential biomarker for androgen signalling activity as a measure of prostatic disease, and at the time very little was known about it apart from the observation that it was localised to glandular epithelial cells in the prostate, and it was strongly up-regulated in response to synthetic androgen treatment, as well as in 75% of prostatic tumours (Xu et al, 2000). A type Ib transmembrane domain was identified between residues 9 and 25 at the N-terminus of the protein, and its size was determined as 252 residues. This would be predictive of subcellular targeting to the secretory pathway, and this was corroborated by the observation that a fluorescent-tagged PMEPA1 construct transiently expressed in LNCaP cells broadly co-localises with the *cis*-Golgi marker GM130 (Xu et al, 2003). Around the same time, an Australian group had used a similar screening method to identify binding partners of Nedd4 in mouse embryos (Jolliffe et al, 2000), one of which was called N4wbp4 and contained two PPxY PY motifs. PMEPA1 was found to share 83% sequence homology with N4wbp4, including the two PY motifs, and was later shown to interact with Nedd4 through those PY motifs (Xu et al, 2003). In the mean time, another Australian group had

independently identified PMEPA1 as being upregulated in renal, stomach and rectal cancers, and dubbed it STAG1 (solid tumour associated gene 1) before acknowledging that the sequence overlapped with that of PMEPA1 (Rae et al, 2001). This group also identified several proline-rich regions as potential SH3 and WW domain interaction motifs, but did not suggest specific interactions with Nedd4 or any other WW-domains containing proteins.

PMEPA1 was definitively identified as a Nedd4 substrate *in vitro* and *in vivo* in 2003, in a paper which also identified that it showed perinuclear localisation with approximate colocalisation with *cis*-Golgi markers, and demonstrated that a growth inhibitory effect in prostate cancer cell lines was abrogated by mutating the PY motifs, and therefore was Nedd4-mediated (Xu et al, 2003). The apparent conflict in subcellular localisation is common to other Nedd4-interacting proteins such as Ndfip2, which has 3 transmembrane domains and is Golgi- and late endosome-associated (Shearwin-Whyatt et al, 2004), so evidently is no barrier to binding *in vivo*. In fact it has been proposed that Ndfip2 sequesters Nedd4 and Nedd4-2 in the secretory pathway, specifically vesicular bodies, as a form of activity regulation (Konstas et al, 2005).

The two motifs, designated PY1 and PY2 according to their position in the primary sequence of PMEPA1, had the sequences $PPPY_{126}$ and $PPTY_{197}$ respectively. The functional loss of either of these two motifs resulted in significant loss of binding to Nedd4 WW domains, as measured using *in vivo* immunoprecipitation studies on prostate cancer lines (Xu et al, 2003), with this paper reporting PY2 as having a larger role in binding that PY1. However, it was simultaneously observed that the loss of PY1 had a greater impact on the growth inhibitory effects of PMEPA1, as measured by *in vivo* colony formation. Later studies confirmed the importance of the PY motifs in PMEPA1-androgen receptor interaction (see section 1.4.5) but did not expand on these initial

observations that the two may not be equal in terms of binding affinity and function (Li et al, 2008).

1.4 Androgen receptor function, regulation and interplay with PMEPA1

1.4.1 Function and structure of the androgen receptor

The androgen receptor (AR) is one of a family of nuclear hormone receptors which bind to steroids and act as ligand-regulated transcription factors. The activation cycle of AR is shown in figure 1.8; the natural ligands of AR are the male hormone testosterone and its metabolite dihydrotestosterone (DHT). Of the two, DHT binds more strongly to AR (Wilson & French, 1976), as well as dissociating more slowly and stabilising the receptor more effectively than testosterone (Zhou et al, 1995), and therefore acts as a more potent activator of the receptor. The development and maintenance of male sexual characteristics commonly associated with testosterone, including embryonic sexual differentiation, pubertal secondary sexual development, and spermatogenesis (George & Wilson, 1994), are all mediated by the androgen receptor. Its importance is demonstrated by the fact that androgen insensitivity syndrome (AIS) caused by mutations on the AR gene is associated with normal, indeed often elevated, levels of testosterone, but varying degrees of androgeny ranging from a completely female appearance at birth to infertility (Gottlieb et al, 1999). In addition to being expressed at high levels in prostatic and testicular tissues, AR has also been detected immunohistochemically in breast and vaginal tissue, as well as in cardiac muscle, hepatocytes and certain skin tissues in both males and females (Ruizeveld de Winter et al, 1991); that AR plays a role in breast cancer is widely accepted and the focus of intense research at present, as it has been

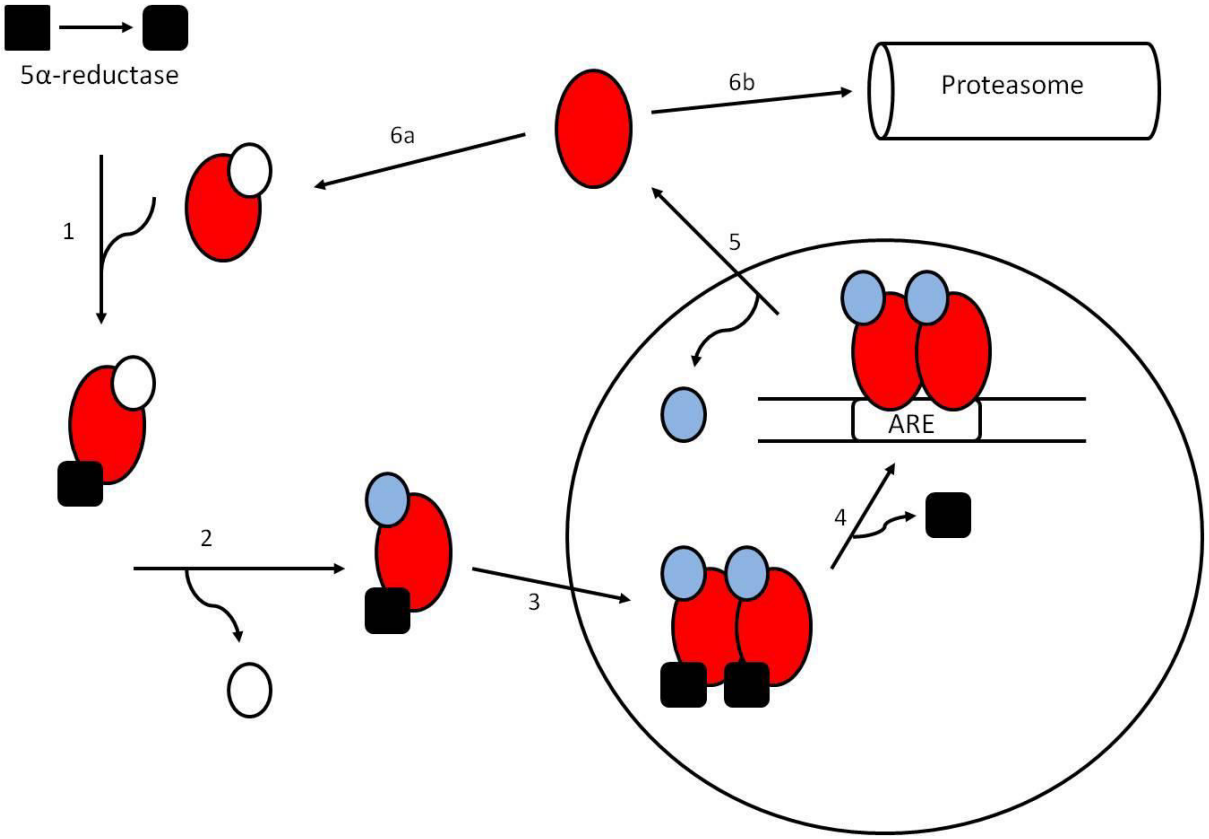

Figure 1.8. Schematic representation of the androgen receptor cycle. Testosterone is converted to DHT (black squares in top left) by the cytosolic enzyme 5α-reductase. AR (red) is maintained in a stable, inactive state in the cytoplasm by chaperones such as heat shock protein (white). Upon binding to DHT (1), a conformational change occurs and the HSPs dissociate (2), facilitating binding of coactivators (blue) such as importin α, which enable AR to move into the nucleus (3). Dimerisation occurs, and the AR dimer moves into the nucleus (3) and binds to androgen receptor elements on DNA, with concurrent dissocation of DHT (4). Once transcription is complete, the unliganded AR dissociates from the DNA and from the coactivators, and moves back into the cytoplasm (5), where it is free to bind stabilising HSPs (6a) or be degraded by the ubiquitin-proteasome system (6b).

found that a higher proportion of tumours show elevated AR (70-90%) than elevated oestrogen (70-80%) or progesterone (50-70%) receptors, the female steroid hormone receptors, yet AR levels correlate strongly with patient survival in non-metastatic cases (Gonzalez et al, 2008). In skin, AR is associated with slight inhibition of wound healing (Ashcroft & Mills, 2002), as well as with hormonally-induced conditions such as pubertal acne, for which anti-androgen have been used as a treatment for over 20 years (Greenwood et al, 1983; Muhlemann et al, 1986), and male pattern baldness, as part of its role as a mediator of the effects of circulating testosterone and DHT. AR has been detected in both male and female cardiac muscle, but the higher levels of circulating androgens in males is the likely cause of the relative hypertrophy of the cardiac muscle in males of several species (Marsh et al, 1998) as well as the basis of myocardial infarction as a consequence of anabolic steroid abuse (Melchert & Welder, 1995).

Structurally, AR is 110kDa in size and shares a common domain structure, and a high degree of sequence homology, with other steroid hormone receptors (Maclean et al, 1997). The N-terminal region consists of a polyglutamine repeat tract, a repeating sequence of glutamine residues with polymorphic repeat number which is associated with endocrinological and neurological disorders (Palazzolo et al, 2008), and an AF-1 domain, less well conserved compared to the other steroid hormone receptors, containing two overlapping transcriptional activation signals, both of which are required to initiate transcription, dubbed TAU1 and TAU5 (Jenster et al, 1995). The DNA-binding domain, which mediates transcriptional activation, is conserved throughout the steroid hormone receptor superfamily and contains 2 zinc finger motifs with a 66-residue core sequence (Luisi et al, 1991). It is located in the central region of the protein and mediates dimerization as well as DNA binding; the question of how such a well-conserved domain can mediate such different responses to the different steroids is ongoing, but there is a

large number of coactivators and a complex network of regulation involved, covered in more detail in section 1.4.3. The hinge region downstream from the DNA-binding domain is less well-studied, but plays a role in ligand-mediated nuclear translocation and DNA binding; there is conflicting evidence as to how this occurs as mutations in this region result in lower translocation efficiency but a stronger androgen response (Haelens et al, 2007). Finally the ligand-binding domain is at the C-terminus, unique among the steroid hormone receptors in that it is solely a ligand-binding region with no role in nuclear translocation. While the sequence homology between hormone receptors in this region is relatively low, they share a common folding pattern, known as an α-helical sandwich, consisting of a small section of β-sheet surrounded by a variable number of α helices (Matias et al, 2000), shown in figure 1.9. This fold is the basis of the structural change that occurs when a ligand is bound; one of the helices moves from being in an 'open' conformation to adopting a more compact, closed conformation that encloses the binding pocket. The specific residues within this binding pocket determine the ligand specificity of the receptor, for example this is the location of the T877A mutation found in the AR of the LNCaP prostate carcinoma cell line, resulting in a much greater binding affinity, and lower specificity, for steroids including progesterone (Matias et al, 2000)

1.4.2 Role in prostate cancer

There are over 10,000 known androgen receptor binding sites on the human genome, identified through chromatin immunoprecipitation (ChIP) sequencing (Sharma et al, 2013; Lamb et al, 2014), and several recent papers have reported the discovery of a significantly altered transcriptional profile in both early and late-stage prostatic tumours compared to normal tissue, both in cell lines *in vitro* and in tissue samples *in vivo*; these

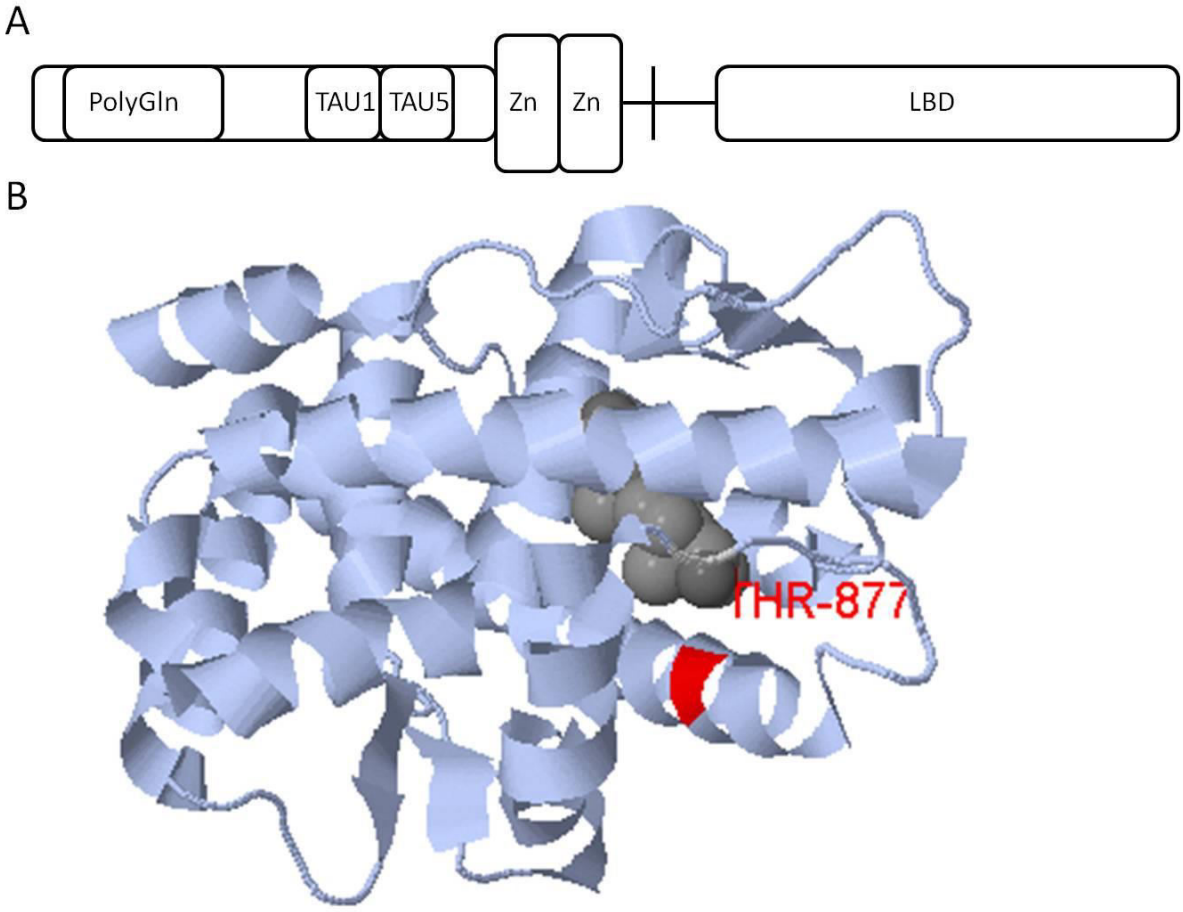

Figure 1.9. Schematic of the domain structure of androgen receptor (**A**), showing the N-terminal transactivation domain, containing the polyglutamine tract (PolyGln) and the two transcriptional activation regions TAU1 and TAU5, the two DNA-binding zinc finger motifs (Zn), the hinge region and the C-terminal ligand binding domain (LBD). Also shown is a crystallographic structure of the LBD of human AR at 1.9Ä resolution, bound to DHT (**B**). AR is shown with secondary structures in light grey, while DHT is shown as dark grey spheres. The small section of β-sheet characteristic of the α-helical sandwich is shown in the bottom left, surrounded by 12 α-helices. The threonine residue which is mutated in the LNCaP cell line is highlighted in red. RCSB PDB reference 2AMA with original structure published by Pereira de Jesus-Tran et al, 2006.

are presented in more detail in figure 1.10. The most immediately striking characteristic of this selection of transcriptional targets is the widely ranging functionality, from MUC6, which encodes gastric mucin, to CHRM1, an acetylcholine-binding G-protein coupled receptor. However, patterns have emerged; Perets et al (2012) identified seven ontology categories that were significantly over-represented in early stage prostatic tumour cells in the presence and absence of an agonist, including transcriptional regulators and ligand-gated ion channels. While the correct functioning of AR is essential for normal prostate development and function (Yeh et al, 2002), there are over 50 identified functional mutations in the AR gene which are associated with prostatic cancer (Heinlein & Chang, 2004). A high level of AR expression is predictive of progession to less treatable forms of the disease, as well as lower long-term survival (Lee, 2003). In normal prostate tissue, cells are turned over at a slow but balanced rate, keeping the overall organ size constant, but during early stages of cancerous development the rate of proliferation increases while the rate of death remains the same, allowing a slow but significant increase in size. As the disease progresses, the rate of death increases to balance the increased proliferation rate, meaning that although the growth is slowed, the number of splitting cycles each cell undergoes increases along with the chance of accumulating further mutations (Berges et al, 1995). The primary course of treatment for prostate cancer is androgen ablation therapy, which has been in use for over 70 years (Huggins et al, 1941) – today, this consists of a combination of chemical or surgical castration and AR antagonists, blocking the production of testosterone and DHT and simultaneously preventing them binding to AR. This treatment is effective in 80% of cases, but sometimes ceases to work after a period of 12-18 months, after which the disease is said to be androgen-independent, hormone-refractory or castration-resistant (the preferred term, as this form of the disease is still dependent on steroid hormones),

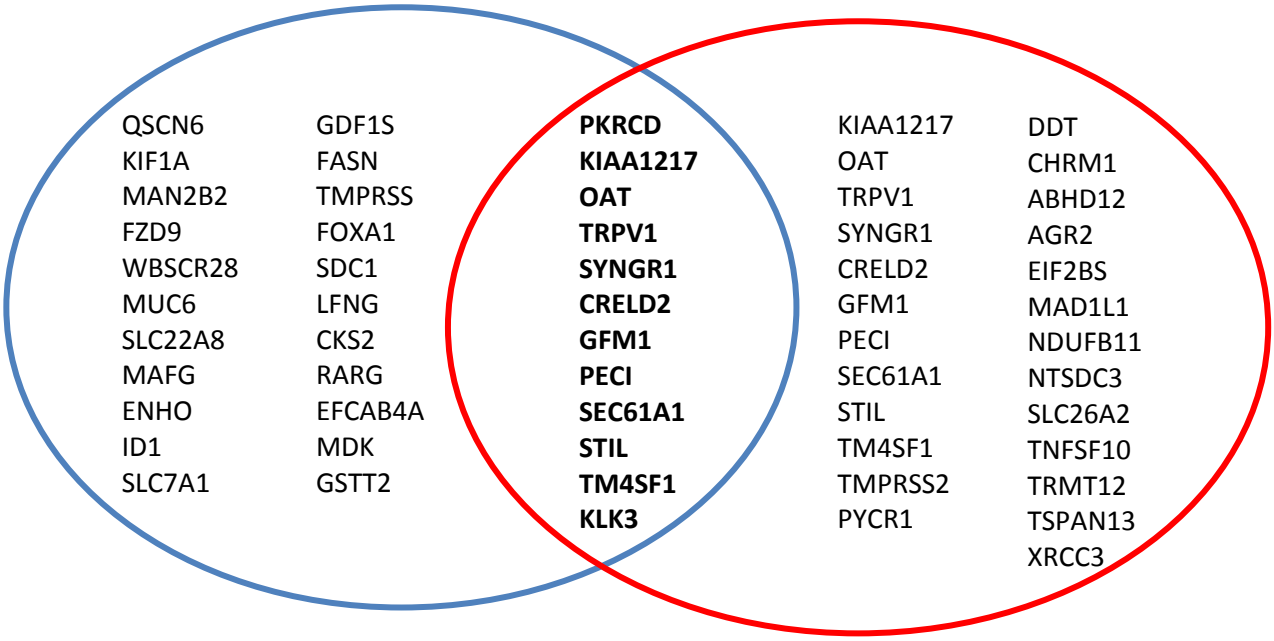

Figure 1.10. Venn diagram showing transcriptional targets of AR associated with prostatic cancer *in vitro* and *in vivo*. There are over 2,500 identified transcriptional targets of AR which have been identified as up-regulated, compared to normal tissue, in either cell line models of prostate cancer or tissue samples from prostatic tumours. This diagram represents a sample of identified genes from three publications (Lamb et al, 2013; Jariwala et al, 2007; Decker et al, 2012) which used ChIP sequencing and microarray techniques to pinpoint specifically novel genes which were significantly up-regulated in cell lines and/or prostatic tumours. Gene targets identified *in vitro* are bounded by the blue line and have refer to those found in the LNCaP and/or its derivative, C4-2B cell lines. Gene targets identified *in vitro* are bounded by the red line and refer to those found in human prostatic tissue samples. Those which overlap are highlighted in bold text.

(Heinlein & Chang, 2004). Paradoxically, withdrawal of anti-androgen therapy can result in a period of rapid symptomatic improvement and tumour regression (Scher et al, 1996), however this is temporary, and the mean survival time once the disease has progressed to that stage is 40-68 months (Oefelein et al, 2004). Second line therapy for castration-resistant prostate cancer is also dependent on anti-androgens, especially less commonly used treatments such as nilutamide, as well as adrenal suppressants and oestrogens (Chang, 2007).

The two transcriptional elements of the N-terminal AF-1 domain of AR both show several polymorphic variants associated with altered transcriptional activation (Gao et al, 1996) and variable rate of prostate growth (Zitzmann et al, 2003); while these seem to be common polymorphisms within the male population, the penetrance of associated cancer is relatively low (Nwosu et al, 2001). In terms of androgen-dependent, early stage cancers, AR has been shown to mediate androgen-dependent cell cycle progression, particularly during the transition from G1-S stage (Knudsen et al, 1998) via activation of cyclin-dependent kinases and subsequent phosphorylation & inactivation of repressors (Sherr, 1996), so androgen ablation therapy halts cell cycle progression. However, AR may also have a context-dependent protective role; it has been reported that mice lacking AR in the prostatic endothelium developed more aggressive prostate cancers and did not live as long as wild type mice (Niu et al, 2008). Similarly, AR can act indirectly to promote cell survival by upregulating cytoprotective proteins and downregulating others, such as the clusterin isoforms (Cochrane et al, 2007).

Rather than the initial development of prostate cancer however, the most striking association is between AR and the progression to the more advanced and less treatable castration-resistant form of the disease. AR levels in androgen-independent tumours are an average of six times higher than in early stage or benign tumours (Linja et al, 2001),

and amplification of the AR gene has been reported in patients who have developed hormone refractory prostate cancer after androgen ablation, but not before (Koivisto et al, 1997), suggesting that progression is at least partly caused by selection for increased AR copy number during low androgen therapy. In addition, there is a high frequency of AR mutations in advanced metastatic prostate cancer compared to early stages of the disease (Marcelli et al, 2000), again possibly due to selection pressure during treatment. These mutations may cause the AR to respond improperly to steroids other than testosterone and DHT ("promiscuous receptor pathway") such as the CaP T877A mutation, found in the LNCaP cell line and approximately 25% of androgen independent tumours (Gaddipati et al, 1994), or to become activated in the absence of steroids ("outlaw receptor pathway"). The tyrosine kinase HER-2/neu is strongly associated with breast and ovarian cancers (Slamon et al, 1989), both linked to the oestrogen receptor (ER) which is very closely related to AR. The drug Herceptin acts to bind HER-2/neu and blocks binding to the ER, and HER-2/neu has been shown to activate AR-dependent genes in the absence of steroid binding via the MAP kinase pathway (Yeh et al, 1999), emphasising again the varied roles of AR and the many potential pathways for its involvement in prostatic cancers. Which of these pathways is dominant, or even significant, in the development of castration-resistant cancer is not known and probably varies from case to case, but it is certain that AR plays an important role not only in the transformation of prostate tumours from androgen-dependent to androgen-independent, but in maintaining androgen-independent growth through an entirely different transcriptional program to that found in normal tissue and androgen-dependent tumours (Wang et al, 2009), including higher levels of histone methylation and upregulation of cell cycle progression.

1.4.3 Regulatory mechanisms

The regulation of androgen receptor activity is hugely complex, involving many pathways and other signalling molecules as well as steroids and intramolecular interaction of AR itself. Figure 1.11 illustrates the interplay and complementary nature of the intra- and selected intermolecular regulatory processes and their effect on ligand binding stability and AR activity. The intramolecular interaction, called the N/C interaction, involves an FQNLF motif on the N-terminal domain (Dubbink et al, 2004) and AF-2 region on the C-terminal ligand binding domain. On other steroid hormone receptors, the AF-2 region strongly binds coactivator complexes through the same motif, but AR is unique in that this is a much weaker binding compared to the binding to itself (He et al, 1999). This N/C interaction stabilises bound testosterone and potentiates the action of the receptor, but is abolished on translocation to the nucleus and binding to DNA, opening up the C-terminal binding site to coregulators (van Royen et al, 2007). In addition, it was recently reported that the DNA-binding and ligand-binding domains interact directly with each other when AR dimerizes, and that the loss of this interaction negatively impacts the ability of AR to bind ligands and to transactivate target DNA (Helsen et al, 2012). This novel interface is the site of several mutations associated with androgen insensitivity syndrome and highlights the holistic nature of the receptor activity, with the function of each domain being dependent on allosteric interactions with the rest of the protein.

One of the most important ways in which AR, in common with other steroid hormone receptors, is regulated is through over 130 identified coregulators which can both negatively and positively affect AR function (Chmelar et al, 2006). Of these, the canonical example is the p160 family, which consists of three large 160 kDa proteins

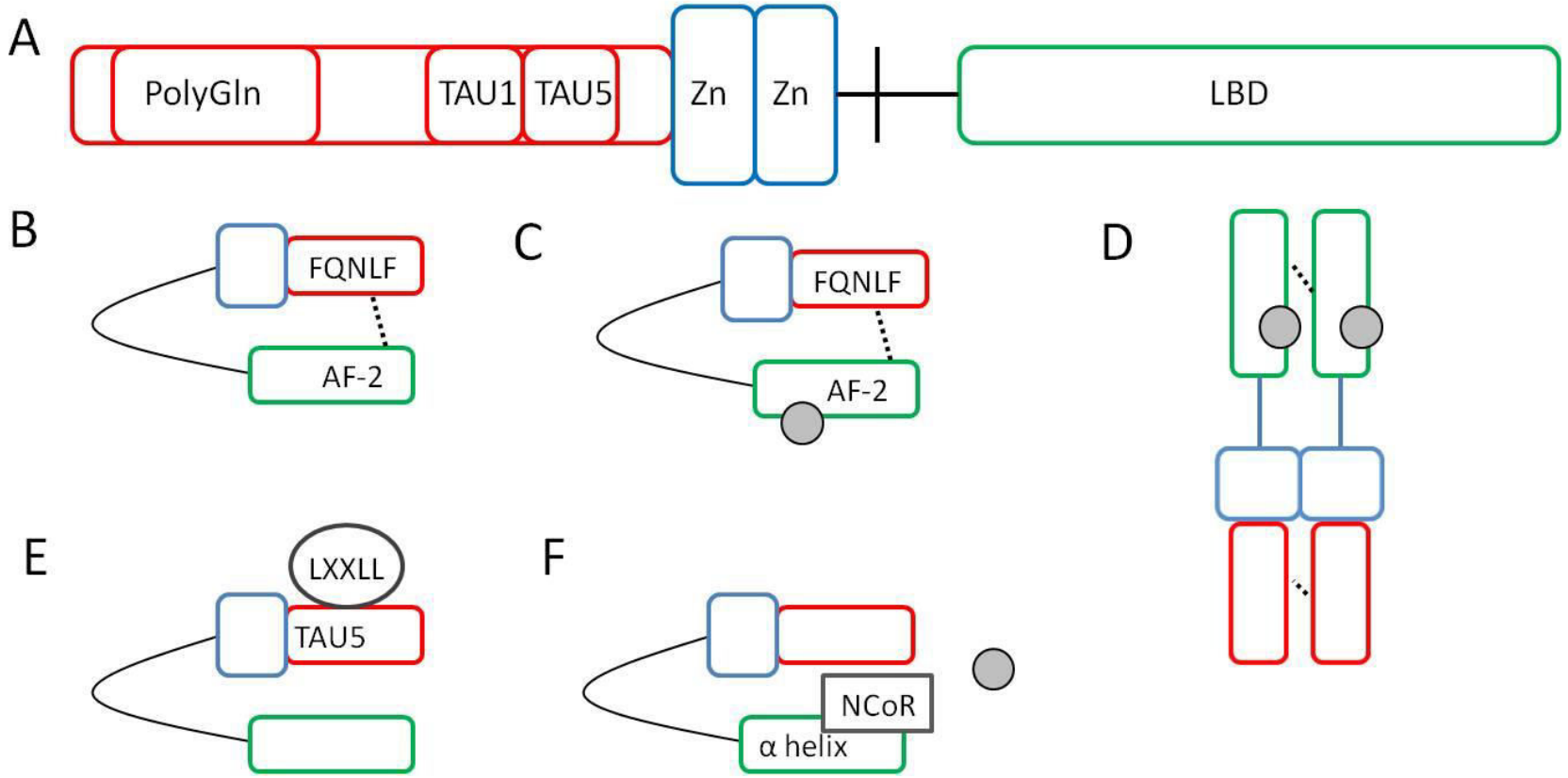

Figure 1.11. Schematic illustration of inter- and intra-molecular regulatory mechanisms of AR. The domain structure of AR is shown with the three main domains colour coded (A); the N-terminal domain (NTD) is shown bounded in red, the DNA binding domain (DBD) is shown bounded in blue, the hinge region is shown in black and the ligand binding domain (LBD) is shown bounded in green. These colours are retained throughout the figure to illustrate which parts of the protein are involved in the various interactions. The intramolecular N/C interaction is shown in (B) by the black broken line; this binding is maintained during ligand binding (C) but lost during dimerisation and DNA binding (D), during which the NTD and LDB domains of the two AR monomers interact, again shown by black broken lines. Two examples of intermolecular regulatory interactions, the binding of a p160 family co-activator to the TAU5 region of the NTD via the LXXLL motif (E) and the binding of the nuclear receptor co-repressor (NCoR) to the DBD (F), are also shown.

named SRC (steroid receptor coactivator) 1, 2 (aka TIF2 or GRIP1) and 3 (alternatively RAC3/AIB1). The SRCs are recruited mainly through the transcription activation domain TAU5 in the N-terminal region of AR (Callewaert et al, 2006), but the precise nature of the DNA promoter region being targeted and the internal regulation of the N/C interaction seem to play a part (Christiaens et al, 2002). These p160s bind AR via LXXLL motifs which compete for the AF-2 binding with the internal N-terminal site described above (Ding et al, 1998) and act as co-activators, stabilising the ligand-AR complex and enhancing the duration and efficiency of transcription. Other AR-associated coactivators are numerous and diverse, with no structural similarity, and for simplicity are named for their molecular weight e.g. ARA267, which mediates apoptosis (Wang et al, 2004). There are also a number of AR co-repressors, such as the nuclear receptor corepressor (NCoR), which interacts with the ligand-binding domain of AR, specifically the α helix which encloses the ligand when bound, and suppresses transcriptional activity (Cheng et al, 2002). Figure 1.11 illustrates several examples of intra- and intermolecular regulatory mechanisms for clarity. Many AR corepressors also have histone deacetylase (HDAC) activity, meaning that they inhibit transcription by preventing RNA polymerases from accessing promoter regions (Mathis et al, 1978).

The other major system of AR regulation is through post-translational modification (PTM), with a summary of the known modifications and their functions presented in figure 1.12. AR has been demonstrated to undergo ubiquitination mediated by the RING ligase Mdm2 (Gaughan et al, 2005), in a process which also requires the deacetylase HDAC1, resulting in decreased activity and increased AR turnover. Ubiquitination of AR is also associated with response environmental toxins such as dioxins, during which the dioxin receptor acts as a component of an E3 ligase complex to mediate enhanced degradation of sex hormone receptors (Ohtake et al, 2011). As well as regulating histone

Modification	Catalysed by	Modification site(s)	Net effect(s) on AR activity
Phosphorylation	Multiple kinases including PKC, MAPK, p38 and Src	At least 17 serine residues, 3 tyrosine residues, 1 threonine residue	Either increased or decreased; associated with increased translocation when carried out in the cytoplasm and both up- and down-regulation in the nucleus
Acetylation	Acetylases including p300, PCAF	Lysines within KLKK/ motif	Increased activation and recruitment to AREs; reported oncogenic effects
Ubiquitination	Ubiquitin E3s including Mdm2, CHIP and RNF6	K845, K847	Decreased activity due to increased proteasomal degradation
SUMOylation	Several SUMO E3s including PIAS1, RanBP2 and Pc2	Lysines within the consensus sequence ψKxE	Reduction of transcriptional activity, possibly by interfering with intramolecular stabilisation
Methylation	Methyltransferase Set9; possibly others	Lysines within the hinge region	Enhanced transcriptional activation

Figure 1.12. Table summarising post-translational modification (PTM) of AR. The type of PTM is shown as well as the enzyme that catalyses the reaction, the target residue(s) in human AR and the reported effect on AR activity.

acetylation status, HAT enzymes also modify AR directly, for example the coactivators p300 and P/CAF, which selectively modify specific lysine residues at the C-terminal end of the DNA-binding domain (Fu et al, 2000); this mutation of these lysines resulted in a loss of DHT-dependent transactivation of AR. Phosphorylation is a particularly well-studied and important PTM, and AR undergoes multiple phosphorylation events which serve several purposes. It is constitutively phosphorylated very soon after synthesis, and impairment of this process results in loss of effective ligand binding and a drop in transcriptional activity (Blok et al, 1998). Ligand binding in turn induces a further increase in phosphorylation to almost twice the initial extent, which is linked to increased nuclear translocation (van Laar et al, 1991) and is linked to ligand-induced conformational change increasing the availability of AR to kinases (Yang et al, 2007), and phosphorylation of AR alone has been shown to make the difference between ligands acting as agonists or antagonists (Wang et al, 1999). There are at least 17 conserved serine residues in AR which act as targets for phosphorylation (Coffey & Robson, 2012), which are preferentially modified depending on the subcellular location of AR in a further level of regulation (Kesler et al, 2007). There is a high degree of interplay between PTMs and other forms of regulation, for example overexpression of the activating kinase HER-2/neu mentioned earlier enhances phosphorylation of AR *in vivo,* while inhibition of HER-2/neu reduces phosphorylation of AR and curtails its transactivation (Sugita et al, 2004), as well as between different forms of PTMs. Phosphorylation of AR has been shown to be crucial for recruitment of the ubiquitin ligase Mdm2 to AR bound to DNA, and mutation of the conserved modified serine results in the preferential recruitment of a different ligase, CHIP, and the accumulation of AR at the PSA promoter (Chymkowitch et al, 2011). The final major PTM on AR is SUMOylation, which is discussed in more detail as a modification in section 1.5. SUMO

is an ubiquitin-like molecule which is conjugated to substrates via an enzymic cascade in much the same way, but has its own specific E1-E3 enzymes. SUMOylation is associated with functional repression of transcription factors in a process that depends on chromatin association (Stielow et al, 2008), and AR contains two SUMOylation motifs which, when mutated, result in enhanced transcriptional activity of AR and are clinically associated with testicular cancer, AIS and prostate cancer (Mukherjee et al, 2011). This is a dynamic process, triggered by ligand binding, during which extant AR is constantly cycling through SUMOylation and deSUMOylation in order to facilitate rapid response to stress signals such as heat (Rytinki et al, 2012).

1.4.4 A published feedback loop between AR and PMEPA1

In 2008, an American group published a report in which they laid out a potential negative feedback loop between AR and PMEPA1 (Li et al, 2008). PMEPA1 is now well-established as a transcriptional target of AR alongside PSA and others (Xu et al, 2012), and was previously shown to exhibit a negative effect on prostate cancer cell growth, both *in vitro* in laboratory cells lines and *in vivo* through a correlation between lower PMEPA1 expression and more advanced tumours (Xu et al, 2003). The new paper confirmed that this was mediated by ligand activation of AR, as well as showing a physical interaction between PMEPA1 and AR via co-immunoprecipitation. The most significant finding in terms of the feedback loop hypothesis was that induction of PMEPA1 expression in LNCaP prostate cancer cells, which express high levels of endogenous AR, caused a complete loss of detectable AR. Similarly, when PMEPA1 expression was silenced, detectable AR levels, as well as transcriptional activity as measured by PSA expression, increased slightly, as did S-phase cell cycle progression,

inferring that cell growth rate had also risen. Inhibition of the ubiquitin-proteasome system using the 26S proteasome inhibitor MG132 reinstated normal endogenous AR, as did another proteasome-specific inhibitor LLnL and, to a much lesser extent, lactacystin, although the non-proteasomal cysteine protease inhibitor E64 did not demonstrate this ability. Co-transfection of AR with HA-tagged ubiquitin and PMEPA1 resulted in a larger high molecular weight smear of ubiquitinated AR compared to AR and HA-Ub alone, and the downregulation of AR was shown to be attenuated when a PMEPA1 construct with both PY motifs mutated out was used in place of wild type, and Mdm2 knockout cells showed a reduced PMEPA1-mediated effect on AR levels.

Based on these findings, the group put forward a model for PMEPA1 acting to recruit Nedd4 to promote ubiquitin-mediated degradation of AR as a negative feedback loop, in which ligand binding initiates AR translocation to the nucleus and initiates PMEPA1 transcription. PMEPA1 in turn recruits Nedd4 and triggers degradation of AR, abolishing its effects. An additional layer of complexity is added by more recent findings by the same group; not only does Nedd4 down-regulation result in an increase of AR levels, but overexpression of AR results in a drop in Nedd4 levels (Li et al, 2012). However, there are several holes in this theory that the 2007 paper does not address; firstly, they do not make any suggestions as to how PMEPA1, which has been shown to associate strongly with the Golgi apparatus (Xu et al, 2003) but is absent from the nucleus and cystoplasm, makes physical contact with AR, which is cytoplasmic until testosterone binding triggers nuclear shuttling (Saporita et al, 2003). Secondly, they interpret the inhibition of the 26S proteasome and the subsequent restoration of cellular AR levels as showing that the effect of PMEPA1 on AR is proteasome-mediated i.e. is a degradation effect. While this is certainly a feasible explanation, inhibiting the proteasome does not result in lower levels of ubiquitination, rather it causes a build-up of ubiquitinated products which

would usually be broken down by the proteasome and their ubiquitin conjugates recycled into the cell's free ubiquitin pool. This in turn means that the pool of free ubiquitin is depleted, and other ubiquitin-dependent processes, such as trafficking and endocytosis, are also halted. There is some evidence in the paper itself that this is the reason for the observations; one of the experiments detailed was a transient transfection of HEK 293 kidney cells with a tagged form of ubiquitin and exogenous AR, with and without PMEPA1. It was observed that on addition of PMEPA1, increased high molecular weight conjugates of AR were seen on Western blots compared to AR and ubiquitin alone. However, this result clearly does not replicate their reported loss of AR in the presence of PMEPA1. If the result were due to increased proteasomal turnover of AR mediated by PMEPA1/Nedd4, the addition of exogenous ubiquitin should not make any difference to AR levels, however if it were due to another function of ubiquitin signalling, the additional ubiquitin would compensate for the depletion of the ubiquitin pool caused by the inhibition of the proteasome, and AR levels would remain stable, at least for a longer period of time. The ubiquitin experiment seems to suggest the latter. Finally, it is not clear from the paper whether PMEPA1 acts as an adaptor to mediate Nedd4 ubiquitination of AR, or whether PMEPA1 itself is ubiquitinated, and possibly trafficked to a location in which it can interact with AR as a result; the paper does not address physical interactions of either protein with Nedd4, only infers its involvement by the importance of the PY motifs in PMEPA1.

1.5 Summary and outstanding questions

This work focuses on clarifying the interaction between the ubiquitin ligase Nedd4 and its known substrate PMEPA1, a membrane protein showing altered expression in prostate cancer. PMEPA1 contains two well-documented canonical PY motifs, both required for interaction with Nedd4, and recent work has identified a third motif with a variant PY (vPY) sequence, QPTY. The roles of the multiple PY motifs in PMEPA1, as well as the importance of the precise nature of the amino acid residues within and surrounding the vPY motif, are not yet clear.

PMEPA1 is involved in regulating the cellular response to testosterone via the androgen receptor (AR) and has been shown to decrease cellular AR via a negative feedback loop involving Nedd4. This process is attenuated in PMEPA1 mutants that cannot interact with Nedd4, implying that receptor regulation is dependent on ubiquitination. However AR and PMEPA1 are reported to be located in different subcellular compartments, raising questions about the mechanism of interaction between them; this leads back to the indeterminate precision of the PMEPA1 localization reported in the original paper, discussed previously. While the individual interactions between PMEPA1 and Nedd4, as well as between PMEPA1 and AR, have been confirmed and studied, the interplay between the mechanisms involved, including how the ubiquitin-proteasome system might underpin the PMEPA1-mediated androgen receptor regulation cycle, remains unresolved.

The specific questions that this project aimed to answer were:

- What is the difference, if any, in functionality between the vPY motif and the two canonical PY motifs in PMEPA1?
- How flexible is the vPY motif, in terms of its precise sequence?
- Does altering the residues immediately flanking all three PY motifs have any impact on their function?
- What is the *in vivo* significance of each of the three PY motifs in PMEPA1?
- Does altering the Nedd4 binding ability of PMEPA1 affect *in vivo* cellular protein levels and subcellular localisation?
- What are the precise roles of PMEPA1, Nedd4 and ubiquitin in the AR/PMEPA1 feedback cycle?

1.6 Hypotheses

1 The vPY motif will, in a similar way to that identified in Bsd2p (Sullivan et al, 2007), be involved in ubiquitination of PMEPA1, and that this unique role will be related to differential binding to WW domains through this motif compared to the two canonical motifs.

2 A soluble variant of PMEPA1, lacking the N-terminal transmembrane domain, will be free to colocalise with the cytosolic proteins AR and Nedd4

3 The *in vitro* significance of the PY motifs in PMEPA1 reflect a prominent *in vivo* role in mediating Nedd4 ubiquitination, and this interaction is implicated in regulation of AR.

4 The proposed feedback loop between AR and PMEPA1 is dependent on a direct interaction as described above, and this is triggered by a ubiquitin-mediated trafficking process rather than ubiquitin acting as a degradation signal.

2. MATERIALS AND METHODS

2.1 Cloning

2.1.1 Plasmids

For the *in vitro* ubiquitination assays, a construct of PMEPA1 lacking the N-terminal hydrophobic domain (first 23 amino acids), with an N-terminal S-tag and 6xHis tag, cloned previously by Dr. Jim Sullivan into a pET30a vector (Novagen) was used. Each alteration was made as a single point mutation, first in the wild type construct, and then on the resulting plasmids as necessary to make double and triple mutants. N-terminal GST-tagged Nedd4 and Uba1 were both previously cloned by Dr Aipo Diao and Dr. Jim Sullivan, respectively, into pGEX-6P2 (GE Healthcare). The circular dichroism experiments, which required an ultraviolet-invisible tag, necessitated cloning an additional Nedd4 construct with a 6xHis-tag for bacterial expression. This was done by ligating the Nedd4 ORF from the GST-tagged construct into pET30a via BamHI and SalI restriction sites.

For the microscopy, full length PMEPA1 with C-terminal green fluorescent protein (GFP) or mCherry tags, in a pGRIP vector (obtained from Alison Gillingham, MRC-LMB, Cambridge), was used. This plasmid has a CMV promoter for mammalian expression, along with a polyadenylated terminator sequence and an ampicillin resistance gene. The wild-type Nedd4 constructs with N-terminal GFP and mCherry tags used were similarly cloned into the same plasmid. The PMEPA1 triple ΔPY mutant was made in the same way as the bacterial expression plasmid described above, using the same SDM primers to sequentially introduce the mutations. The ΔNT truncated mutant was made

using PCR as detailed below to produce a DNA fragment coding for PMEPA1 without the first 23 amino acids, using the full length ORF in the pGRIP vector as a template, with sticky ends to ligate directly into the same pGRIP17 plasmid via existing AfeI and ClaI restriction sites. The AR-GFP plasmid was made by first cloning human AR from the IMAGE clone (number 40146997) into a pGRIP intermediate vector using BamHI & XhoI restriction enzymes to introduce additional cloning sites, and then inserting the ORF into the pGRIP mammalian expression plasmid downstream of the GFP tag via BamHI and XbaI restriction sites. To introduce the CaP (T877A) mutation into the androgen receptor, oligonucleotides were designed as described below, and SDM was performed as previously. A GFP-only plasmid was cloned previously into the pGRIP vector for mammalian expression, and an mCherry-only plasmid was cloned by inserting the mCherry sequence from a previously cloned mCherry-SUMO (Giulia Benná, unpublished) plasmid into pCMV (Addgene) via SacI & BamHI restriction sites.

For the epitope tagged mammalian expression constructs, firstly PCR was used (see 2.1.2) to introduce additional restriction sites at either end of the PMEPA1 ORF. This fragment was then digested & inserted into a variant of the pGRIP17 plasmid (cloned previously by Dr. J. Sullivan) via BamHI and XhoI restriction sites, to give a single ORF with a C-terminal tag (2x Myc + IgG binding domain of Protein A) fused to full-length PMEPA1. This new plasmid was then used to clone a ΔNT truncated PMEPA1 construct using a similar method to that used for the fluorescent protein tagged ΔNT PMEPA1 plasmid; PCR was used to amplify out a fragment containing the entire PMEPA1-Myc-IgG ORF, without the N-terminal transmembrane domain and with the addition of extra restriction sites at both ends, which was then ligated into a p3HA plasmid (provided by Thomas Mund, MRC-LMB, Cambridge) via BamHI and SalI restriction sites. AR was cloned directly from the GFP plasmid into pGRIP in place of PMEPA1 using BamHI and

XhoI restriction sites, and an untagged construct, created by ligating the IMAGE clone into pGRIP-HA cut using BamHI and XhoI restriction enzymes, was also made. In addition, TAP-Nedd4 was cloned into pGRIP17 previously by Nasra Diriye (QMUL, undergraduate project student), and 8xHis-FLAG-ubiquitin was cloned into p3HA previously by Arfa Jalil (QMUL, undergraduate project student).

2.1.2 Primer Design

For site directed mutagenesis (SDM), oligonucleotides were designed using the Primer X online program available at http://www.bioinformatics.org to ensure the melting temperatures and GC content were suitable for use in SDM, and purchased from Eurofins MWG. KOD Hot Start 2x Master Mix (Novagen) and Phusion Hot Start Flex 2x Master Mix (New England Biolabs) were used as described in 2.1.3 below, and success was confirmed using the Eurofins MWG DNA sequencing service.
See figure 2.1 for a complete list of all the primers used for PCR.

2.1.3 Polymerase Chain Reaction (PCR)

For all PCR reactions a PeqStar 96 thermocycler (Peqlab) was used. Primers were supplied as lypophilised powder and reconstituted using an appropriate volume of sterile distilled water to a stock concentration of 100 µM.

Target	Mutation	Forward primer sequence (5'-3')	Reverse primer sequence (5'-3')
PMEPA1	Y102A (PY1)	CCG CTT CCA GCC CAC CGC TCC GTA CCT GCA G	CTG CAG GTA CGG AGC GGT GGG CTG GAA GCG G
PMEPA1	Y126A (PY2)	GAC GAG CCC CCA CCC GCC CAG GGC CCC TG	CAG GGG CCC TGG GCG GGT GGG GGC TCC TC
PMEPA1	Y197A (PY2)	GGC CGC CGC CCA CCG CCA GCG AGG TCA TCG	CGA TGA CCT CGC TGG CGG TGG GCG GCG GCC
PMEPA1	Q99A	CGC TTC CAC CGC TTC AAT CCC ACC TAT CCG TAC	GTA CGG ATA GGT GGG ATT GAA GCG GTG GAA GCG
PMEPA1	Q99D	CGC TTC CAC CGC TTC GAT CCC ACC TAT CCG TAC	GTA CGG ATA GGT GGG ATC GAA GCG GTG GAA GCG
PMEPA1	Q99A	CTT CCA CCG CTT CGC GCC CAC CTA TCC G	CGG ATA GGT GGG CGC GAA GCG GTG GAA G
PMEPA1	T101S	CGC TTC CAG CCC AGC TAT CCG TAC CTG	CAG GTA CGG ATA GCT GGG CTG GAA GCG
PMEPA1	T101E	CAC CGC TTC CAG CCC GAA TAT CCG TAC CTG CAG	CTG CAG GTA CGG ATA TTC GGG CTG GAA GCG GTG
PMEPA1	T101A	CGC TTC CAG CCC GCG TAT CCG TAC CTG	CAG GTA CGG ATA CGC GGG CTG GAA GCG
PMEPA1	T101P	CAC CGC TTC CAG CCC CCG TAT CCG TAC CTG CAG	CTG CAG GTA CGG ATA CGG GGG CTG GAA GCG GTG
PMEPA1	Q99P	CTT CCA CCG CTT CCC GCC CAC CTA TCC G	CGG ATA GGT GGG CGG GAA GCG GTG GAA G
PMEPA1	F98A	CGC TTC CAC CGC GCG CAG CCC ACC TAT C	GAT AGG TGG GCT GCG CGC GGT GGA AGC G
PMEPA1	F98E	GCG CTT CCA CCG CGA ACA GCC CAC CTA TC	GAT AGG TGG GCT GTT CGC GGT GGA AGC GC
PMEPA1	P103A	CAG CCC ACC TAT GCG TAC CTG CAG C	GCT GCA GGT ACG CAT AGG TGG GCT G
PMEPA1	P103E	CTT CCA GCC CAC CTA TGA ATA CCT GCA GCA CGA G	CTC GTG CTG CAG GTA TTC ATA GGT GGG CTG GAA G
AR	Introduction of NheI site at 3' end of ORF	GAC AAG GCC ATG GCT GAT ATC GGA TCC ATG	GTG GTG GTG GTG GTG GTG CTC GAG TCA CTG
PMEPA1	Introduction of SalI site at 5' and BglII site at 3' end of ORF	CTA CTC ACT ATA GGG AGA CCG GAA GCT TAT G	CAT CTC CCG GGG ATC TCT AGA TTA CGC
PMEPA1	Introduction of BamHI and SalI sites at 5' and XhoI site at 3' end of ORF	CGA CTC ACT ATA GGG GAT CCG GGT CGA CAT GGC GGA GCT GG	ATT TTT TTC TCC ATC TCG AGG AGA GGG TGT CC
AR	Introduction of NdeI site and 5' and BamHI site at 3' end of ORF	GCC AGA GAT CAA CAT ATG AAA AGG CAG TCA GGT	GGG TGG GGA AAT AGG GGA TCC AAT GCT TCA CTG
AR	T877A	GAG AGC TGC ATC AGT TCG CGT TTG ACC TGC TAA TCA AG	CTT GAT TAG CAG GTC AAA CGC GAA CTG ATG CAG CTC TC
PMEPA1	Removal of first 23 residues with insertion of SacI site at 5' and BamHI site at 3' end of ORF	TGA TGG TGA TGG AGC TCG GAT CCA CGA TGC TGC TGA GCC AC	AGT TAG CCT CCG TCG ACT CCC GGG GAT C

Figure 2.1. Table of all primers used in PCR for SDM and cloning. Includes the name of the gene to be altered, forward and reverse primer sequences and a brief explanation of the residue(s) to be altered. Single letter abbreviations are used for amino acid sequence changes. Complete DNA and amino acid sequences of PMEPA1 are included for reference in chapter 1.

2.1.3.1 Kod Hot Start Master Mix

The Kod Hot Start Master Mix (Novagen) was provided at 2x concentration, and 25 µL was used in a reaction mixture containing 1 µL plasmid DNA (approx. 10-20 pg), 2 µL forward primer & 2 µL reverse primer (both at 10 µM working concentration), with sterile distilled water to make up the volume to 50 µL.

The Kod PCR conditions were an initial incubation of 2 min at 95 ^{o}C, followed by 20-30 cycles of 1 min at 95 ^{o}C, 1 min at 54-55 ^{o}C and 20 sec/kb at 70 ^{o}C, and a final incubation of 5 min at 70 ^{o}C.

2.1.3.2 Phusion Hot Start Flex Master Mix

The Phusion Hot Start Flex Master Mix (New England Biolabs) was also provided at 2x concentration, and 25 µL was used in a 50 µL volume containing 1 µL plasmid DNA (10-20 pg), 2 µL forward primer and 2 µL reverse primer (at 10 µM), with the volume made up with sterile distilled water.

The Phusion PCR conditions were an initial incubation of 2 min at 98 ^{o}C, followed by 25-30 cycles of 10 sec at 98 ^{o}C, 20 sec at 75-92 ^{o}C and 30 sec/kb at 72 ^{o}C, and a final incubation of 5 min at 72 ^{o}C. The annealing temperature was adjusted for each primer pair with reference to the Thermo Scientific melting temperature calculator available at http://www.thermoscientificbio.com/webtools/tmc/.

2.1.3.3 DNA digestion and cleanup for SDM

Following the PCR reaction, methylated template DNA was removed by the addition of 10 units DpnI (New England Biolabs) per 50 µL reaction, which was then incubated overnight at 37 ^{o}C. The digested PCR product was cleaned up using a commercial kit according to manufacturer's protocol (Bioneer or Fermentas), by adding 500 µL binding buffer (5.5 M guanidine thiocyanate, 20 mM Tris-HCl pH 6.6), 20µL 3 M sodium acetate pH 5.2, and 100 µL isopropanol to the PCR reaction. This mixture was added to a DNA binding column in a 2 ml tube and centrifuged for 1 minute at 14,000 rpm, then the flow-through was loaded back onto the column and the centrifugation repeated. The column was washed by centrifuging for 1 minute at 14,000 rpm with 700 µL of a buffer containing 80% v/v ethanol with 20 mM sodium chloride and 2 mM Tris-HCl pH 7.5, then dried by removing the flow-through and centrifuging at 14,000 rpm for 2 minutes. The DNA was eluted by incubation with 55 µL autoclaved, ultrapure water at room temperature for 5 minutes, then centrifuging at 14,000 rpm for 1 minute. 5 µL of the eluted PCR product was run on a 1% w/v agarose gel in order to assess the purity and yield, before being used in downstream applications.

2.1.3.4 Agarose gel electrophoresis

An appropriate weight (0.8-2 g) of powdered agarose (Web Scientific) was dissolved in 100 ml TAE buffer (40 mM Tris acetate with 1 mM EDTA) and heated in the microwave until the agarose was completely dissolved. Once the liquid agarose had cooled sufficiently, but not started to set, ethidium bromide (Sigma Aldrich) was added to a final concentration of 0.5 µg/ml and the mixture was poured into a Submarine horizontal electrophoresis unit (Hoefer) with one or more combs in place to form wells.

Once the gel had set, the unit containing the gel was submerged in TAE buffer and the comb removed. A 6x DNA loading buffer (New England Biolabs) was added to the sample(s) and they were run at 100-120 V for 20-60 min alongside a 2-log 0.1-10 kb size comparison ladder (New England Biolabs). Gels were visualised using the Syngene G:BOX gel imaging system with GeneSnap software.

2.1.3.5 Gel slice extraction

A gel slice containing the appropriate DNA fragment was cut out of the agarose using a scalpel blade; this was done using a standard UV transilluminator (UVP). The DNA was purified from the gel slice using a commercial kit according to manufacturer's protocol (Bioneer/Fermentas) by dissolving the gel slice in an equal volume (400-600 µL) of DNA binding buffer (5.5 M guanidine thiocyanate, 20 mM Tris-HCl pH 6.6) at 60 ^{o}C, then adding 100 µL isopropanol and 20 µL 3M sodium acetate pH 5.2. This mixture was added to a DNA binding column in a 2 ml tube and centrifuged for 1 min at 14,000 rpm, then the flow-through was loaded back onto the column and the centrifugation repeated. The column was washed by centrifuging for 1 min at 14,000 rpm with 700 µL of a buffer containing 80% v/v ethanol with 20 mM sodium chloride and 2 mM Tris-HCl pH 7.5, then dried by removing the flow-through and centrifuging at 14,000 rpm for 2 min. The DNA was eluted by incubation with 55 µL autoclaved, ultrapure water at room temperature for 5 min, then centrifuging at 14,000 rpm for 1 minute.

2.1.4 Restriction digestion and ligation

Endonuclease enzymes were supplied by New England Biolabs, Promega and Thermo Scientific. Digests were performed in a 20 µL volume containing 100-500 ng DNA (5-10 µL), 2 µL appropriate reaction buffer as supplied by the manufacturer of the enzyme(s) at 10x concentration, 2 µL 10 mg/ml bovine serum albumin (BSA), and 5 units each enzyme, and the volume was made up with autoclaved distilled water. The reaction mixture was incubated at 37 ^{o}C for 1-3 hours, and then 4 µL 6x loading buffer (New England Biolabs) was added before the mixture was run on an appropriate percentage agarose gel as described previously.

The digested, cleaned up DNA fragments were ligated using T4 DNA ligase (New England Biolabs). The ligation mixture contained varying ratios of vector to insert DNA depending on their relative sizes, between 1:2 and 1:30, for a total volume of 10-15 µL DNA, as well as 2 µL buffer provided by the manufacturer at 10x concentration, and 400 units of ligase. The volume was made up to 20 µL with sterile, double-distilled water and the reaction was incubated at 16 ^{o}C overnight or at 4 ^{o}C for 72 h. The ligation mixture was transformed directly into chemically competent *E. coli* as described below.

2.1.5 Bacterial transformation

Four strains of *E. coli* were used; Rosetta-Gami 2 (Novagen) and BL21-CodonPlus (DE3) (New England Biolabs), for overexpression of recombinant proteins, DH5α (New England Biolabs) and XL1-Blue (Stratagene) for DNA production and cloning.

To make chemically competent bacteria for transformation, we used a modified version of the standard protocol published by Inoue et al (1990). Individual colonies of *E. coli* were isolated by streaking a liquid culture out onto a plate containing 2XYT broth

(Melford) containing 16 g/L digest peptone, 10 g/L yeast extract and 5 g/L sodium chloride with 100 g/L high gel strength agar (Melford) under sterile conditions, and incubating overnight at 37 ^{o}C. A single colony was grown up in 5 ml liquid 2XYT broth overnight at 37 ^{o}C on an orbital shaker at 180 rpm, then 1 ml of this culture was inoculated into 100 ml 2XYT broth and incubated at 37 ^{o}C on an orbital shaker at 180 rpm for 2 h. The cells were cooled on ice for 15 min, then centrifuged at 4000 rpm for 7 min at 4 ^{o}C. The resulting pellet was resuspended in 50 ml ice cold buffer containing 30 µM potassium acetate, 50 µM manganese (II) chloride tetrahydrate, 100 µM potassium chloride, 10 µM calcium chloride dihydrate and 15% v/v glycerol, incubated on ice for 15 min then spun again at 7000 rpm for 7 min. Finally the pellet was resuspended again in 4 ml ice cold buffer containing 10 µM MOPS, 75 mM calcium chloride dihydrate, 10 µM potassium chloride and 15% v/v glycerol, aliquotted into 100 µL volumes and flash-frozen in liquid nitrogen before being stored at -80^{o}C.

For transformation, a 100 µL aliquot of competent cells was combined gently with 50-300 ng plasmid DNA, or 10 µL of ligation reaction, and incubated on ice for 30 min. The mixture was heat shocked at 42 ^{o}C for 45 sec, then incubated on ice for a further 2 min. 900 µL of 2XYT broth, without any antibiotic selection, was added and the tube was incubated at 37 ^{o}C for 1 h. The tube was spun in a microcentrifuge for 1 min at 14,000 rpm, then 900 µL of supernatant was removed and the pellet resuspended in the remaining 100 µL. The resuspended cells were streaked or spread over a 2XYT-agar plate, with appropriate antibiotic selection under sterile conditions (see figure 2.2), then incubated at 37 ^{o}C overnight.

Name of antibiotic	Stock concentration	Working concentration
Chloramphenicol	50mg/ml in ethanol	50µg/ml
Kanamycin	50mg/ml in distilled water	50µg/ml
Ampicillin	100mg/ml in distilled water	200µg/ml

Figure 2.2. Antibiotics used to maintain selection in E. coli.. The stock concentrations as well as the solvent used are given; these stocks were aliquotted and frozen at -20^{o}C. The working concentrations are the final concentrations of the stocks diluted in 2XYT media, with or without agar. Kanamycin was obtained from Melford which ampicillin and chloramphenicol were obtained from Sigma Aldrich.

2.1.6 Plasmid DNA preparation

Small-scale plasmid DNA extraction ("Minipreps") was either performed using a commercial kit or using a variation of the alkaline lysis method (Birnboim & Doly, 1979). DNA concentration was determined using a Nanovue (GE Healthcare) microspectrophotometer. Typical yield was 100 ng/µL for the column-based method and 2000 ng/µL for the alkaline lysis protocol.

2.1.6.1 Small (mini) scale extraction via kit

One of two commercial columns based kits (Bioneer/Thermo Scientific) was used; the names of the buffers varied but the protocol for both was the same. The buffers for each are given in figure 2.3 but are referred to here as 1, 2, 3 and 4. 3 ml of an overnight bacterial culture transformed with the plasmid of interest was centrifuged at 14,000 rpm for 1 min and the pellet resuspended in 250 µL of buffer 1. Then 250 µL buffer 2 was added, followed by 350 µL of buffer 3 and gently mixed by inversion. The tube was then centrifuged at 14,000 rpm for 10 min, and the supernatant was added to a DNA-binding column and centrifuged for 1 min at 14,000 rpm. The flow-through was discarded, 700 µL buffer 4 was added to the column and centrifuged for 1 min at 14,000 rpm, then the flow-through was discarded and the column was dried by centrifugation at 14,000 rpm for 2 min. The DNA was eluted by placing the column into a clean tube and incubating with 55 µL sterile distilled water for 5 min at room temperature, followed by centrifuging at 14,000 rpm for 1 min.

Notation in text	Bioneer Accuprep notation	Thermo Scientific GeneJET notation
1	1	Resuspension Solution
2	2	Lysis Solution
3	3	Neutralisation Solution
4	4	Wash Solution

Figure 2.3. Names of buffers in commercial kits used for plasmid minipreps. The first column indicates how each buffer is designated in the text, which the specific manufacturer names for each solution are given in the second and third columns. The formulae for all buffers are equivalent in both kits.

2.1.6.2 Alkaline lysis

3 ml of overnight bacterial culture transformed with the plasmid of interest was centrifuged at 14,000 rpm for 1 min. The supernatant was discarded and the pellet resuspended in 150 µL resuspension buffer (50 mM Tris-HCl, 10 mM EDTA and 100 µg/ml RNAse A, at pH 8). Then 250 µL lysis buffer (200 mM sodium hydroxide and 1% w/v SDS) was added to the mixture, followed by 350 µL neutralisation buffer (3M potassium acetate pH 5.5). The tube was gently inverted to mix and centrifuged at 14,000 rpm for 10 min. The supernatant was transferred to a clean tube, then 400 µL phenol:chloroform:isoamyl alcohol 25:24:1 (Sigma Aldrich) was added, and centrifuged for 3 min at 14,000 rpm. The top aqueous layer, containing the DNA, was removed and transferred to a clean tube. 880 µL ethanol and 40 µL 3 M sodium acetate (pH 5.2) was added and the mixture was incubated on ice for 30 min to precipitate the DNA, which was pelleted by centrifugation at 14,000 rpm for 15 min. The pellet was resuspended in 200 µL 70 % v/v ethanol, then the tube was spun again for 2 min at 14,000 rpm, the ethanol was removed and the pellet was allowed to air dry at 37 ^{o}C for 5 minutes. Finally the DNA pellet was resuspended in 55 µL sterile double-distilled water.

2.1.6.3 Larger (midi) scale extraction via kit

For larger scale production of plasmid DNA, a peqGOLD XChange midi-prep kit (PEQlab) was used, providing a typical total yield of 100-400 µg DNA. This method is based on a technique described by Prazeres et al (1998). 100 ml of overnight bacterial culture transformed with the plasmid of interest was pelleted by centrifugation at 4000 rpm for 20 min. The pellet was resuspended in 8 ml of Buffer I, then 8 ml of Buffer II was added, followed by 8 ml Buffer III. The resulting mixture was incubated on ice for 5

min before being cleared by centrifugation at 10,000 rpm for 25 min at 4 ^{o}C, and additionally filtered through a wad of Miracloth (Millipore) before being added onto the column (which was pre-equilibrated with 2.5 ml EQ buffer) and allowed to drip through completely by gravity flow. The column was then washed using 12 ml DNA Wash Buffer and the DNA eluted using 5 ml Elution Buffer by gravity flow. Excess salt was removed by precipitating the DNA in 3.5 ml room temperature isopropanol and centrifuging at 13,500 rpm for 30 min at 4 ^{o}C. The resultant DNA pellet was resuspended in 2 ml 70% v/v ethanol and spun again at 20-25 ^{o}C for 10 min. The supernatant was carefully removed and any remaining ethanol allowed to evaporate by air drying at room temperature for 5-10 min. Finally the pellet was redissolved in 100 µL sterile distilled water.

2.2 Recombinant protein production

2.2.1 Small scale

500 µL of a 5 ml bacterial culture, grown overnight and expressing the construct of interest, was seeded into 11 ml 2XYT broth with appropriate antibiotic selection (chloramphenicol to select for the codon plus plasmid, as well as ampicillin or kanamycin to select for the transfected plasmid) and grown at 37 ^{o}C on an orbital shaker at 180 rpm for 2 h. 1.5 ml was harvested, centrifuged at 14,000 rpm for 1 min and the pellet resuspended in 1 ml SDS sample buffer (4% w/v SDS, 20% v/v glycerol, 5% v/v β-mercaptoethanol and 0.05% w/v bromophenol blue) as a pre-induction sample. Protein expression was induced in the remaining 10 ml using 1 mM IPTG (Melford). The induced bacteria were grown for an additional 4 h at 30 ^{o}C, then another 1.5 ml was harvested as an induced sample. The induced sample was sonicated using a Sonics

Vibra-Cell VCX130 at 80% amplitude for 90 sec (30 sec on, 30 sec off) to break the cell membranes, and the debris pelleted by centrifugation at 14,000 rpm for 10 min. The supernatant was removed and had an equal volume of SDS sample buffer added to it; this was the soluble fraction. The pellet was resuspended in 1 ml SDS sample buffer as the insoluble fraction. The samples were run out on an appropriate percentage SDS-PAGE gel and stained with Coomassie as described in 2.3.1.

2.2.2 Large scale

5 ml bacterial culture, grown overnight and expressing the construct of interest, was seeded into 1 L 2XYT broth with appropriate antibiotics and incubated for 4-5 h at 37 ^{o}C with shaking at 180 rpm. Protein expression was induced with 1 mM IPTG, following which the cultures were incubated overnight with shaking at 16 ^{o}C. The cells were harvested by centrifugation at 6,000 rpm for 5 min and resuspended in 50 ml lysis buffer, the composition of which varied according to the affinity tag on the protein as described below. The resuspended cells were lysed by homogenisation using an EmulsiFlex-C2 (Avestin) at 15,000 kPa, and the cell debris pelleted by centrifugation at 20,000 rpm for 10 min. The pellet was discarded and an appropriate binding resin was added to the cleared lysate.

For 6xHis-tagged proteins the lysis buffer contained 50 mM sodium dihydrogen phosphate, 300 mM sodium chloride, 10 mM imidazole, 1 mM PMSF and protease inhibitor cocktail (Roche) at pH 8.0. For 1 L of bacterial culture, 400 µL HisSelect nickel affinity gel (Sigma Aldrich) was used; this was centrifuged at 14,000 rpm for 30 sec, the storage buffer removed and the resin resuspended in 400 µL His lysis buffer. The centrifugation was repeated, the supernatant was discarded and the pellet resuspended again in 400 µL His lysis buffer; this washed resin was added directly to the 50 ml

cleared lysate, and incubated at 4 ^{o}C for 1-2 h with rotation. The bound resin was washed using 2 column volumes of a His wash buffer (50 mM sodium dihydrogen phosphate, 300 mM sodium chloride and 20 mM imidazole at pH 8.0), and the protein was eluted in a total volume of 2.5 ml His elution buffer, added in 0.5 ml aliquots, containing 50 mM sodium dihydrogen phosphate, 300 mM sodium chloride and 500 mM imidazole, also at pH 8.0.

For GST-tagged proteins, Super-Glu glutathione fast flow resin (Generon) was used, with 800 µL resin slurry, washed in the same way as the HisSelect resin, but using GST wash buffer (50 mM Tris base and 150 mM sodium chloride at pH 7.4). The resin was added to 50 ml cleared lysate, and incubated at room temperature for 1-2 h with rotation. The GST lysis buffer contained 50 mM Tris base, 150 mM sodium chloride, 5 mM DTT, 1 mM PMSF and protease inhibitors at pH 7.4. The bound resin was washed using 2 column volumes of GST wash buffer and the protein was eluted by capping the column and adding 0.5 ml elution buffer (50 mM Tris and 10 mM reduced glutathione at pH 8.0) incubating for 5 min at room temperature then allowing the eluant to drip through, and repeating 5 times to give a total volume of 2.5 ml. For Nedd4, adding 1% Triton X-100 (Sigma Aldrich) to the GST lysis buffer and increasing the DTT concentration to 5 mM improved stability and yield.

2.2.3 Buffer exchange and FPLC

Purified proteins were desalted using PD10 columns (GE Healthcare), by equilibrating with 25 ml storage buffer containing 50 mM Tris pH 8.0 with 10% glycerol, adding 2.5 ml of protein solution and eluting with 3.5 ml storage buffer. If necessary, the resulting protein solution was concentrated using Generon Vivaspin concentrating spin columns with an appropriate molecular weight cut off (100 kDa for

Nedd4 [~120kDa], 30 kDa for PMEPA1 [~36kDa]). ÄKTA FPLC (detector model UPC-900, pump model P-920) was used with a Superdex 200 10/300 GL column (GE Healthcare). The column was equilibrated using a buffer containing 20 mM phosphate pH 7.4 and 10% v/v glycerol. The sample was run at a flow rate of 0.5 ml/min, and eluted into 0.5 ml fractions. 20 µL of each fraction containing protein was run out on an SDS-PAGE gel and stained with Coomassie to confirm the size (see 2.3.1); fractions containing the correct protein were combined into a single sample and concentrated again if necessary.

2.3 Protein analysis

2.3.1 Protein separation and visualisation

2.3.1.1 Polyacrylamide gel electrophoresis (PAGE)

For most applications, we used denaturing SDS-PAGE for separation of proteins based on the Laemmli method (Laemmli, 1970). This involved the use of the OmniPAGE mini vertical electrophoresis system (Cleaver Scientific) to pour and run 10x10cm gels. A solution of 40% acrylamide:bisacrylamide 37.5:1 (Melford) was diluted to the appropriate percentage based on the size of the protein to be resolved. The acrylamide was mixed with 5 ml buffer containing 0.75 M Tris base and 7 mM SDS at pH 8.8, 100 µL 10% w/v AMPS (Sigma Aldrich) in distilled water and 5 µL undiluted TEMED (Melford), with the volume made up to 10 ml with distilled water. This mixture was pipetted between 2 glass plates and allowed to polymerise at room temperature for 10-30 minutes. A 5 % acrylamide stacking gel was mixed by adding 625 µL 40 % acrylamide:bisacrylamide 37.5:1 to 2.5 ml buffer containing 0.25 M Tris base and 7 mM

SDS at pH 6.8, along with 50 µL 10 % w/v AMPS and 5 µL undiluted TEMED, with the volume made up to 5 ml with distilled water. This stacker was pipetted on top of the resolving gel around a plastic comb to form 8-12 wells and allowed to polymerise at room temperature for 10 min.

Once the gel was prepared, the samples were added to an equal volume of SDS sample buffer, and heated at 95 ^{o}C for 10 min in a hot block. The electrophoresis tank was filled with running buffer containing 25 mM Tris base, 200 mM glycine and 3.5 mM SDS, and 20-50 µL of the samples were loaded. A marker containing pre-stained proteins of known sizes from 10-230 kDa (New England Biolabs) was loaded alongside the samples for reference. The gel was run at a constant voltage (180-220 V) for approximately 1 h, until the dye front ran almost to the bottom of the gel.

For native PAGE, the resolving gel consisted of an appropriate volume of acrylamide:bisacrylamide 37.5:1 in a final concentration of 0.375 M Tris-HCl pH 8.8, 0.05 % w/v AMPS and 0.05 % v/v TEMED, with the volume made up to 10 ml with distilled water. The stacking gel consisted of 3 % acrylamide:bisacrylamide 37.5:1 in 0.125 M Tris-HCl pH 6.8 with 0.1 % w/v AMPS and 0.1 % v/v TEMED, and the volume made up to 4 ml with distilled water. The gel was poured and the wells formed in the way described above, but the sample was added to an equal volume of sample buffer containing 100 mM Tris pH 6.8, 20 % v/v glycerol, 5 % v/v β-mercaptoethanol and 0.05 % bromophenol blue, and was heated at 37 ^{o}C for 30 min. The samples were loaded in the same way as a denaturing gel, with the same marker, but the running buffer used consisted only of 25 mM Tris base and 200 mM glycine, and the gel was run at a much lower voltage (100 V) for longer, up to 2 h, to avoid overheating.

2.3.1.2 Coomassie Brilliant Blue staining

Gels were stained using a solution of 25 % v/v isopropanol, 10 % v/v glacial acetic acid, and 0.05 % Coomassie Brilliant Blue R-250, according to Meyer & Lambert (1965), for about 30 min with gentle shaking, then the nonspecific polyacrylamide staining was removed by gentle shaking in 30 % methanol and 10 % glacial acetic acid for 1-12 h, adding fresh destaining solution 2-3 times.

2.3.2 Western blotting

Proteins were transferred from a polyacrylamide gel using a 200x200 mm semi-dry blotting system (Jencons) onto a 7.5x8 cm piece of low background fluorescence Immobilon PVDF membrane (Millipore), which was soaked in methanol to activate it and then washed for 5 min in transfer buffer (50 mM Tris base, 380 mM glycine, 20 % v/v methanol, 0.1 % w/v SDS) before being stacked in a 'sandwich' with the gel on top (i.e. closer to the cathode) and three 8x8 cm pieces of 0.8 mm blotting paper (Whatman) soaked in transfer buffer on top and underneath to stop the membrane drying out. The blotting apparatus was secured and the transfer was run at a constant current of 400 mA for 1-2 h, depending on the size of the protein of interest.

Once the transfer was complete the membrane was blocked using a solution of 5 % w/v skimmed milk powder in TBS for one hour at room temperature with gentle shaking, then the membrane was transferred to a 1.5 % w/v solution of milk in TBS containing the primary antibody at an appropriate concentration, and incubated overnight at 4 ^{o}C with gentle shaking (a complete list of all primary antibodies used during this project is shown in figure 2.4). After washing 3 times for 1 min with TBS, the membrane was then incubated with gentle shaking in a 1.5% w/v solution of milk in TBS containing an

Epitope recognition sequence	Clonality	Supplier	Working dilution
α S-tag (KETAAAKFERQHMDS)	Monoclonal	Novagen	1:5000
α GST	Polyclonal	Sigma Aldrich	1:1000
α Nedd4 (WW2 domain)	Polyclonal	Abcam	1:2000
α GFP	Monoclonal	Roche	1:2000
α AR (441)	Monoclonal	Santa Cruz	1:200
α Actin	Polyclonal	UCL	1:3000
α Tubulin	Polyclonal	Abcam	1:1000
α GAPDH	Monoclonal	UCL	1:5000
α HA	Monoclonal	Thermo Scientific	1:5000
α FLAG clone M2	Monoclonal	Sigma Aldrich	1:1000
α Myc clone 9E10	Monoclonal	Sigma Aldrich	1:5000
α CBP clone C167	Monoclonal	Millipore	1:5000

Figure 2.4. Epitope recognition sites, clonality, suppliers and working concentrations of all primary antibodies used for detection of proteins via Western blotting. Where supplier is given as 'UCL', these antibodies were provided by Sergei Novoselov at University College, London.

appropriate concentration of secondary antibody for 60 min at room temperature. Finally, the membrane was washed for at least 30 min in TBS, with 5 changes of buffer. The washed blot could then be analysed by one of the two methods described below.

2.3.3 Odyssey detection

For detection of most immunoblotted proteins, we used the Licor Odyssey infrared scanning system. A combination of goat anti-rabbit IRDye 680LT (Licor), goat anti-mouse IRDye 680LT (Licor) and CF680 goat anti-mouse (Biotium) was used to image in the 700nm (red) channel, and goat anti-rabbit IRDye 800CW (Licor), goat anti-mouse IRDye 800CW (Licor) and CF770 goat anti-mouse (Biotium) to image in the 800nm (green) channel. The Licor 680LT dyes were used at a 1:20000 dilution, while the Licor 800CW dyes were used at a 1:3000 dilution and the Biotium CF dyes were used at a 1:30000 dilution. The Licor software accompanying the Odyssey scanner was used to image the blots at 89 µm resolution and obtain relative quantification data by using the integrated intensity calculation function. Adobe Photoshop C4 was used for limited image manipulation such as brightness adjustments.

2.3.4 Enhanced chemiluminescence (ECL) detection

After incubation with an appropriate primary antibody, the blot to be imaged was incubated in an HRP-conjugated secondary antibody raised in goat, either anti-mouse or anti-rabbit (Sigma Aldrich), at a concentration of 1:10000 in a 1.25% w/v solution of skimmed milk in TBS for 1 h. Alternatively, proteins fused to the TAP tag were detected using a single step by incubating in peroxidase-anti-peroxidase (Sigma Aldrich) at 1:10000. After being thoroughly washed in TBS, the blot was incubated in a 1:1 mixture

of each of the 2 components of the Immobilon Western HRP substrate (Millipore) for 5 min, then the excess was drained and the blot placed into a cassette and held in place with clear plastic wrap.

To image the blot, a piece of 13x18 cm X-ray film (Kodak) was placed over the plastic wrap in a dark room, and the cassette was closed and locked to prevent external light from entering. After a suitable exposure period, varying from 30 sec to 1 h depending on the level of signal, the film was removed and immersed in photographic developer and fixer (Champion Photochemistry).

2.4 Mammalian cell culture and transfections

2.4.1 Cell culture

2.4.1.1 Maintenance and passage

HeLa cervical cancer cells, as described by Scherer et al (1953) were maintained in modified Eagle media with Earle's salts (PAA Laboratories) containing 2 mM glutamine, 1 % v/v penicillin-streptomycin and 10 % v/v foetal bovine serum (FBS, PAA). LNCaP prostate cancer cells, as described by Horoszewicz et al (1983), (provided by Yong-Jie Lu, Barts & the London, School of Medicine & Dentistry) were maintained in the same media with the addition of 1 % v/v supplementary non-essential amino acids (PAA) containing 890 mg/L alanine, 1500 mg/L asparagine, 1330 mg/L aspartic acid, 1470 mg/L glutamic acid, 750 mg/L glycine, 1150 mg/L proline and 1050 mg/L serine. Both cell lines were maintained at 37 ^{o}C and a 5 % CO_2 atmosphere, in 25 cm^2 and 75 cm^2 flasks with plasma treated surfaces to optimise adherence and caps containing a 22 µM

filter to allow gas exchange (PAA). Sterile conditions were maintained by working in a Jencons Microflow biological safety cabinet.

Cells were grown to 80-90 % confluency then, to subculture, the media was removed and the cells washed with Dulbecco's PBS (PAA). A sterile solution of 0.05 % trypsin and 0.02 % EDTA (PAA) was added to the adhered cells and the flask was incubated at 37 ^{o}C for 5 min to allow the cells to detach from the plasticware. An equal volume of media with 10 % FBS (containing protease inhibitors) was then added to deactivate the trypsin and a fraction of the trypsinised cells were added to fresh media in a new flask. The time between passages depended on the rate of growth of the cells, for example HeLa cells divided more quickly and adhered better than LNCaP cells, and how densely the cells were seeded into the culture vessel, but was usually 3-4 days.

2.4.1.2 Freezing & thawing cell cultures

Cells with low passage numbers were routinely frozen to maintain a stock of healthy cell lines. The cells were trypsinised as described above, and then pelleted by centrifugation at 1000 rpm for 5 min at 4 ^{o}C. The pellet was resuspended in complete medium containing 10 % v/v DMSO and aliquoted into 1 ml volumes in 2 ml, internal-thread cryogenic vials. The aliquots were frozen slowly, at a rate of 1 ^{o}C/minute, to -80 ^{o}C using a Mr. Frosty freezing container (Nalgene), then transferred to liquid nitrogen for long term storage. To reanimate the cells, an aliquot was first warmed quickly to 37 ^{o}C, then added to a fresh flask containing a large volume (10-20 ml) complete media.

To maximise the number of healthy cells, particularly of the LNCaP line, surviving this practice, plasticware was pre-coated with an autoclaved 0.1 % w/v solution of porcine gelatine (Sigma Aldrich) in distilled water and incubated at 37 ^{o}C for 60 min.

The gelatine was then aspirated and fresh medium added to the flask before the defrosted cells were added as described above.

2.4.2 Transfection of mammalian cells

2.4.2.1 FuGene

For the majority of this project, FuGene HD (Promega), a multi-component lipid-based reagent, was used for mammalian cell transfection. The cells to be transfected were seeded into a 10 cm^2 dish and grown to 80 % confluency in complete media, then washed with Dulbecco's PBS. 1 ml serum-free growth medium, containing glutamine, pen/strep and amino acids as described previously but no FBS, was added to the cells, then 6 µL FuGene HD reagent and 2 µg DNA was added and mixed by gentle rocking. The mixture was incubated at 37 ^oC for 4 h, then aspirated off and 2 ml complete medium added to the cells. The dish was returned to the incubator and allowed to express the protein of interest for 24-72 h; the optimal time of incubation was determined by the expression construct and the cell line, with LNCaP cells requiring longer incubation times than HeLa. An apparent transfection efficiency of 40-80 % was observed in both cell lines using FuGene HD. This was calculated by counting the number of cells exhibiting fluorescence in the spectral range expected from the transfected gene of interest in a sample of transfected cells compared to a control sample of untransfected cells of the same line.

2.4.2.2 JetPRIME

JetPRIME (PolyPlus), a cationic polymer-based reagent, was used alongside FuGene HD. The cells were grown to 80 % confluency in a 10 cm^2 in complete media and washed with PBS as for the FuGene protocol, but instead of using serum-free media, 2 ml of complete growth media was added to the cells. 2 µg DNA and 4 µL JetPRIME reagent were added to 200 µL JetPRIME buffer, mixed and incubated at room temperature for 10 min. The mixture was added drop-wise to the cells and incubated for 4-16 h at 37 ^oC, and the media was aspirated and replaced with 2 ml fresh complete media. The dish was then incubated at 37 ^oC for 24-72 h, once again with the time between transfection and harvesting being dependent on the cell line and protein being expressed. An apparent transfection efficiency of 70-90 % was observed in both cell lines using JetPRIME. This was calculated by counting the number of cells exhibiting fluorescence in the spectral range expected from the transfected gene of interest in a sample of transfected cells compared to a control sample of untransfected cells of the same line.

2.4.2.3 Calcium chloride

For applications such as pull-downs, a transfection protocol based on a technique first described by Graham & van der Eb (1973) and refined by Wigler et al (1977) and Lewis et al (1980) using calcium chloride and HEPES, was used

Cells to be transfected were trypsinised and seeded into a 35 mm dish, then transfected after 4 h. A transfection mixture was prepared containing 400 µL HEPES-buffered saline (20 mM HEPES, 140 mM sodium chloride, 5 mM D-glucose, 50 mM potassium chloride and 0.1 mM disodium hydrogen phosphate heptahydrate, pH 7.1), 8

µg plasmid DNA and 16 µL 2.5 M calcium chloride, incubated at room temperature for 25 min, then added drop-wise to the cells in complete growth media. The dish was incubated at 37 ^{o}C overnight, then the media aspirated, the cells washed twice with PBS, and fresh complete media added. The protein of interest was harvested after a further 12-24 h. A lower apparent transfection efficiency of approximately 20-40% was observed using this transfection method. This was calculated by counting the number of cells exhibiting fluorescence in the spectral range expected from the transfected gene of interest in a sample of transfected cells compared to a control sample of untransfected cells of the same line.

2.4.3 Harvesting mammalian cells for Western blotting

Two methods were used for harvesting total cell lysates from mammalian cells; TCA precipitation as described by Schwert (1973) and detergent lysis method as described by described by Li et al (2008).

2.4.3.1 TCA precipitation

The cells were grown in 6-well plate wells and, at a suitable time following transfection, the media was aspirated and the cells were washed with PBS. 1 ml of lysis buffer (0.2 M NaOH with 0.2 % β-mercaptoethanol) was added to the cells and the plate was incubated on ice for 30 min, then a pipette tip was used to manually scrape any remaining cells off the bottom of the well. 160 µL 30 % w/v TCA in distilled water was added to the supernatant, then the mixture was incubated on ice for 10 min, and the precipitated proteins were pelleted by centrifugation at 14,000 rpm for 10 min. The

resulting pellet of protein was resuspended in 20 µL Tris base before 80 µL SDS sample buffer was added and the sample was run on SDS-PAGE as described previously.

2.4.3.2 Detergent lysis

The cells were transfected & grown as described, then the media was aspirated and the cells washed with PBS. 100 µL lysis buffer containing 50 mM Tris-HCl pH 8, 1 mM EDTA, 1 % v/v Triton X-100, 150 mM sodium chloride and 10 % v/v glycerol, with 0.1 % v/v protease inhibitor cocktail in DMSO (Sigma Aldrich), was added to the cells and the plate was incubated on ice for 30 min. Cell debris and insoluble cell fractions were pelleted by centrifugation at 14,000 rpm for 5 min, then the pellet was discarded and 100 µL SDS sample buffer was added to the supernatant. These samples were then run on SDS-PAGE as described, except that they were heated at 37 ^{o}C, instead of 95 ^{o}C, for 20-30 min in a heat block.

2.5 Immunoprecipitation

2.5.1 IgG sepharose

Cells were transfected and grown as described previously in 6-well plate wells; usually 3-5 wells of transfected cells, in addition to an equal number of untransfected cells as a control. 2.5 mM NEM was added to the growth medium and incubated at room temperature for 30 min, then the media was aspirated and the cells washed twice with 4mM NEM in PBS (NEM-PBS). The cells were trypsinised as described previously, but without the addition of media to inactivate the trypsin. Instead, the detached cells were placed into a Falcon tube and the cells washed with an equal volume of NEM-PBS, then

this was aspirated and added to the same tube. The cells were pelleted by centrifugation at 1,000 rpm for 5 min at 4 ^{o}C, then washed with NEM-PBS and spun again. 1 ml IP buffer (50 mM Tris-HCl pH 8, 250 mM sodium chloride, 2 % v/v Triton X-100, 20 % v/v glycerol, 3 mM magnesium chloride and 0.1 % protease inhibitor cocktail in DMSO [Sigma Aldrich]) was added to the pellet and incubated on ice for 10 minutes, then the pellet was resuspended and sonicated at 20 % amplitude for 30 sec (10 sec on, 30 sec). Cell debris was pelleted at 14,000 rpm for 1 min, then the pellet was discarded and 50 µL supernatant placed aside, with 50 µL SDS sample buffer added, as the "Input" i.e. pre-pulldown sample.

0.5 ml of IgG Sepharose 6 Fast Flow (GE Healthcare) resin was washed by centrifuging at 1000 rpm for 1 min, removing the supernatant, resuspending the pellet in 1 ml 100 mM glycine pH 3 and centrifuging again. The pellet was resuspended in 1 ml IP buffer, and centrifuged again. This was repeated with 1 more wash in glycine pH 3, then 2 more washes in IP buffer, before the washed pellet was resuspended in 800 µL IP buffer. 50 µL of this washed resin was added to the remaining lysate and incubated with rotation at 4 ^{o}C for 16 h. The bound resin was pelleted by centrifugation at 1000 rpm for 1 min and the supernatant was removed without disturbing the pellet. The bound resin was washed 5 times by resuspending in 1 ml IP buffer, resuspending, then pelleting at 1000 rpm for 1 min and removing the supernatant. After the last wash, 50 µL glycine pH 3 was added to elute the bound protein; the pellet was resuspended in the glycine solution and incubated for 2 min at room temperature, then the tube was centrifuged at 5000 rpm for 1 min, the supernatant was retained and the elution was repeated on the pellet 4 times, giving 200 µL total eluate volume.

A 10 µL aliquot of the eluate was set aside for analysis and 19 µL 20 % w/v sodium deoxycholate (Melford) was added to the remaining 190 µL of sample followed by 209

µL 30 % w/v TCA. This mixture was incubated on ice for 30 min then centrifuged for 15 min at 14,000 rpm. The supernatant was discarded and the pellet neutralised by the addition of 20 µL 1 M Tris base, followed by 30 µL SDS sample buffer to produce the final pull-down sample. Both the input and pull down samples were run on an appropriate percentage SDS-PAGE gel and a Western blot performed as described previously.

2.5.2 Protein A sepharose

Protein A coupled to sepharose resin (Amersham Biosciences) was used to bind an appropriate primary antibody to interact with a tagged protein expressed in mammalian systems.

The first part of the process is as described in 2.5.1; the cells were washed in PBS-NEM and trypsinised, then pelleted, washed and pelleted again. The pellet was resuspended in 1.05 ml A-IP buffer (20 mM Tris pH 7.5, 150 mM NaCl, 1 mM EDTA, 1 mM EGTA, 1 % sodium deoxycholate and 1 % Triton X-100) and incubated on ice for 10 min, then lysed by sonication and centrifuged to remove cell debris. 50 µL of the supernatant was set aside with 50 µL SDS sample buffer as the input sample, and the remaining 1 ml was split into two 500 µL aliquots (referred to here as A and B). Primary antibody was added into tube A only at an appropriate dilution, and both tubes were incubated at 4 ^{o}C with rotation for 16 h. The protein A resin was reconstituted in TBS at a concentration of 1 mg/ml and 50 µL was added to each tube A and B, then both tubes were incubated at 4 °C with rotation for a further 4-12 h.

The bound beads were pelleted by centrifugation at 1000 rpm for 1 min and the supernatant removed. 1 ml cold A-IP buffer was added to each tube and the pellets were resuspended then centrifuged again. This process was repeated for a total of 4 washes in

A-IP buffer, then the washed pellets were each resuspended in 50 µL 100 mM glycine at pH 3.0 and incubated for 2 min at room temperature. The tubes were centrifuged at 5000 rpm for 1 min and the supernatant transferred to clean tubes (also designated A & B here); this process was repeated 3 times to yield a total volume of 200 µL from each sample. 20 µL 20 % w/v sodium deoxycholate and 220 µL TCA was added to each tube and incubated on ice for 30 min. The tubes were centrifuged for 15 min at 14,000 rpm, the supernatant was discarded and the pellets were resuspended in 20 µL 1 M Tris base and 30 µL SDS sample buffer to give the eluted samples; tube B is a control, with only the protein A and no primary antibody present, while tube A is the experimental sample.

2.5.3 HisSelect resin

Transfected cells were incubated in media containing 4 mM NEM for 30 min then washed with PBS. One well of a 6-well plate was harvested using TCA precipitation as described in 2.4.5 and set aside as the input sample. Each of the pull-down samples consisted of 3 wells of a 6-well plate; the cells from all 3 wells were lysed by the addition of a total of 5 ml denaturing lysis buffer (DLB) containing 6 M guanidine hydrochloride (Melford), 100 mM monosodium phosphate, 10 mM Tris, 1 % v/v Triton X-100 and 4 mM NEM at pH 8.0. The lysate was centrifuged at 4,000 rpm for 15 min at 4 ^{o}C and 100 µL HisSelect resin (Sigma Aldrich), washed twice and resuspended in DLB, was added to the cleared lysate and incubated at room temperature with rotation for 2-4 h.

The bound resin was pelleted by centrifugation at 1,000 rpm for 1 min and the buffer removed. The pellet was washed in 1 ml DLB twice, then once in a 50:50 mixture of DLB and His wash buffer, then twice more in the wash buffer alone. After the final wash, the sample was centrifuged at 4,000 rpm and the supernatant removed. 100 µL

SDS sample buffer was added directly to the resin and heated at 95 ^{o}C for 10 min to elute the protein and form the pull-down sample.

2.6 Recombinant protein analyses

2.6.1 In vitro assays

2.6.1.1 Ubiquitination assays

The purified proteins to be assayed were first run out on a Western blot with Odyssey detection as described above, and the relative protein levels calculated using Odyssey intensity values. The loading volumes were equalised accordingly. Based on the relative loading volumes, an appropriate volume of each protein was then added to a mixture containing (final concentrations) 5 mM Tris pH 7.4, 0.01 M magnesium chloride, 0.01 M ATP, along with 100 ng recombinant human Uba1 (Boston Biochem), 100 ng recombinant yeast Ubc1 (cloned & produced in house) and 1 µg methylated human ubiquitin (Boston Biochem). 100-500 µg recombinant human Nedd4 or yeast Rsp5 was added to initiate the reaction and samples were incubated at 30 ^{o}C for 45 min. For autoubiquitination assays where the E3 enzyme is also the substrate, a negative control consisting of all the above with no ubiquitin was incubated and run alongside. For ubiquitination assays where the activity of the E3 on a substrate was being assessed, the negative control instead lacked the E3. The reaction was stopped by heating to 95 ^{o}C with an equal volume of SDS sample buffer and the samples were analysed by running on an appropriate percentage SDS-PAGE gel and Western blotting.

2.6.1.2 SUMOylation assays

As with the ubiquitination assays, the E3 proteins to be assayed were approximately equalised by running them out on an SDS-PAGE gel and performing a Western blot with Odyssey detection to assess the relative protein levels. An appropriate relative volume based on these results was used in the assays. The E3, acting as both ligase and substrate, was added to a reaction volume containing (final concentrations) 0.05 M Tris pH 7.4, 0.01 M magnesium chloride and 0.01 M ATP, along with 150 ng E1 conjugating complex (Uba2/Aos1, cloned & produced in house), 150 ng E2 activating enzyme Ubc9 (cloned and produced by Dr. Jim Sullivan) and 1 µg Smt3 (cloned and produced by Dr. Jim Sullivan). The reaction volume was made up to 30 µL with ddH_2O and the E3 added last to initiate the reaction. The mixture was incubated at 30 ^oC for 2 h then stopped by the addition of an equal volume of SDS sample buffer, then run on a 7.5 % SDS-PAGE gel alongside a negative control containing the reaction mixture with no SUMO present, followed by a Western blot as described previously.

2.6.2 Microscale thermophoresis

Recombinant proteins to be assayed were produced and run through FPLC as described previously. C-terminal GST-tagged full length Nedd4 was concentrated to 80 µM (using spin columns as described in section 2.2.3) and 16 serial dilutions were prepared, ranging from 80 µM to 2 nm. Each of the N-terminal 6xHis-tagged ΔNT PMEPA1 constructs used was either concentrated or diluted with a buffer containing 20mM phosphate as 10% v/v glycerol to 5-20 µM, then mixed with an equal volume of 30 µM NT-red dye (Nanotemper Technologies) and incubated on ice for half an hour. The labelled protein was then passed through a desalting column and eluted with 600 µL

phosphate buffer, and 10 µL was added to an equal volume of each Nedd4 dilution, resulting in a total 20 µL reaction volume. The mixture was allowed to incubate at room temperature for 10-15 minutes, and then each reaction was taken up into a glass capillary and loaded into a Monolith NT.115 (Nanotemper Technologies) for analysis by Dr. James Wilkinson of Nanotemper Technologies. By titrating Nedd4 and PMEPA1 solutions of known concentration, it is possible to estimate the binding affinity (K_D) by plotting the change in fluorescence of the labelled PMEPA1 (when exposed to the high temperature of the laser beam) against the concentration of Nedd4. This produces a sigmoid curve which can be fitted against the equilibrium solution given by the Law of Mass Action, given that the magnitude of the 'reaction' produced by the interaction of the two proteins, and the concentrations are already known and leaving the affinity constant K_D as the calculated unknown.

2.7 Cell imaging

2.7.1 Fixing and mounting

Cells were seeded into 6-well plate wells each containing a single, circular 16 mm diameter, 1 mm sterile coverslip (Scientific Laboratory Supplies), grown and transfected as described in section 2.4. After 24-48 h, growth media was removed and the cells were washed with PBS. The cells were fixed on the coverslip by immersion in 4 % w/v PFA (Sigma Aldrich) in PBS at pH 7.0 for 15 minutes, then washed three times in PBS. The fixed, washed cells on the coverslip were mounted on a microscope slide using 3 µL Fluoromount-G (Southern Biotechnology Associates) and sealed with nail varnish, then stored at 4 ^{o}C in a low light environment, if necessary, until imaging.

2.7.2 Immunostaining

Cells were fixed following transfection in 4 % PFA as described above, then washed three times in PBS containing 100 mM glycine (Melford) and permeabilized by immersion in PBS containing 0.1 % v/v Triton X-100 for 4 min. Nonspecific protein binding sites were blocked by immersion in PBS containing 1 % v/v FBS for 1 h at room temperature and the cells were incubated in an primary antibody diluted in the blocking buffer for 16 h at room temperature, or for 48 h at 4 ^{o}C.

The primary antibody was removed with three 5-min washes with PBS and the cells incubated in an appropriate dilution of Alexa Fluor (Life Technologies) secondary antibody, conjugated to either a green-fluorescent or red-fluorescent dye, in the blocking buffer for 1 hour at room temperature. The fixed cells were washed five times for 10 min, then mounted and sealed on microscope slides as described previously.

2.7.3 Confocal microscopy

We used confocal microscopy to directly visualise fluorescent-tagged proteins, cloned as described in 2.1, as well as untagged, endogenous proteins detected via immunofluorescence as described previously. For brevity, the notation ‘green channel’ is used to refer to both green-fluorescent-protein-tagged transfected proteins and to endogenous proteins detected using Alexa Fluor 488-congugated secondary antibodies. The notation ‘red channel’ is used to refer to both mCherry-tagged transfected proteins and to endogenous proteins detected using Alexa Fluor 594-conjugated secondary antibodies.

Confocal images were captured and processed using a Leica TCS SP5 type DMI6000 microscope with Leica LAS AF software. The pinhole was set to 95 µm diameter and the

objective used was a 63x oil immersion lens with Immersol microscopy immersion oil (Zeiss). Green channel fluorophores were excited, using an argon laser at 25% power, at 488 nm and emission was collected across the region 500-570 nm. Red channel fluorophores were excited at 633 nm using a HeNe laser and emission was collected across the region 660-750 nm. For fluorescence resonance electron transfer (FRET) analysis, green channel fluorophores were excited using an argon laser at 25% power, at 488 nm and emission was collected across the region 660-750 nm. Non-overlap of the green and red emission spectra was confirmed by calibrating the spectral range with single-channel images before gathering FRET data.

Captured images were taken in 2048x2048 pixel format at 200 Hz, and subjected to two line averages and two frame averages. These images were saved in .TIFF format and subsequently adjusted using Adobe Photoshop CS4 to convert to monochrome as necessary and ensure that images were directly comparable.

2.8 Statistical & *in silico* analysis

2.8.1 Relative ubiquitination

The ubiquitination assay results were quantified by assessing the relative intensity of the bands corresponding to the unmodified protein compared to those corresponding to the ubiquitinated products. The combined value of the modified and unmodified protein was taken to represent the total protein in that assay, and the value of the ubiquitinated products was calculated as a percentage of the total protein in each column to give values for percentage ubiquitination. For each PMEPA1 assay, these values were then adjusted so that the wild type construct was always given an arbitrary value of 1.0, and the degree of modification of the mutant constructs were represented as a proportion of that value.

These adjusted values were used to find the mean and standard deviation of the data. The statistical significance was calculated using a 2-tailed t-test, assuming unequal variance, on all repeats of the assays.

2.8.2 Localization of cellular proteins

The localisation of GFP-AR in HeLa and LNCaP cells was visualised using confocal microscopy and categorised as cytoplasmic, nuclear or a combination of the two. The number of cells showing each localisation distribution was counted in three treatments; expressing wild type AR with no hormonal treatment, expressing wild type AR following treatment for 24 h with 10 μM DHT, and expressing AR with the CaP mutation (T877A). Cell counts for each treatment were repeated a minimum of 5 times. To determine whether observed differences between treatments were statistically significant, several statistical analyses were carried out using the statistical computing programme R (Strubig et al, 2012). For each cell line (HeLa and LNCaP), an analysis of variance (ANOVA) was carried out on the variance of the experiments to see if any differences in cellular localisation between treatments were significant. An F-test compared the variance within treatments to variance between treatments and returned a calculated *F* value, which was compared to a table of critical values to determine whether the difference between treatments was significant ($P<0.05$). Tukey's post-hoc test was applied to the means of the cell numbers in each experiment to compare treatments pairwise, generating a *q* value which was compared to a table of critical values to determine whether differences are statistically significant ($P<0.05$).

2.8.3 In silico prediction of PMEPA1 localisations

Protein localisation was predicted using five online programs; the University of Queensland's PProwler (http://bioinf.scmb.uq.edu.au/pprowler_webapp_1-2/), National Chaio Tung University's CELLO (http://cello.life.nctu.edu.tw/), University of Tübingen's MultiLoc (http://abi.inf.uni-tuebingen.de/Services/MultiLoc/), Technical Univeristy of Denmark's TargetP (http://www.cbs.dtu.dk/services/TargetP/) and Japan's National Institute of Advanced Industrial Science & Technology's WoLF PSORT (http://wolfpsort.org/). Full length wild type PMEPA1, a truncated form with the N-terminal 23 amino acids absent (ΔNT) and a full length form with all three PY motifs mutated at the tyrosine residues (Y102A/Y126A/Y197A; ΔPY) were all run through the prediction software with and without a GFP tag at the C-terminus (full sequences available for reference in the appendices).

2.8.4 In silico production of 3D molecular images

3D images were produced using Polyview-3D (http://polyview.cchmc.org/polyview3d.html) with source information from entries included in the RCSB Protein Data Bank (http://www.rscb.org). Image orientation was set using the Jmol application for Windows (http://jmol.sourceforge.net/) and images were resized & made equivalent using Adobe Photoshop CS4.

3. RESULTS

3.1 Investigating the interaction between Nedd4 and PMEPA1 *in vitro*

3.1.1 Introduction

3.1.1.1 WW domains and PY motifs

The tryptophan-containing substrate recognition (WW) domains of Nedd4 and related proteins have long been reported as binding to proline-rich (PY) motifs (Staub et al, 1996). The recognition sequence required for WW-PY interaction varies from protein to protein and dictates how the WW domain is classified (Chong et al, 2006); in the case of the Nedd4 family of E3 ligases, the core consensus motif required for substrate recognition and binding is generally accepted as Pro-Pro-x-Tyr (PPxY, sometimes represented as xPPxY), where X can represent any amino acid (Staub et al, 1996). Occasionally variant motifs with the sequence LPxY (Bruce et al, 2008; Kanelis et al, 2006) have been reported, but the canonical PPxY consensus sequence remains the most frequently cited (Aragón et al, 2011; Kotorashvili et al, 2009; Lu et al, 2007).

The human prostatic androgen-induced protein PMEPA1 has been known and studied as a PY motif-mediated binding partner for Nedd4 for a decade (Xu et al, 2003). With respect to the interaction between Nedd4 and PMEPA1 two PY motifs were originally identified (Xu et al, 2003) and are accepted as the only WW-domain binding motifs present in PMEPA1 (Shi et al, 2010). Previous studies looking at the relationship between Nedd4 and PMEPA1 have assumed that eliminating the binding capacity of

these two motifs equates to a functional loss of interaction between the two proteins (Li et al, 2008).

3.1.1.2 The role of vPY motifs and multiple PY motifs

A variant PY (vPY) motif, with sequence APSY, has been reported in the yeast protein Bsd2p an adaptor for the yeast Nedd4 ligase Rsp5p (Sullivan et al, 2007). This vPY motif was shown to be absolutely required for Bsd2p to function as an adaptor *in vivo* and when absent, Rsp5p was unable to ubiquitinate and thereby regulate the manganese transporter Smf1p. It was postulated that, given the observation that between the adaptors Tre1p and Bsd2, there are 3 PY motifs required for Smf1p modification, but only 2 of the 3 WW domains on Rsp5p are involved, there is a sequential binding event occurring. The vPY motif may bind transiently to Rsp5p to ensure correct orientation of the ligase with respect to the adaptor, therefore enhancing the ubiquitination of the substrate. The *Drosophila* protein *Commissureless* has a similar binding site LPSY that specifically binds a different WW domain to the stronger PPxY sequence (Kanelis et al, 2006), adding further weight to the theory that the vPY motifs are conserved in order to preserve an orientation function.

3.1.1.3 Additional factors that may affect the Nedd4/PMEPA1 interaction

3.1.1.3.1 Phosphorylation

Phosphorylation is being increasingly implicated in regulation of Nedd4-family dependant ubiquitination; the ability of the family member Itch to bind to the PY motif-containing substrate p63 was shown to be affected by the absence of a conserved threonine/serine residue just downstream from the PY motif (Bellomaria et al, 2010),

suggesting a phosphorylation event at that position. In addition, phosphorylation by protein kinases can act to regulate the activity of some Nedd4-family adaptors; a proline-rich region of Itch is phosphorylated on a specific serine and threonine residues by the MAPK family kinase JNK1, activating it and greatly enhancing its activity (Gallagher et al, 2006). The ability of specific residues of PMEPA1 to be phosphorylated must therefore be considered, as this may impact the ability of Nedd4 to interact with some or all of the PY motifs present.

3.1.1.3.2 SUMOylation

SUMO consensus motifs have the consensus sequence ΨKxD/E, where Ψ represents a large, hydrophobic amino acid and x can be any residue (Rodriguez et al, 2001). A variant SUMO interacting motif with sequence Ψ(I)x(S)KE was identified in the HECT domain of Nedd4, and preliminary investigations seemed to show that, when the lysine in this variant motif was mutated, a reduction in modification of Nedd4 mediated by the SUMO E2 protein Ubc9 was observed, indicating that this variant motif might play a role in SUMOylation of Nedd4 (Sullivan, personal communication).

SUMOylation can alter ubiquitin ligase activity both up and down depending on the particular ligase involved; when the RING-type E3 BRCA1 is SUMOylated by the PIAS family of SUMO E3 enzymes, it results in an increase in the ubiquitination activity of BRCA1 (Morris et al, 2009). However, in contrast it has been shown that SUMOylation of the yeast Nedd4-family protein Rsp5p, by the PIAS homologues Siz1p and Siz2p, reduces Rsp5p activity (Novoselova et al, 2013).

3.1.2 Results

3.1.2.1 PMEPA1 mutagenesis

3.1.2.1.1 Identification and confirmation of a variant PY motif 'PY1'

Through a process of analysis of the human proteome, searching specifically for proteins containing at least one canonical (PPxY) motif in addition to a motif with sequence xPxY (where the first residue was not proline), PMEPA1 was identified as containing a third putative PY motif, QPTY, upstream from the two canonical motifs (Cotton & Sullivan, personal communication). This PY motif has not been previously identified or studied due to its variant nature, and so presented an ideal model for investigating the binding of WW domains to PY motifs, particularly with regards to the environment surrounding the interaction site, as well as the potential role of multiple PY motifs. The vPY motif was designated PY1 due to its location at the N-terminus of the protein, and the two canonical motifs $PPPY_{126}$ and $PPTY_{197}$ were designated PY2 and PY3 respectively.

To investigate whether the newly identified vPY motif in PMEPA1 was necessary for ubiquitination of PMEPA1 by Nedd4 *in vitro*, ubiquitination assays were performed. Given the difficulties of working with recombinant integral membrane proteins, an N-terminally truncated form of PMEPA1 was expressed and purified in *E. coli* containing only the soluble cytoplasmic domain. Mutated versions of this protein were produced in which the putative vPY and the 2 previously identified PY motifs were functionally eliminated by mutating the tyrosine at the fourth position in the motif (Y102, Y126 and Y197) to alanine, which is known to prevent the site from being able to interact with WW domains (Goulet et al, 1998). Recombinant PMEPA1 and versions lacking each of

the three PY motifs alone, in double and triple combinations, were prepared and the ability of these proteins to be ubiquitinated by recombinant Nedd4 was assessed *in vitro*. Figure 3.1.1 shows a workflow diagram of the process behind each experiment

3.1.2.1.2 Initial investigation of PY1 vs. PY2 and PY3

The initial mutagenesis, the results of which are shown in figure 3.1.2, indicated that the loss of the canonical PY motifs PY2 or PY3, results in a reduction in Nedd4-dependent ubiquitination of 55.2% and 43.9% respectively, as compared to the wild-type protein. Similarly, the loss of PY1 results in a reduction in ubiquitination of 26.9%, which is much less than either of the canonical motifs, but still a statistically significant ($P = 0.014$) deviation from the wild type. In addition, although there was no significant difference between the PY3 mutant (Y197A) when PY1 was functionally removed or left intact ($P = 0.230$), leaving PY1 intact actually decreases the ubiquitination of the PY2 mutant (Y126A) by 19 % compared to the double mutant where both are functionally removed (Y102A/Y126A, $P = 0.090$). However, there was no significant difference in the amount of ubiquitination between the triple mutant (with all three PY motifs functionally removed), and the mutant with only PY1 motif present (Y126A/Y197A) ($P = 0.104$), indicating that the vPY motif alone is not sufficient to facilitate ubiquitination of PMEPA1 by Nedd4 in the absence of the two canonical sites. In summary, while the newly identified vPY motif contributes significantly to the efficiency of Nedd4-mediated ubiquitination of PMEPA1 *in vitro,* this motif alone cannot enable a significant degree of ubiquitination to occur, in contrast to either of the two previously identified canonical motifs.

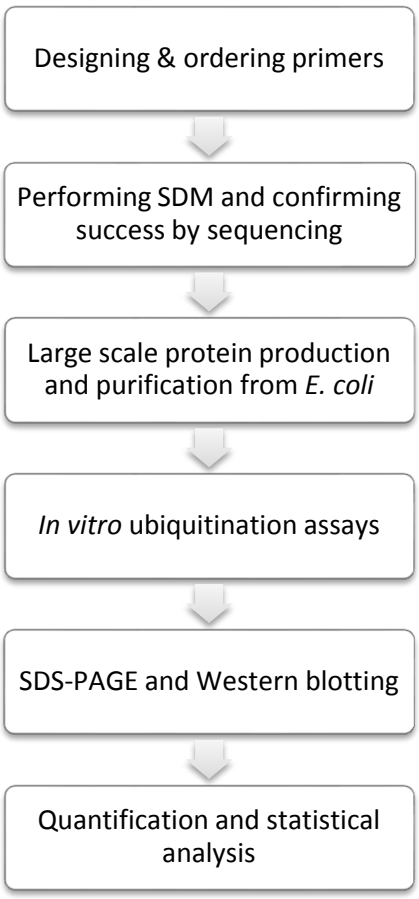

Figure 3.1.1. Workflow schematic to show the process behind each ubiquitination assay blot and histogram. Each protein used was individually cloned via site-directed mutagenesis, produced in *E. coli* using 2-3 L of culture per protein, and purified using HisSelect resin. The resulting recombinant protein was used in ubiquitination assays and analysed using SDS-PAGE and Western blotting using Odyssey detection. The relative extent of ubiquitination was assessed using the Odyssey software and a student's t-test was carried out to assess significance, where applicable. All methods are explained fully in section 2.

3.1.2.1.3 Altering the variant residues in PY1

The differences in the ability of the motifs to mediate ubiquitination by Nedd4 must be dependent on the two residues that are variable in the newly identified PY1 motif of PMEPA1, i.e. first and third (Q99, T101). In order to investigate this, an initial mutagenesis trial was performed. Each iteration was only a single mutation, with the whole designed to see if these small alterations had any impact on subsequent ubiquitination of PMEPA1. Each single mutation, as well as those described later on, were carried out in a construct of PMEPA1 lacking a functional PY2 motif (Y126A) as initial experimental data produced by a previous member of the group initially indicated that any effect on PY1 would be more pronounced in absence of PY2. While the data presented in figure 3.1.2 shows that this is not in fact the case, these constructs had already been made, and experimental work begun, when this was realised.

Figure 3.1.3 shows the results of the *in vitro* ubiquitination assays from this round of mutagenesis. Interestingly, none of the mutations had a significant effect on PMEPA1 ubiquitination, with the exception of the T102S mutant, which showed an increase in ubiquitination of 14.3 % ($P = 0.017$). However it should be noted that the presence of a phosphomimic (Androutsellis-Theotokis et al, 2006), glutamic acid, at this position did not increase ubiquitination. It can also be seen in figure 3.1.3 that in the case of the T101S mutant, both the modified and unmodified protein signal shows a double band characteristic, possibly indicating a post-translational modification event occurring in *E. coli* independent of ubiquitination.

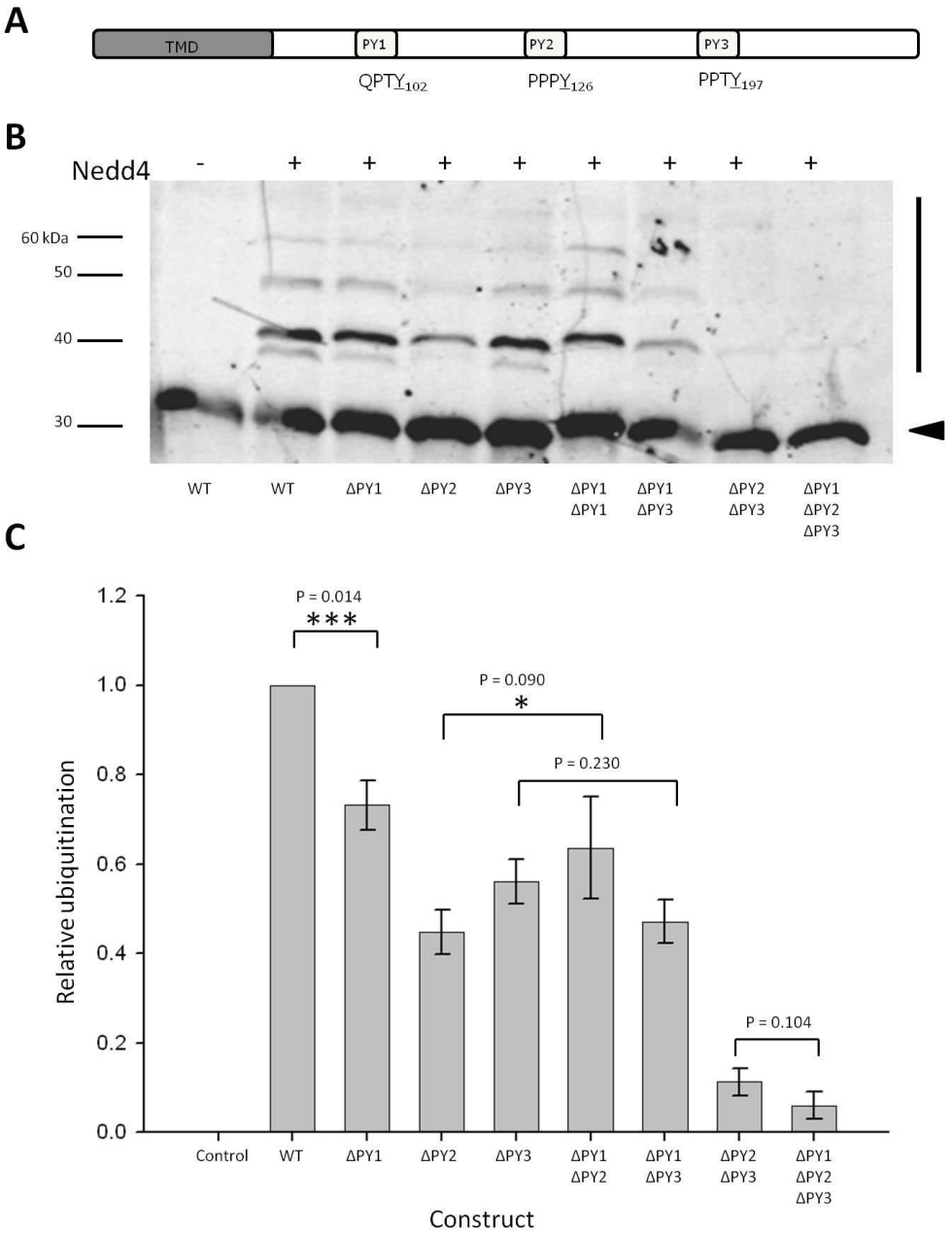

Figure. 3.1.2. Schematic showing the position of the residues motifs being modified within the broad structure of PMEPA1 (**A**). The designated nomenclature, with the vPY motif being labelled PY1, is shown alongside the residue number for clarity. Representative western blot, showing the results of an *in vitro* ubiquitination assay on soluble PMEPA1 constructs lacking the transmembrane domain but with an N-terminal S-tag, with the tyrosine residues in each PY motif mutated to alanine singly and in combination (**B**). Recombinant PMEPA1 was detected using α S-tag primary antibody followed by IR-labelled α mouse secondary antibody and imaged using the Odyssey IR laser scanning system. The relative ubiquitination was calculated by measuring the proportion of unmodified protein (indicated by the arrow) vs. modified protein (indicated by the vertical line). Combined data from 5 replicates with the data normalised to that of the wild-type (WT) sample given an arbitrary value of 1.0 (**C**). Error bars indicate one standard deviation. A 2-tailed students' t-test was carried out to determine the statistical significance of major pairs of data sets as indicated by the horizontal lines. P values indicate the probability that the resulting difference is due to chance, with relative significance of the differences between means indicated by zero ($P>0.1$), one ($0.1>P>0.05$), two ($0.05>P>0.025$) or three ($P<0.025$) asterisks.

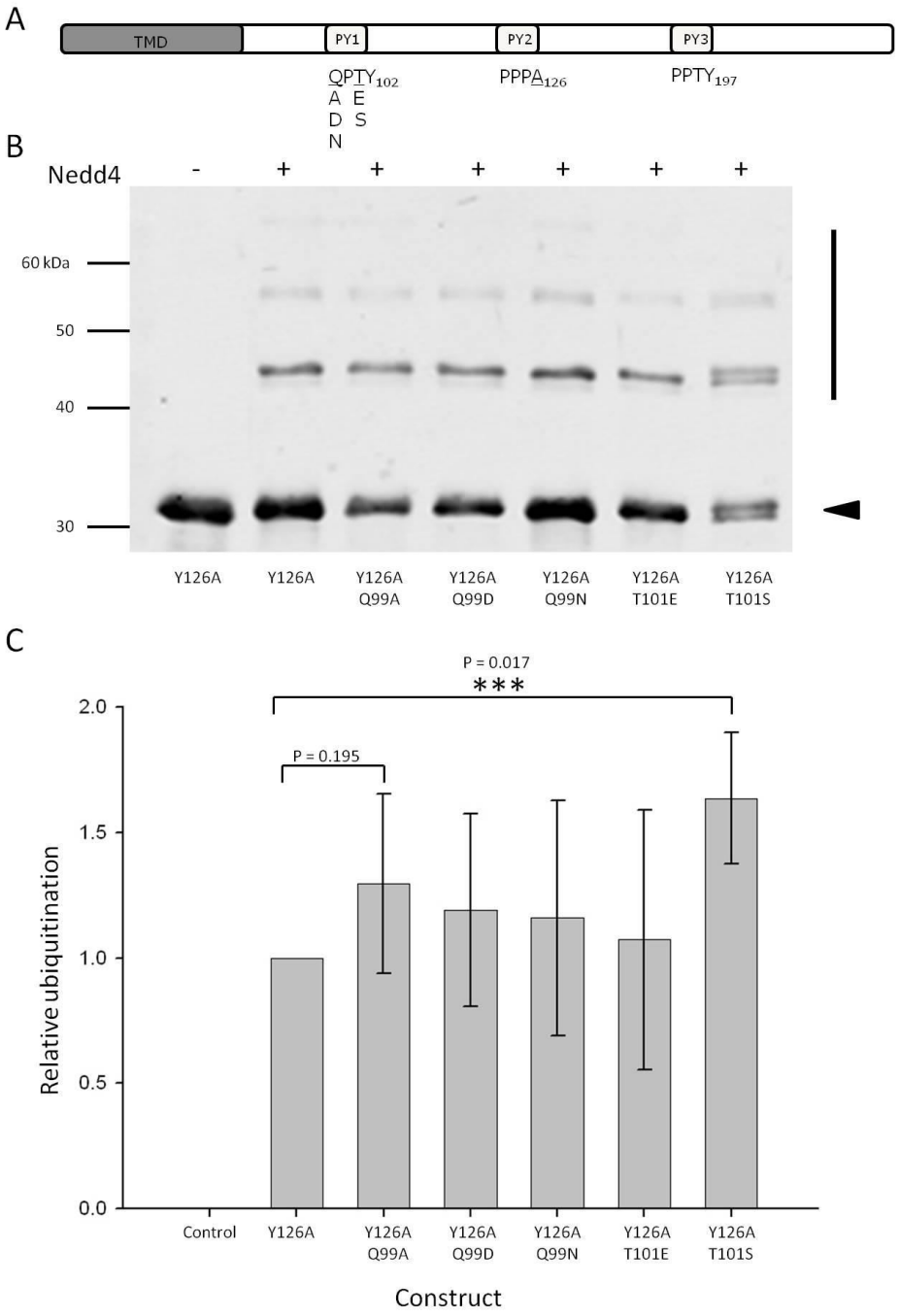

Figure 3.1.3. Schematic showing the broad structure of Y126A PMEPA1 and the mutations made within PY1 (**A**). Representative western blot, showing the results of an *in vitro* ubiquitination assay on soluble S-tagged PMEPA1 constructs, with first and third residues of the vPY motif mutated as indicated in a Y126A construct. (**B**) PMEPA1 was detected using α S-tag primary followed by IR-labelled α mouse secondary antibody and imaged using the Odyssey IR laser scanning system. The relative modification by Nedd4 was calculated by the proportion of unmodified (indicated by the arrow) vs. modified (indicated by the vertical line) protein and shown in the histogram (**C**) as normalised to show Y126A as 1.0. Data are based on four replicates of the experiment, with error bars showing one standard deviation. A 2-tailed students' t-test was carried out to determine the statistical significance of major pairs of data sets as indicated by the horizontal lines. The P values indicate the probability that the resulting difference is due to chance, with relative significance of the differences between the means indicated by zero (P>0.1), or three (P<0.025) asterisks.

3.1.2.1.4 Altering the residues immediately flanking PY1

As well as the core four residues, PY motifs are sometimes reported as extending further e.g. PPPxY (Furuhashi et al, 2005); although this feature is not considered canonical it is commonly found in PY motifs (including the flanking region of PY3 in PMEPA) and it is possible that the nature of the residues flanking the core motif might be important for function. To address the importance of the phenylalanine and proline residues flanking PY1 these residues were altered to an alanine (F98A, P103A), as well as to a glutamic acid (F98E, P103E), in a construct lacking a functional PY2 motif. In addition, T101 was also mutated to proline (T101P) in order to assess the effect, if any, of specifically having a proline in this position as in the canonical motif PY3.
Figure 3.1.4 shows that although altering F98 to a glutamic acid had no significant impact on the level of modification, altering this residue to an alanine resulted in a 53% drop in ubiquitination (P=0.005). The mutation P103A resulted in a significant reduction in ubiquitination of 45% (P=0.035), while the effect of P103E was a less pronounced reduction of 38% (P=0.015. Interestingly, the double mutant P103E/F98E had no significant effect on the ubiquitination of the protein, which may suggest that any structural characteristic that is disrupted by the mutation of one of these residues is compensated for by the mutation of the other, possibly by facilitating access to the PY motif which was previously blocked. In addition, the T101P mutation that alters PY1 to a canonical PY motif did not have any significant impact on the level of ubiquitination (figure 3.1.4).

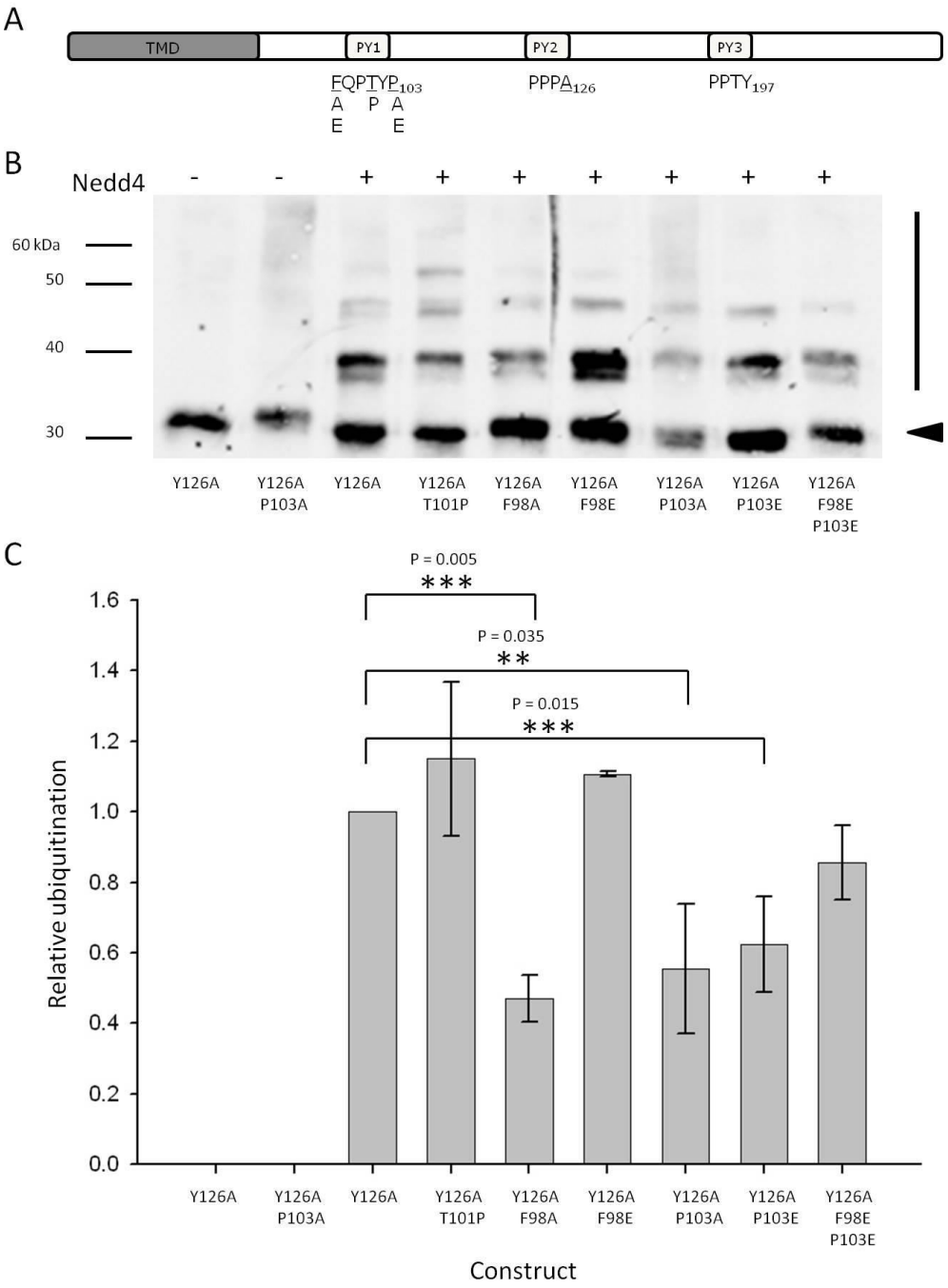

Figure 3.1.4. Schematic showing the broad structure of Y126A PMEPA1 and the mutations made within and around PY1 (**A**). Representative western blot, showing the results of an *in vitro* ubiquitination assay on soluble S-tagged PMEPA1 constructs, with the residues within and flanking the vPY motif mutated as indicated in a Y126A construct (**B**). PMEPA1 was detected using α S-tag primary followed by IR-labelled α mouse secondary antibody and imaged using the Odyssey IR laser scanning system. The relative modification by Nedd4 was calculated by the proportion of unmodified (indicated by the arrow) vs. modified (indicated by the vertical line) protein and shown in the histogram (**C**) as normalised to show Y126A as 1.0. Data are based on three replicates of the experiment, with error bars showing one standard deviation. A 2-tailed students' t-test was carried out to determine the statistical significance of major pairs of data sets as indicated by the horizontal lines. The relative significance of the differences between the means is indicated by zero (P>0.1), two (0.05>P>0.025) or three (P<0.025) asterisks.

3.1.2.1.5 Altering PY1 to resemble the canonical motifs

The final stage of the mutagenesis programme investigated the two variant residues in the vPY motif, altering the character of this motif to make it more similar to the sequence of PY2 (PPTY) and then PY3 (PPPY). This was achieved by introducing the mutation Q99P, alone and in combination with T101P, in both Y126A and Y126A/Y197A constructs to see if making the vPY site more canonical can compensate for the loss of ubiquitination associated with the functional loss of the canonical motifs. The results from the *in vitro* ubiquitination assays are shown in figure 3.1.5. The Q99P mutation alone had no significant impact on the extent of ubiquitination in the Y126A background, but the double mutation Q99P/T101P resulted in a small decrease in ubiquitination of 31% (P=0.012) in the same construct. This supports the hypothesis that the presence of a vPY motif with a non-canonical sequence is important for effective interaction between Nedd4 and PMEPA1. However, the same double mutation in the Y126A/Y197A background did not result in a statistically significant change in ubiquitination.

3.1.2.2 Ubiquitination and SUMOylation assays on Nedd4

To investigate whether the variant SUMO motif on Nedd4 has a significant role in the ability of Nedd4 to autoSUMOylate, SUMOylation assays were carried out (as detailed in section 2) on recombinant wild type Nedd4 and Nedd4 with the lysine of the variant site mutated out (K598R). Rsp5p, the yeast homologue of Nedd4, was assayed alongside as a control as it has no ability to autoSUMOylate under the same conditions as Nedd4, but shows a similar, if not stronger, ability to autoubiquitinate. In addition, a ubiquitination assay was carried out on the same proteins to check whether any effects seen were specific to the SUMOylation pathway and not related to any loss of general catalytic activity. From the ubiquitination assay (figure 3.1.6) it appears that the mutation

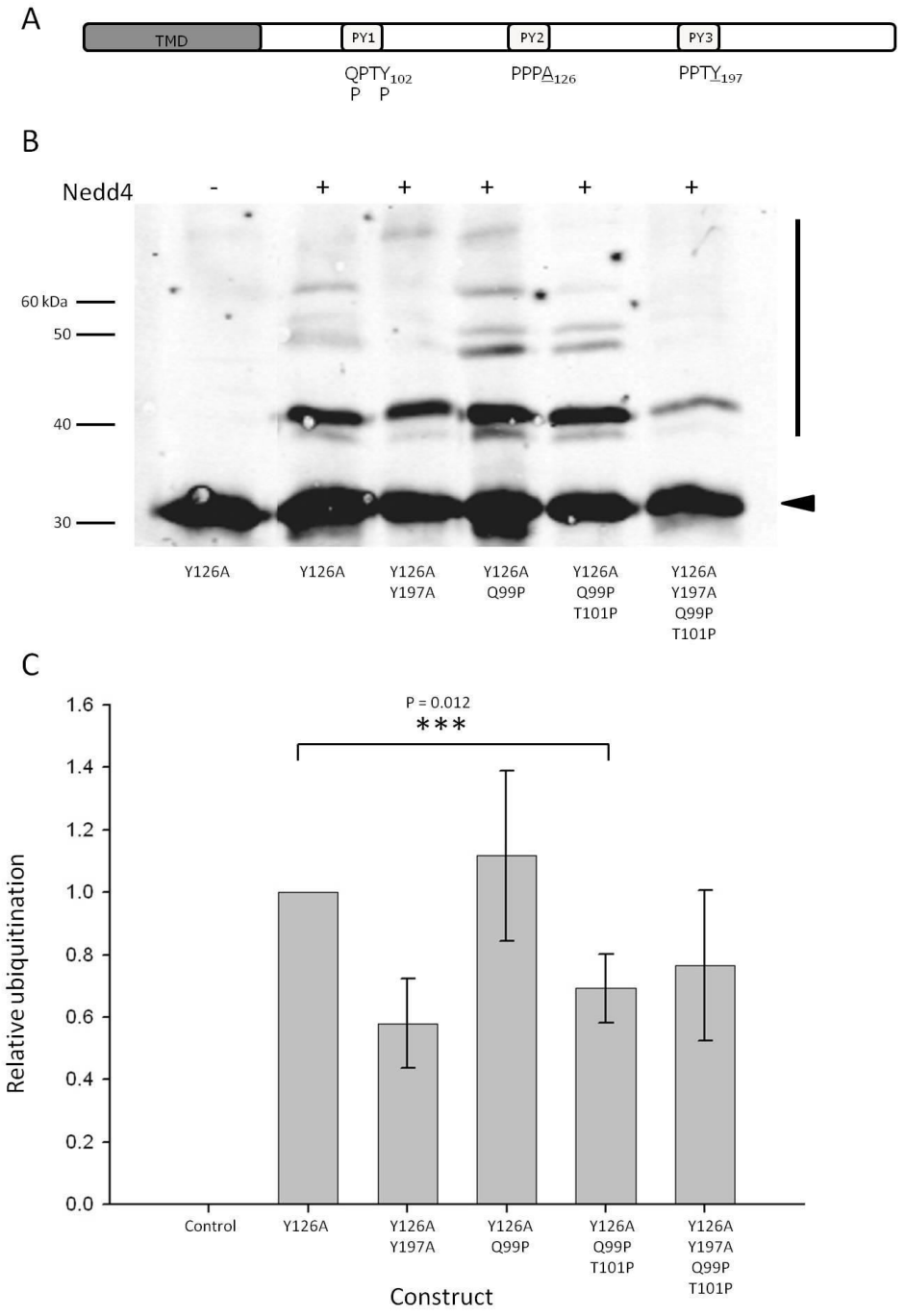

Figure 3.1.5. Schematic showing the broad structure of PMEPA1 and the mutations made within PY1 and PY3 in a Y126A construct (**A**). Representative western blot, showing the results of an *in vitro* ubiquitination assay on soluble, S-tagged PMEPA1 with the residues within and flanking the vPY motif mutated as indicated in a Y126A or Y126A/Y197A construct (**B**). PMEPA1 was detected using α S-tag primary followed by IR-labelled α mouse secondary antibody and imaged using the Odyssey IR laser scanning system. The relative modification by Nedd4 was calculated by the proportion of unmodified (indicated by the arrow) vs. modified (indicated by the vertical line) protein and shown in the histogram (**C**) as normalised to show Y126A protein as 1.0. Data are based on three replicates of the experiment, with error bars showing one standard deviation. A 2-tailed students' t-test was carried out to determine the statistical significance of major pairs of data sets as indicated by the horizontal lines. The relative significance of the differences between the means indicated by zero ($P>0.1$) or three ($P<0.025$) asterisks.

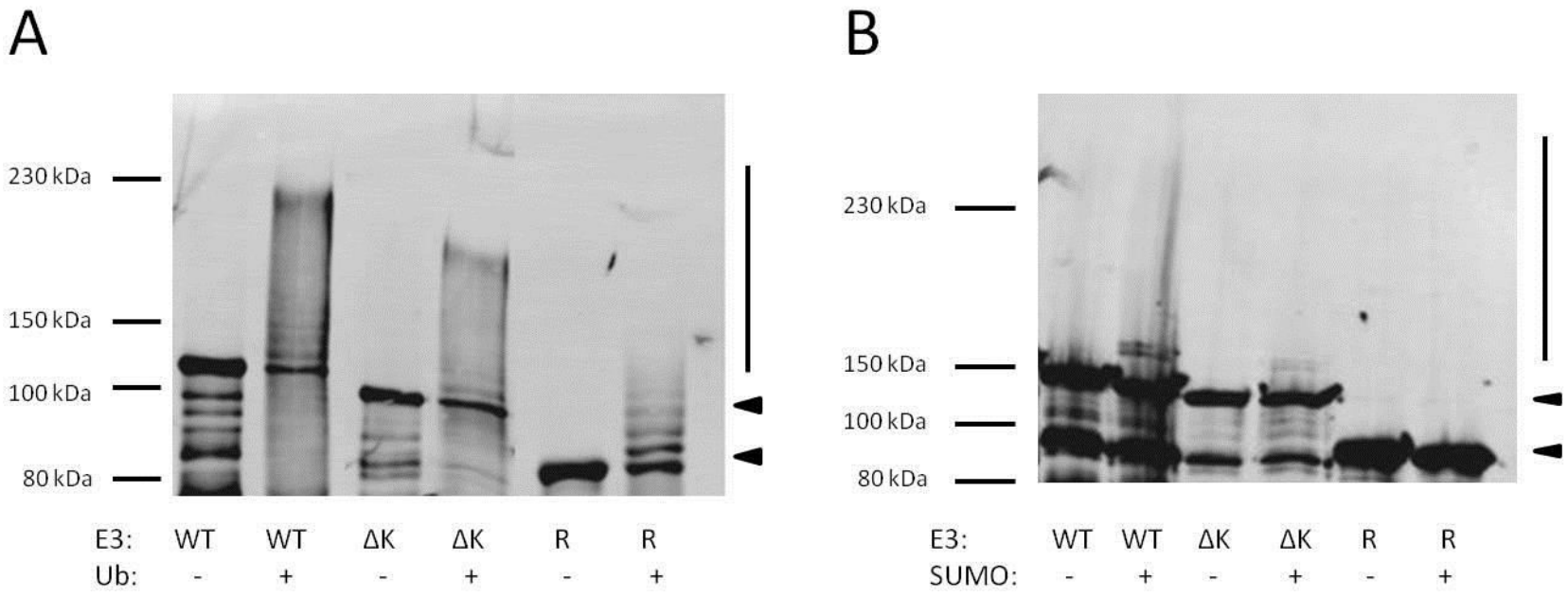

Figure 3.1.6. The results of *in vitro* ubiquitination (**A**) and SUMOylation (**B**) assays on GST-tagged Nedd4 and Rsp5 protein. The ligase being assayed is indicated at the bottom of the blot as WT (wild type Nedd4), ΔK (Nedd4 K598R) or R (Rsp5). The presence or absence of the modifying protein (ubiquitin is represented by Ub) is indicated by the -/+ at the bottom of the blot. Proteins were detected using αNedd4 primary antibody followed by IR-labelled α rabbit secondary antibody and imaged using the Odyssey IR laser scanning system. The unmodified proteins are indicated by the arrows to the right of the blots and the modified forms are the higher molecular weight bands indicated by the vertical line.

K598A has little or no impact on the ability of the Nedd4 to catalyse autoubiquitination, indicating that any effect seen could legitimately be considered the result of the mutated SUMO motif being rendered unavailable. However, there was a small observable decrease in SUMOylated products of K598R compared to the wild type (figure. 3.1.6B*)*. This is particularly obvious when looking at the very high molecular weight products which manifest as a smear towards the top of the blot; however this is possibly an artefact of the lower total protein concentration in the K598R sample compared to the wild type. This would seem to indicate that the variant SUMO motif ISKE does play a role in the autoSUMOylation of Nedd4 *in vitro*.

3.1.2.3 Microscale thermophoresis as a tool for investigating the PMEPA1/Nedd4 interaction

While the results of the PMEPA1 mutant assays provide important information about the functional role of PY motifs in Nedd4-mediated ubiquitination and SUMOylation, they do not give any information about the binding between Nedd4 and PMEPA1. To analyse the binding affinity of recombinant Nedd4 to PMEAPA1 a microthermophoresis experiment was performed (Wienken et al, 2010). The movement of a labelled protein, in this case PMEPA1, inside a narrow capillary is measured. An IR laser is used to heat a very small area of the capillary to a temperature 1000-6000 times higher than the rest of the solution, resulting in a temperature gradient which the labelled molecules move down by diffusion. The time taken for this movement to result in equilibrium depends on the hydration shell, charge or size of a solution, which in turn is dependent on the extent to which the labelled molecule is associating with an unlabelled binding partner. By titrating in increasing amounts of this unlabelled partner (in this case Nedd4), a binding curve is produced, from which the binding affinity can be inferred.

Three PMEPA1 constructs were used – wild type, a triple PY mutant (ΔPY 1,2,3) and the double PY mutant ΔPY 2,3, all with the N-terminal transmembrane domain removed and a C-terminal 6xHis tag, alongside GST-tagged Nedd4, at concentrations of 9.5-14 μM (see figure 3.1.7). A K_D of 40 nM for binding of Nedd4 to wild type PMEPA1 (i.e. at a Nedd4 concentration of 40 nM, half the total Nedd4 in the solution is bound to PMEPA1) was obtained, and a much higher K_D of 16.5μM for binding of Nedd4 to the triple mutant Y102A/Y126A/Y197A. However the result for the double mutant Y126A/Y197A was inconclusive.

3.1.3 Discussion

PY motifs have, until now, been considered well-defined in the literature, with PPxY being commonly cited as the minimal recognition motif for the WW domains of Nedd4 ligases (Chen & Sudol, 1995; Gautam et al, 2013). The data presented in figure 3.1.2 show that in PMEPA1 the variant PY motif QPTY, while not as indispensible as the two downstream canonical motifs, still contributes to Nedd4-dependent ubiquitination *in vitro*. This is consistent with previously published work, which showed that removing a vPY motif from the Rsp5p adaptor Bsd2p eliminated the ability of Bsd2p to function *in vivo* even when another, canonical PY motif was intact (Sullivan et al, 2007). The fact that the reduction in ubiquitination seen when the vPY site is eliminated is relatively small, compared to eliminating either of the two canonical motifs, might indicate weaker binding to the site. However, if this were the case we might expect that making the vPY motif more canonical in nature would result in an increase in Nedd4-dependent ubiquitination. The decrease in modification seen in the Q99P/T101P/Y126A mutant, which makes the vPY1 motif similar to PY3 in character, supports the hypothesis that the

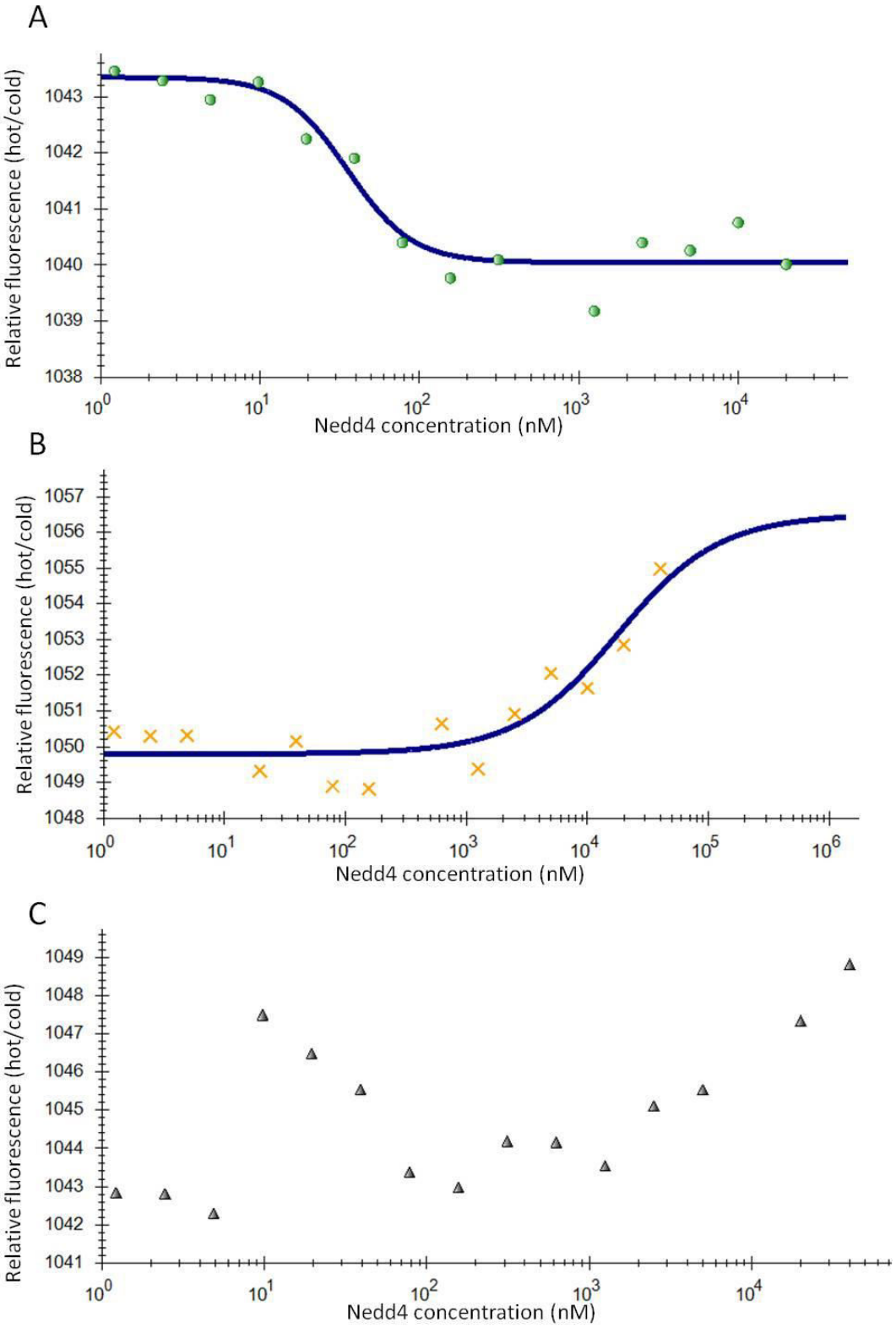

Figure 3.1.7. Microscale thermophoresis data showing PMEPA1 WT (**A**), ΔPY 1,2,3 (**B**) and ΔPY 2,3 (**C**) with titration of increasing concentrations of Nedd4. The x-axis shows the concentration of Nedd4 in nM and the y axis shows the ratio of fluorescence detected under hot and cold conditions, which is used to infer the fraction of molecules bound. While a single binding event is seen in both the WT and ΔPY 1,2,3 spectra, no clear corresponding event is seen in the ΔPY 2,3 data. Experiments were carried out by Dr. James Wilkinson of Nanotemper Technologies (Germany).

'strengthening' of the vPY site is not conducive to efficient ubiquitination, and that the function of this and other variant PY motifs is to bind the ligase transiently in order to bring the canonical PY motifs into contact with the correct WW domains for efficient modification. In fact, the data presented in figure 3.1.5 show that this is not the case, as altering the vPY motif to recreate the canonical sequence has little effect on modification of PMEPA1. This does not fit with the findings of Sullivan et al (2007), which found that mutating the APSY motif to mimic the canonical PY2 site (PPTY) resulted in an increase in ubiquitination, however this was only assessed with the canonical site functionally lost, a scenario in which a proposed orientation function for the vPY motif would be redundant.

One possible explanation for this is that the interaction of Nedd4 with PMEPA1 involves a transient binding event, involving the vPY motif, which precedes the interaction with PY2 and/or PY3. This transient binding may serve to orient PMEPA1 correctly with respect to one of the four Nedd4 WW domains and/or HECT domain in order to facilitate efficient ubiquitination. Ubiquitination targets lysine residues, and four of the five lysines in PMEPA1 are clustered at the very end of the primary sequence (see appendix iii), so it is logical that the PMEPA1 has to be oriented specifically against the ligase in order to avoid restricting access to these residues. If this were the case, we would not expect to see a complete loss of ubiquitination, because the correct orientation could still be achieved, albeit with less efficiency. This fits well with the results as presented in figure 3.1.2. One odd observation is that the level of ubiquitination in the double mutant Y102A/Y126A is higher than the level in the single mutant Y126A, i.e. loss of the vPY motif appears to slightly enhance ubiquitination when only PY3 remains functional. This effect is not seen on the PY3 (Y197A) mutant, or the double PY2/3 mutant (Y126A/Y197A), indicating that the vPY motif seems to have a negative impact

on specifically PY3-mediated interaction (figure 3.1.2). This may be due to the PY2 motif being the 'stronger' binding site; the loss of this site has by far the largest effect on ubiquitination of PMEPA1. It is feasible that the transient binding of the vPY site to Nedd4 has developed to bring the PY2 site in contact with Nedd4 at the optimal position, with the resultant PY3/WW interaction being less productive but still contributing to the overall level of ubiquitination. In the absence of PY2 but the presence of the vPY, this orientation effect would still take place, but with only the 'weaker' PY3 site intact, the ubiquitination reaction would be less efficient. In the absence of both the orienting vPY and PY2, the ligase and substrate are free to interact in such a way that the PY3 site is sometimes in contact with the Nedd4 in the same position as PY2 would be, allowing a small increase in ubiquitination (figure 3.1.8).

The data in figure 3.1.3 indicates that the residues at positions one and three in the vPY motif can apparently be altered with little or no impact on ubiquitination. The major exception to this that we found was that altering Thr_{102} to a serine residue appears to significantly increase the capacity of PMEPA1 to be ubiquitinated, possibly due to increased phosphorylation at the site by non-specific bacterial kinases as has been previously observed with recombinant enzymes (Yang & Liu, 2004). Phosphorylation of this serine would also explain the odd double banding pattern that is only seen in this mutant. It has been found that the protein Sprouty2 has two conserved serine residues in a non-canonical, non-PY, Nedd4-specific interaction region which must be phosphorylated in order to facilitate Nedd4 binding and catalysis of ubiquitination (Edwin et al, 2010). However, threonine is also phosphorylated, often by the same kinases that modify serine, and substituting this residue for the glutamic acid which mimics the change in charge associated with phosphorylation did not have the same effect as the mutation to serine. In addition, as seen in figure 3.1.4, substituting a proline

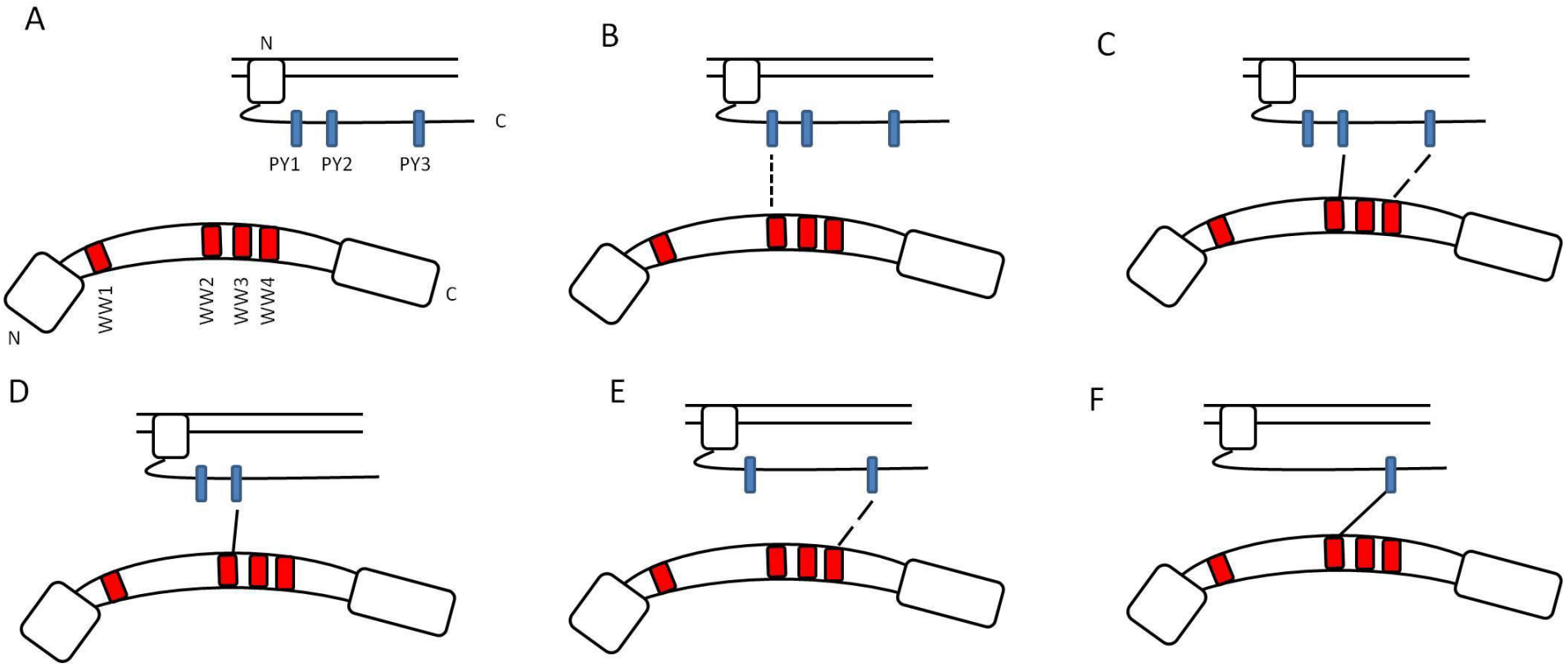

Figure 3.1.8. Schematic of the posited relationship between multiple PY motifs in PMEPA1 and Nedd4, with the three PY motifs represented in blue and the four WW domains in red. Nedd4 in the cytosolic approaches PMEPA1, anchored in the Golgi membrane by the N-terminal transmembrane domain (**A**). The vPY motif (PY1) weakly & transiently interacts with a WW domain of Nedd4, represented by the dotted line, in this case speculated as being WW2 (**B**). This interaction is then replaced by a stronger interaction, represented by the solid line, between PY2 and Nedd4, alongside a slightly weaker interaction between PY3 and Nedd4, represented by the broken line (**C**). When PY3 is absent (**D**), the total ubiquitination on Nedd4 is only slightly reduced as the dominant PY2-mediated interaction can still occur. But when PY2 is absent (**E**), only the weaker PY3-mediated interaction can occur, although Nedd4 is still held in position by the PY1 interaction. When PY1 and PY2 are absent (**F**), the Nedd4 is free to adopt other orientations, including ones which may allow a stronger interaction between the remaining PY3 and Nedd4, represented again by an unbroken line.

did not result in any change in ubiquitination that might be expected if phosphorylation of this residue plays a key role in the function of the motif. The vPY motif identified previously, APSY in Bsd2p, also has a serine in the third position, and there is at least one example, a transcriptional regulator implicated in Charcot-Marie-Tooth disease called LITAF (Shi et al, 2010), of a canonical PY motif also having a serine as the variant residue. Several, including the canonical motif of Bsd2p and PY3 of PMEPA1 have a threonine, also susceptible to phosphorylation, in this position. Lu et al (2009) reported that isolated Nedd4 WW domains bind to phosphoproteins, specifically those rich in phosphoserine and phosphothreonine. Interestingly, the paper identified proline, serine, glutamic acid and threonine (PEST) as creating an environment particularly well suited to these phosphoprotein-WW domain interactions and this may go some way towards explaining why altering the residues flanking the core vPY motif had an effect on ubiquitination. Clearly the threonine in the vPY of PMEPA1 plays some kind of role, as it is universally conserved across species from humans to zebrafish, even when the rest of the protein is only 65% conserved (figure 3.1.9).

Altering the phenylalanine upstream of the vPY motif to an alanine resulted in a significant loss of ubiquitination not seen when a glutamic acid was substituted in the same position (figure 3.1.4). This is unlikely to be due to the phosphomimetic nature of the glutamic acid, as phenylalanine is not phosphosphorylated, so this result is most likely due to a steric effect; the presence of a bulky side chain at this position may increase, or indeed decrease, the availability of the site to interact with WW domains. By contrast, altering the downstream proline residue of the same motif results in a reduction in ubiquitination regardless of the nature of the substituted amino acid, but the effect of having a glutamic acid in this position is less pronounced than an alanine. Once again, proline has a bulky ring side chain, but it is unique in having its primary amine group

Species	Homology with human	Sequence of PY motifs 1-3 & surrounding residues
Human	100%	---- FQPTYP ---- EPPPYQ ---- PPPTYS ----
Orang-utan	98%	---- FQPTYP ---- EPPPYQ ---- PPPTYS ----
Panda	94%	---- FQPTYP ---- EPPPYQ ---- PPPTYS ----
Dog	94%	---- FQPTYP ---- EPPPYQ ---- PPPTYS ----
Cow	94%	---- FQPTYP ---- EPPPYQ ---- PPPTYS ----
Chimpanzee	94%	---- FQPTYP ---- EPPPYQ ---- PPPTYS ----
Mouse	92%	---- FQPTYP ---- EPPPYQ ---- PPPTYS ----
Rat	92%	---- FQPTYP ---- EPPPYQ ---- PPPTYS ----
Cat	92%	---- FQPTYP ---- EPPPYQ ---- PPPTYS ----
Platypus	84%	---- FQPTYP ---- EPPPYQ ---- PPPTYS ----
Opossum	84%	---- FQPTYP ---- EPPPYQ ---- PPPTYN ----
Chicken	84%	---- FQPTYP ---- EPPPYQ ---- PPPTYS ----
Frog	77%	---- FQPTYP ---- EPPPYQ ---- PPPTYN ----
Zebrafish	65%	---- FQPTYP ---- EPPPYQ ---- PPPTYS ----

Figure 3.1.9. PY motif sequence homology in PMEPA1. Comparison of PY motifs and flanking residues in PMEPA1 from 13 mammalian species in addition to the human protein used in all experiments described. The core residues of all 3 PY motifs can be seen to be conserved even in zebrafish PMEPA1, with only 65% overall homology with the human protein. In addition, both flanking residues of PY1 and PY2, and the upstream proline of PY3, are 100% conserved in all 14 species, and the downstream residue of PY3 is a conserved serine in 12 out of 14 species.

involved in that side chain, which induces a 'kink' in the protein chain which cannot be recreated by substitution with any other residue. Therefore the glutamic acid side chain may partly compensate for the loss of the steric environment, but a significant loss of ubiquitination is seen in both mutants. The fact that mutating both residues simultaneously to a glutamic acid seems to compensate for this loss is, however, very curious. It may that having the two additional glutamic acid residues, which are acidic, in place of the proline and phenylalanine, which are both nonpolar, causes a sufficient change in the environment surrounding the motif that the availability of the motif to Nedd4 is increased despite the physical changes surrounding the motif. Alternatively, both residues may be contributing to the topology of the region and the loss of one may cause a specific alteration in the three dimensional structure which can be compensated for by the loss of both. This alteration may cause access to the site to be blocked, or possibly cause the vPY motif to be more exposed to the ligase in a way which results in preferential binding of the WW domain(s) to the weaker motif to the detriment of binding to the canonical motifs. Unfortunately, despite several attempts, the double alanine mutant F98A/P103A could not be successfully cloned; it is possible that this is due to a problem with the primers. This would be an informative experiment to see whether substituting both flanking residues for a small amino acid has any effect on Nedd4 ubiquitination.

PMEPA1 has never been structurally resolved, but there are several examples in the literature of isolated PY-containing peptides bound to individual WW domains (Seo et al, 2006, Kanelis et al, 2001; Chong et al, 2006). The WW domain structure features a conserved, aromatic-rich "XP groove" which binds proline-rich regions, as well as a loop formation which recognises the tyrosine residue of PY motifs (Zarrinpar & Lim, 2000). The PY motif of the ENaC sodium transporter adopts a helical conformation, due to the

rigid structure of the prolines as mentioned above, that fits into the XP groove, supporting the theory that the proline upstream from PY1 in PMEPA1 plays an important structural role. However, there is also a C-terminal leucine residue in the ENaC which is essential for WW domain interaction, but not via the same groove that binds the PY motif (Kanelis et al, 2001). The N-terminal domain of the Epstein-Barr virus associated protein LMP2A has a region between the two PY motifs which NMR analyses showed to contribute to binding WW domains of Nedd4 ligases, although the reason for this is not clear (Seo et al, 2006), and Chong et al (2006) showed that 6 residues immediately downstream of a PY motif in the Smurf2 adapter Smad7 are also implicated in binding, to a variable area of the WW domain separate from the XP groove, and posited that this variability was the source of substrate specificity in Nedd4 family ligases. This all indicates an important role for the residues outside of the PY motifs, and it would be an interesting future experiment to expand the programme of mutagenesis to include residues further out from the vPY motif.

Given the importance of the PMEPA1 vPY *in vitro* for ubiquitination by Nedd4 the role of the N-terminal TMD may need to be investigated, as the presence of this may alter the folding of the protein and therefore the environment of vPY, being the closest to the TMD in the primary sequence. The residues immediately flanking the identified vPY motifs in PMEPA1, Bsd2p (Sullivan et al, 2007) and Commissureless (Kanelis et al, 2006) do not seem to be conserved, although taking the canonical PY motifs into account reveals that proline, serine and aspartic acid are present more than once in the immediate vicinity of a PY motif (see figure 3.1.10). This may be related to the charged nature of these residues (including serine when phosphorylated) or their contribution to the surface exposure of the motif. Clearly the function of the vPY motif is affected by the surrounding environment and not simply governed by the four core residues, and this

Protein	Sequence around PY motifs
PMEPA1	---- FQPTY**P** ---- EPPPYQ ---- **P**PPTY**S** ----
Bsd2	---- IPPTY**D** ---- MAPSYY----
Commissureless	---- **S**PPCYT ---- GLPSY**D** ----

Figure 3.1.10 PY motifs and surrounding residues. Comparison of PY motifs and flanking residues in human PMEPA1, Bsd2 from *S. cerevisiae* and Commissureless from *D. melanogaster.* Residues which are present more than once in the immediate vicinity of a motif are highlighted in bold; proline, aspartic acid and serine are all represented more than once. Of the other residues around the motifs, 6/8 are hydrophobic or nonpolar, and 7/8 are uncharged.

may relate to the specificity of binding to different members of the Nedd4 family, or different WW domains within the ligases.

Nedd4-family ligases have a strong tendency to autoubiquitinate in appropriate conditions *in vitro*, which has been put forward as a regulatory event to limit stability and catalytic activity of the ligase (Bruce et al, 2008). This autoubiquitination event is thought to be linked to a PY motif located close to the catalytic cysteine in the HECT domain (Kasanov et al, 2001). When the ligase has the opportunity to bind with higher affinity to a substrate PY motif, perhaps due to the more canonical sequence, it is presumed that this displaces the intramolecular interaction and the ligase preferentially ubiquitinates the substrate (Bruce et al, 2008). If a lower affinity vPY motif is present on the substrate e.g. PMEPA1, this could result in binding to a single WW domain without breaking the interaction between the HECT PY motif and a different WW domain, bringing the substrate and enzyme into a very specific alignment before the intramolecular interaction is interrupted.

Finally, the observation that the variant SUMO interaction motif (SIM) ΨxKE identified in Nedd4 appears to be a legitimate modification site indicates that this may be an area in which the accepted canonical recognition site for ubiquitin-like protein modification is more flexible than previously thought. While canonical SIMs interact with the 'groove' on SUMO created by the α helix and β sheet folding common to SUMO and other ubiquitin-like proteins (Song et al, 2006; Hecker et al, 2006), a novel motif has been identified which bind specifically to the SUMO1 isoform via several residues in the β sheet and connecting loop (Pilla et al, 2012). While this interaction was shown to be mediated by a valine/isoleucine-rich region on the dipeptidyl peptidase DPP9, it serves as an example of an alternate SUMO interaction, of which this may be another example. The relative loss of SUMOylation in the K598R mutant is small, but

there are no canonical SUMO modification sites in Nedd4, and this is reflected in low levels of SUMOylation, with only two higher molecular weight bands and a small amount of smear being observed in the wild type protein. This small effect, and the fact that the K598R mutant has similar autoubiquitination activity as the wild type, supports the observation as a true consequence of the loss of the variant SUMO site and not of a loss of catalytic activity of Nedd4. It would be extremely interesting to investigate this effect *in vivo* to see whether SUMOylation of Nedd4 has a regulatory effect on ubiquitination activity as demonstrated in Rsp5p, especially as the target SUMOylation lysine is so close to the catalytic cysteine of Nedd4, and subsequently on the regulation of AR.

3.2 *In vivo* localization of PMEPA1 and AR

3.2.1 Introduction

3.2.1.1 PMEPA1 localization

Prostate membrane protein androgen induced 1 (PMEPA1) is a 252 kDa protein with a sequence that is mostly predictive of a soluble structure, with the notable exception of a type Ib transmembrane domain at the N-terminus (Xu et al, 2000). It is described in the literature as being targeted to the secretory pathway, however co-localisation with a cis-Golgi marker is not perfect, with 'spots' of PMEPA1 being observed around the main area of overlap (Xu et al, 2003).

While there have been publications on PMEPA1 since the initial papers by Xu et al, they have mostly focussed on its potential role in tumorigenesis and TGF-β signalling (Nakano et al, 2010; Watanabe et al, 2010). However, Brunschwig et al (2003) identified PMEPA1 as a transcriptional target of TGF-β in its capacity as a tumour suppressor in colon cancer. This paper reported an alternative splice variant lacking the N-terminal transmembrane domain; the RNA of both splice alternatives were directly shown to be present, although the full-length transcript was predominant, and in some cell lines, including the human LNCaP line, the truncated version was absent. The localisation of both splice alternatives were described as 'cytoplasmic' by Brunschwig et al, although the full length protein appeared much more diffuse, in contrast to the concentrated Golgi-like appearance reported by Xu et al. (2003). The truncated variant, lacking the hydrophobic domain, has a much more perinuclear appearance that the authors described as "punctuate clusters", with 'spots' of fluorescence becoming less densely packed further away from the nucleus; this is actually more similar in appearance to the Golgi

colocalisation reported previously. The authors make no comment on the potential reasons for the difference in localisation between the two proteins, but it is not immediately clear why the results do not agree with the previous observations of Xu et al, nor why a variant with the hydrophobic N-terminus removed might show a less diffuse, perinuclear clustering.

3.2.1.2 Androgen receptor localisation

There was initially some uncertainty over the subcellular localisation of AR until it was established that it can vary by cell line (Jenster et al, 1993). The same paper connected several associated ideas about AR localisation, and showed that the addition of testosterone as a ligand induced relocation from the cytoplasm, or a diffuse spread over the cytoplasm and nucleus, into the nucleus exclusively in all cell lines. The same publication used mutation studies to show that blocking ligand binding prevented the movement of AR into the nucleus, and that mutating a bipartite basic region in the DNA binding domain, with similarity to a nuclear targeting domain in the histone-binding protein nucleoplasmin (Robbins et al, 1991), diminished or abolished the movement of AR into the nucleus on ligand binding. Conversely, deletion of a region of the C-terminus resulted in a constitutively active, nuclear-localised AR (Jenster et al, 1991), and non-activational ligands including anti-androgens and oestrogens were able to induce nuclear localisation but not transcription, showing that the two processes are separate (Jenster et al, 1993). The report concluded that a novel nucleoplasmin-like nuclear localisation signal functions in tandem with a previously postulated signal (Simental et al, 1991) to mediate shuttling of the AR from the cytoplasm into the nucleus in an ATP-dependent manner.

Later research revealed that the glucocorticoid receptor, a nuclear hormone receptor in the same family as AR, is trafficked into the nucleus in an importin α-dependent process (Savory et al, 1999) that is mediated by a nuclear localisation signal of basic residues, conserved in AR, with the sequence RKxxxxxxxxxxRKLKK. Importin α was then shown to co-immunoprecipitate with AR both in the presence and absence of a ligand, and the structure of the bound complex revealed the hinge region between the N and C termini to be crucial for this (Cutress et al, 2008). The loss of this region resulted in a loss of binding to importin and subsequent inability of AR to move into the nucleus as a response to ligand stimulation, however this report reiterated that nuclear import is necessary but not sufficient for transcriptional activation. The reverse process, the export of AR from the nucleus back into the cytoplasm, is triggered by ligand withdrawal and it has been suggested that ligand binding suppresses a nuclear export signal on the ligand-binding domain and causes accumulation of nuclear protein (Saporita et al, 2003). It was also confirmed that cytosolic AR was trafficked out of the nucleus rather than synthesised *de novo*, that the nuclear export signal is in the ligand-binding domain between residues 743 and 814, and that it is partially conserved in the oestrogen and mineralocortocoid nuclear receptors (Saporita et al, 2003). The regulation of AR transactivation is complex and still being unravelled, but the postulated feedback loop between PMEPA1 and AR, described in detail in section 1.4.4, relies on a physical interaction between the two proteins. This does not tie with their published localisations, but no evidence has been presented to date regarding whether, when expressed together under different conditions, there is any alteration in those localisations which may support this theory.

3.2.2 Results

3.2.2.1 In silico predictions of PMEPA1 localization

While the presence of a transmembrane domain in PMEPA1 is indicative of membrane targeting, to date there has been no published localisation prediction of PMEPA1, based on anything other than its transmembrane domain. This was addressed by using five independent online prediction programmes to calculate the probability of wild type PMEPA1, a variant with the N-terminal transmembrane domain removed, and another with the three PY motifs rendered inactive, localising to different subcellular compartments. The results of these programmes is summarised in figure 3.2.1. Pprowler (Boden & Hawkins, 2005) predicted a secretory pathway targeting for the wild type protein, based entirely on the region between residues 1 and 32 i.e. the transmembrane domain, as did TargetP (Emmuelsson et al, 2000), with a reliability class of 1, the highest denomination. MultiLoc2 (Hoeglund et al, 2006) returned a more specific prediction of endoplasmic reticular localisation with 87% certainty, despite an absence of specific ER retention motif. CELLO (Yu et al, 2006) returned a completely different result, predicting a nuclear localisation, although with some composition elements returning a low-probability of targeting to the plasma membrane, and WoLF PSORT concurred, predicting with 69.6% certainty nuclear localisation based on comparison with 23 'nearest neighbours' sequence homologues despite the identification of a transmembrane domain with the C-terminus facing inwards and the lack of any nuclear localisation signal.

The localisation of the wild type proteins were not altered in the absence of the three PY motifs described in section 3.1, confirming that any effects on localization seen experimentally would be likely to be due to the resultant loss of Nedd4-interactions.

	PProwler	CELLO	MultiLoc	TargetP	WoLF PSORT	Consensus
PMEPA1 WT	Secretory pathway	Nucleus	ER	Secretory pathway	Nucleus	Secretory pathway
PMEPA1 ΔNT	Mitochondria	Nucleus	Cytosol	Mitochondria	Mitochondria	Mitochondria
PMEPA1 ΔPY	Secretory pathway	Nucleus	ER	Secretory pathway	Nucleus	Secretory pathway

Figure 3.2.1. Predicted subcellular localisation of wild type (WT), ΔNT (with residues 1-23 of the wild type sequence removed) and ΔPY (Y102A /Y126A/Y197A) PMEPA1 according to five online prediction programs. While removing the PY motifs, and therefore preventing interaction of PMEPA1 with Nedd4, has no effect on the predicted localisation, removing the N-terminal transmembrane domain appears to expose a mitochondrial targeting sequence.

Similarly, running the full sequence of PMEPA1 with a C-terminal fluorescent protein tag had no impact on the resultant sequence predictions. In contrast, repeating the process with an N-terminal truncated form of PMEPA1 yielded very different results. The N-terminal mutant sequence lacked the initial N-terminal 23 residues containing the transmembrane domain, and was the soluble protein used in the *in vitro* assays detailed in section 3.1. This construct was predicted to be targeted to the mitochondria, through a region corresponding to residues 24-59 in the full length protein, by PProwler, and this was corroborated with 56.5% certainty by WoLF PSORT and with the second-highest reliability class by TargetP. CELLO predicted nuclear localisation by every measured parameter, while MultiLoc2 returned a cytoplasmic prediction with 85%, despite the identification of a mitochondrial targeting peptide.

3.2.2.2. Comparison of PMEPA1 localization with and without the transmembrane domain

In order to try and establish which localisation of the wild type PMEPA1 was observable in our experimental system, as well as to clarify the effects of removing the transmembrane domain on PMEPA1, green (GFP) and red (RFP) C-terminal fluorescent-tagged mammalian expression constructs of both versions of PMEPA1 (see figure 3.2.3) were cloned and transiently transfected into HeLa cells both individually and together. Having established that the tag used is likely to have no effect on PMEPA1 localisation and could therefore be discounted as a contributing factor (figure 3.2.3 G-I), it then became clear that the wild type (WT) protein shows a diffuse distribution throughout the cytoplasm, with apparent exclusion from the nucleus when expressed in both HeLa and LNCaP cells (figures 3.2.2B & D), but in contrast to the evenly distributed appearance displayed by GFP, unconnected specks and spots of concentrated protein were observed.

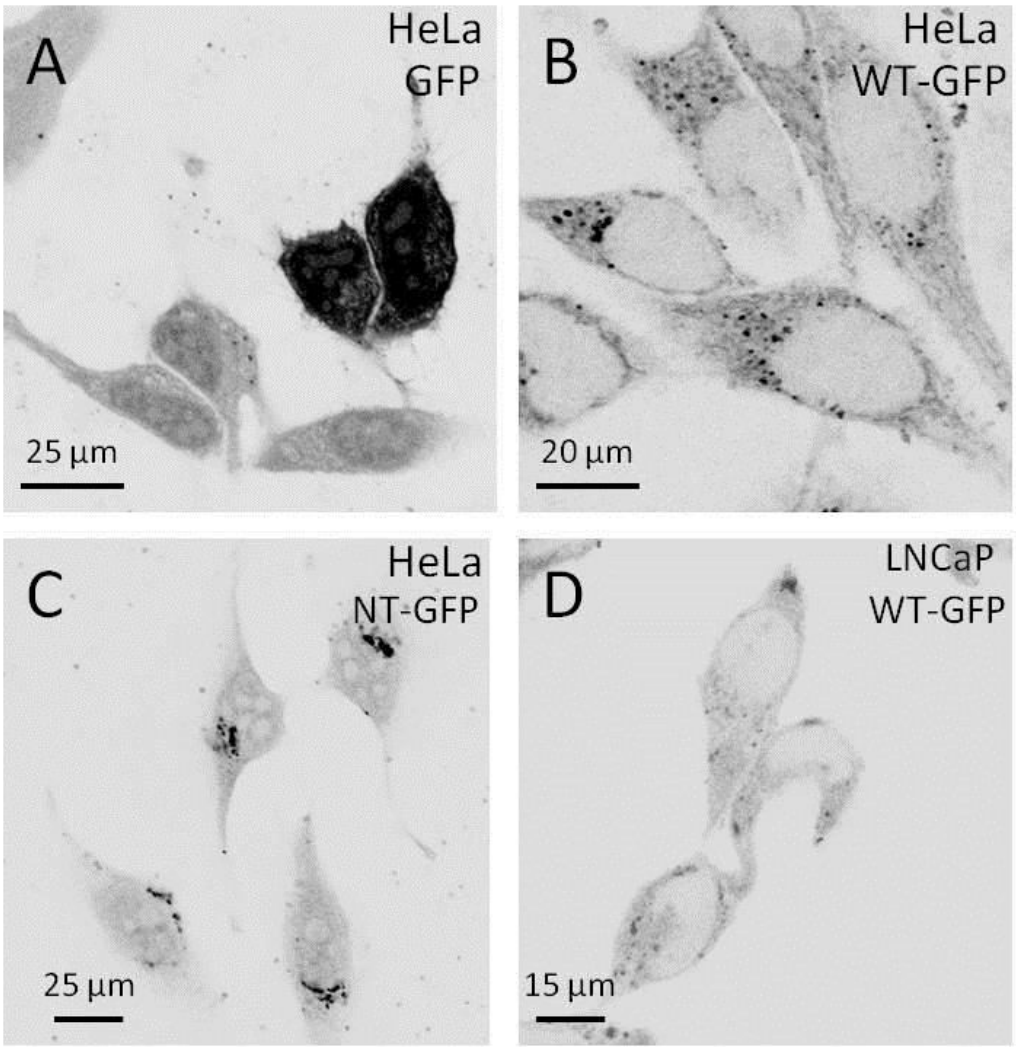

Figure 3.2.2. Confocal microscope images of fixed HeLa cells transiently transfected with free GFP (**A**) compared to GFP-tagged wild-type (WT) PMEPA1 (**B**) PMEPA1 lacking the N-terminal transmembrane domain (NT) (**C**) all expressed in HeLa cells, and LNCaP cells transfected with GFP-tagged WT (**D**). These are all representative images of three fields of view, each containing an average of 19 expressing cells. Cells were fixed using paraformaldehyde 48 hours post-transfection, mounted and a representative cell cluster was imaged using excitation at 488 nm to produce an emission spectrum across 500-570 nm. Images were desaturated and reversed to produce black-on-white images for easy comparison.

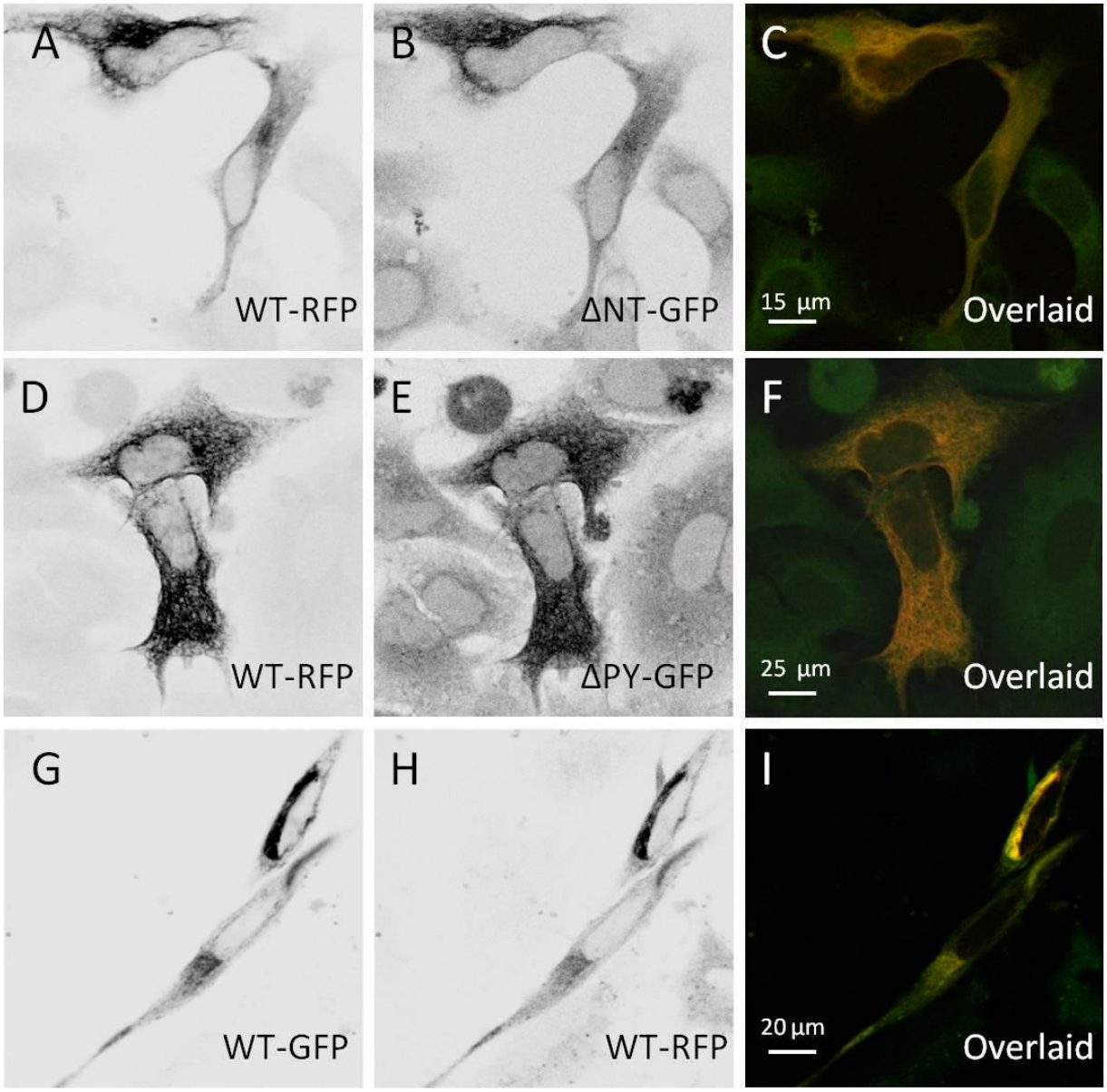

Figure 3.2.3. Confocal microscope images of fixed HeLa cells transiently cotransfected with RFP-tagged WT (**A**) and GFP-tagged ΔNT (**B**) PMEPA1, and an overlay of the two channels showing almost overlap (**C**). RFP-tagged WT (**D**) and GFP-tagged ΔPY (**E**) are also shown overlaid in (**F**). For comparison, WT-PMEPA1 tagged with GFP (**D**) and RFP (**E**) are shown separately and overlaid (**F**). These are all representative images of three fields of view, each containing an average of 4 doubly expressing cells. Cells were fixed using paraformaldehyde 48 hours post-transfection, mounted and a representative cell cluster was imaged. Red channel (A) was excited at 633nm to produce an emission spectrum across 660-750 nm, green channel (B) was excited at 488 nm to produce an emission spectrum across 500-570 nm. Images were desaturated and reversed to produce black-on-white images for easy comparison.

The protein showed a similar appearance in both HeLa (figure 3.2.2B) and LNCaP (figure 3.2.2D), although overall fluorescence was generally lower in LNCaP. This is the opposite effect to that predicted based on the activated status of AR in the LNCaP line, which might be expected to increase PMEPA1 production, but this effect may be lost because the transfected PMEPA1 expression levels are higher than the endogenous protein. The N-terminal truncated protein (ΔNT) appears to show the same distribution despite lacking the transmembrane domain region (figure 3.2.2C), and this was corroborated by double transfections showing almost complete overlap between RFP-tagged WT and GFP-tagged ΔNT (figure 3.2.3).

3.2.2.3 Coexpression of PMEPA1 and subcellular markers

To see if the observed punctate distribution of PMEPA1 could be identified as representing any specific subcellular compartment, both WT and ΔNT PMEPA1, as well as a triple PY mutant Y102A/Y126A/Y197A (ΔPY), were transfected into HeLa cells and immunofluorescence was used to visualise markers of the secretory system, nucleus and mitochondria. The results of these experiments are shown in figures 3.2.4 and 3.2.5. Again the characteristic shattered appearance of PMEPA1 is seen throughout the cytoplasm, both with and without the N-terminal transmembrane domain, and this does not seem to be dependent on the PY motifs being intact (see also section 3.3.2). The signal partly overlaps with that of GM130, a cis-Golgi marker protein (Nakamura et al, 1995), particularly in a region towards the centre of the PMEPA1 distribution close to the nucleus, but there is a large amount of PMEPA1 further out in the cytosol which does not correspond to a Golgi location, as well as areas of Golgi which are free of PMEPA1. Similarly, there is a smaller degree of overlap with the ER-Golgi intermediate compartment, as shown by the marker ERGIC-53 (Schweizer et al, 1988), particularly

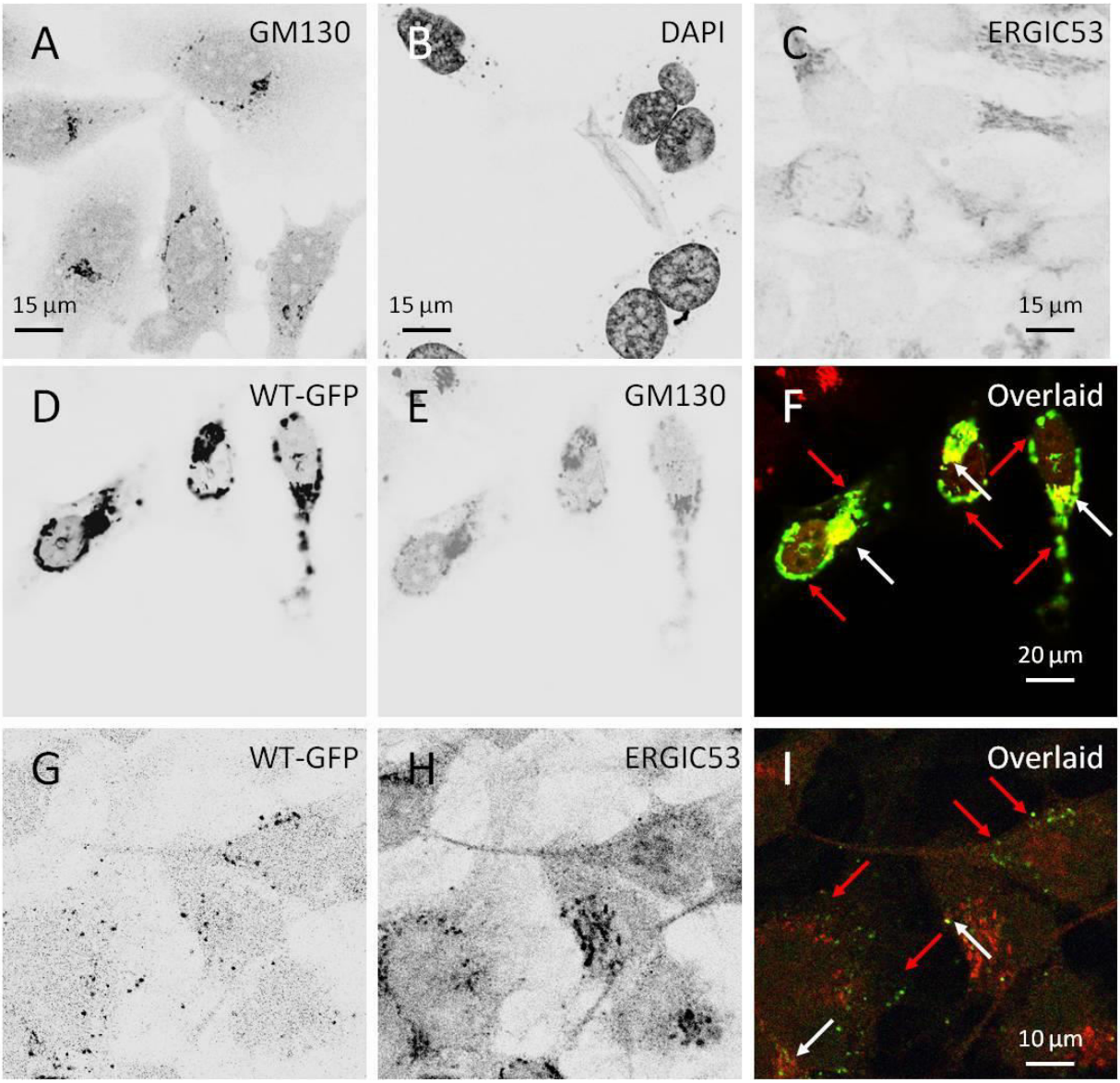

Figure 3.2.4. Confocal microscope images of fixed HeLa cells showing the degree of overlap between wild-type GFP-tagged PMEPA1 and various subcellular compartment markers. The immunolocaization of the cis-Golgi using anti GM130 antibodies (**A**), the nucleus as imaged by DAPI staining (**B**) and the ERGIC as imaged using anti ERGIC53 (**C**) is shown in untransfected cells. The localization of wild-type PMEPA1-GFP (WT-GFP) is shown in cells counterstained using anti-GM130 (**D, E**) and anti-ERGIC-53(**G, H**) and the two channels are merged in (**F**) and (**I**). In both cases a degree of overlap can be seen, appearing yellow and highlighted using the white arrows, but with distinct areas where the two do not colocalize, highlighted using red arrows. These are all representative images of three fields of view, each containing an average of 24 immunostained cells, plus an average of 12 expressing cells if transfected with labelled protein. Cells were fixed using paraformaldehyde 48 hours after transfection, then permeabilised and stained for immunofluorescence using an appropriate primary antibody followed by AlexaFluor-594. A representative cell cluster was imaged; red channel (**A, C, E, H**) was excited at 633nm to produce an emission spectrum across 660-750 nm, green channel (**D, G**) was excited at 488 nm to produce an emission spectrum across 500-570 nm. DAPI was excited at 356 nm to produce an emission spectrum across the range 400-475 nm. Single channel images were desaturated and reversed to produce black-on-white images for easy comparison, merged images were produced using Leica LAS AF software.

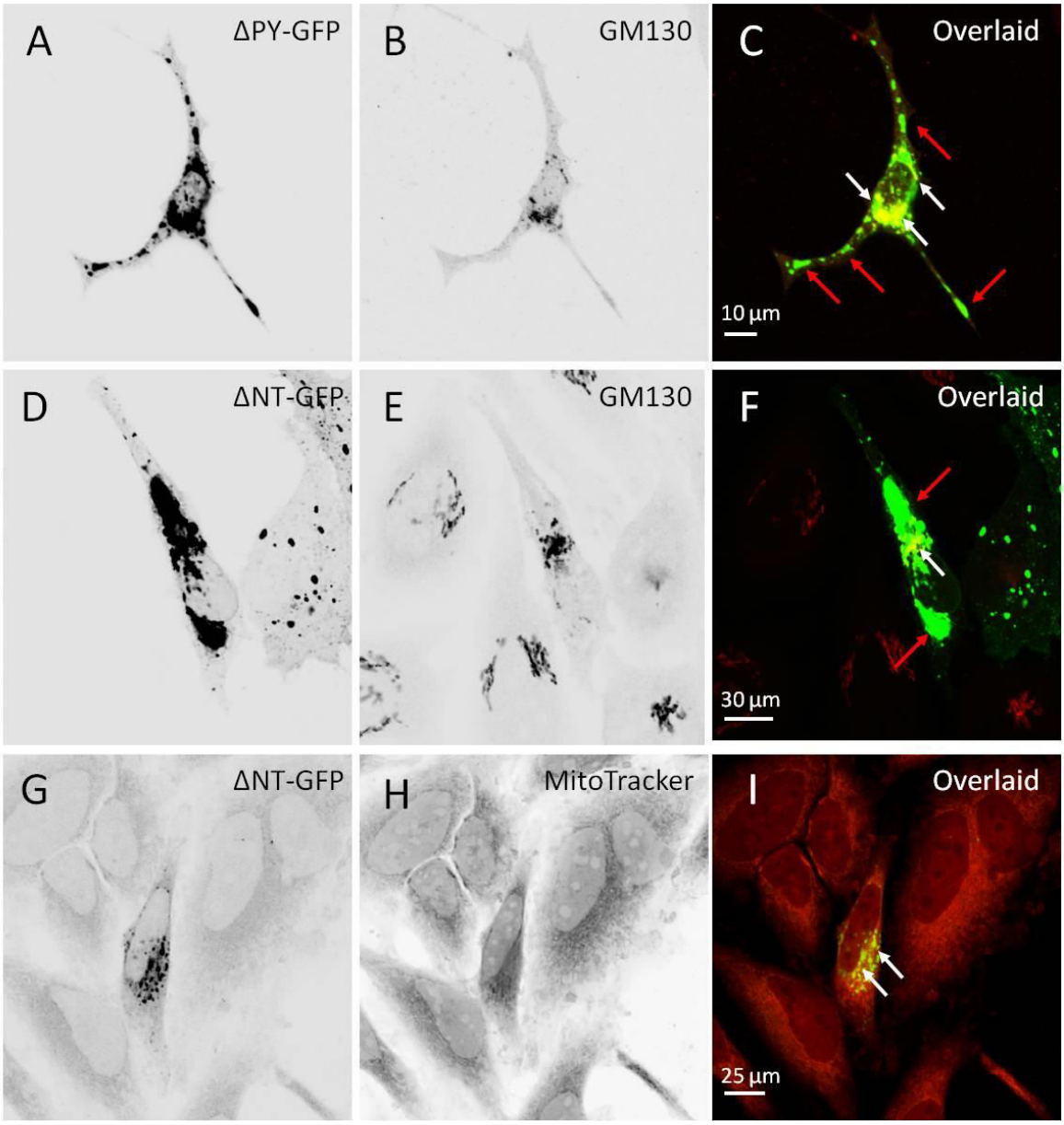

Figure 3.2.5. Confocal microscope images of fixed HeLa cells showing the degree of overlap between PMEPA1 ΔPY and ΔNT mutants and various subcellular compartment markers. ΔPY PMEPA1-GFP is shown in cells counterstained using anti-GM130 (**A, B**) and the two channels are merged in (**C**). ΔNT PMEPA1-GFP is shown in cells counterstained using anti-GM130 (**D, E**) and Mitotracker Red (**G, H**), and the merged images are presented in (**F**) and (**I**). In both cases a degree of overlap can be seen, appearing yellow and highlighted using the white arrows, but ΔPY appears to overlap slightly better with the *cis*-Golgi than ΔNT. These are all representative images of three fields of view, each containing an average of 24 immunostained cells, plus an average of 8 expressing cells if transfected with labelled protein. Cells were fixed using paraformaldehyde 48 hours after transfection, then permeabilised and stained for immunofluorescence using an appropriate primary antibody followed by AlexaFluor-594. A representative cell cluster was imaged; red channel (**B, E, H**) was excited at 633nm to produce an emission spectrum across 660-750 nm, green channel (**A**, **D, G**) was excited at 488 nm to produce an emission spectrum across 500-570 nm. Mitotracker Red was added to cell growth medium at a concentration of 200nm for 45 minutes prior to fixation. Images were desaturated and reversed to produce black-on-white images for easy comparison, merged images were produced using Leica LAS AF software.

around the edges of the cluster formed by the marker, but there are still large regions of PMEPA1 expression which don't overlap with this marker. As predicted the absence of all 3 PY motifs made no difference to the co-localization with GM130 (figure 3.2.5 A-C). By this point it seemed clear that the ΔNT PMEPA1 was not, as predicted by the online software, localised differently to the wild-type protein or to the mitochondria, but this was tested by staining HeLa cells transfected with GFP-tagged ΔNT with Mitotracker red (Minamikawa et al, 1999). The mitochondrial signal was diffuse and evenly distributed throughout the cytosol, but the ΔNT construct retained the completely different spotty, concentrated appearance seen previously, with some areas of slight overlap apparently caused by the fact that the red signal was present throughout the cell (figure 3.2.5). This supports the WT/ΔNT overlap data shown in figure 3.2.2 suggesting that the ΔNT mutant is in fact retained in the same compartment as the wild type protein. For completion, transfections of ΔPY and ΔNT mutants with α-GM130 staining are also presented in figure 3.2.5, showing a similar pattern to the wild type; some overlap with the *cis*-Golgi marker, especially in the perinuclear region, but the majority scattered throughout the cytosol and not overlapping with the GM130 signal.

3.2.2.4 Nuclear vs. cytoplasmic localization of AR in the presence and absence of ligand

While it is well-established that AR can localise either to the cytosol or the nucleus, the exact distribution between the two compartments varies between cell lines. To try and establish precisely what percentage of AR is present in each compartment under different conditions, and to re-examine the AR localisation with a view to identifying possible areas of interaction with PMEPA1, we used GFP-tagged constructs (see appendix 5.2.4) to transiently transfect HeLa and LNCaP cell lines. The constructs used were wild type (WT) AR and a mutant containing a single point mutation at position 877

in the ligand-binding domain, T877A. This mutation is found in the endogenous AR of LNCaP line cells (Veldscholte et al, 1990) and affects the ligand-binding pocket, resulting in a decreased ligand binding specificity and greater transactivational activity (Sack et al, 2001). Examination of these tagged proteins expressed in cells showed that the addition of DHT to cells expressing wild type AR induced a large-scale shift, from either an exclusive cytosolic or diffuse cytosolic and nuclear pattern, to an almost exclusively nuclear pattern which also seemed to show higher levels of expression. This shift was recreated in cells transfected with tagged T877A-AR, and the presence or absence of ligand had no effect on the targeting of this mutant (figure 3.2.6). Figures 3.2.7 and 3.2.8 show examples of each of these distributions as well as the results of a statistical analysis involving ANOVA testing, to assess whether the number of cells showing each pattern differed between conditions, and pairwise post-hoc Tukey's tests to establish which of the conditions differed significantly from each other. In both Hela and LNCaP, there was a statistically significant difference in localisation between wild type protein in the absence of ligand, and wild type protein in the presence of ligand. There was also a significant difference between wild type protein in the absence of ligand and T877A in the absence of ligand, however there was no significant difference in localisation between wild type protein in the presence of DHT and T877A in the absence of DHT. In HeLa cells, 73.9% of cells transfected with WT-AR in the absence of DHT showed a nuclear and cytosolic distribution, 23.3% showed an exclusively cytosolic localisation and only 2.8% showed an exclusively nuclear localisation (n=180). When DHT was added to the culture medium for 24 hours, 65.1% of cells showed an exclusively nuclear localisation, 33.0% showed a nuclear-cytosolic distribution and only 1.9% showed an exclusively cystosolic distribution (n=106). When AR-T877A was expressed in the absence of ligand, 46.9% of cells showed an exclusively nuclear

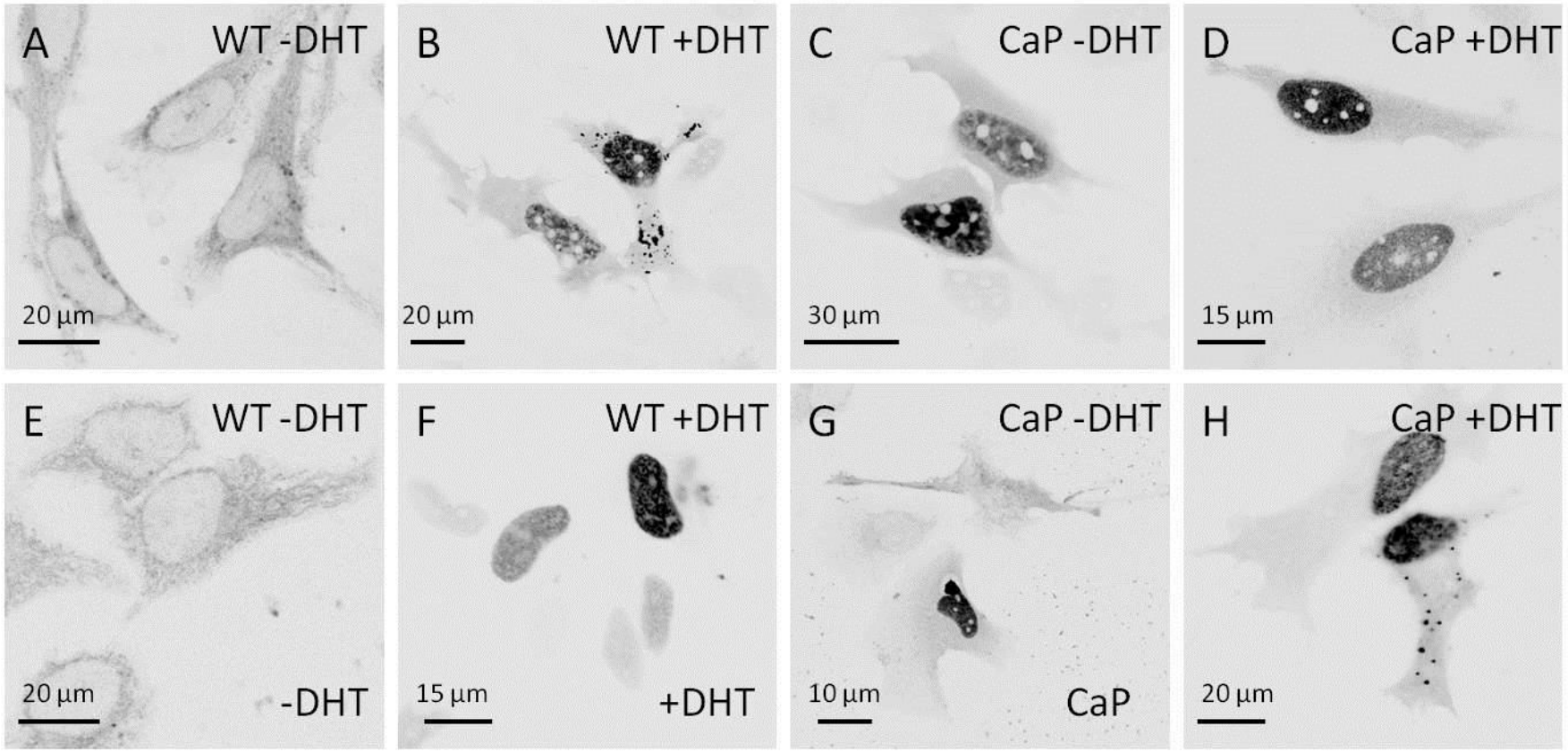

Figure 3.2.6. Confocal microscope images of GFP-AR transiently expressed in HeLa (**A-D**) and LNCaP (**E-H**) human cell lines. These are all representative images of five fields of view, each containing an average of 25 expressing cells. Cells were grown for 24 hours following transfection, then either 100 nM DHT or an ethanol control was added and the cells left for a further 24 hours prior to fixation. Cells were fixed using paraformaldehyde 48 hours after transfection and a representative cell cluster was imaged; GFP was excited at 488 nm to produce an emission spectrum across 500-570 nm. Images were desaturated and reversed to produce black-on-white images for easy comparison. For each cell line, WT-AR in the absence (**A, E**) and presence (**B, F**) of DHT is shown alongside AR-T877A (CaP) under the same conditions(**C, D, G, H**). AR-T877A, shows the same nuclear distribution as the activated wild type protein even in the absence of DHT or other ligands, as distinct from the cytosolic appearance of WT-AR when not activated by ligand binding.

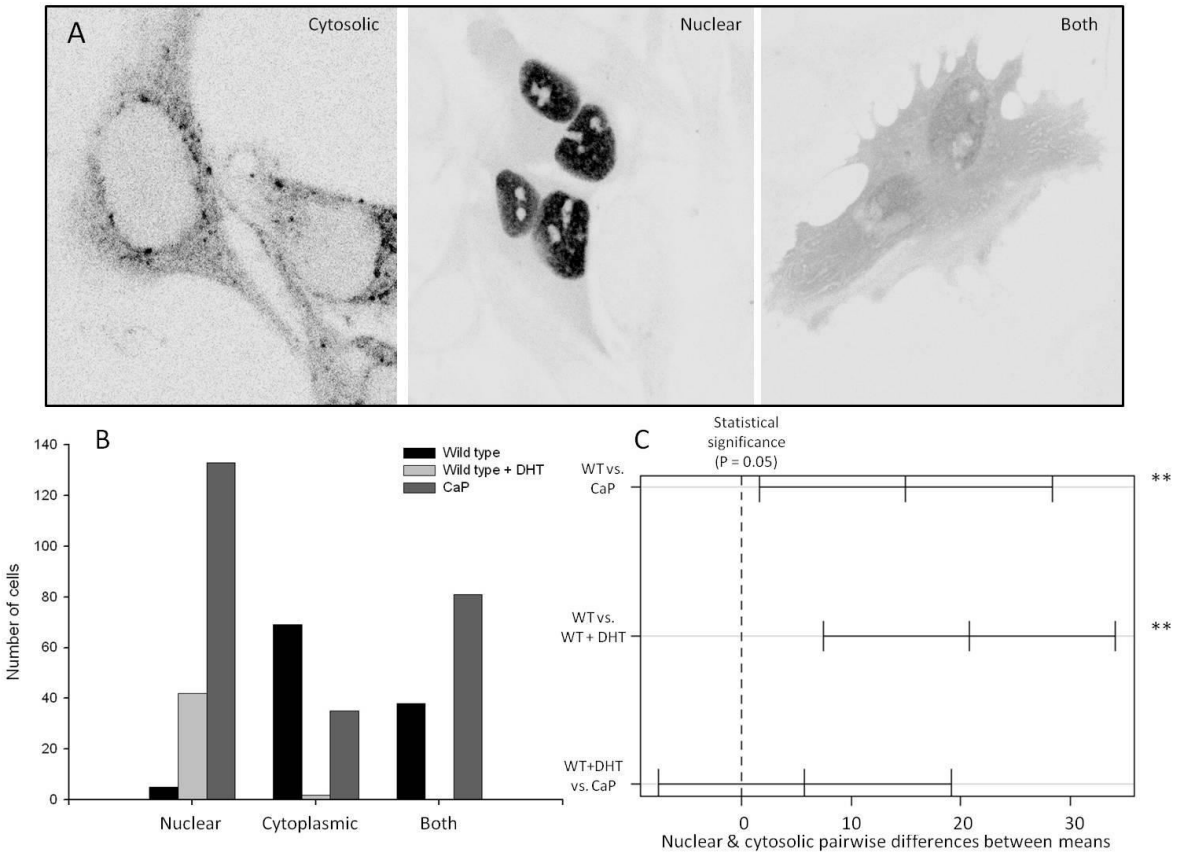

Figure 3.2.7. Panel (**A**) shows representative confocal microscope images of the three observed localisations of AR in HeLa cells - exclusively cytosolic, exclusively nuclear and nuclear/cytosolic. Cells were grown for 24 hours following transfection, then either 100 nM DHT or an ethanol control were added for a further 24 hours prior to fixation. Cells were fixed using paraformaldehyde 48 hours after transfection and a representative cell cluster was imaged; GFP was excited at 488 nm to produce an emission spectrum across 500-570 nm. Images were desaturated and reversed to produce black-on-white images for easy comparison. The histogram (**B**) shows the number of cells in each treatment category – WT-AR with only an ethanol control, WT-AR + DHT and AR-CaP (T877A) – showing each of these localisations. Panel (**C**) shows the results of Tukey's post-hoc testing showing pairwise comparisons of means of each group; the degree of difference is represented by the horizontal axis and each line spans 95% confidence when comparing two groups, as shown on the vertical axis. A statistically significant ($p<0.05$) difference between a given two groups is represented by asterisks on the right hand side.

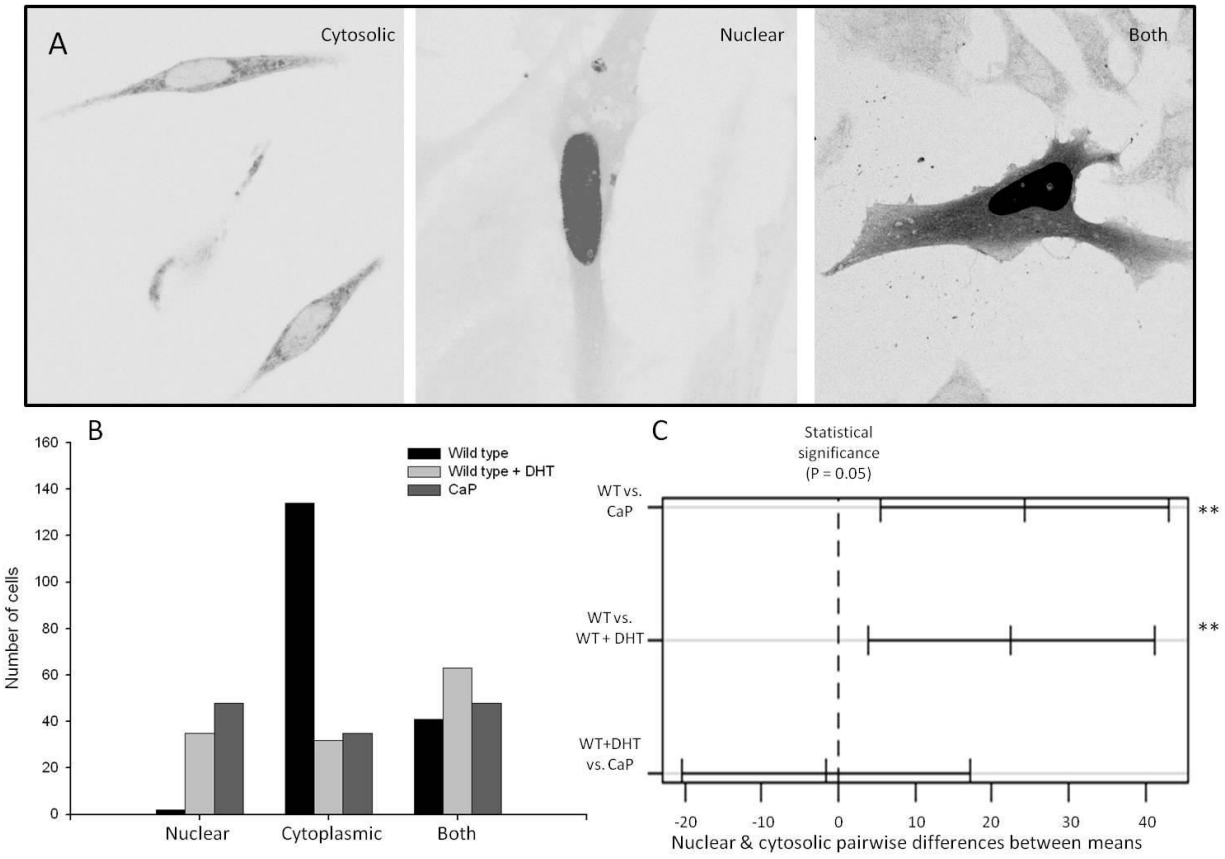

Figure 3.2.8. Panel (**A**) shows representative confocal microscope images of the three observed localisations of AR in LNCaP cells - exclusively cytosolic, exclusively nuclear and nuclear/cytosolic. . Cells were grown for 24 hours following transfection, then either 100 nM DHT or an ethanol control were added for a further 24 hours prior to fixation. Cells were fixed using paraformaldehyde 48 hours after transfection and a representative cell cluster was imaged; GFP was excited at 488 nm to produce an emission spectrum across 500-570 nm. Images were desaturated and reversed to produce black-on-white images for easy comparison. The histogram (**B**) shows the number of cells in each treatment category – WT-AR with only an ethanol control, WT-AR + DHT and AR-CaP (T877A) – showing each of these localisations. Panel (**C**) shows the results of Tukey's post-hoc testing showing pairwise comparisons of means of each group; the degree of difference is represented by the horizontal axis and each line spans 95% confidence when comparing two groups, as shown on the vertical axis. A statistically significant ($p<0.05$) difference between a given two groups is represented by asterisks on the right hand side.

distribution and 53.1% showed a nuclear/cytosolic distribution, but none were observed at all showing an exclusively cytosolic distribution (n=81). In LNCaP cells, the differences were slightly less stark but were still shown to be significant (see figure 3.2.5); 75.7 % of WT-AR in the absence of ligand was exclusively cytosolic, 23.2 % was nuclear-cytosolic, and only 1.1 % was nuclear (n=177), compared to 26.7 % cytosolic, 48.5 % nuclear-cytosolic and 26.9 % nuclear in the presence of DHT (n=130). 24.7 % of cells expressing AR-T877A showed cytosolic distribution, 36.6 % showed nuclear-cytosolic and 36.7 % showed exclusively nuclear (n=131).

3.2.3 Discussion

The initial observation that WT-PMEPA1 localises in a pattern that resembles part of the Golgi-ER pathway, but does not completely correspond to either the Golgi or the ERGIC, is consistent with the 2003 observation of Xu et al, which reported a *cis*-Golgi localisation. However on closer examination of the figures presented by Xu et al (2003) it is clear that PMEPA1 partially but by no means completely overlaps with the *cis*-Golgi marker. This is in contrast with other proteins reported as Golgi-localised, such as COH1 (Seifert et al, 2011), which overlaps almost completely with immunostained GM130. The fact that there is a slight overlap with the ERGIC may indicate that PMEPA1 is rapidly trafficked through the cell and is consequently only transiently present in specific compartments in a particular moment, but the high levels of protein, especially in transiently transfected cells, would be expected to compensate for that resulting in a signal which overlapped each of the compartments rather than none. Another possibility is that the spotted distribution observed actually corresponds to a different part of the secretory pathway, or another cellular compartment altogether, or

that the transmembrane domain of PMEPA1 in fact targets to several different membrane bound organelles, such as the perinuclear membrane and the lysosomal network. If PMEPA1 does localise to the secretory pathway, high levels of protein in transfected cells might cause a disruption to the Golgi morphology, such as that seen when the GTPase acceptor PRA1 is mutated and overexpressed (Gougeon et al, 2002). This is something that would certainly merit further investigation, possibly using alternative markers, along with the expression of mutants in the LNCaP line as well as HeLa. Figure 3.2.2 shows that wild type PMEPA1 expression in LNCaP is similar to that seen in HeLa, with weak, diffuse cytosolic signal and small, irregular areas of stronger signal in the same punctuate arrangement.

A very interesting observation is that that the removal of the transmembrane domain, which was predicted across four of the five localisation prediction programmes to completely alter the targeting of PMEPA1, has absolutely no impact on the protein's appearance within the cell. This construct was used extensively *in vitro* for the assays reported in chapter 3.1, because it was found to be much more soluble than the full length protein, which resisted recombinant purification. There is a possibility that the transiently transfected soluble PMEPA1 is associating with endogenous full-length protein at membranes, however there no evidence of dimerization in the literature. This would have been the subject of future experimentation if time permitted, and would be a priority for future experimentation. Alternatively, there may be a non-canonical means by which PMEPA1 is localising to its correct compartment, possibly mediated by other proteins; the RNA helicase RIG-1 translocates from the cytosol to the mitochondrial membrane in a process that relies on the chaperones TRIM25 (also a RING type E3 ligase) and 14-3-3ε, and is also ubiquitination-mediated (Liu et al, 2012). Another relevant example is the bacterial secretin PulD, which is targeted to the outer membrane

by binding to a dedicated chaperone called PulS (Nickerson et al, 2011). This binding causes a shift from mostly disordered secondary structure in PulD to a slightly more ordered, α-helical structure which is then targeted to the outer membrane; PMEPA1 is also predicted to have a mostly unstructured nature, so something similar may be occurring. Eliminating the three Nedd4-binding PY motifs has no effect on PMEPA1 localisation (see section 3.3) but the targeting process may be mediated by other, yet to be identified proteins.

The location studies on AR presented here are the first to show that the subcellular targeting of AR-T877A mimics that of the ligand-bound wild type protein, even in the absence of any activating molecules. This is in contrast to several previous findings; a 2002 paper on endogenous AR in LNCaP cells, which carries the T877A mutation, reported that the mutant protein accumulated in the nucleus following activation by oestrogens (Maggiolini et al, 2002), and that this was associated with upregulation of the AR target gene PSA. However, the immunostaining detection used in this study did not detect any AR in cells prior to the addition of ligand, in contrast to our studies and others which show that AR-T877A is constitutively expressed in LNCaP cells at relatively high levels regardless of the presence or absence of steroids (Nakauchi et al, 2007). Another paper, published around the same time and focussing on the xenoandrogenic properties of bisphenol A, reported only 20-40% of endogenous AR-T877A in LNCaP cells as showing nuclear distribution under androgen-depleted conditions, rising to 90-95% after the addition of DHT (Wetherill et al, 2002). While my statistical data supports the initial observation, finding that 36.7 % of transfected AR-T877A showed a nuclear distribution, my qualitative data (figure 3.2.6) does not indicate the same significant shift towards an exclusively nuclear arrangement. The similarity in the behaviour of both the wild type and mutant receptors in LNCaP cells compared to HeLa is interesting; Nakauchi et al

(2007) found significant differences in the distribution of transiently transfected wild type and T877A mutant AR between prostate and non-prostate cancer cell lines. This group reported that COS-1 cells showed a predominantly cytoplasmic distribution of AR-T877A in the absence and low concentrations of ligand, although their representative figures show some fluorescence in the nucleus at T-0 after the addition of DHT, while LNCaP cells showed a diffuse nuclear-cytosolic distribution that showed a rapid, complete shift to nuclear on addition of even a very low concentration (0.1 nM) of DHT. The authors conclude that the T877A mutation alone is not sufficient for the androgen hypersensitivity associated with LNCaP, but rather must be influenced by other intracellular factors, such as differently active cofactors or chaperone proteins; this is contradictory both to the findings presented here, and to functional analyses of the effects of the mutation on PSA expression in LNCaP and other cell lines (Magiollini et al, 2002; Wetherill et al, 2002). The differences in microscopy results may be put down to the use of living cells in the 2007 paper, while our experiments are based upon fixed, preserved cells, but this does not account for the inconsistency with the gene product analyses. Finally, a 2009 paper showed that endogenous AR-T877A in LNCaP cells showed a diffuse nuclear-cytosolic (with a large proportion of the protein shown in the nucleus) distribution when grown in the absence of steroids, but showed absolute nuclear translocation upon exposure to the synthetic androgen R1881 (Stan & Singh, 2009). However, these authors present only single cell images, and no statistical data to indicate that these observations are consistent; indeed, the focus of the paper is more on *in vivo* immunohistochemical data. Unfortunately, I did not carry out statistical analysis on AR-T877A in the presence of ligand, as the primary purpose of these experiments was to show that the mutant receptor behaves in a quantifiably similar way to the activated wild

type receptor, but this would certainly shed more light on which of these prior observations this data can be said to support.

The increased promiscuity of AR-T877A, a result of the single residue mutation making the ligand-binding pocket larger and more accessible to ligands other than testosterone and DHT (Sack et al, 2001), may account for the behaviour of the mutant if the receptor is constantly binding to and being activated by other components of the growth media, although the charcoal-stripped serum used should contain only trace amounts of steroid, if any. Alternatively, the mutation may interfere with the N/C regulation of AR, the intracellular association of the ligand-binding domain and with the DNA-binding domain, which stabilises the bound ligand and potentiates the receptor activity (see section 1.4.3) and is usually terminated on translocation to the nucleus, resulting in potentiated activation even in the absence of ligand binding. However, this is not such a clear-cut conclusion; while AR-T877A is apparently localised in the same way as the ligand-bound wild type, it is not necessarily the case that the transcriptional activation capacity is constitutively raised, as follows DHT-binding to the wild type. AR-T877A, as the only endogenous AR present in the LNCaP line, has been shown to mediate increased cell proliferation in the presence of DHT compared to controls, and to have increased levels of expression induced by the addition of androgens (Yeap et al, 1999). A more recent study found a high level of transcriptional activity of AR-T877A in the absence of ligand (Sun et al, 2006), but there is no evidence in this paper that the experiments performed in the 'absence' of steroid were performed using stripped media of any kind. However, the fact that the T877A mutation is prevalent in advanced metastatic prostate cancers (Gaddipati et al, 1994), and that the LNCaP cell line is sensitive to androgens (Horoszewitz et al, 1983), indicate that the steroid binding to the mutant protein must precipitate some function that the unbound mutant cannot fulfil. The

constitutive nuclear localisation and raised expression levels may in fact be indicative of low transcriptional activity, for example if the presence of more AR than would normally be expected in the nucleus resulted in increased exposure to co-repressors which inhibit its activity, resulting in a large amount of inactive, nuclear mutant protein. Regardless of transcriptional activation of the endogenous mutant in LNCaP cells, the mechanism behind the nuclear localisation does not induce the same pattern in the exogenous wild type protein, as evidenced by the fact that the majority of GFP-tagged wild type AR expressed in LNCaP in the absence of steroid was cytosolic, with a shift to nuclear/cytosolic or nuclear distribution observed only on the addition of DHT. This is the same pattern observed in HeLa cells, without the activated endogenous AR, and indicates that the processes set in motion by the activation of AR, whether that is selective degradation, increases nuclear import or both, are not self-perpetuating and are dependent on the structural alterations that occur on AR following ligand binding. Future work to investigate the impact of inhibiting protein degradation and intracellular trafficking on the DHT-mediated localisation shift would help shed light on the intricacies of this process.

In conclusion, the data presented here represent a systematic study of the localisation PMEPA1 and AR, in various forms, for the first time. The role of the transmembrane domain of PMEPA1 seems more complex than was previously thought, as its absence does not preclude the trafficking of PMEPA1 to the secretory pathway and an as-yet unidentified compartment. The mutant T877A androgen receptor is shown to be located almost exclusively in the nucleus, and to mimic the distribution of ligand-bound wild type even in the absence of steroid, however further work on the transcriptional activity of both forms of AR is required to clarify if the ligand-precipitated functions are also mimicked by this mutant. An interesting side observation, seen particularly clearly in

figure 3.2.6B, is that occasionally AR appears to have a spotty distribution in the cytoplasm, either alone or alongside some protein in the nucleus, in contrast to the even appearance seen more commonly and shown in figures 3.2.6A, C and D. This looks remarkably similar to the distribution of PMEPA1 shown in figures 3.2.2 & 3.2.3, and could shed some light on the physical interactions behind the proposed PMEPA1-AR feedback mechanism. This possibility is examined in more detail in the next chapter.

3.3 *In vivo* association between Nedd4, PMEPA1 and AR

3.3.1 Introduction

3.3.1.1 Physical interaction between Nedd4, PMEPA1 and AR

PMEPA1 has been shown to interact directly and non-transiently with Nedd4 through co-immunoprecipitation studies (Xu et al, 2003). Similarly, AR has been shown to co-precipitate with PMEPA1 (Li et al, 2008). However, there is no direct evidence of a direct interaction between AR and Nedd4, and the basis for the hypothesised negative feedback loop, described in detail in section 1.4.4, between AR and PMEPA1 is that PMEPA1 acts as an adaptor to facilitate Nedd4-mediated ubiquitination of AR. Ubiquitination of AR has been widely reported, mediated by several RING-type ligases including Mdm2 (Lin et al, 2002), RNF6 (Xu et al, 2009) and Siah2 (Qi et al, 2013), however Nedd4 has never been directly shown to utilise AR as a substrate. The fact that the loss of the 2 canonical PY motifs in PMEPA1 appears to attenuate its ability to downregulate AR points to Nedd4 involvement, corroborated by a direct observation that Nedd4 levels are influenced by AR levels and *vice versa* (Li et al, 2012). However, there are some aspects of the theory that warrant further investigation in order to clarify the precise nature of the association between AR and Nedd4. AR is well-documented as localising to the nucleus or cytoplasm, or a combination of the two (Jenster et al, 1993) and this is corroborated by the results detailed in section 3.2 showing redistribution of AR into the nucleus on addition of a ligand. PMEPA1, however, shows a spotty distribution over the perinuclear and cytoplasmic region, and although PMEPA1 and AR were shown to co- immunoprecipitate in the LNCaP line (Li et al 2008), no consideration has been given to this apparent difference in localization. In addition, although there is

abundant *in vitro* evidence for PMEPA1 and Nedd4 interaction, it is not clear where in the cell this takes place, as Nedd4 adopts a cytosolic distribution similar to that of AR prior to ligand binding (Anan et al, 1998).

3.3.1.2 Testosterone activation of AR and the effects on PMEPA1 and Nedd4

AR binds specifically to the male hormone testosterone, with approximately half the affinity as to its potentiated metabolite dihydrotestosterone (DHT) (Grino et al, 1990). The conversion from testosterone to DHT is catalysed by the enzyme 5α-reductase, the cellular distribution of which varies by age and gender. When AR binds to a ligand, AR alters conformation from a relatively unfolded, loose structure to a more compact, tightly folded shape in which the N- and C-termini are closely associated; this is followed by movement of the receptor into the nucleus and rapid dimerization (Schaufele et al, 2005). The subsequent transcriptional activation of a variety of genes, including PMEPA1, is the basis of all testosterone-mediated cellular effects. PMEPA1 is a direct transcriptional target of AR, and is highly androgen-induced, with expression levels reported as 29 times higher in the presence of the artificial AR ligand R1881 (Xu et al, 2000), and this is the theoretical basis for the negative feedback loop for regulation of AR. Up-regulation of PMEPA1 has also been noted in other endocrine cancers, such as breast cancer (Singha et al, 2010) but this does not appear to be induced by other hormones such as oestrogen or progestogen, indeed the tissues in which enhanced expression was found are receptor-negative tumours.

None of the Nedd4 family ligases, unlike PMEPA1, are known to be directly induced by androgens, however there is some evidence of an indirect association, indicated by the observation that AR up-regulates expression of Nedd4, although a full methodology is yet to be published (Li et al, 2012). In addition, the PMEPA1-mediated regulation of AR

described in detail previously is attenuated upon the loss of the two canonical PY motifs in PMEPA1, strongly implying a Nedd4-mediated mechanism. Nedd4-2 has previously been identified as binding to the aldosterone-induced kinase SGK-1 as part of the regulation of the sodium transporter ENaC (Wiemuth et al, 2010), a nuclear receptor response pathway with parallels to that induced by testosterone.

3.3.1.3 Potential role of the proteasome vs. ubiquitin-mediated trafficking

As well as its best-studied and widely-known role as a proteasome targeting signal, the modification of proteins by ubiquitination has several other functions. With regards to the role of ubiquitination in AR-mediated signalling, the RING E3 ligase RNF6 catalyses the formation of K6- and, to a lesser extent, K27-linked chains on AR, however this is not associated with any decrease in stability (Xu et al, 2009). Recruitment of another RING ligase, Siah2, has been reported to decrease the half-life of AR by a factor of three (Qi et al, 2013), and this is consistent with the identified K48-linked chain topology, associated with proteasomal targeting (Finley et al, 2004). Conversely, MDM2 is associated with increased turnover of AR in a process that is proteasome dependent and regulated by phosphorylation of AR (Chymokowitch et al, 2010), despite previous reports of MDM2 catalysing specifically the formation of K63-linked lysine chains (Sehat et al, 2008), which are generally a marker for non-proteasomal activity. Nedd4 has previously been identified as catalysing the formation of predominantly K63-linked (Fan et al, 2013, Tofaris et al, 2011), as well as occasionally K11-linked chains (Platta et al, 2012), which would seem to indicate a non-proteasomal role in PMEPA1-mediated AR regulation, but that is not consistent with the negative feedback mechanism proposed by Li et al in 2008.

3.3.2 Results

3.3.2.1 In vivo interaction between PMEPA1 and Nedd4

While we have been able to efficiently and consistently reproduce *in vitro* interactions between recombinant Nedd4 and PMEPA1, and shown these to be dependent on the two canonical and single variant PY motifs on PMEPA1 (see chapter 3.1), *in vivo* interactions are more difficult to quantify. Xu et al (2003) used immunoprecipitation to show binding between transiently transfected, tagged PMEPA1 and Nedd4 expressed in HEK293 cells, but there has not been any subsequent published investigation of this complex formation. To investigate the *in vivo* interaction between Nedd4, PMEPA1 and AR initial experiments involved overexpressing wild-type PMEPA1 and PY motif mutants, in order to assess the outcome of interfering with the ability of PMEPA1 to interact with Nedd4 a construct of full length PMEPA1, with a dual epitope tag of cMyc (MEQKLSEED) and the IgG-binding domain of protein A at the C-terminus (giving a predicted MW of 45.7 kDa) was expressed in HeLa cells (figure. 3.3.1A). In addition to the wild-type PMEPA1 sequence mutated versions each with a single PY motif inactivated through tyrosine-alanine substitution at the crucial fourth position (see section 3.1) were also transiently expressed in HeLa cells. The results of this transient expression are, shown in figure 3.3.1, where an expected band of approximately 45kDa was observed with wild-type PMEPA1 with both anti-myc (figure 3.3.1A) and peroxidase-anti-peroxidase that binds the protein A domain (figure 3.3.1B). Very interestingly, a smaller epitope-positive fragment of approximately 25 kDa was also observed with wild-type and all of the PY motif mutants used except Y216A (ΔPY2) where a single band of approximately 38 kDa was observed (figures 3.3.1A and B) with both epitopes. All constructs were sequenced prior to recombinant expression and known

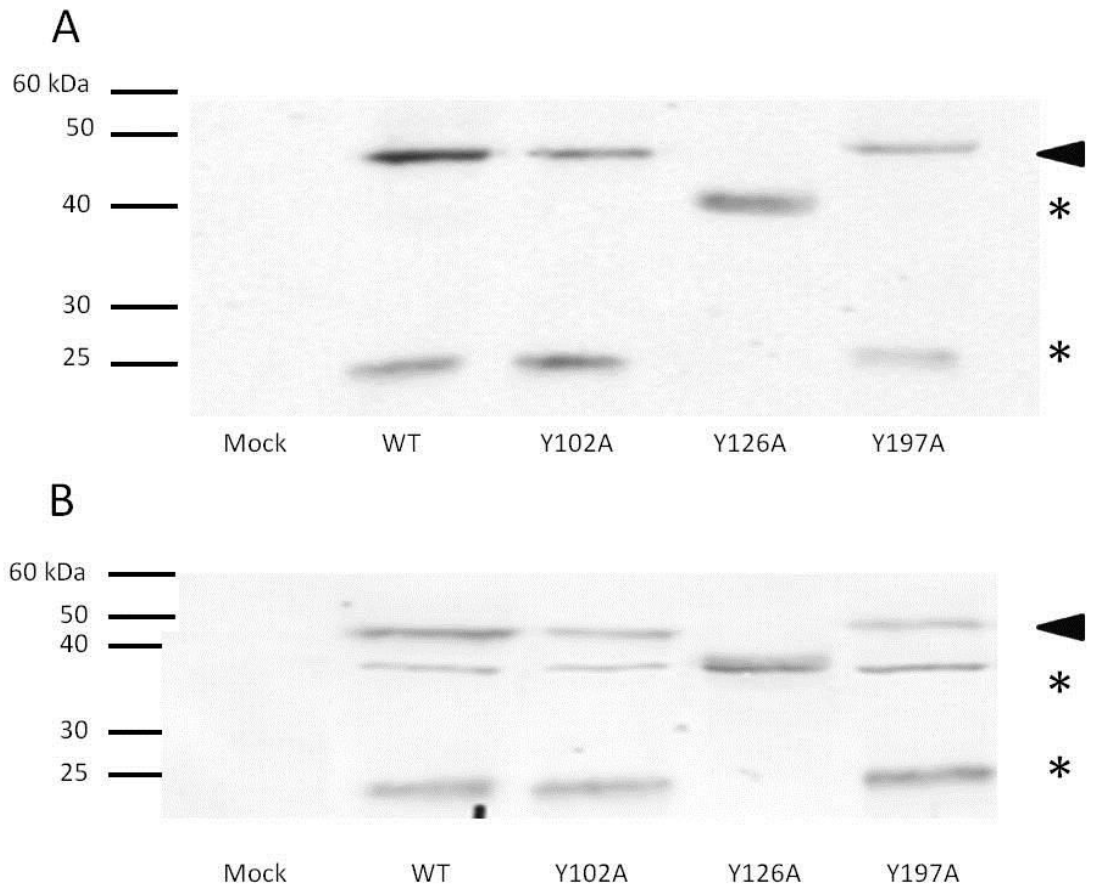

Figure 3.3.1. Western blots showing Myc-IgG-tagged PMEPA1 transiently expressed in HeLa cells. Proteins were harvested using detergent lysis and visualised using SDS-PAGE followed by Western blotting using anti-Myc primary and anti-mouse HRP-conjugated secondary (**A**) or peroxidase anti-peroxidase (**B**). Mock lanes show lysate from cells transfected with empty vector under the same conditions. Bands corresponding to tagged PMEPA1 were observed at the expected size, ~45kDa, at indicated by the black arrow on the right hand side, as well as ~38kDa and ~25kDa, indicated by asterisks. The largest and smallest bands are observed in every PMEPA1 construct with the exception of Y126A. The band corresponding to the 38 kDa size is observed in Y126A, but is absent or greatly reduced in the wild type protein, as well as the Y102A and Y197A single mutants.

to produce proteins of the same size, with only substitution mutations introduced as opposed to truncations or additional stop codons. Although not visible when using anti-myc, when the more sensitive peroxidase-anti-peroxidase detection was used, the 38 kDa was visible with all constructs although was clearly more abundant with Y126A (figure 3.3.1B).

Unfortunately, attempts to recreate the 2003 co-immunoprecipitation experiment failed due to difficulties in obtaining sufficiently high protein levels for accurate detection This could have been due to using a different cell line (HeLa instead of HEK293) or a different protein tag (PMEPA1-Myc instead of PMEPA1-V5), or simply due to the size of the culture vessels used. Attempts to use fluorescence resonance energy transfer (FRET) to elucidate if subcellular locations of Nedd4 and PMEPA1 are in close enough proximity (<10 nm) for photon transfer were partially successful (figure 3.3.2), showing some FRET signal in the perinuclear and cytoplasmic regions of some cells expressing both proteins. This signal also appears, although somewhat fainter, in cells co-expressing Nedd4 and a triple mutant Y102A/Y126A/Y197A (ΔPY) which is prevented from interacting with Nedd4; the triple PY mutant retained a small (< 10% compared to wild type) ability to be ubiquitinated by Nedd4 so it is possible that this signal is due to the same residual interaction. However, this is much less likely in a crowded cellular environment compared to *in vitro,* where protein levels are much higher, so difficult to be sure whether this is a true signal or due to some bleed-through from the overlapping emission spectra of the green and red fluorescent proteins. As reported in section 3.2, confocal microscope images of PMEPA1 WT and ΔPY co-expressed with different fluorescent tags in HeLa have already been established as showing no difference in subcellular localisation or apparent expression levels

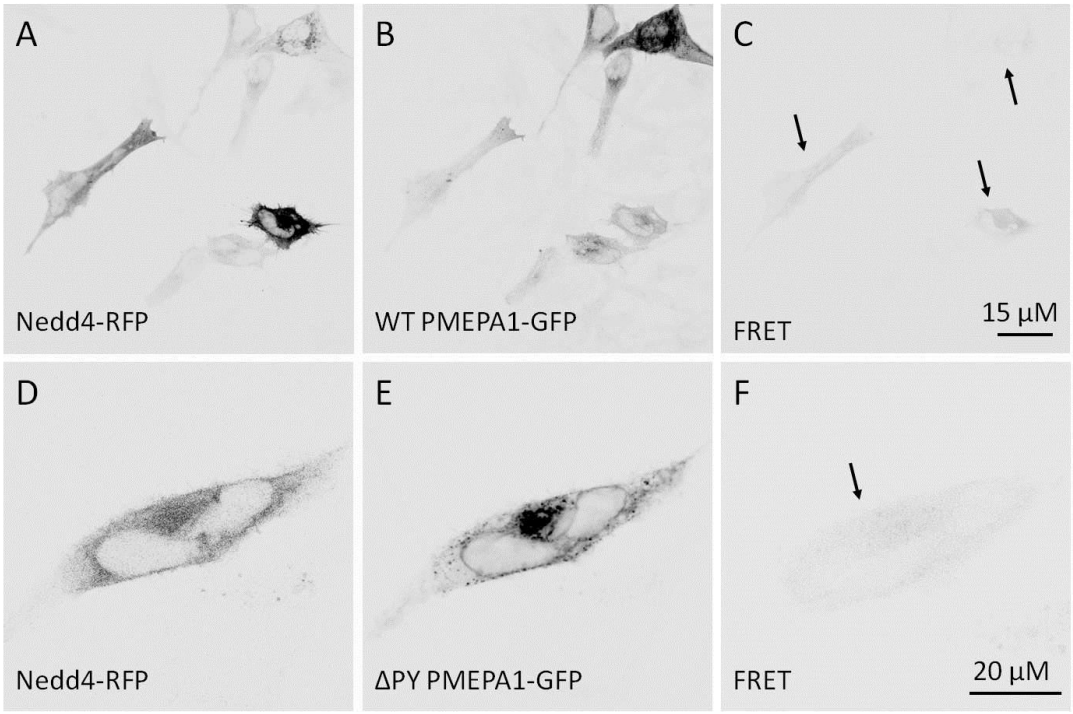

Figure 3.3.2. Confocal microscope images of fixed HeLa cells transiently cotransfected with PMEPA1-GFP, wild type (WT) or Y102A/Y126A/Y197A (ΔPY), and Nedd4-RFP. Cells were fixed using paraformaldehyde 48 hours post-transfection, mounted and a representative cell cluster was imaged. Red channel (**A** and **D**) was excited at 633nm to produce an emission spectrum across 660-750nm, green channel (**B** and **E**) was excited at 488nm to produce an emission spectrum across 500-570nm. To produce FRET images (**C** and **F**), the green fluorescence was excited at 488nm, but the emission spectrum was collected across 660-750nm, to ensure only RFP-spectrum excitation was detected. Images were desaturated and reversed to produce black-on-white images for easy comparison. There appears to be some FRET signal produced by interaction with both WT and to a lesser extent ΔPY, indicated by the black arrows.

(figure 3.2.2) when the Nedd4-interacting motifs are removed.

3.3.2.2 Effect of testosterone on Nedd4 levels and implications for Nedd4-AR interaction

I used a succession of experiments to infer a role for AR in Nedd4 regulation, or *vice versa*, by altering the levels of ligand, and therefore AR transcriptional activity. The hypothesis being tested was that induction of AR activity is the signal for up-regulation of PMEPA1, which in turn seems to regulate AR in a process which recruits Nedd4; therefore any alteration in Nedd4 levels or localisation associated with increased cellular DHT would be linked to the activation of AR. There was sufficient quantity of lysate from these experiments to run an α-Nedd4 blot concurrently with the α-AR blot, which also offered the opportunity to examine any potential effect on Nedd4 levels as a result of AR activation, in light of the increasing literature evidence of a two-way interplay between the two proteins (Li et al, 2012). Initial observations were undertaken to assess endogenous Nedd4 and AR levels in the presence and absence of DHT and in cell lines with (LNCaP) and without (HeLa) AR expression. The results are shown in figure 3.3.3; while the western blots are of poor quality due to the relative lack of control over signal intensity afforded by the ECL method, it can be seen that there is a no apparent variation in Nedd4 abundance on addition of DHT within both cell lines. However, this cannot be quantified in the absence of a loading control; provisional indications are that Nedd4 is neither up-regulated nor degraded when AR is activated. Higher levels of AR are seen in response to DHT treatment in the LNCaP cell line, consistent with previous findings; as expected, there is no AR present in the HeLa cell line.

Figure 3.3.4 shows the results of the addition of the Eukaryotic protein synthesis inhibitor cycloheximide to both HeLa and LNCaP cell lines on endogenous Nedd4

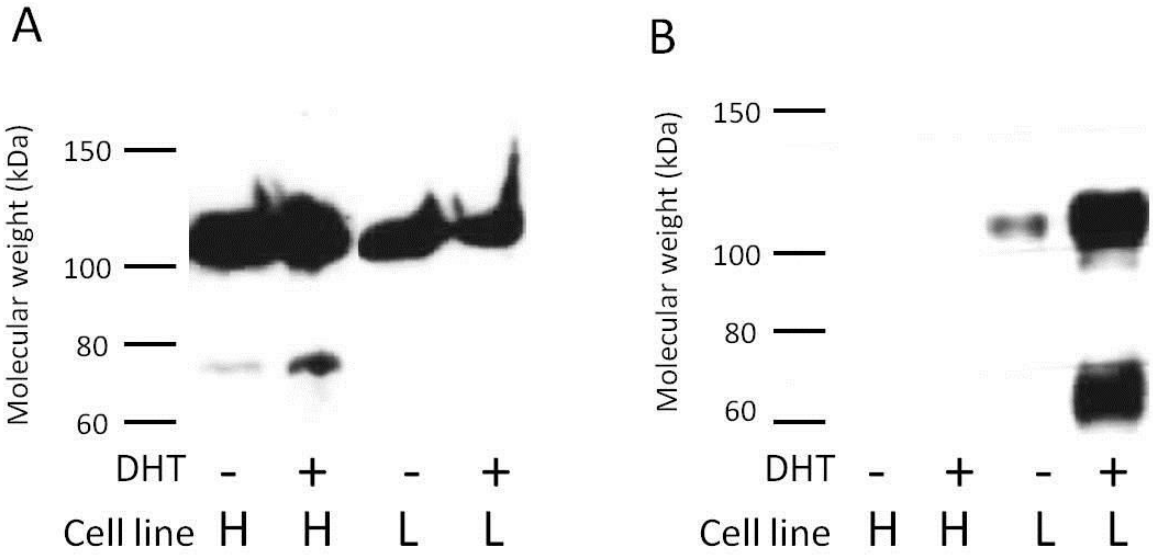

Figure 3.3.3. Western blots showing endogenous Nedd4 (**A**) and AR (**B**) from untransfected cells harvested by detergent lysis. The cell line is indicated by H (HeLa) or L (LNCaP). Cells were grown in charcoal-stripped MEM for 48 hours following passage, then either 100 nM DHT or an ethanol control was added to the medium for a further 24 hours. Lysates were run on SDS-PAGE followed by western blotting using anti-Nedd4 primary and anti-rabbit HRP-conjugated secondary or anti-AR primary and anti-mouse HRP-coupled secondary The main band for Nedd4 is ~120kDa in size compared to ~110kDa for AR. Both proteins seem to show higher levels of the main band of protein, as well as lower molecular weight degradation products, in HeLa compared to LNCaP. Nedd4 undergoes no change in cellular levels on the addition of DHT while AR levels are increased in LNCaP.

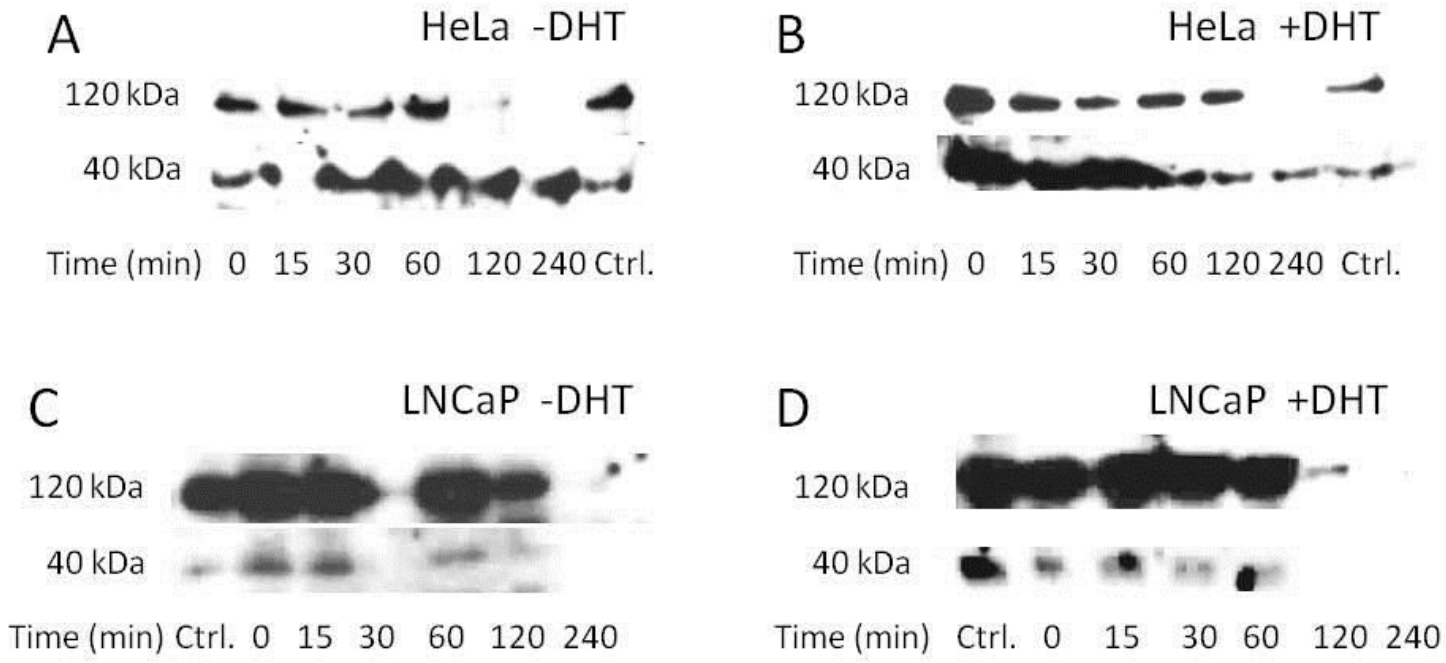

Figure 3.3.4. Western blots showing endogenous Nedd4 from untransfected cells following the addition of 50µg/ml cycloheximide to the growth medium and harvested by detergent lysis. Panels (**A**) and (**B**) show the products of HeLa cell lysates in the absence and presence of DHT, while panels (**C**) and (**D**) show the products of LNCaP cell lyastes. Cells were grown in charcoal-stripped MEM for 48 hours following passage, then either 100 nM DHT or an ethanol control was added to the medium for a further 24 hours. Control samples had water added in place of cycloheximide and were harvested after 240 minutes. Lysates were run on SDS-PAGE followed by western blotting using anti-Nedd4 primary and anti-rabbit HRP-conjugated secondary. The membranes were then stripped by incubating in a solution of 0.1M glycine and 1% w/v SDS (pH 2.2) and reincubated in anti-actin primary and anti-rabbit HRP-conjugated secondary. The Nedd4 band at 120 kDa shows declining levels over four hours, while the actin loading control (40 kDa band) shows that overall protein levels in the LNCaP cell line are lower than in HeLa, despite the Nedd4 signal being stronger.

levels. This experiment was to attempt to determine the half-life of Nedd4 and AR in the presence and absence of DHT since if the activation of AR results in Nedd4 and/or PMEPA1 recruitment that might be associated with a decrease in Nedd4 stability when activated by the ligand. Unfortunately the anti-AR blots produced no signal at all over several attempts, even in a control lane with no cycloheximide present, so I was not able to infer anything about the stability of endogenous AR in different activation states. However, I was able to detect Nedd4 in the lysates; the role of Nedd4 in the PMEPA1 feedback mechanism is still unclear, but following addition of cycloheximide in the absence of DHT an apparent decrease in Nedd4 levels can be seen in both HeLa and LNCaP cells over the course of 4 hours, particularly between 60 and 120 minutes (figures 3.3.4A and 3.3.4C). In HeLa, addition of DHT appears to slightly stabilise Nedd4 with some protein being observed 120 minutes following the addition of cycloheximide following DHT treatment (figure 3.3.4B). However in LNCaP, the opposite appears to be true in that addition of DHT results in lower Nedd4 abundance at 120 min although the actin signal suggests that the overall protein level in that particular sample may also lower. It should also be noted that in relative to the actin loading controls the levels of endogenous Nedd4 appear to be higher in extracts from LNCaP cells as compared to HeLa (figures 3.3.4A and 3.3.4C) supporting the hypothesis that DHT (or a mutation that mimics AR binding to DHT) stabilizes Nedd4. However, signal from the loading controls is relatively low and inconsistent, meaning that the Nedd4 signal unfortunately cannot be accurately quantified; these are speculations rather than conclusions.

3.3.2.3 Effect of testosterone on Nedd4 and AR localisation

The question of where in the cell any interaction between Nedd4 and AR might occur was still unanswered, given that the trigger for such an interaction appears to be activation of AR and movement into the nucleus, when Nedd4 is a soluble, cytosolic protein. While the effect of DHT on AR has been shown to induce nuclear localisation (see section 3.2), the potential effect on Nedd4 has not been assessed. To see whether there was any co-localisation between Nedd4 and AR upon ligand binding, which might point to a direct interaction, confocal microscopy was used to visualise the response of Nedd4 to DHT on a subcellular level. Figure 3.3.5 shows the result of the addition of DHT which, as seen previously, causes a distinctive large-scale shift from a diffuse cellular expression pattern to an exclusively nuclear localisation for AR (Fig. 3.3.5D). In contrast, in these cells RFP-Nedd4 remains cytoplasmic regardless of the presence of DHT (Fig. 3.3.5E). There is, however, an apparent change in the Nedd4 distribution from diffuse signal in the absence of DHT to a more punctate appearance in the presence of DHT. While this does not coincide with any increased association with AR, in fact the opposite is true as AR is almost entirely excluded from any compartment except the nucleus under these conditions, it intriguingly does resemble the localisation pattern of PMEPA1 (as shown in figure 3.2.1)

3.3.2.4 Investigating the postulated feedback loop between AR and PMEPA1

In order to further elucidate the potential mechanism of the observed interplay between PMEPA1 and AR, LNCaP cells were transiently transfected with FLAG-histidine-tagged ubiquitin (figure 6.2.5; derived from that used in Novoselova et al 2013) alongside PMEPA1 and/or Nedd4. The cells were lysed in a guanidine-based denaturing

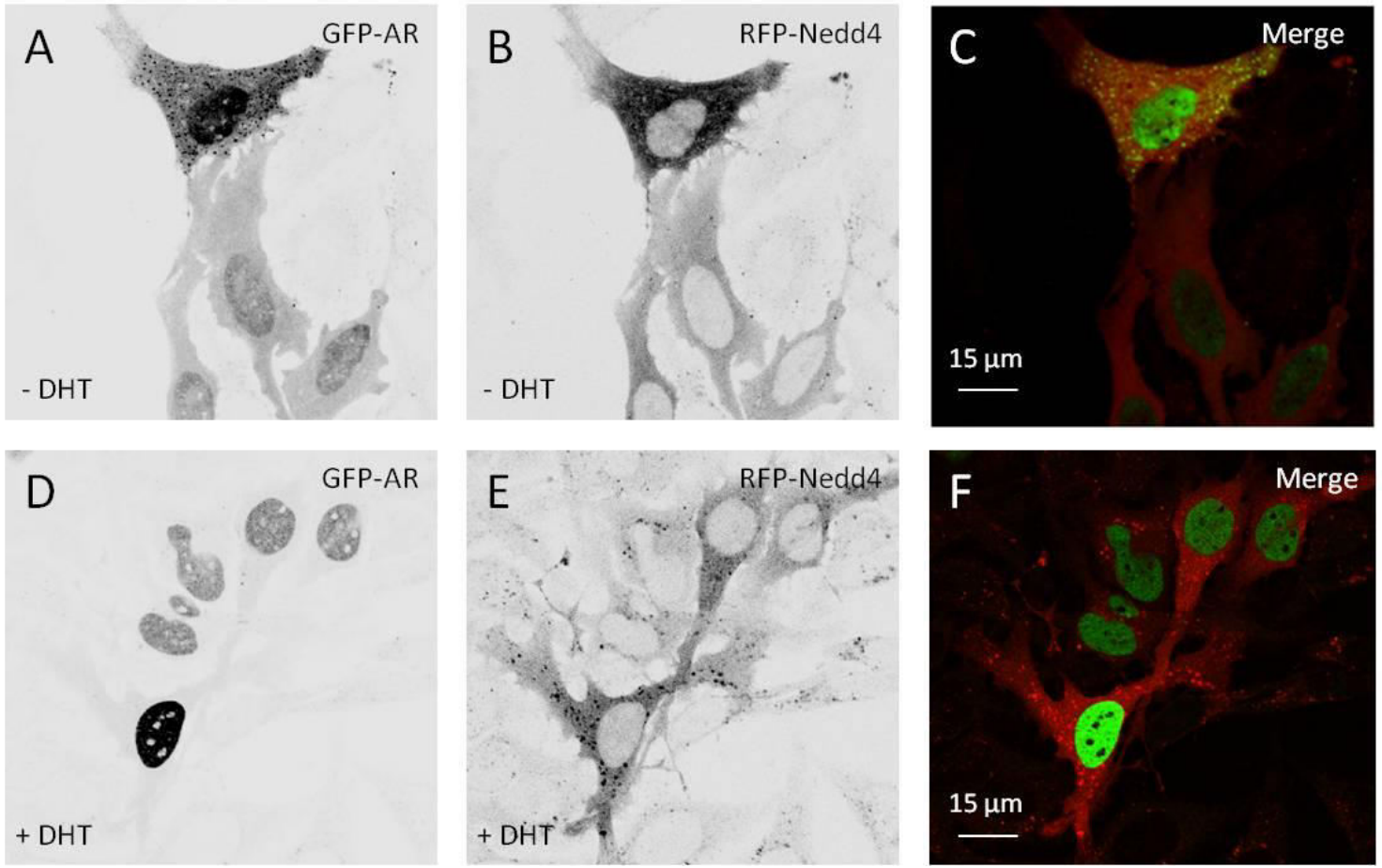

Figure 3.3.5. Confocal microscope images of HeLa cells transiently co-transfected with RFP-Nedd4 and GFP-AR. Cells were fixed using paraformaldehyde 48 hours post-transfection, mounted and a representative cell cluster was imaged. Green channel (**A & D**) was excited at 488nm to produce an emission spectrum across 500-570nm. Red channel (**B & E**) was excited at 633nm to produce an emission spectrum across 660-750nm, The single channel images were desaturated and reversed to produce black-on-white images for easy comparison, and the overlaid channels are shown in sections **C & F.** Nedd4 can be clearly seen to be expressed in the cytoplasm at variable levels, and this does not appear to be altered by the addition of DHT, although its appearance in panel E resembles the Golgi-like distribution of PMEPA1. In contrast AR can be seen to switch from a nuclear-cytosolic, diffuse expression pattern throughout the cell to an exclusively nuclear localisation on the addition of DHT, and this eliminates any areas of overlap in the merged images.

buffer, and HisSelect nickel resin (Sigma Aldrich) was used to capture the His-tagged ubiquitin, along with any covalently attached proteins. A western blot was performed on the samples using anti-AR antibody in order to determine whether directly ubiquitinated endogenous AR could be detected, and whether the level of protein and extent of ubiquitination was affected by increased levels of PMEPA1 and/or Nedd4. The result is presented in figure 3.3.6; a higher molecular weight AR band is clearly seen in the presence of PMEPA1 and ubiquitin but this modification appears to be lost on the addition of Nedd4. However, levels of Nedd4 were not high enough to be detected in the same sample, although ubiquitin was highly expressed, making interpretation of the result difficult. AR does appear to be modified, but whether this is mediated by Nedd4 or a result of previously reported *in vivo* interactions is unclear, and the fact that these experiments were not able to be repeated means that any conclusions are at best preliminary.

Having assessed the modification status of AR, the next step was to try to establish whether the PMEPA1-mediated regulatory effect previously reported was ubiquitin-proteasome mediated, or dependent on a non-proteasomal function of ubiquitination. The original experiment (Li et al, 2008), expressing AR in the presence and absence of PMEPA1 and assessing the effect of adding the proteasomal inhibitor lactacystin, did not factor in the potential effect of depletion of the free ubiquitin pool on cellular processes. In order to assess whether compensating for this depletion, by overexpressing transiently transfected ubiquitin, eliminates the observed PMEPA1 down-regulation of AR, the experiment was repeated with ubiquitin co-expressed in each well. The results are shown in figure 3.3.7; the significant drop in AR levels reported by Li et al in 2008 in response to co-expressing PMEPA1 in the absence of ubiquitin is not seen when ubiquitin levels are increased in this way, and adding lactacystin in this case does not seem to result in

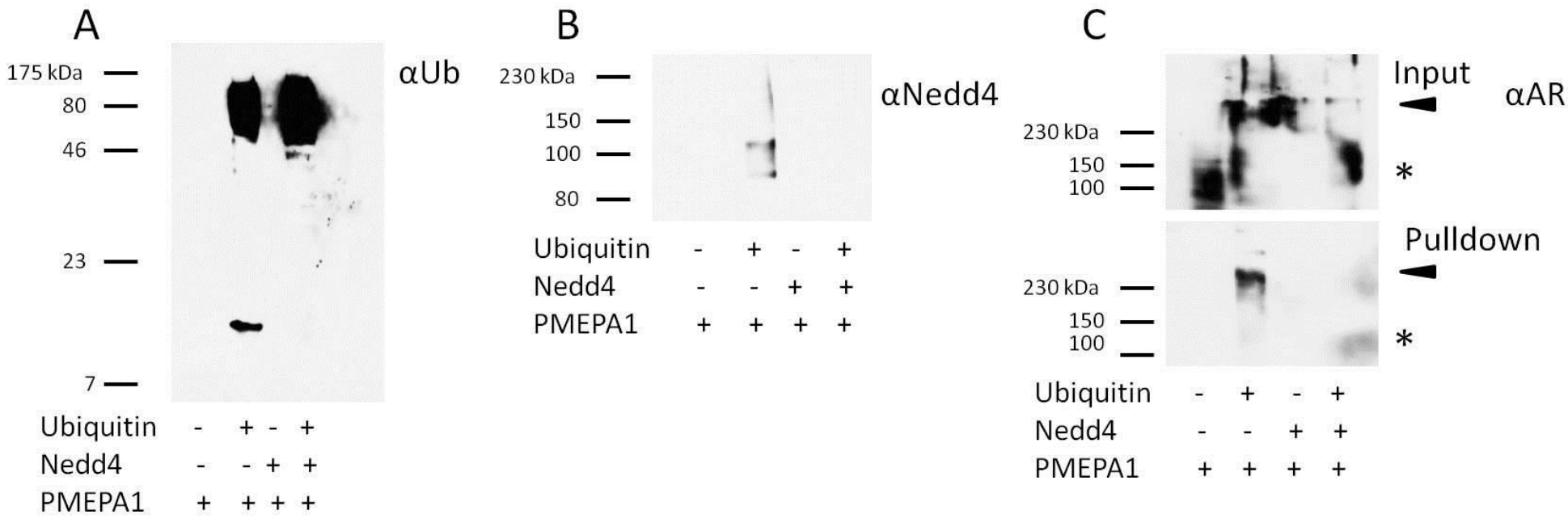

Figure 3.3.6. Results of a denaturing immunoprecipitation of a histidine-FLAG tagged ubiquitin construct, expressed alongside PMEPA1 and in the presence and absence of GFP-tagged Nedd4, in HeLa cells 48 hours post-transfection. Ubiquitin was precipitated via the histidine tag using HisSelect nickel resin in denaturing conditions. Panels (**A**) and **(B**) shows the same input samples detected using anti-FLAG primary (**A**) and anti-Nedd4 primary (**B**); ubiquitin is clearly expressed in both positive samples and is absent from the controls as expected. A greater proportion of the exogenous ubiquitin appears to be incorporated into conjugates in the presence of Nedd4, as indicated by the absence of an ~8 kDa band representing free ubiquitin. Unfortunately Nedd4 itself is only visible in one of the two lanes it was transfected in, and that is the control lane. Panel (**C**) shows total lysate (input) and pulldown samples with endogenous AR detected by western blots using anti-AR primary and anti-mouse HRP-conjugated secondary. A smeared band corresponding to the expected size of unmodified AR (~110 kDa) is visible but only in the negative contol lane of the input sample without Nedd4, indicated by the asterisk on the right hand side. A higher molecular weight product, indicating post-translational modification, is visible in three of the four input lanes and in the pull-down samples without Nedd4, indicated by the black arrow on the right hand side.

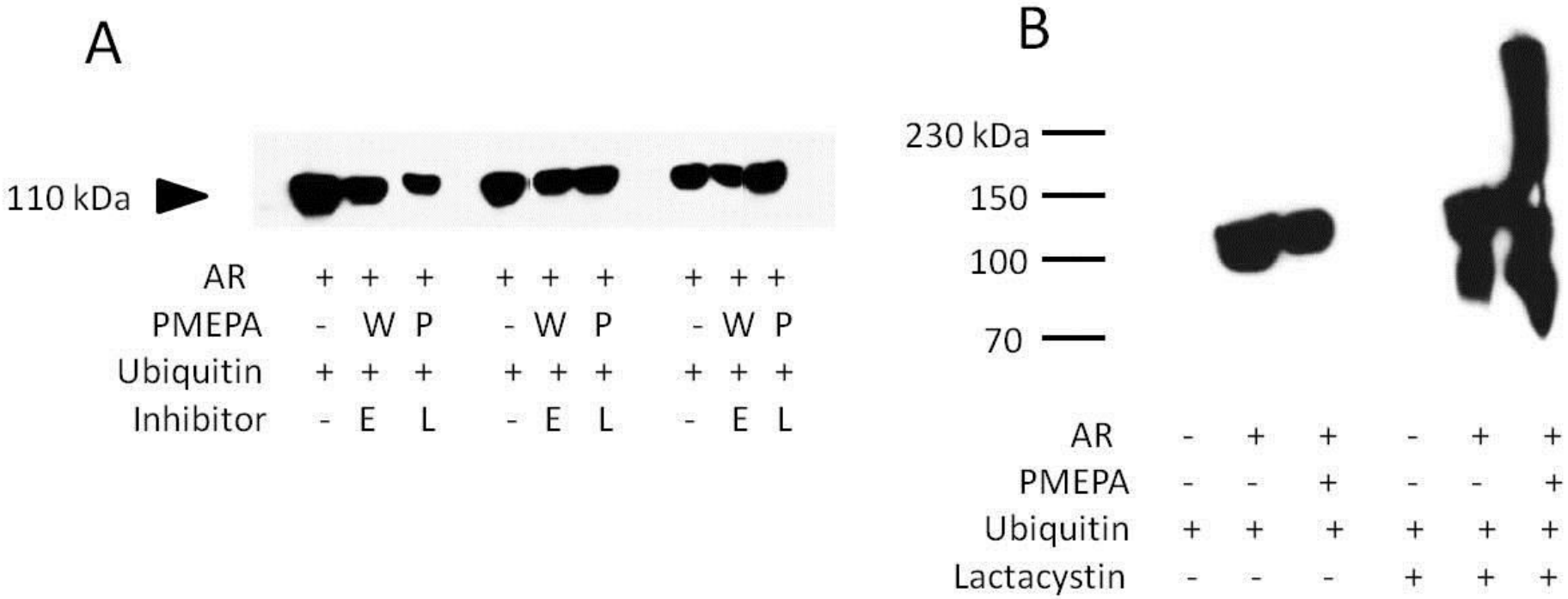

Figure 3.3.7. Levels of transiently transfected wild type AR, in the presence and absence of PMEPA1, in HeLa cells coexpressing exogenous ubiquitin. Both panels (**A**) and (**B**) show cell lysates harvested by detergent lysis and detected using SDS-PAGE following by western blotting with α-AR primary and α-mouse HRP-conjugated secondary antibodies. Panel (**A**) shows, for comparison, the effect of the non-proteasomal protease inhibitor E-64 (E) compared to lactacystin (L) and controls, in the presence and absence of wild type PMEPA1 (W) and the triple PY mutant Y102A/Y126A/Y197A (P). Panel (**B**) shows a repeat of the experiment using only WT PMEPA1 and lactacystin. Cells were grown in charcoal stripped media for 24 hours following transfection, then either 100μM E-64 or an ethanol control was added to the medium. Cells were then grown for a further 18 hours, then either 10μM lactacystin or a DMSO control was added for the final 6 hours. The addition of ubiquitin appears to eliminate the previously observed loss of AR on the addition of PMEPA1, and the addition of lactacystin has no effect on the levels of unmodified AR, in contrast to the previous findings.

any increase in AR levels, although in one experimental replicate (figure 3.3.7B) there was an accumulation of higher molecular weight products which is presumably ubiquitinated protein as a result of the proteasomal machinery being rendered non-functional.

Figure 3.3.8 shows the results of overexpressing the constitutively active form of AR, the mutant T877A, which has already been shown in section 3.2 to behave in a manner similar to the wild type protein bound to testosterone, with and without PMEPA1, similar to the experiment conducted originally on the wild type protein, but with the addition of ubiquitin to assess whether this has any effect on the mutant AR as it did on the wild type. In the HeLa cell line, the addition of PMEPA1 results in an apparent decrease in AR T877A, consistent with the previously published wild type result, but the addition of ubiquitin as a co-transfected plasmid appears to reverse this effect to some extent. However the levels of AR in the absence of PMEPA1 seem to be lower in the presence of ubiquitin, and a stain for total protein (figure 3.3.8 C) shows that this is not due to higher DNA levels arising from multiple co-transfections leading to increased toxicity and lower overall protein; it, could be the case that turnover of AR-T877A is more rapid than that of the wild type, for example if its constitutively active state triggers upregulation and recruitment of ubiquitin-proteasome machinery. In this scenario, having more free ubiquitin in the cell may allow that process to occur more readily, resulting in the lower cellular levels of mutant AR observed. Alternatively this may be an artefact due to cell number or variability in transfection efficiency, but the fact that the same pattern is seen in the LNCaP cell line seems to indicate that is not the case.

The final experiment to assess where in the cell any direct interaction between PMEPA1 and AR could take place was to image PMEPA1 in the presence and absence of DHT i.e. when AR is active and the proposed negative feedback mechanism between

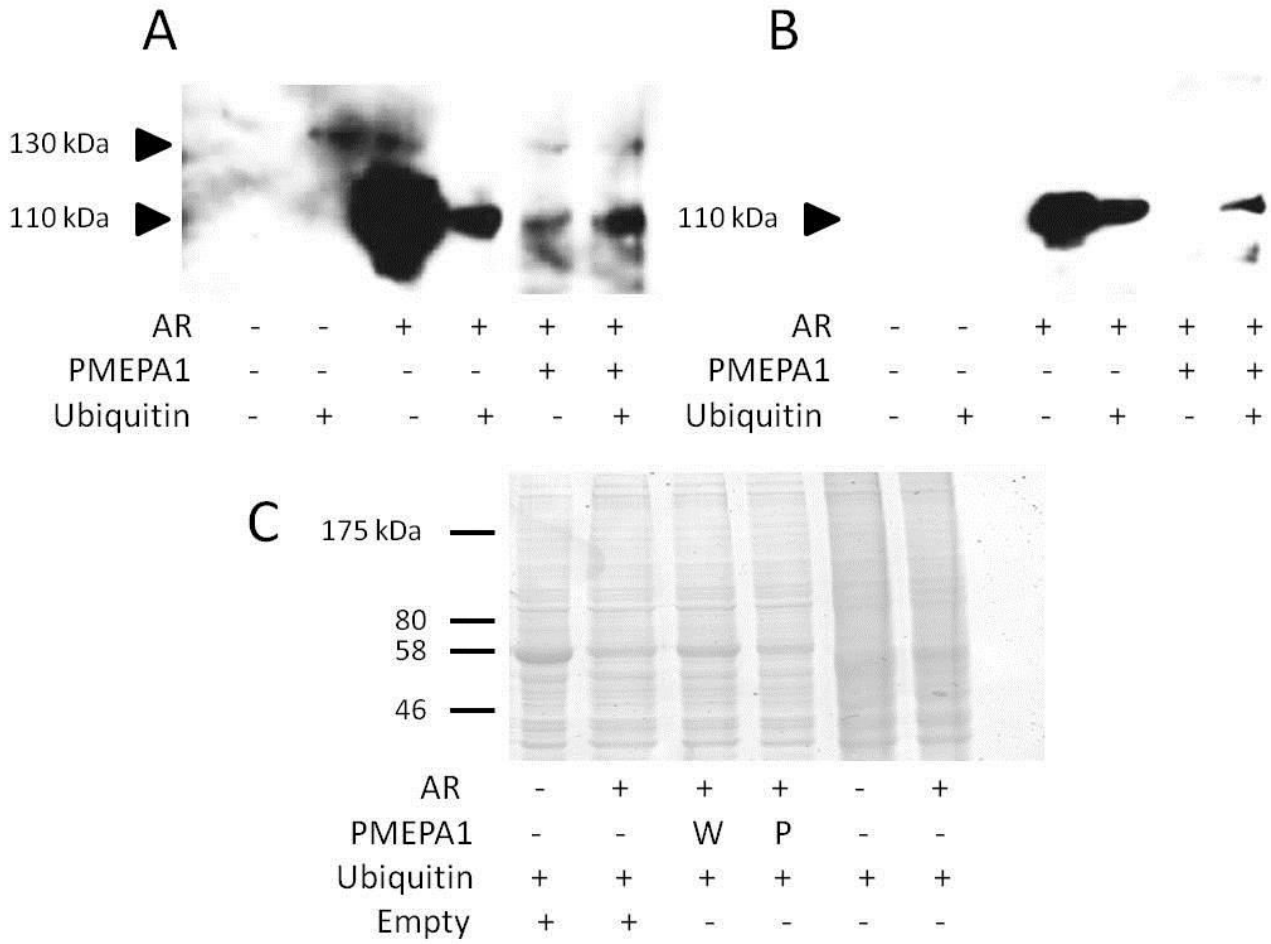

Figure 3.3.8. HeLa (**A**) and LNCaP lysates (**B**), harvested by detergent lysis and detected using SDS-PAGE following by western blotting with α-AR primary and α-mouse HRP-conjugated secondary antibodies, of cells overexpressing mutant AR-T877A in the presence of ubiquitin with and without PMEPA1, alongside negative controls. The ~110 kDa band, corresponding to the expected size of the mutant AR, and a higher molecular weight ~130 kDa band seen in the HeLa cell lysates are indicated by black arrows to the left of the blot. Levels of unmodified AR-T877A were much lower or absent when coexpressed with PMEPA1, an effect that was partially reversed when ubiquitin was also coexpressed. The 130 kDa band seen in panel (**A**) may be modification but its presence in the negative control lanes indicates a possible nonspecific cross reaction with bacterial protein. Also shown is a Coomassie stained 7.5% SDS-PAGE gel showing total protein levels in the same cell lysates as those used in lanes 2, 4 and 6 of panel (**A**), along with repeats of the same experiments carried out with the addition of empty vectors to bring the total amount of DNA used up to the same level in each transfection (**C**). The additional DNA actually appears to reduce the total level of protein compared to the same experiments performed without their addition.

AR and PMEPA1 would be ongoing. Figure 3.3.9 shows the localization of GFP-tagged PMEPA1 wild type and Y102A/Y126A/Y197A (ΔPY) in HeLa cells in the presence and absence of DHT. PMEPA1 localisation is never seen to cross the nuclear membrane regardless of the presence of steroid, either in the wild type or in the mutant which cannot interact with Nedd4.

3.3.3 Discussion

The observation of lower molecular weight forms of PMEPA1 suggests that more than one cleavage event is occurring, at least one of which appears to be dependent on the canonical PY2 (Fig. 3.3.1). The predicted size of PMEPA1 with the Myc-IgG-binding-domain tag on is 45 kDa, the size of the largest observed band. As the tag being detected is on the C-terminus of the protein, the reduction in size must be caused by truncation from the N-terminus. A reduction in weight from 45 kDa to 38 kDa, the only band of PMEPA1 Y126A observed, reflects a reduction in size of full length PMEPA1-IgG of approximately 64 residues, encompassing approximately 25% of the PMEPA1 protein, including the hydrophobic transmembrane domain, but leaving all three PY motifs intact. Similarly, truncation to 25 kDa would reflect truncation at approximately residue 182, encompassing approximately 72% of the PMEPA1 part of the protein; this leaves only one PY motif, PY3 ($PPTY_{197}$) intact, removing both the variant PY1 and the canonical PY2. The apparent disruption to this process caused by a mutation in PY2, but not either of the other PY motifs, suggests that this process is Nedd4-mediated, and also fits with the idea put forward in section 3.1.3 that the PY2 motif on PMEPA1 plays the most significant role in interaction with Nedd4 and subsequent modification. Interestingly in these assays no modified, i.e. higher molecular weight, forms of

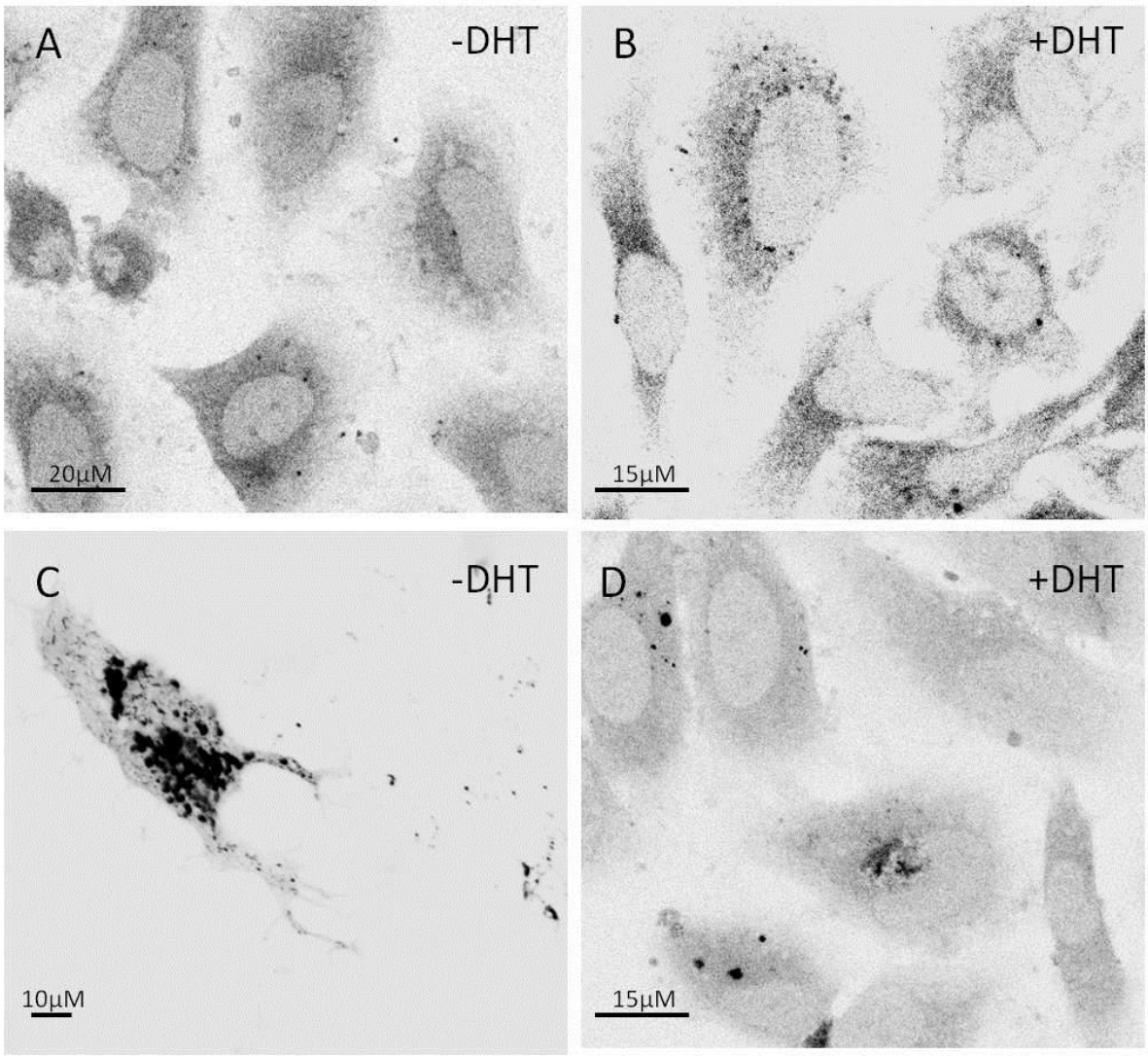

Figure 3.3.9. Confocal microscope images of fixed HeLa cells transiently transfected with wild-type (**A & B**) and ΔPY (**C & D**) PMEPA1-GFP. Cells were grown in charcoal-stripped medium for 24 hours post-transfection then either 100 nm DHT or an ethanol control was added for a further 24 hours. Cells were fixed using paraformaldehyde, mounted and a representative cell cluster was imaged. GFP was excited at 488nm to produce an emission spectrum across 500-570nm. The images were desaturated and reversed to produce black-on-white images for easy comparison**.** Regardless of the presence or absence of PY motifs and DHT, AR concentrates in the nucleus following ligand binding, but PMEPA1 is never seen to cross the nuclear membrane.

PMEPA1 were observed in any lane. The purpose of the partial digestion *in vivo* is unclear, as the loss of all PY motifs has no effect on the localisation of PMEPA1 compared to wild type, even in the presence of DHT, when it might be expected to inhibit some form of nuclear transfer to represent an interaction with activated AR (figures 3.3.2 & 3.3.9).

Levels of Nedd4 don't seem to differ significantly in the presence or absence of steroid (figure 3.3.3), but the Nedd4 turnover rate (figure 3.3.4) does seem to be affected by ligand-activation of AR in LNCaP, however the lack of quantification in the cycloheximide chases make it impossible to draw any definite conclusions in that regard.

There is no change in Nedd4 localisation (figure 3.3.5), again in spite of ligand-induced activation of AR and significant change in AR localisation upon DHT binding. This indicates that the role of Nedd4 in AR regulation is confined to an indirect effect, possibly mediated by an adaptor – a role PMEPA1 may fill. It is plausible that the role of Nedd4, which is implied by the role of PY motifs in the paper that first described the AR regulatory cycle, and later confirmed directly by the same group (Li et al, 2008; Li et al, 2012) is to catalyse a ubiquitin-mediated partial proteolysis of PMEPA1, producing the observed fragments, and that this fragment in turn plays a role in regulation of AR. There are parallel examples of such a process in the literature, for example, the activation of two yeast transcription factors, Spt23p and Mga2p, which is mediated by Rsp5p and regulates production of unsaturated fatty acids by transcriptional control of the desaturase enzyme Ole1p (Hoppe et al, 2000; Shcherbik et al, 2003). Like PMEPA1, the homologues Spt23p and Mga2p are membrane-associated with a ~20 residue transmembrane domain, contain a PY motif LPKY and localise to the secretory pathway (ER). Rsp5p-mediated ubiquitination triggers the processing of the 120 residue precursor protein to a 90 residue active form, with subsequent passage into the nucleus where they

function as transcription factors. However, the question remains why PMEPA1 is never seen in the nucleus, as this is where AR is confined to once activated and therefore where any negative regulatory effect would be expected to occur (see figures 3.3.5 and 3.3.9). It would be interesting to detect endogenous proteins, rather than, as shown here, using transfected, tagged proteins; the transfection process itself subjects the cells to significant stress, which may mean that the expressed constructs do not localise as they would under normal growth conditions. In addition, the highly variable expression levels of transiently expressed protein can both interfere with normal cellular function and cause misleadingly high levels of fluorescence that may be difficult to pinpoint accurately. Use of immunofluorescence would not preclude co-detection of two proteins if appropriate antibodies were used, and would bypass these potential problems, but would rely heavily on consistently detectable levels of endogenous protein which, as demonstrated by the difficulty in obtaining Western blot and immunoprecipitation results, may present a problem in this instance.

The results in figure 3.3.7B, showing that wild type, transiently transfected AR expressed in HeLa cells does not disappear when PMEPA1 is co-expressed in the presence of an artificially expanded ubiquitin pool, seems to indicate that the drop in AR levels in the presence of PMEPA1 observed by Li et al (2008) were artifactual; certainly their result is valid in showing a PMEPA1-mediated event, but the assumption that this is necessarily proteasome mediated is incorrect. Repeating this experiment with the use of a loading control such as co-detection of actin would provide more concrete evidence of this, but the fact that the addition of lactacystin and similar proteasome inhibitors, in the initial paper, rescues the PMEPA1-associated loss of AR is fundamentally not reason enough to conclude a proteasomal involvement, because there is a finite pool of free ubiquitin available in the cell. Ordinarily this pool is turned over continuously because

the proteins are deubiquitinated upon entry to the proteasome, but inhibiting the degradation mechanism causes a build-up of polyubiquitinated proteins, resulting in a loss of the ubiquitin reserves as they cannot be replenished. Therefore a point is reached where non-proteasomal ubiquitin-mediated processes also cannot occur, as the cellular free ubiquitin is no longer available; the therapeutic proteasome inhibitor bortezomib has been shown to precipitate such an event, with processes such as histone regulation and the IκBα pathway also being affected (Xu et al, 2004). Evidence for this can be seen in figure 3.3.8; the addition of PMEPA1 apparently precipitates an increase in AR ubiquitination, and a smear of high molecular weight protein is seen in that lane which is absent in the equivalent experiment without the inhibitor as the modified protein accumulates in the cell. While these experiments were carried out on HeLa cells, rather than the LNCaP prostate cancer model used in the 2008 paper, the results in figure 3.3.9, showing a similar pattern in the CaP mutant AR (T877A) to that reported in the wild type, indicate the model is valid. The drop or complete loss of AR in the presence of PMEPA1 is apparently rescued by the addition of supplementary ubiquitin even in the absence of proteasome inhibitors; this is an odd result, and may be due to total DNA levels in the transfections being higher and leading to less efficient transfection. However, analysis of the total protein in the samples by SDS-PAGE and Coomassie staining (see figure 3.3.9C) shows that there is actually more protein present in cell lysates transfected with less DNA, although this does not distinguish between endogenous and transfected proteins. Repeating the proteasome inhibitor experiments in LNCaP would be a future extension of the experiment.

AR is a 110 kDa protein, while the cutoff for passive diffusion across the nuclear envelope is around 60 kDa (Alberts et al, 2002); nuclear localisation of AR occurs through a combination of importin-dependent (i.e. active transport through nuclear pores)

and importin-independent processes (Kaku et al, 2008). One alternative pathway for nuclear translocation would be through the Golgi apparatus/endosomal pathway, which would afford opportunity for AR to interact with PMEPA1. The observation (figure 3.3.6) that some Nedd4 appears to localise in a Golgi-like pattern in the presence of DHT may indicate that the activation of AR by ligand binding precipitates the recruitment of Nedd4 to the endosomal trafficking pathway, with could in turn facilitate association of Nedd4 with AR and regulation through its interception between the cytosol and nucleus. However, this would presumably be a transient event that could only result in a small proportion of the total cellular AR being targeted, whereas the almost total loss of cellular AR seen in response to PMEPA1 up-regulation, both in the 2008 paper and our own data (figure 3.3.9) implies this is not the case.

There were a lot of difficulties encountered while undertaking co-immunoprecipitation experiments, and no Nedd4 or AR signal was detectable even in input samples. While no definite conclusions can be drawn from this, overexpression of Nedd4 would certainly be expected to destabilise AR if indeed the Nedd4/PMEPA1 complex is responsible for the negative feedback previously observed; the lack of Nedd4 signal means that the lack of AR signal could also be due to poor detection or low overall protein, although this is countered by the observation of a strong FLAG-ubiquitin signal in the same experiment.

It is possible that, despite the discrepancy in observed localisations of the three proteins, a direct interaction is occurring. In *Arabidopsis*, the RING ligase KEG localises to the early endosome, while the transcription factor AB15 is seen exclusively in the nucleus, yet the two interact directly in the cytoplasm (Liu & Stone, 2013) and when this process is blocked, AB15 accumulates in the cytoplasm. AB15 contains both nuclear import and nuclear export signals, and is transported both ways across the nuclear

envelope, but the cytoplasmic levels are kept low by this compartment-selective degradation. It is therefore feasible that the truncated PMEPA1 products seen, the release of which is dependent on Nedd4-mediated ubiquitination, enter the cytoplasm as soluble fragments where they recruit the ubiquitin-proteasome pathway to precipitate the degradation of AR in the cytosol only.

The use of controls to assess whether the high molecular weight band is still observed in lysates which are not overexpressing PMEPA1 would be a logical extension of this experiment, and I would also like to see a direct interaction between PMEPA1 and AR, as seen in the 2008 paper; multiple attempts to detect this interaction using tagged PMEPA1 or bound α-AR were not successful.

4. EXPERIMENTAL WORK NOT INCLUDED DUE TO LACK OF CONCLUSIVE FINDINGS

4.1. Attempted structural analyses on PMEPA1 and Nedd4

A significant portion of my time between November 2009 and November 2010 was spent preparing large quantities of highly pure protein with the intention of undertaking X-ray crystallography studies. This involved repeated culture of large quantities (4-8 L) of *E. coli* expressing recombinant 6xHis-PMEPA1 lacking the transmembrane domain, followed by affinity column purification. Further steps were necessary to obtain the 95 % purity required for successful structural analysis, and this was achieved using FPLC. The difficulties arose due to the low solubility of PMEPA1, even with the transmembrane domain removed; a typical prep yielded 2.5 ml protein at a concentration of around 0.5 µL, with a large proportion of the cellular protein lost in the insoluble fraction. While it was possible, using concentrating columns, to obtain a reduced volume at higher concentration, attempting to obtain concentrations higher than 2 mg/ml resulted in PMEPA1 precipitating out of the aqueous solution and the prep being rendered unusable. I attempted various solutions, including the use of detergents and stabilising agents such as glycerol in the lysis buffers, but when these were subsequently removed by buffer exchange during the FPLC process, any stabilising effect was lost. In addition, PMEPA1 degrades rapidly; initial samples that were stored at 4 ^{o}C overnight were completely unusable after 24 hours. These factors all combined to make obtaining sufficient protein at sufficient concentration for crystallography – approximately 1 mL at 1.5 mg/ml – an extremely long and arduous process. When I did succeed in obtaining samples of this quality, I laid down Hampton I and II crystal screens on two occasions and waited the required 2 weeks for any crystals to form, the result was only unusable precipitate.

Experimental work not included elsewhere due to lack of conclusive findings

Alternative structural analysis was attempted during July-September 2012, in the form of circular dichroism spectroscopy to try and quantify any structural alterations that arise upon PMEPA1 binding to Nedd4, and whether this was affected by the loss of any of the PY motifs. Again, this required extremely pure protein at a concentration of 1.5-2 mg/ml, but in smaller quantities, so I was able to obtain sufficient quantity of samples and pass these on to a collaborator. Unfortunately, the GST tag on Nedd4 interfered with the CD spectra, and attempts to remove the tag using PreScission protease (GE Healthcare) were unsuccessful due to the stability of Nedd4 in the required buffer; a construct of Nedd4 with a 6xHis tag in place of GST was successfully cloned near the end of the project.

4.2. Developing stable cell lines and use of inducible expression vectors

The initial idea, when planning the mammalian cell culture aspect of the project, was to use a tetracycline-inducible vector to express both PMEPA1 and AR simultaneously from a controlled time point, a similar technique to that used by Li et al (2007). This required multiple steps; following purchase of the vector system in March 2011, I undertook multiple cloning procedures in order to obtain both AR and PMEPA1, with appropriate affinity tags that could be simultaneously detected, and with restriction sites that would allow those fragments to be introduced into the inducible vector downstream of the two promoters already present in the plasmid. This alone took several months (alongside other experiments). Between September 2011 and July 2012, a significant proportion of my time was spent repeatedly attempting to clone both proteins into a single vector, optimising doxycycline concentration to induce expression of these proteins *in* vivo, and using linear selection markers to try to establish stable cell lines, an extremely time consuming process which required multiple dilutions to try and establish

monoclonal cultures in what is necessarily a stress-inducing selective media. Unfortunately, these attempts were not successful and, due mostly to time constaints, I instead used simultaneous transient transfections as described in this thesis.

5. DISCUSSION

5.1 The in vitro interaction between PMEPA1 and Nedd4

The identification of the novel variant PY motif in PMEPA1 is very interesting, as it is only the third WW domain-interacting PY motifs with a non-canonical xPxY sequence, and the first confirmed in a human protein. The fact that inactivating the vPY and each of the canonical PY motifs has a different level of impact on the level of Nedd4-mediated ubiquitination on PMEPA1 indicates that they are not equivalent, and their roles differ. In theory, if the role of a PY motif is purely to bind WW domains as strongly as possible to facilitate ubiquitination on as many sites as possible, then changing the nature of the vPY motif to mimic the two stronger sites would have been expected to increase the ability of Nedd4 to ubiquitinate PMEPA1, however the data presented in section 3.1 appear to show that this is not the case.

The motif now labelled PY2 appears to play the most significant role in PMEPA1 ubiquitination, as the removal of this motif has the largest impact on the extent of modification by Nedd4 *in vitro*. This seems to be due to more than simply the sequence of this motif (PPPY), as altering the gluatamic acid and threonine PY1 (QPTY) to mimic this sequence does not 'rescue' ubiquitination in a Y126A mutant (figure 3.1.5). A possible explanation for this is (as outlined as figure 3.1.8) is that the vPY motif interacts only transiently with Nedd4 in order to align the enzyme with PMEPA1, allowing the two canonical PY motifs to interact with specific WW domains. The spacing and sequence of the three PY motifs is perfectly conserved across many different species, and selective binding of PY motifs to specific WW domains of the Nedd4 family has been previously observed (Ingham et al, 2005). In addition, the paper that identified the vPY

Bsd2p in yeast posited a similar theory, based additionally on the observation that Bsd2 interacts specifically with WW3 in Rsp5p (Sullivan et al, 2007). The next stage of *in vitro* experimentation on the PMEPA1/Nedd4 interaction would involve the use of individual WW domain mutants in ubiquitination assays to pinpoint the specificity of each PY motif on PMEPA1. This would be a relatively simple way to test whether the theory that the vPY motif has an orientation effect is correct, as it assumes that both PY2 and PY3 interact predominantly with a single WW domain and that this reaction is so specific that the vPY needs to be conserved in order to allow the Nedd4 to align correctly with PMEPA1. Further experimental work with the microscale thermophoresis technique, or alternatives such as SPR, may also be useful in this regard, as a way of quantifying the precise binding affinity of wild type and mutant PMEPA1 to Nedd4 and therefore clarifying whether the vPY motif does indeed bind with lower affinity to the enzyme. The data presented in figure 3.1.7 show a clear binding curve between WT PMEPA1 and Nedd4, as well as a much weaker binding event between Nedd4 and a triple mutant ΔPY 1,2,3 PMEPA1, but the data for the ΔPY 2,3 PMEPA1 mutant does not show any clear binding event corresponding to either interaction. This is due to the first six data points appearing displaced from one another; it is not clear whether points 1-3 or points 4-6 are the anomalies which make drawing a binding curve impossible. Since August 2013, we have been in contact with Nanotemper Technologies and have repeated these experiments, with PMEPA1 ΔPY 2,3 as well as the original wild type, triple mutant and the mutant ΔPY 1. Unfortunately, this data had to be gathered off-site due to technical limitations, and despite being stored on dry ice during transport, PMEPA1 became highly aggregated and usable results could not be obtained.

Further *in vitro* assays that might shed more light on the nature of the interaction would be to use a wild type construct as the base for further mutations; all the mutations

detailed in section 3.1 were made in PMEPA1 with the PY2 motif inactivated by the Y126A mutation, as early on in the project, initial results of the experiment shown in figure 3.1.2 seemed to indicate that the reduction in ubiquitination observed in a double ΔPY1/2 mutant, compared to ΔPY2 alone, was greater than the reduction observed in a ΔPY1 mutant compared to wild type. As the experiment was repeated and statistical data accumulated, this turned out to be a false assumption (see figure 3.1.2), and repeating the experiments with both PY motifs intact may allow differences which were not statistically significant, such as those resulting from the vPY motif being altered to mimic the canonical motifs, to be amplified.

The mutagenesis experiments on the residues either side of the four core PY motif amino acids (see figure 3.1.4) show that those residues immediately flanking the PY motif are also important for PMEPA1 ubiquitination. This raises the possibility that the PY motif should be considered to extend beyond those four residues; while such motifs are usually referred to as PPxY or LPxY, it has already been discussed in detail here that a motif that does not adhere to this convention is still recognised by WW domain-containing proteins and has a role in modification by those proteins. It is absolutely reasonable that their functionality is not restricted to those residues alone. There are already examples of extended recognition motifs, such as the PY motif of ENaC being considered as PPPxY (Furuhasi et al, 2005) and six residues downstream from the PY motif of Smad7 being essential for recognition by Smurf2 (Chong et al, 2006). However, further research through mutagenesis studies on the residues surrounding the vPY motif, as well as the canonical motifs, of PMEPA1 would be very informative as to what exactly their role is. The nature of the upstream residues are almost universally conserved in PMEPA1 (the only exception being an S198N substitution of the residue immediately downstream of PY3 in two species) possibly indicating a functional role. In

addition, the particular substitution of the phenylalanine upstream of PY1 has profound effects on ubiquitination *in vitro*, clearly demonstrating its importance. However, at present the precise role of these flanking residues is not yet clear and it would be useful to shed some light their specific molecular significance.

The potential impact of other post-translational modifications on the PMEPA1-Nedd4 interaction is another intriguing area for future study. The interesting observation that the substitution of the threonine of the vPY motif for a serine results in an increase in ubiquitination, combined with the fact that phosphorylated residues have been shown to provide a favourable environment for Nedd4 WW domain binding (Lu et al, 2009) implies that substrate phosphorylation plays a regulatory role in ubiquitination by these enzymes. In addition, phosphorylation of the Rsp5p adaptors, Bul1p and Bul2p has recently been implicated as a regulatory mechanism in the ubiquitination of the amino acid permease Gap1p; in a low-nitrogen environment, the adaptors are phosphorylated by the kinase Npr1, preventing their ubiquitination by Rsp5p and subsequent ubiquitination and degradation of Gap1. However, when cellular amino acid levels increase, the Bul proteins are dephosphorylated and released from binding to chaperones, releasing them to interact with Rsp5p and Gap1p (Merhi and André, 2012). Therefore it might be useful to use a technique such as assessing kinase activity, both *in vitro* in *E. coli* as a model system, and *in vivo* in mammalian cultures, to see whether there is significant phosphorylation of PMEPA1 occurring that may have a regulatory effect.

As well as PMEPA1, there is evidence that the ubiquitin ligase activity of Nedd4 may be regulated by alternative modification events; a recent paper has identified conserved threonine residues in each of the WW domains of Rsp5p, at least one of which is constitutively phosphorylated (Sasaki & Takagi, 2013). Mutation of the conserved threonine in the WW2 domain causes the Gap1p permease to be downregulated by

targeting to the vacuole instead of the plasma membrane. In combination with the data presented in figure 3.1.6, showing that the non-canonical SUMO modification site in the HECT domain of Nedd4 has a role in autoSUMOylation, and a recently-discovered modification of Nedd4 by the UBL protein ISG15 that inhibits its ability to bind E2 enzymes (Malakhova & Zhang, 2008), suggests that this might be a focus for future work on the effects of non-ubiquitin modifications on the Nedd4 ligases themselves. Finally, autoubiquitination of Nedd4 may warrant investigation; autoubiquitination assays (figure 3.1.6) show that Nedd4 is extensively self-modified, and the original paper which identified the PY motif in the HECT domain postulated that this is a regulatory phenomenon, acting to control Nedd4-2 activity levels when the substrate ENaC is not bound (Bruce et al, 2008). It should be relatively easy to simultaneously assess PMEPA1 and Nedd4 ubiquitination using antibodies for both and western blotting with Odyssey detection, to see whether the degree of autoubiquitination is altered when Nedd4 is modifying wild type and ΔPY PMEPA1.

5.2 In vivo and structural analyses on PMEPA1 and Nedd4

The most important observation from the *in vivo* experiments detailed in section 3.2 is that the N-terminal transmembrane region of PMEPA1 challenges both the *in silico* prediction and current published thinking, as it does not appear to play any significant role in subcellular targeting of PMEPA1. An important next phase of experimentation to define this phenomenon would be to establish in exactly what compartment PMEPA1 is found. As seen in figure 3.2.4, there is some overlap between fluorescent tagged PMEPA1 and markers for both the *cis*-Golgi and the ER-Golgi intermediate compartment, but neither is a perfect match. Ubiquitination itself has been identified as a targeting signal for Golgi proteins to be transported to the yeast vacuole (Scheuring et al,

2012), and this may have a counterpart in mammalian cells involving trafficking to the lysosome. If PMEPA1 is being constantly turned over and trafficked between the Golgi and lysosome, this might explain the Golgi-like appearance and partial overlap with markers for different parts of the secretory pathway. If ubiquitination rather than the TMD is the trigger for PMEPA1 localization, this might explain why the removal of the N-terminus does not affect it. An alternative explanation, mentioned briefly in section 3.2.3, is that the transfected PMEPA1 is dimerising with endogenous protein; there is no direct evidence for this, but it would explain why none of the PMEPA1 mutants showed any altered localization compared to wild type, and the fact that the PY mutant still showed some FRET signal (see figure 3.3.3) despite having no intact Nedd4 interaction motifs. The priority experiment to assess this possibility would be to use a gene silencing technique such as RNAi to knock down expression of the endogenous protein and see whether this makes any difference to the expression of transfected PMEPA1. An alternative method would be to use anti-PMEPA1 antibodies to detect endogenous protein via immunofluorescence, rather than using tagged protein; there are no published examples of endogenous localization studies in PMEPA1, but such antibodies have been used successfully in Western blotting and immunoprecipitation experiments (Li et al, 2008). I did attempt, by using GFP-only controls, to ensure that the observed targeting is genuinely a product of the tagged protein, not the tag itself, but (as discussed in section 3.3.2) it is possible that, by the nature of the transfection process itself, these localizations are not representative of what would be the case *in vivo.*

Structural information, both on PMEPA1 alone and the Nedd4/PMEPA1 complex, would be extremely useful in understanding the nature of PMEPA1 and its role as a substrate for Nedd4; during this project, we attempted both circular dichroism (CD) and crystallographic studies, but these were hindered by various factors (see section 4.1). X-

ray crystallography would have provided atomic-level imaging of both proteins in solution; there is a possibility that this could be attempted again in the future, either using a different tag to increase the solubility of PMEPA1, such as MBP, or cleaving the existing tag after purification. As an alternative, CD is a useful technique for assessing changes in protein structure resulting from binding events; although it cannot give atomic-level resolution in the same way as other spectrographic techniques, circular dichroism (CD) uses the chiral nature of amino acids to predict secondary structure of proteins. The relative levels of random coil, helices, turns and β-sheet can be broadly inferred, and the technique is most useful for assessing the degree of structural change that occurs under different conditions; in this case, in the presence and absence of Nedd4. During the project, an attempt was made by Dr. Robert Janes to assess the spectra of the same recombinant PMEPA1 constructs used in the microscale thermophoresis experiments (described in section 3.1), alone and in solution with Nedd4, using synchrotron radiation circular dichroism (SRCD). However, this was hindered by the same solubility problems with PMEPA1 restricting the concentration of solutions, and the fact that the GST tag on Nedd4 produced a UV-wavelength spectrum that interfered with the ability of the technique to detect the impact of the enzyme on PMEPA1 (see section 4.1).

5.3 In vivo interactions between Nedd4, PMEPA1 and AR

While the experiments detailed here represent significant experimental work, drawing firm conclusions with regards to the multiple interactions between AR and Nedd4/PMEPA1 has proved difficult due to the high proportion of negative and inconclusive results. The priority for future experiments would be to successfully recreate the experiments of Li et al (2008) involving protease inhibitors (see figure 5.1).

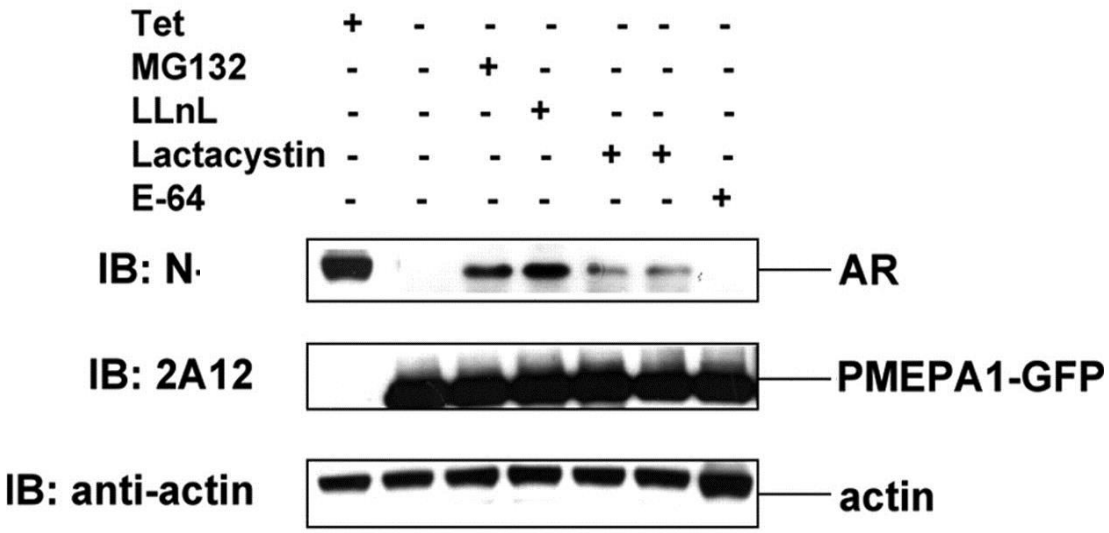

Figure 5.1. Original image from Li, H. et al, *J. Biol. Chem.* 2008; **283** 28988-28995 showing cell lysates from LNCaP cells stably expressing PMEPA1-GFP in a Tet-Off vector, grown with or without tetracycline for 11 days then incubated in either a DMSO control, 50 µM MG132, 50 µM LLnL, 10 µM lactacystin or 50 µM E-64 for an additional 5 hours. Lysates were harvested by detergent lysis, run on a 4-12% SDS-PAGE gradient gel and detected by western blotting using α-AR, α-GFP or α-actin as indicated.

During this project several attempts were made to repeat the experiment as described in the original paper, but AR levels in the resultant lysates were too low to be detected. This may be due to the fact that we were using transient transfections rather than stably expressing cell lines; in fact constructs based on the Clontech Tet-On system, expressing both PMEPA1 and AR in a plasmid containing a tetracycline-induced promoter, were created during this project and around 6 months was dedicated to attempting to cultivate stable, clonal cell lines using antibiotic selection (see section 4.2). However the rate of cell adherence and division in the antibiotic-containing media was very low, and even once a usable population had been established, no induction was observed upon addition of tetracycline. In theory AR should have been detectable in the transiently transfected cells, as we have on several occasions detected both endogenous (figure 3.3.3) and transiently transfected AR (figure 3.3.7) using the same detection method, and the fact that this was not the case may indicate a problem with the cells, possibly due to high passage number, which could be eliminated by repeated attempts. The use of multiple plasmids using the same pCMV promoter may also need to be addressed; figure 3.3.8C appears to show that introducing empty vectors does not result in increased cell toxicity, which can be an adverse effect of increasing DNA in transient transfections, but is both a poor quality blot, and therefore possibly inaccurate, and does not take into account the possibility that introducing additional plasmids using the same promoter may result in competition for a limited pool of cellular transcription factors or that the higher negative charge may result in a lower transfection efficiency. This could be compensated for by using cloning vectors containing a CMV promoter but no gene to express.

The issue of potential low expression may also explain why the immunoprecipitation experiments, which were attempted on several occasions (figure 3.3.6), were unsuccessful. Variability in levels of expression between experiments is a factor which

cannot be controlled in transient transfections, and at the very least a loading control, such as simultaneous detection of an abundant protein such as actin, would be required upon repeat of these experiments. However, there is evidence that the reasons for the negative results are not as simple as this; especially in figure 3.3.6, the transfected FLAG-ubiquitin is detectable in the input samples, but Nedd4, which was cotransfected using the same amount of DNA, is not. Neither is the endogenous Nedd4, which is detectable using the same antibodies and detection method in figures 3.3.3 and 3.3.4, visible in these blots. This is an extremely odd result which implies that a fundamental change in the experimental protocol may be required; we used NEM as a protease inhibitor, to prevent proteolytic cleavage of ubiquitin modification prior to lysis, however there is no equivalent step in the protocol used by Li et al (2008), and there are published protocols describing detection of ubiquitinated proteins *in vivo* without using any such inhibitors (Choo & Zhang, 2009). In addition, we used a modified TCA precipitation protocol to ensure that proteins with low solubility were detectable, however Li et al (2008) used a much less aggressive detergent lysis method, which may be more effective in the case of mammalian pull-downs as opposed to yeast or bacteria, which produce much higher yields. Certainly in the future, refinement and repeats of the immunoprecipitation experiments would be very valuable in order to establish whether AR and Nedd4 are directly interacting. For example, if the reaction is transient or weak, *in vivo* crosslinking using NHS-ester reagents would be a relatively quick and simple technique that could be used to stabilise the bonds and enable detection using immunological techniques or mass spectrometry.

Alternative experiments which could shed light on the mechanism of the potential AR/Nedd4/PMEPA1 interaction include *in vitro* ubiquitination assays along the lines of those performed on PMEPA1 (see section 3.1). One thing that could be tentatively

concluded from figure 3.3.6 is that AR does co-precipitate with ubiquitin, indicating *in vivo* modification. AR contains what resembles a variant PY motif very close to the C terminus ($KPIY_{855}$) and this may mediate direct interaction with Nedd4, or alternatively PMEPA1 may be acting as an adaptor in a similar way to Bsd2p in yeast (Sullivan et al, 2007). If PMEPA1 is essential for AR ubiquitination by Nedd4, *in vitro* assays in the presence and absence of PMEPA1 would be a quick and efficient way to establish this, and similarly mutation of the KPIY sequence will quickly show whether this has a significant role. In addition, the surface plasmon resonance (SPR) technique might be a good way to detect direct protein-protein interaction between AR and ubiquitin or AR and Nedd4, as this is a way to determine binding affinity between two proteins without the multi-step labelling process involved in microscale thermophoresis, and requires achievable analyte concentrations, as low as 100 nM. However, this technique requires specialised equipment and expensive consumables, and therefore was not a practical option for us during the course of this project.

The CaP mutation (T877A) in AR appears, in the results presented here, to localize in the same way as wild type AR activated by DHT, even in the absence of ligand (figures 3.2.7 & 3.2.8). This is not in agreement with previous published results (see section 3.2.3), but does represent consistent observations subjected to rigorous statistical analysis. Interestingly, the experiments shown in figure 3.3.8 involving AR-CaP were repeated at the same time, under the same conditions, using the wild type protein, but these were not successful, producing only blank western blots with no protein, endogenous or transfected, detectable. In addition, the GFP signal from both the CaP-AR and wild type AR (in the presence of DHT), seen in the confocal microscopy images (figure 3.2.6) is much stronger than the wild type in the absence of DHT. It has previously been shown that when bound to a ligand *in vivo*, AR does show up-regulated

expression, but that this is due to increased transcription efficiency rather than stability of existing protein, as mRNA levels actually fall following androgen treatment (Krongrad et al, 1991). Therefore the apparent increase in detectable protein when using AR-CaP as opposed to wild type supports the evidence from the confocal microscopy studies that the mutant behaves in a way which mimics the wild type bound to DHT; this may provide a useful tool in the future to understand the metabolic behaviour of the LNCaP cell line, but it must first be qualified with studies on endogenous protein to compliment these transfection-based results (see section 3.3.3).

5.4 Evidence for an altered model for the PMEPA1/AR feedback system

The issue of where in the cell any potential interaction between PMEPA1 and AR may occur is still unresolved; logically, this would be expected to be the nucleus as this is where AR is concentrated in the presence of DHT i.e. in an activated state, but these results indicate (figure 3.3.9) that PMEPA1 is excluded from the nucleus regardless of whether there is a ligand present to activate AR. The same image also appears to show that wild type PMEPA1 has a more punctuate appearance in the presence of DHT, while the ΔPY triple mutant has a more diffuse appearance when AR is activated. However, these are representative images chosen from multiple repeats of the experiments, and this may not be consistent observation, rather it is more likely due to variation in imaging & signal intensity. While the consistent exclusion of PMEPA1 from the nucleus is in agreement with previous localisation studies on PMEPA1 (Xu et al, 2003), these studies are limited and, as mentioned earlier, focus on the use of fluorescent tagged proteins which may produce an artificial result.

Other interesting observations are that Nedd4 appears more punctuate in appearance in the presence of DHT (figure 3.3.5) and that DHT may also increase the half-life of

Nedd4 (figure 3.3.4); both of these are supportive of a role for Nedd4 which involves both up-regulation and recruitment to a cellular compartment which resembles the Golgi, although this is an extremely provisional statement and would require further experimentation to confirm, including co-imaging with cellular markers to identify the precise position of Nedd4 in the presence and absence of DHT, and a repeat of the cycloheximide chase experiments, or an alternative such as radioactivity pulse-chase assay, to confirm the precise half-life of both Nedd4 and AR under different conditions.

The result shown in figure 3.3.7, suggesting that the addition of supplementary ubiquitin to cells over-expressing PMEPA1 appears to compensate for the complete loss of AR reported by Li et al (2008), is important in our understanding the interaction between the two proteins, and it is disappointing that repeating the experiment produced such different results in terms of the apparent modification of AR under these conditions. An extremely useful future experiment would be to corroborate this result with repeats of this experiment, including loading controls and preferably using a time-controlled, inducible construct, to address the question of why the higher molecular weight AR is visible in one iteration of the experiment (figure 3.3.7B) but not the other (figure 3.3.7A). Such a build up of modified protein could be considered an expected effect of inhibition of the proteasome by lactacystin, and this does not seem to have been accounted for at all in the original paper. Their published result is shown in figure 5.1 and clearly shows that the increase in androgen receptor, interpreted as being due to the PMEPA1-mediated degradation being prevented, is actually an increase in the unmodified protein, running at the same position on a gel as that observed in the absence of any proteasome inhibitor. As previously mentioned, the fact that, in the same paper, an immunoprecipitation of AR bound to ubiquitin showed a smear of high molecular weight protein (figure 5.2), in contrast to the result shown here in figure 5.1, demonstrates that

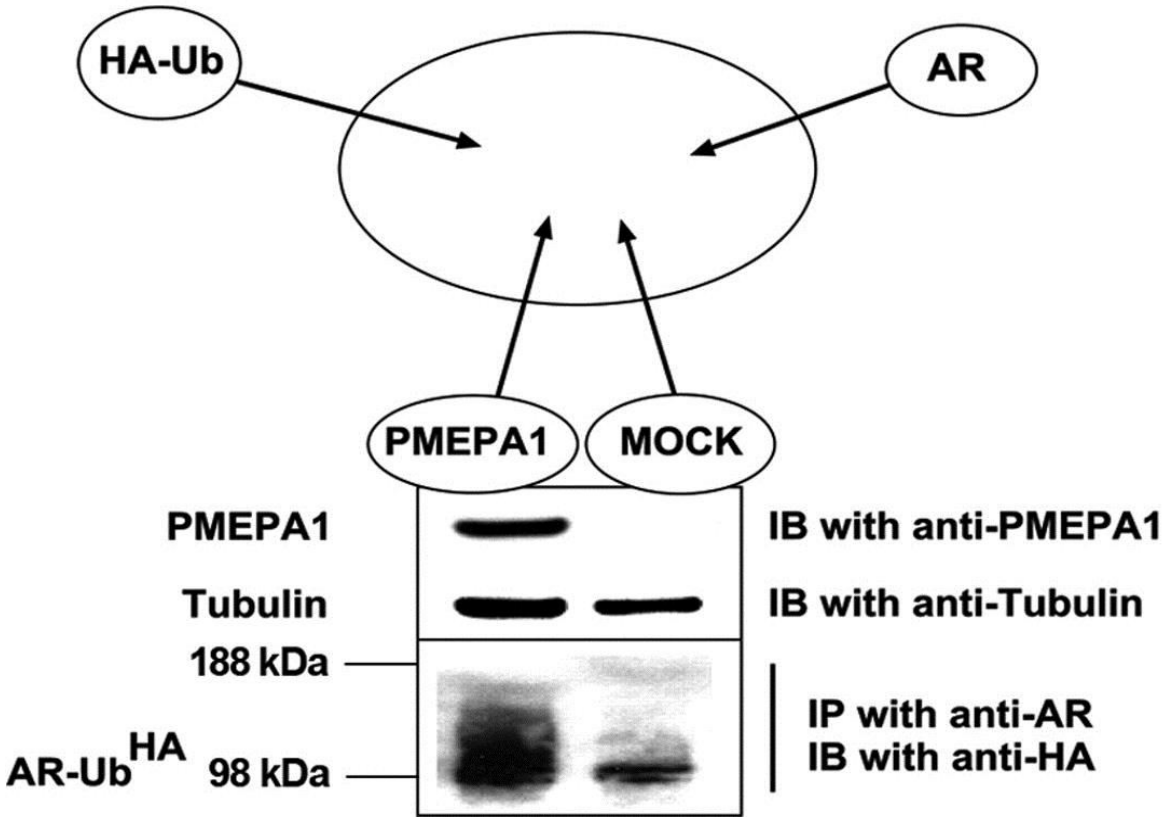

Figure 5.2. Original image from Li, H. et al, *J. Biol. Chem.* 2008; **283** 28988-28995 showing immunoprecipitated AR HEK 293 cell lysates transiently expressing AR as well as HA-tagged ubiquitin and either PMEPA1 or an empty plasmid. After 24 hours growth, the cells were treated with both 10 nm R1881 and 5 μM MG132, then incubated further for 16 hours. Cell contents were harvested by detergent lysis and immune-precipitated with α AR and a western blot was performed using anti-HA antibody.

the proposed model is oversimplified even if we have not been able to confirm a viable alternative.

Bearing in mind the inconsistencies and unanswered questions in the original paper, and the (albeit limited) data obtained throughout this project, I do not believe that the proposed simple feedback loop between AR and PMEPA1, in which PMEPA1 initiates ubiquitin-mediated proteasomal degradation of AR, is correct. Instead, PMEPA1, possibly in a truncated form as a result of partial proteolysis resulting from a precise Nedd4-mediated ubiquitination event, may be acting as an adaptor to mediate Nedd4 interaction with AR to initiate selective degradation in the cytosol. This degradation may be occurring via the lysosomal pathway, or it may in fact be a trafficking event initiated by saturation of the primary importin-α pathway at high ligand concentrations. Figure 5.3 shows a simple schematic of such a model, postulating that the initial Nedd4-PMEPA1 interaction occurs through a different WW domain (illustrated as WW3/4) to that involved in the modification of AR. The use of a specific inhibitor of the importin-α nuclear import pathway, such as ivermectin (Wagstaff et al, 2012), could be used to assess the impact of blocking this pathway on the cellular localisation of AR and clarify its role in the model.

5.5 Concluding remarks

In summary, the work presented here indicates that the N-terminal transmembrane domain of PMEPA1 is not, as was previously thought, responsible for targeting PMEPA1 to the Golgi apparatus, that the apparent localisation of both the wild type and ΔNT mutant are in fact to the same compartment, and that this compartment does not align with the Golgi network. In addition, the variant PY motif in PMEPA1 has a

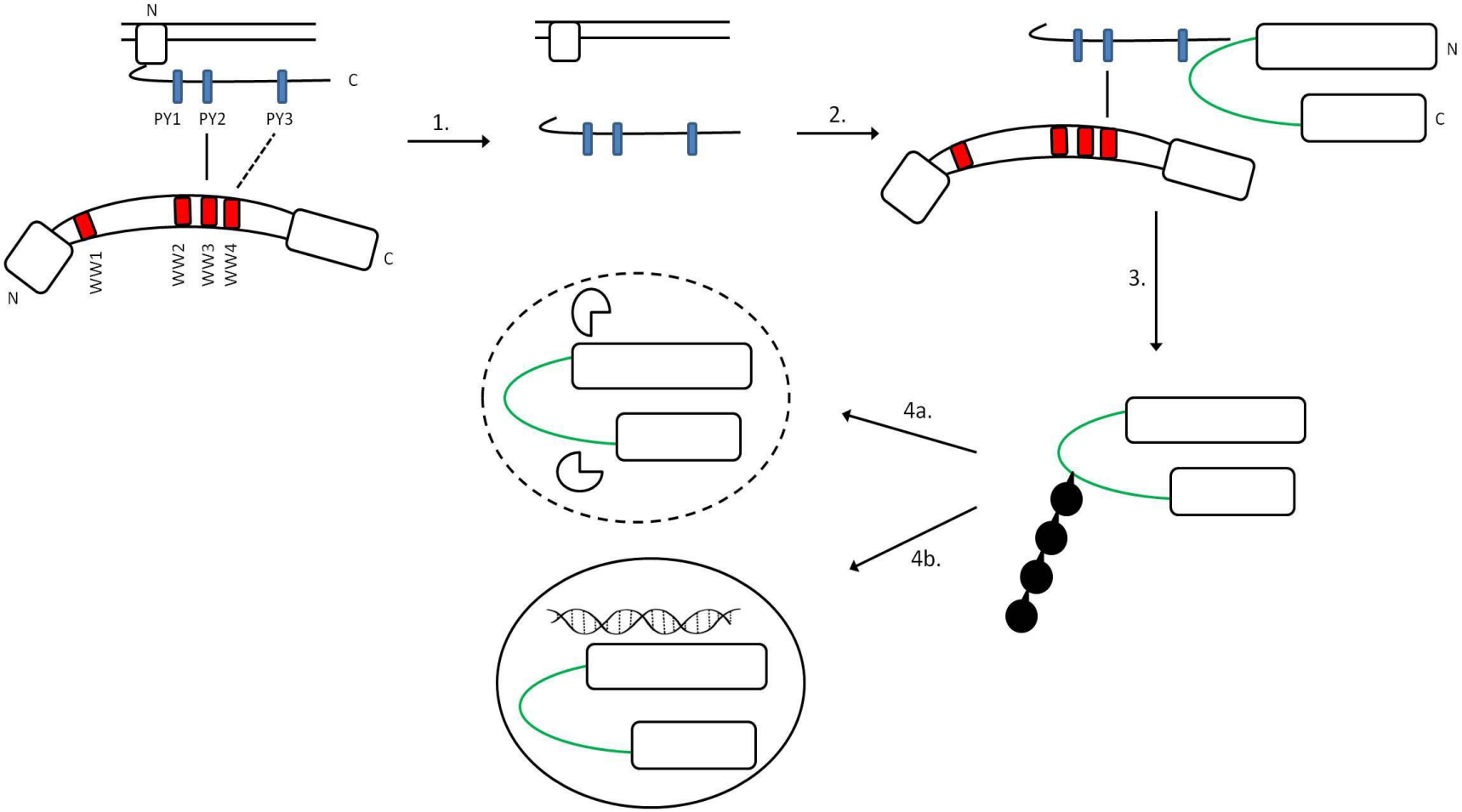

Figure 5.3. Potential alternative model of the interaction between androgen receptor, PMEPA1 and Nedd4. PMEPA1, anchored in the membrane by the TMD, is ubiquitinated by Nedd4 in an interaction that relies heavily on PY2. A partial proteolysis event follows (1) which results in a soluble fragment of PMEPA1 being released into the cytosol, where a second interaction involving both Nedd4 and AR occurs (2). PMEPA1 acts as an adaptor to facilitate Nedd4 ubiquitination of AR (3) and the ubiquitinated protein either triggers autophagosome formation and subsequent targeting to the lysosome (4a) or uptake into the Golgi network and subsequent delivery to the nucleus (4b).

functional role in interaction with Nedd4, and flanking residues, as well as the core four considered to be a minimal interaction motif, play a significant role in Nedd4-mediated ubiquitination *in vitro.* The variant residues within the newly identified PY1 motif are flexible at least *in vitro*, to some extent, but replacing the variant motif with a canonical motif counter-intuitively results in a decrease in ubiquitination; in this report, a hypothesis is put forward that relies on a weak interaction between the variant motif and WW domains to orientate PMEPA1 correctly for optimal ubiquitination.

Using a combination of *in vivo* imaging and immunoassay techniques, the data presented here imply that the CaP mutation of AR, associated with the development of advanced prostatic cancer, behaves in the same way as ligand-bound wild type AR, both in terms of localisation and stability. Finally I have tried to show, though re-interpretation of the results presented by Li et al (2008) and some additional experimentation, that the previously published model of AR/PMEPA1 interaction as a straightforward feedback cycle in which AR is targeted to the proteasome for degradation is oversimplified, and postulated an alternative model which relies on PMEPA1 acting as an adaptor between Nedd4 and AR, and a non-proteasomal role for ubiquitination of AR. Future work should build on this to test the hypotheses presented and elucidate the precise nature of the interaction between Nedd4 and PMEPA1 in the regulation of the androgen receptor, and possibly identify new therapeutic targets for the treatment of the fourth most deadly cancer in the UK.

6. APPENDICES

6.1 List of abbreviations

AMPS	Ammonium persulphate
AR	Androgen receptor
ATP	Adenosine triphosphate
Bsd2p	Bypass Sod1p defects protein
CaP	Cancer of the prostate
CBP	Calmodulin binding protein tag
CMV	Cytomegalovirus
DHT	5α-dihydrotestosterone
DMSO	Dimethyl sulfoxide
DNA	Deoxyribonucleic acid
DTT	Dithiothreitol
E. coli	*Escherichia coli*
EDTA	Ethylenediaminetetraacetic acid
EGTA	Ethylene glycol tetraacetic acid
FBS	Foetal bovine serum
FLAG	Trademarked affinity peptide tag with sequence DYKDDDDK
Gap1p	General amino acid permease 1 protein
GFP	Green fluorescent protein
GST	Glutathione S-transferase
HEPES	4-(2-hydroxyethyl)-1-piperazineethanesulfonic acid
His	Histidine
HRP	Horseradish peroxidase
IgG	Immunoglobulin G
IPTG	Isopropyl β-D-1-thiogalactopyranoside
kDa	KiloDalton
kPa	KiloPascal
MOPS	3-(N-morpholino)propanesulfonic acid
Myc	Peptide affinity tag with sequence N-EQKLISEEDL-C

Nedd4	Neural precursor cell expressed developmentally down-regulated protein 4
NEM	N-Ethylmaleimide
ORF	Open reading frame
PAGE	Polyacrylamide gel electrophoresis
PBS	Phosphate buffered saline
PCR	Polymerase chain reaction
PFA	Paraformaldehyde
PMEPA1	Prostate transmembrane protein, androgen-induced 1
PMSF	Phenylmethanesulfonylfluoride
RNAse	Ribonuclease enzyme
Rpm	Revolutions per minute
Rsp5p	Reverses Spt-phenotype protein
SDS	Sodium dodecyl sulfate
S-tag	N-terminal region of ribonuclease S (KGTAAAKFERQHMDS)
SUMO	Small ubiquitin-like modifier
TAE	Tris-Acetic acid-EDTA buffer
TAP	Tandem affinity purification tag
TBS	Tris-buffered saline
TCA	Trichloroacetic acid
TEMED	Tetramethylethylenediamine
Tris	Tris(hydroxymethyl)aminomethane
Uba1	Ubiquitin activating enzyme 1
Ubc1	Ubiquitin-conjugated enzyme E2K

6.2 Plasmid maps

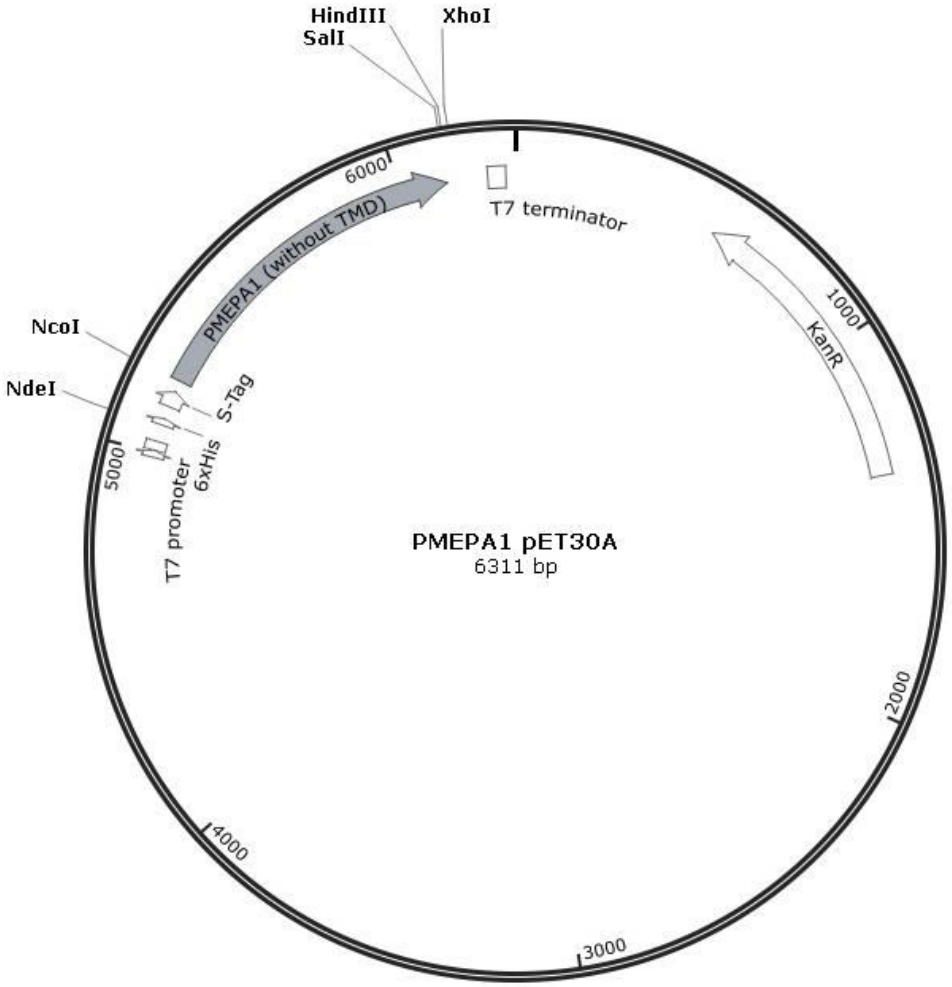

Figure 6.2.1. Soluble PMEPA1 in pET30a**.** Map showing construct for bacterial expression of recombinant, soluble PMEPA1 subsequently used in *in vitro* assays. The bacterial T7 promoter, 6xHis and S-tags, PMEPA1 ORF and kanamycin resistance ORF are shown along with restriction sites used for cloning. This plasmid was also used to clone a 6xHis-tagged Nedd4 for recombinant expression. Note that the N-terminal 23-residue transmembrane domain is absent. Created using SnapGene Viewer version 1.5.2.

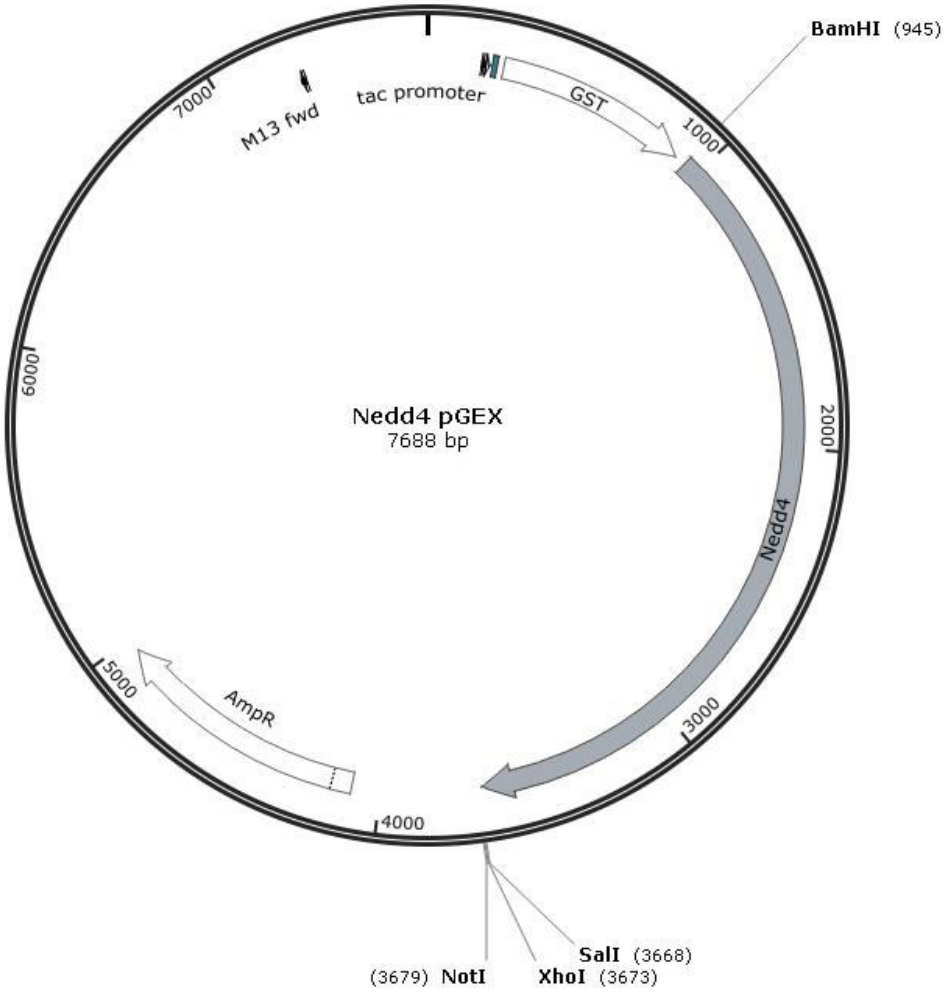

Figure 6.2.2. Nedd4 in pGEX6P2**.** Map showing construct for bacterial expression of recombinant GST-tagged human Nedd4 subsequently used in *in vitro* assays. The bacterial tac promoter, GST tag, Nedd4 ORF and ampicillin resistance ORF are shown along with restriction sites used for cloning. Created using SnapGene Viewer version 1.5.2.

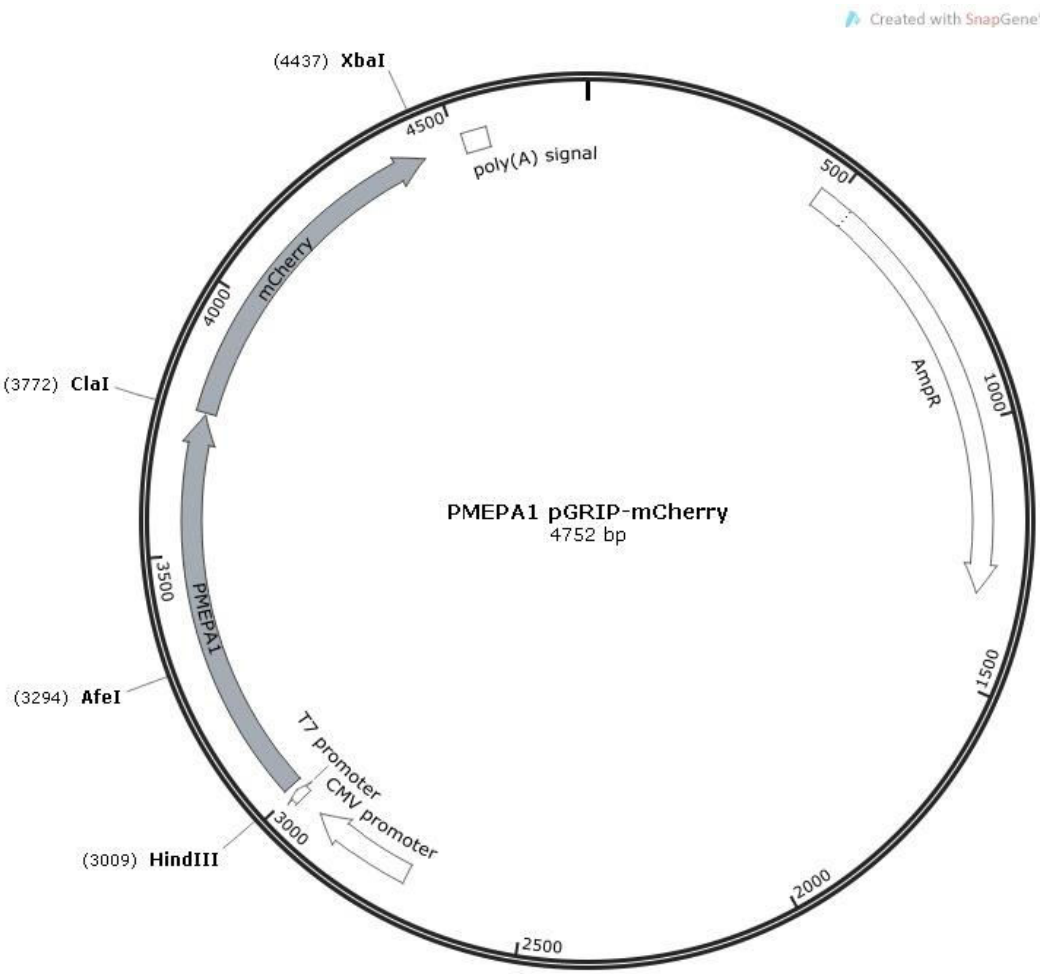

Figure 6.2.3. PMEPA1 in pGRIP**.** Map showing construct for mammalian expression of full-length, mCherry-tagged PMEPA1 for use in microscopy and western blotting. The bacterial T7 promoter, mammalian CMV promoter, mCherry tag, PMEPA1 ORF and ampicillin resistance ORF are shown along with restriction sites used for cloning. Note that this plasmid, with the same restriction sites, was used to clone GFP and mCherry-tagged AR, Nedd4 and non-WT PMEPA1 for microscopy, as well as Myc-IgG-tagged PMEPA1 for the western blotting experiments described in section 3.3.2.Created using Snapgene viewer version 1.5.2.

Figure 6.2.4. AR in pGRIP**.** Map showing construct for mammalian expression of HA-tagged human AR for use in western blotting. The bacterial T7 promoter (not labelled), mammalian CMV promoter, HA tag, AR ORF and ampicillin resistance ORF are shown along with restriction sites used for cloning. Created using Snapgene Viewer version 1.5.2.

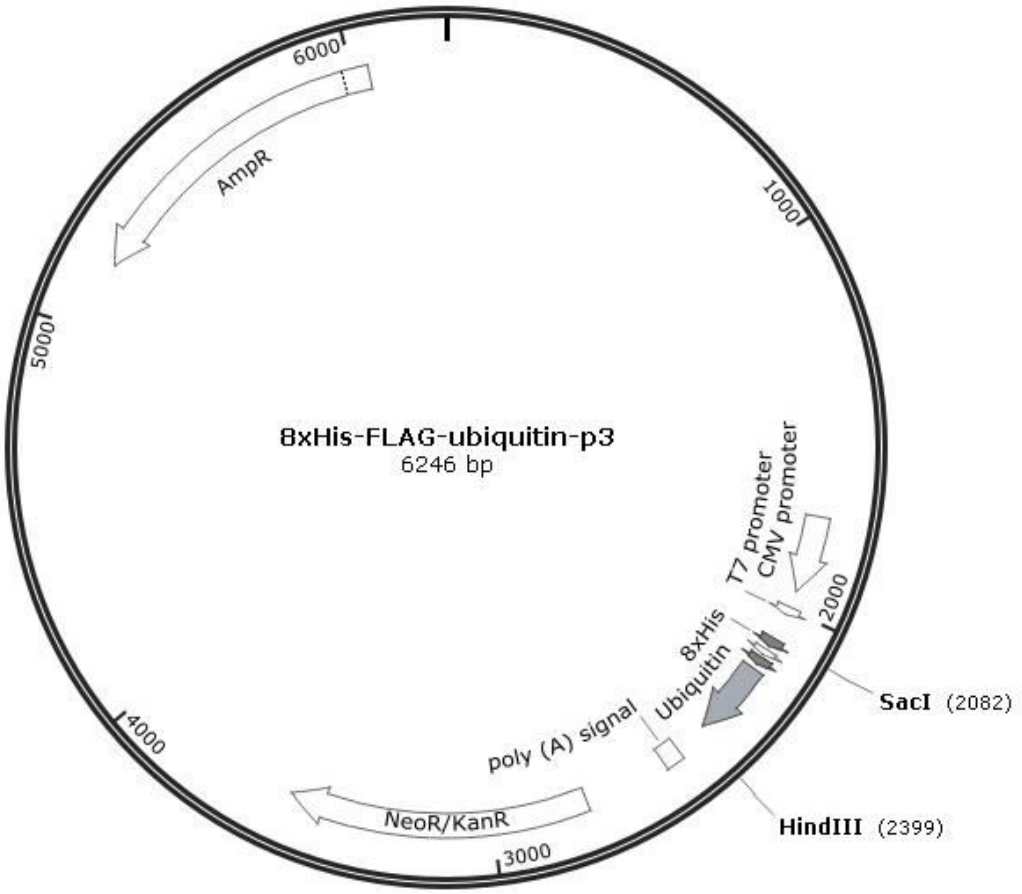

Figure 6.2.5. Ubiquitin in p3**.** Map showing construct for mammalian expression of ubiquitin with an N-terminal 8xHis-FLAG tag, for use in western blotting and pulldowns. The bacterial T7 promoter, mammalian CMV promoter, 8xHis tag, thrombin cleavage site and FLAG tag (not labelled), ubiquitin ORF, neomycin resistance ORF and ampicillin resistance ORF are shown along with restriction sites used for cloning. Created using Snapgene Viewer version 1.5.2.

6.3 Annotated PMEPA1 protein sequence

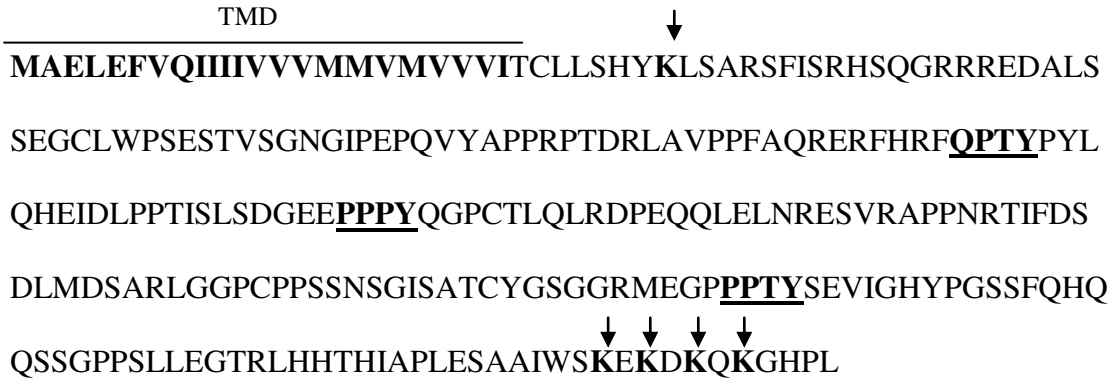

The annotated 252-amino acid protein sequence of PMEPA1, shown above, includes the transmembrane domain, which encompasses the first 23 residues of the sequence and is removed in constructs encoding a soluble form of the recombinant protein, as well as in some mammalian expression constructs. The arrows indicate the locations of the five lysine residues (K_{31}, K_{242}, K_{244}, K_{246}, K_{248}); note that apart from one, all are located at the far C-terminus of the protein. The three PY motifs are highlighted in bold and underlined.

7. REFERENCES

Ahmed, N., Zeng, M., Sinha, I., Polin, L., Wei, W.Z., Rathinam, C., Flavell, R., Massoumi, R. & Venuprasad, K. (2011) The E3 ligase Itch and deubiquitinase Cyld act together to regulate Tak1 and inflammation. *Nat. Immunol.* 12 (12) 1176-1183

Amos, W.B., White, J.G. & Fordham, M. (1987) Use of confocal imaging in the study of biological structures. *Appl. Opt.* 26 (16) 3239-3243

Anan, T., Nagata, Y., Koga, H., Honda, Y., Yabuki, N., Miyamoto, C., Kuwano, A., Matsuda, I., Endo, F., Saya, H. & Nakao, M. (1998) Human ubiquitin-protein ligase Nedd4: expression, subcellular localization and selective interaction with ubiquitin-conjugating enzymes. *Genes Cells.* 3 (11) 751-763

Androutsellis-Theotokis, A., Leker, R.R., Soldner, F., Hoeppner, D.J., Ravin, R., Poser, S.W., Rueger, M.A., Bae, S.K., Kittappa, R. & McKay, D. (2006) Notch signalling regulates stem cell numbers *in vivo* and *in vitro*. *Nature* 442 (7104) 823-826

Aragón, E., Goerner, N., Xi, Q., Gomes, T., Gao, S., Massagué, J. & Macias, M.J. (2012) Structural basis for the versatile interactions of Smad7 with regulator WW domains in TGF-β pathways. *Structure* 20 (10) 1726-1736

Ashcroft, G.S. & Mills, S.J. (2002) Androgen receptor-mediated inhibition of cutaneous wound healing. *J. Clin. Invest.* 110 (5) 615-624

Ashida, H., Toyotome, T., Nagai, T. & Sasakawa, C. (2007) *Shigella* chromosomal IpaH proteins are secreted via the type III secretion system and act as effectors. *Mol. Microbiol.* 63 (3) 680-693

Ashida, H., Nakano, H. & Sasakawa, C. (2013) *Shigella* IpaH0722 E3 ubiquitin ligase effector targets TRAF2 to inhibit PKC-NF-κB activity in invaded epithelial cells. *PLoS Pathog.* 9 (6) e1003409

Bayer, P., Arndt, A., Metzger, S., Mahajan, R., Melchior, F., Jaenicke, R. & Becker, J. (1998) Structure determination of the small ubiquitin-related modifier SUMO-1. *J. Mol. Biol.* 280 (2) 275-286

Bedford, M.T., Chan, D.C. & Leder, P. (1997) FBP WW domains and the AbI SH3 domain bind to a specific class of proline-rich ligands. *EMBO J.* 16 (9) 2376-2383

Bedford, M.T., Reed, R. & Leder, P. (1998) WW domain-mediated interactions reveal a spliceosome-associated protein that binds a third class of proline-rich motif: the proline glycine and methionine-rich motif. *Proc. Natl. Acad. Sci. USA* 95 (18) 10602-10607

Bellomaria, A., Barbato, G., Melino, G., Paci, M. & Melino, S. (2010) Recognition of p63 by the E3 ligase ITCH: Effect of an ectodermal dysplasia mutant. *Cell cycle* 9 (18) 3730-3739

Ben-Saadon, R., Zaaroor, D., Ziv, T. & Ciechanover, A. (2006) The polycomb protein Ring1B generates self atypical mixed ubiquitin chains required for its *in vitro* histone H2A ligase activity. *Mol. Cell* 24 (5) 701-711

Berges, R.R., Vukanovic, J., Epstein, J.I., CarMichel, M., Cisek, L., Johnson, D.E., Veltri, R.W., Walsh, P.C. & Isaacs, J.T. (1995) Implication of cell kinetic changes during the progression of human prostatic cancer. *Clin. Cancer Res.* 1 (5) 473-480

Birnboim, H.C. & Doly, J. (1979) A rapid alkaline extraction procedure for screening recombinant plasmid DNA. *Nucleic Acids Res.* 7 (6) 1513-1523

Blok, L.J., de Ruiter, P.E., Brinkmann, A.O. (1998) Forskolin-induced dephosphorylation of the androgen receptor impairs ligand binding. *Biochemistry* 37 (11) 3850-3857

Bodén, M. & Hawkins, J. (2005) Prediction of subcellular localization using sequence-biased recurrent networks. *Bioinformatics* 21 (10) 2279-2286

Brakenhodd, G.J., Blom, P. & Barends, P. (1979) Confocal scanning light microscopy with high aperture immersion lenses. *J. Microscopy* 117 (2) 219-232

Bremm, A., Freund, S.M. & Komander, D. (2010) Lys11-linked ubiquitin chains adopt compact conformations and are preferentially hydrolyzed by the deubiquitinase Cezanne. *Nat. Struct. Mol. Biol.* 17 (8) 939-947

Bruce, M.C., Kanelis, V., Fouladkou, F., Debonneville, A., Staub, O. & Rotin, D. (2008) Regulation of Nedd4-2 self-ubiquitination and stability by a PY motif located within its HECT domain. *Biochem. J.* 415 (1) 155-163

Brunschwig, E.B., Wilson, K., Mack, D., Dawson, D., Lawrence, E., Willson, J.K., Lu., S., Nosrati, A., Rerko, R.M., Swinler, S., Beard, L., Lutterbaugh, J.D., Willis, J., Platzer, P. & Markowitz, S. (2003) PMEPA1, a transforming growth factor beta-induced marker of terminal colonocyte differentiation whose expression is maintained in primary and metastatic colon cancer. *Cancer Res.* 63 (7) 1568-1575

Busch, H. & Goldknopf, I.L. (1981) Ubiquitin-protein conjugates. *Mol. Cell. Biochem.* 40 (3) 173-187

Cao, X.R., Lill, N.L., Boase, N., Shi, P.P., Croucher, D.R., Shan, H., Qu, J., Sweezer, E.M., Place, T., Kirby, P.A. & Daly, R.J. (2008) Nedd4 controls animal growth by regulating IGF-1 signalling. *Sci. Signal.* 1 (38)

Callewaert, L., van Tilborgh, N. & Claessens, F. (2006) Interplay between two hormone-independent activation domains in the androgen receptor. *Cancer Res.* 66 (1) 543-553

Cary, P.D., King, D.S., Crane-Robinson, C., Bradbury, E.M., Rabbani, A., Goodwin, G.H. & Johns, E.W. (1980) Structural studies on two high-mobility-group proteins from calf thymus, HMG-14 and HMG-20 (ubiquitin), and their interaction with DNA. *Eur. J. Biochem.* 112 (3) 577-580

Chan, D.C., Bedford, M.T. & Leder, P. (1996) Formin binding proteins bear WWP/WW domains that bind proline-rich peptides and functionally resemble SH3 domains. *EMBO J.* 15 (5) 1045-1054

Chang, H.C., Paek, J. & Kim, D.H. (2011) Natural polymorphisms in *C. Elegans* HCW-1 E3 ligase affect pathogen avoidance behaviour. *Nature* 480 (7378) 525-529

Chen, H.I. & Sudol, M. (1995) The WW domain of Yes-associated protein binds a proline-rich ligand that differs from the consensus established for Src homology 3-binding modules. *Proc. Natl. Acad. Sci. USA* 92 (17) 7819-7823

Chen, C., Sun, X., Guo, P., Dong, X.Y., Sethi, P., Zhou, W., Zhou, Z., Petros, J., Frierson, H.F. Jr., Vessella, R.L., Atfi, A. & Dong, J.T. (2007) Ubiquitin E3 ligase WWP1 as an oncogenic factor in human prostate cancer. *Oncogene* 26 (16) 2386-2394

Cheng, S., Brzostek, S., Lee, S.R., Hollenberg, A.N. & Balk, S.P. (2002) Inhibition of the dihydrotestosterone-activated androgen receptor by nuclear receptor corepressor. *Mol. Endocrinol.* 16 (7) 1492-1501

Chmelar, R., Buchanan, G., Need, E.F., Tilley, W. & Greenberg, N.M. (2007) Androgen receptor coregulators and their involvement in the development and progression of prostate cancer. *Int. J. Cancer* 120 (4) 719-733

Chong, P.A., Lin, H., Wrana, J.L. & Forman-Kay, J.D. (2006) An expanded WW domain recognition motif revealed by the interaction between Smad7 and the E3 ubiquitin ligase Smurf2. *J. Biol. Chem.* 281 (25) 17069-17075

Choo, Y.S. & Zhang, Z. (2009) Detection of protein ubiquitination. *J. Vis. Exp.* (30) 10.3791/1293

Christiaens, V., Bevan, C.L., Callewaert, L., Haelens, A., Verrijdt, G., Rombauts, W. & Claessens, F. (2002) Characterization of the two coactivator-interacting surfaces of the androgen receptor and their relative role in transcriptional control. *J. Biol. Chem.* 277 (51) 49230-49237

Chymkowitch, P., Le May, N., Charneau, P., Compe, E. & Egly, J.M. (2011) The phosphorylation of the androgen receptor by TFIIH direct the ubiquitin/proteasome process. *EMBO J.* 30 (30) 468-479

Ciechanover, A., Hod, Y. & Hershko, A. (1978) A heat-stable polypeptide component of an ATP-dependent proteolytic system from reticulocytes. *Biochem. Biophys. Res. Commun.* 81 (4) 1100-1105

Ciechanover, A., Heller, H., Elias, S., Haas, A.L. & Hershko, A. (1980) ATP-dependent conjugation of reticulocyte proteins with the polypeptide required for protein degradation. *Proc. Natl. Acad. Sci. USA* 77 (3) 1365-1368

Cochrane, D.R., Wang, Z., Muramaki, M., Gleave, M.E. & Nelson, C.C. (2007) Differential regulation of clusterin and its isoforms by androgens in prostate cells. *J. Biol. Chem.* 282 (4) 2278-2287

Coffey, K., Robson, C.N. (2012) Regulation of the androgen receptor by post-translational modifications. *J. Endocrinol.* 215 (2) 221-237

Creamer, T.P. (1998) Left-handed polyproline II helix formation is (very) locally driven. *Proteins* 33 (2) 218-226

Cutress, M.L., Whitaker, H.C., Mills, I.G., Stewart, M. & Neal, D.E. (2008) Structural basis for the nuclear import of the human androgen receptor. *J.Cell Sci.* 121 (Pt. 7) 957-968

De Craene, J.O., Soetens, O. & Andre, B. (2001) The Npr1 kinase controls biosynthetic and endocytic sorting of the yeast Gap1 permease. *J. Biol. Chem.* 276 (47) 43939-43948

De Duve, C., Gianetto, R., Appelmans, F. & Wattiaux, R. (1953) Enzymic content of the mitochondria fraction. *Nature* 172 (4390) 1143-1144

De la Fuente, N., Maldonado, A.M. & Portillo, F. (1997) Glucose activation of the yeast plasma membrane H+-ATPase requires the ubiquitin-proteasome proteolytic pathway. *FEBS Lett.* 411 (2-3) 308-312

Ding, X.F., Anderson, C.M., Ma, H., Hong, H., Uht, R.M., Kushner, P.J. & Stallcup, M.R. (1998) Nuclear receptor-binding sites of coactivators glucocorticoid receptor interacting protein 1 (GRIP1) and steroid receptor coactivator 1 (SRC-1): multiple motifs with different binding specificities. *Mol. Endocrinol.* 12 (2) 302-313

Dohmen, R.J., Stappen, R., McGrath, J.P., Forrová, H., Kolarov, J., Goffeau, A. & Varshavsky, A. (1995) An essential yeast gene encoding a homolog of ubiquitin-activating enzyme. *J. Biol. Chem.* 270 (30) 18099-18109

Dubbink, H.J., Hersmus, R., Verma, C.S., van der Korput, H.A., Berrevoets, C.A., van Tol, J., Ziel-van der Made, A.C., Brinkmann, A.O., Pike, A.C. & Trapman, J. (2004) Distinct recognition modes of FXXLF and LXXLL motifs by the androgen receptor. *Mol. Endocrinol.* 18 (9) 2132-2150

Duda, D.M., Borg, L.A., Scott, D.C., Hunt, H.W., Hammel, M. & Schulman, B.A. (2008) Structural insights into NEDD8 activation of cullin-RING ligases: conformational control of conjugation. *Cell* 134 (6) 995-1006

Dunn, R., Klos, D.A., Adler, A.S. & Hicke, L. (2004) The C2 domain of the Rsp5 ubiquitin ligase binds membrane phosphoinositides and directs ubiquitination of endosomal cargo. *J. Cell Biol.* 165 (1) 135-144

Edwin, F., Anderson, K. & Patel, T.B. (2010) HECT domain-containing E3 ubiquitin ligase Nedd4 interacts with and ubiquitinates Sprouty2. *J. Biol. Chem.* 285 (1) 255-264

Egner, R., Mahé, Y., Pandjaitan, R. & Kuchler, K. (1995) Endocytosis and vacuolar degradation of the plasma membrane-localized Pdr5 ATP-binding cassette multidrug transporter in *Saccharomyces cerevisiae*. *Mol. Cell Biol.* 15 (11) 5879-5887

Emanuelsson, O., Nielsen, H., Brunak, S. & von Heijne, G. (2000) Predicting subcellular localization of proteins based on their N-terminal amino acid sequence. *J. Mol. Biol.* 300 (4) 1005-1016

Espanel, X. & Sudol, M. (1999) A single point mutation in a group I WW domain shifts its specificity to that of group II WW domains. *J. Biol. Chem.* 274 (24) 17284-17289
Fan, C.D., Lum, M.A., Xu, C., Black, J.D. & Wang, X. (2013) Ubiquitin-dependent regulation of phospho-AKT dynamics by the ubiquitin E3 ligase, NEDD4-1, in the insulin-like growth factor-1 response. *J. Biol. Chem.* 288 (3) 1674-1684

Finch, J.S., Bonham, K., Krieg, P., Bowden, G.T. (1990) Murine polyubiquitin mRNA sequence. *Nucleic Acids Res.* 18 (7) 1907

Finley, D., Ciechanover, A. & Varshavsky, A. (2004) Ubiquitin as a central cellular regulator. *Cell* 116 (2 Suppl.) S29-32

Fisk, H.A. & Yaffe, M.P. (1999) A role for ubiquitination in mitochondrial inheritance in *Saccharomyces cerevisiae*. *J. Cell Biol.* 145 (6) 1199-1208

Flasza, M., Gorman, P., Roylance, R., Canfield, A.E. & Baron, M. (2002) Alternative splicing determines the domain structure of WWP1, a Nedd4 family protein. *Biochem. Biophys. Res. Commun.* 290 (1) 431-437

Foot, N.J., Dalton, H.E., Shearwin-Whyatt, L.M., Dorstyn, L., Tan, S.S., Yang, B. & Kumar, S. (2008) Regulation of the divalent metal ion transporter DMT1 and iron homeostasis by a ubiquitin-dependent mechanism involving Ndfips and WWP2. *Blood* 112 (10) 4268-4275

Fotia, A.B., Ekberg, J., Adams, D.J., Cook, D.I., Poronnik, P. & Kumar, S. (2004) Regulation of neuronal voltage-gated sodium channels by the ubiquitin-protein ligases Nedd4 and Nedd4-2. *J. Biol. Chem.* 279 (28) 28930-28935

Freemont, P.S., Hanson, I.M. & Trowsdale, J. (1991) A novel cysteine-rich sequence motif. *Cell* 64 (3) 483-484

Fu, M., Wang, C., Reutens, A.T., Wang, J., Angeletti, R.H., Siconolfi-Baez, L., Ogryzko, V., Avantaggiati, M.L. & Pestell, R.G. (2000) p300 and p300/cAMP-response element-binding protein-associated factor acetylate the androgen receptor at sites governing hormone-dependent transactivation. *J. Biol. Chem.* 275 (27) 20853-20860

Furuhashi, M., Kitamura, K., Adachi, M., Miyoshi, T., Wakida, N., Ura, N., Shikano, Y., Shinshi, Y., Sakamoto, K., Hayashi, M., Satoh, N., Nishitani, T., Tomita, K. & Shimamoto, K. (2005) Liddle's syndrome caused by a novel mutation in the proline-rich PY motif of the epithelial sodium channel beta-subunit. *J. Clin. Endocrinol. Metab.* 90 (1) 340-344

Gaddipati, J.P., McLeod, D.G., Heidenberg, H.B., Sesterhenn, I.A., Finger, M.J., Moul, J.W. & Srivastava, S. (1994) Frequent detection of codon 877 mutation in the androgen receptor gene in advanced prostate cancers. *Cancer Res.* 54 (11) 2861-2864

Galan, J.M., Moreau, V., André, B., Volland, C. & Haguenauer-Tsapis, R. (1996) Ubiquitination mediated by the Npi1p/Rsp5p ubiquitin-protein ligase is required for endocytosis of the yeast uracil permease. *J. Biol. Chem.* 271 (18) 10946-10952

Galan, J.M. & Haguenauer-Tsapis, R. (1997) Ubiquitin Lys63 is involved in ubiquitination of a yeast plasma membrane protein. *EMBO J.* 16 (19) 5847-5854

Gallagher, E., Gao, M., Liu, Y.C. & Karin, M. (2006) Activation of the E3 ubiquitin ligase Itch through a phosphorylation-induced conformational change. *Proc. Natl. Acad. Sci. USA* 103 (6) 1717-1722

Gao, T., Marcelli, M., McPhaul, M.J. (1996) Transcriptional activation and transient expression of the human androgen receptor. *J. Steroid Biochem. Mol. Biol.* 59 (1) 9-20

Garcia-Gonzalo, F.R. & Rosa, J.L. (2005) The HERC proteins: functional and evolutionary insights. *Cell. Mol. Life Sci.* 62 (16) 1826-1838

Gaughan, L., Logan, I.R., Neal, D.E. & Robson, C.N. (2005) Regulation of androgen receptor and histone deacetylase 1 by Mdm2-mediated ubiquitylation. *Nucleic Acids Res.* 33 (1) 13-26

Gautam, V., Trinidad, J.C., Rimerman, R.A., Costa, B.M., Burlingame, A.L. & Monaghan, D.T. (2013) Nedd4 is a specific E4 ubiquitin ligase for the NMDA receptor subunit GluN2D. *Neuropharmacology* 74: 96-107

Gavilanes, J.G., Gonzalez de Buitrago, G., Perez-Castellis, R. & Rodriguez, R. (1982) Isolation, characterization, and amino acid sequence of a ubiquitin-like protein from insect eggs. *J. Biol. Chem.* 257 (17) 10267-10270

Goldknopf, I.L. & Busch, H. (1977) Isopeptide linkage between nonhistone and histone 2A polypeptides of chromosomal conjugate-protein A24. *Proc. Natl. Acad. Sci. USA* 74 (3) 864-868

Goldstein, G., Scheid, M., Hammerling, U., Schlesinger, D.H., Niall, H.D. & Boyse, E.A. (1875) Isolation of a polypeptide that has lymphocyte-differentiating properties and is probably represented universally in living cells. *Proc. Natl. Acad. Sci. USA* 72 (1) 11-15

Gonzales, L.O., Corte, M.D., Vasquez, J., Junquera, S., Sanchez, R., Alvarez, A.C., Rodriguez, J.C., Lamelas, M.L. & Vizoso, F.J. (2008) Androgen receptor expression in breast cancer: Relationship with clinicopathological characteristics of the tumors, prognosis, and expression of metalloproteases and their inhibitors. *BMC Cancer* 8 (149)

Gossen, M. & Bujard, H. (1992) Tight control of gene expression in mammalian cells by tetracycline-responsive promoters. *Proc. Natl. Acad. Sci. USA* 89 (12) 5547-5551

Goto, E., Yamanaka, Y., Ishikawa, A., Aoki-Kawasumi, M., Mito-Yoshida, M., Ohmura-Hoshino, M., Matsuki, Y., Kajikawa, M., Hirano, H. & Ishido, S. (2010) Contribution of lysine 11-linked ubiquitination to MIR2-mediated major histocompatibility complex class I internalization. *J. Biol. Chem.* 285 (46) 35311-35319

Gottlieb, B., Pinsky, L., Beitel, L.K. & Trifiro, M. (1999) Androgen insensitivity. *Am. J. Med. Genet.* 89 (4) 210-217

Gougeon, P.Y., Prosser, D.C., Da-Silva, L.F. & Ngsee, J.K. (2002) Disruption of Golgi morphology and trafficking in cells expressing mutant prenylated rab acceptor-1. *J. Biol. Chem.* 277 (39) 36408-36414

Goulet, C.C., Volk, K.A., Adams, C.M., Prince, L.S., Stokes, J.B. & Snyder, P.M. (1998) Inhibition of the epithelial Na+ channel by interaction of Nedd4 with a PY motif deleted in Liddle syndrome. *J. Biol. Chem.* 273 (45) 30012-30017

Graham, F.L. & van der Eb, A.J. (1973) A new technique for the assay of infectivity of human adenovirus 5 DNA. *Virology* 52 (2) 456-567

Greenwood, R., Burke, B., Brummit, L. & Cunliffe, W.J. (1983) Cyclic cyproterone/ethinyloestradiol for acne. *Lancet* 2 (8353) 796

Grino, P.B., Griffin, J.E. & Wilson, J.D. (1990) Testosterone at high concentrations interacts with the human androgen receptor similarly to dihydrotestosterone. *Endocrinology* 126 (2) 1165-1172

Gu, Z., Rubin, M.A., Yang, Y., Deprimo, S.E., Zhao, H., Horvath, S., Brooks, J.D., Loda, M. & Reiter, R.E. (2005) Reg IV: a promising marker of hormone refractory metastatic prostate cancer. *Clin. Cancer Res.* 11 (6) 2237-2243

Haas, A.L. & Rose, I.A. (1982) The mechanism of ubiquitin activating enzyme. A kinetic and equilibrium analysis. *J. Biol. Chem.* 257 (17) 10329-10337

Haelens, A., Tanner, T., Denayer, S., Callewaert, L. & Claessens, F. (2007) The hunge region regulates DNA binding, nuclear translocation and transactivation of the androgen receptor. *Cancer Res.* 67 (9) 4514-4523

Haglund, K., Sigismund, S., Polo, S., Szymkiewicz, I., Di Fiore, P.P. & Dikic, I. (2003) Multiple monoubiquitination of RTKs is sufficient for their endocytosis and degradation. *Nat. Cell Biol.* 5 (5) 461-466

Harlalka, G.V., Baple, E.L., Cross, H., Kühnle, S., Cubillos-Rojas, M., Matentzoglu, K., Patton, M.A., Wagner, K., Coblentz, R., Ford, D.L., Mackay, D.J., Chioza, B.A., Scheffner, M., Rosa, J.L. & Crosby, A.H. (2013) Mutation of HERC2 causes developmental delay in Angelman-like features. *J. Med. Genet.* 50 (2) 65-73

Hatfield, P.M. & Vierstra, R.D. (1992) Multiple forms of ubiquitin-activating enzyme E1 from wheat. Identification of an essential cysteine by *in vitro* mutagenesis. *J. Biol. Chem.* 267 (21) 14799-14803

He, B., Kemppainen, J.A., Voegel, J.J., Gronemeyer, H. & Wilson, E.M. (1999) Activation function 2 in the human androgen receptor ligand binding domain mediates interdomain communication with the NH(2)-terminal domain. *J. Biol. Chem.* 274 (52) 37219-37225

Hein, C., Springael, J.Y., Volland, C., Haguenauer-Tsapis, R. & André, B. (1995) NPI1, an essential yeast gene involved in induced degradation of Gap1 and Fur4 permeases, encodes the Rsp5 ubiquitin-protein ligase. *Mol. Microbiol.* 18 (1), 77-87

Heinlein, C.A. & Chang, C. (2004) Androgen receptor in prostate cancer. *Endocr. Rev.* 25 (2) 276-308

Helsen, C., Dubois, V., Verfaillie, A., Young, J. Trekels, M., Vancraenenbroeck, R., De Maeyer, M. & Claessens, F. (2012) Evidence for DNA-binding domain-ligand binding domain communications in the androgen receptor. *Mol. Cell Biol.* 32 (15) 3033-3043

Henry, P.C., Kanelis, V., O'Brien, M.C., Kim, B., Gautschi, I, Forman-Kay, J., Schild, L. & Rotin D. (2003) Affinity and specificity of interactions between Nedd4 isoforms and the epithelial Na+ channel. *J.Biol. Chem.* 278 (22) 20019-20028

Hershko, A., Ciechanover, A., Heller, H., Haas, A.L. & Rose, I.A. (1980) Proposed role of ATP in protein breakdown: conjugation of protein with multiple chains of the polypeptide of ATP-dependent proteolysis. *Proc. Natl. Acad. Sci. USA* 77 (4) 1783-1786

Hershko, A., Heller, H., Elias, S. & Ciechanover, A. (1983) Components of ubiquitin-protein ligase system. Resolution affinity purification, and role in protein breakdown. *J.Biol. Chem.* 258 (13) 8206-8214

Höglund, A., Dönnes, P., Blum, T., Adolph, H.W. & Kohlbacher, O. (2006) MultiLoc: prediction of protein subcellular localization using N-terminal targeting sequences, sequence motifs and amino acid composition. *Bioinformatics* 22 (10) 1158-1165

Hoppe, T., Matuschewski, K., Rape, M., Schlenker, S., Ulrich, H.D. & Jentsch, S. (2000) Activation of a membrane-bound transcription factor by regulated ubiquitin/proteasome-dependent processing. *Cell* 102 (5) 577-586

Horak, J. & Wolf, D.H. (2001) Glucose-induced monoubiquitination of the *Saccharomyces cerevisiae* galactose transporter is sufficient to signal its internalization. *J. Bacteriol.* 183 (10) 3083-3088

Horoszewicz, J. C. Leong, S. S. Kawinski, E. Karr, J. P. Rosenthal, H. Chu, T. M. Mirand, E. A. & Murphy, G. P. (1983) LNCaP model of human prostatic carcinoma. *Cancer Res.* 43 1809-1818

Huang, L., Kinnucan, E., Wang, G., Beaudenon, S., Howley, P.M., Huibregtse, J.M. & Pavletich, N.P. (1999) Structure of an E6AP-UbcH7 complex: insights into ubiquitination by the E2-E3 enzyme cascade. *Science* 286 (5443) 1321-1326

Huang, Y., Liao, H., Li, W., Hu, Y., Huang, L., Wang, X., Sun, J., Chen, W., Deng, C., Liang, C., Wu, Z., Li, X., Xu, J. & Yu, X. (2013) Identification, sequence analysis and characterisation of *Clonarchis sinensis* ubiquitin. *Esp. Parasitol.* 133 (1) 62-29

Huggins, C., Stevens, R.E. Jr., Hodges, C.V. (1941) Studies on prostatic cancer II. The effects of castration on advanced carcinoma of the prostate gland. *Arch. Surg.* 43: 209-223

Huibregtse, J.M., Yang, J.C. & Beaudenon, S.L. (1997) The large subunit of RNA polymerase II is a substrate of the Rsp5 ubiquitin-protein ligase. *Proc. Natl. Acad. Sci. USA* 94 (8) 3656-3661

Hunt, L.T. & Dayhoff, M.O. (1977) Amino-terminal sequence identity of ubiquitin and the nonhistone component of nuclear protein A24. *Biochem. Biophys. Res. Commun.* 74 (2) 650-655

Hwang, Y.S., Lee, H.S., Kamata, T., Mood, K., Cho, H.J., Winterbottom, E., Ji, Y.J., Singh, A. & Daar, I.O. (2013) The Smurf ubiquitin ligases regulate tissue separation via antagonistic interactions with ephrinB1. *Genes Dev.* 27 (5) 491-503

Ingham, R.J., Raajimakers, J., Lim, C.S., Mbamalu, G., Gish, G., Chen, F., Matskova, L., Ernberg, I., Winberg, G. & Pawson, T. (2005) The Epstein-Barr virus protein, latent membrane protein 2A, co-opts tyrosine kinases used by the T-cell receptor. *J. Biol. Chem.* 280 (40) 34133-34142

Inoue, H. Nojima H. & Okayama H. (1990) High efficiency transformation of Escherichia coli with plasmids. *Gene* 96 (1) 23-28

International Human Genome Sequencing Consortium (2004) Finishing the euchromatic sequence of the human genome. *Nature* 431 (7011) 931-945

Isasa, M., Katz, E.J., Kim, W., Yugo, V., González, S., Kirkpatrick, D.S., Thomson, T.M., Finley, D., Gypi, S.P. & Crosas, B. (2010) Monoubiquitination of RPN10 regulates substrate recruitment to the proteasome. *Mol. Cell* 38 (5) 733-745

Jensen, O.N. (2004) Modification-specific proteomics: characterization of post-translational modifications by mass spectrometry. *Curr. Opin. Chem. Biol.* 8 (1) 33-41

Jenster, G., van der Krorput, H.A., van Vroonhoven, C., van der Kwast, T.H., Trapman, J. & Brinkann, A.O. (1991) Domains of the human androgen receptor involved in steroid binding, transcriptional activation and subcellular localization. *Mol. Endocrinol.* 5 (10) 1396-1404

Jenster, G., Trapman, J. & Brinkmann, A.O. (1993) Nuclear import of the human androgen receptor. *Biochem. J.* 293 (Pt. 3) 761-768

Jenster, G., van der Korput, H.A., Trapman, J. & Brinkmann, A.O. (1995) Identification of two transcription activation units in the N-terminal domain of the human androgen receptor. *J. Biol. Chem.* 270 (13) 7341-7356

Jentsch, S. (1992) The ubiquitin-conjugation system. *Annu. Rev. Genet.* 26; 179-207

Jolliffe, C.N., Harvey, K.F., Haines, B.P., Parasivam, G. & Kumar, S. (2000) Identification of multiple proteins expressed in murine embryos as binding partners for the WW domains of the ubiquitin-protein ligase Nedd4. *Biochem. J.* 351 (Pt. 3) 557-565

Kaku, N., Matsuda, K., Tsujimura, A. & Kawata, M. (2008) Characterization of nuclear import of the domain-specific androgen receptor in association with the importin alpha/beta and Ran-guanosine 5'-triphosphate systems. *Endocrinology* 149 (8) 3960-3969

Kamura, T., Koepp, D.M., Conrad, M.N., Skowyra, D., Moreland, R.J., Iliopoulous, O., Lane, W.S., Kaelin, W.G. Jr., Elledgem S.J., Conaway, R.C., Harper, J.W. & Conaway, J.W. (1999) Rbx1, a component of the VHL tumor suppressor complex and SCF ubiquitin ligase. *Science* 284 (5414) 657-661

Kanelis, V., Rotin, D. & Forman-Kay, J.D. (2001) Solution structure of a Nedd4 WW domain-ENaC peptide complex. *Nat. Struct. Biol.* 8 (5) 407-412

Kanelis, V., Bruce, M.C., Skrynnikov, N.R., Rotin, D. & Forman-Kay, J.D. (2006) Structural determinants for high-affinity binding in a Nedd4 WW3* domain-Comm PY motif complex. *Structure* 14 (3) 543-553

Kasanov, J., Pirozzi, G., Uveges, A.J. & Kay, B.K. (2001) Characterizing Class I WW domains defines key specificity determinants and generates mutant domains with novel specificities. *Chem. Biol.* 8 (3) 231-241

Katz, M., Shtiegman, K., Tal-Or, P., Yakir, L., Mosesson, Y., Harari, D., Machluf, Y., Asao, H, Jovin, T., Sugamura, K & Yarden, Y. (2002) Ligand-independent degradation of epidermal growth factor receptor involves receptor ubiquitylation and Hgs, an adaptor whose ubiquitin-interacting motif targets ubiquitylation by Nedd4. *Traffic* 3 (10) 740-751

Kesler, C.T., Gioeli, D., Conaway, M.R., Weber, M.J. & Paschal, B.M. (2007) Subcellular localization modulates activation function 1 domain phosphorylation in the androgen receptor. *Mol. Endocrinol.* 21 (9) 2071-2084

Kim, H.T., Kim, K.P., Lledias, F., Kisselev, A.F., Scaglione, K.M., Skowyra, D., Gypi, S.P. & Goldberg, A.L. (2007) Certain pairs of ubiquitin-conjugating enzymes (E2s) and ubiquitin-protein ligases (E3s) synthesize nondegradable forked ubiquitin chains containing all possible isopeptide linkages. *J. Biol. Chem.* 282 (24) 17375-17386

Kishino, T., Lalande, M. & Wagstaff, J. (1997) UBE3A/E6-AP mutations case Angelman syndrome. *Nat. Genet.* 15 (1) 70-3. Erratum in: *Nat. Genet.* (1997) 15 (4) 411

Knudsen, E.S., Arden, K.C. & Cavenee, W.K. (1998) Multiple G1 regulatory elements control the androgen-dependent proliferation of prostatic carcinoma cells. *J. Biol. Chem.* 273 (32) 20213-20222

Koivisto, P., Kononen, J., Palmberg, C., Tammela, T., Hyytinen, E., Isola, J., Trapman, J., Cleutjens, K., Noordzij, A., Visakorpi, T. & Kallioniemi, O.P. (1997) Androgen receptor gene amplification: a possible molecular mechanism for androgen deprivation therapy failure in prostate cancer. *Cancer Res.* 57 (2) 314-319

Komander, D., Reyes-Turcu, F., Licchesi, J.D., Odenwalder, P., Wilkinson, K.D. & Barford, D. (2009) Molecular discrimination of structurally equivalent Lys 63-linked and linear polyubiquitin chains. *EMBO Rep.* 10 (5) 466-473

Konstas, A.A., Shearwin-Wyatt, L, Fotia, A.B., Degger, B., Riccardi, D., Cook, D.I., Korbmacher, C. & Kumar, Sharad. (2002) Regulation of the epithelial sodium channel by N4WBP5A, a novel Nedd4/Nedd4-2 interaction protein. *J. Biol. Chem.* 277 (33) 29406-29416

Kotorashvili, A., Russo, S.J., Mulugeta, S., Guttentag, S. & Beers, M.F. (2009) Anterograde transport of surfactant protein C proprotein to distal processing compartments requires PPDY-mediated association with Nedd4 ubiquitin ligases. *J. Biol. Chem.* 284 (24) 16667-16678

Krongrad, A., Wilson, C.M., Wilson, J.D., Allman, D.R & McPhaul, M.J.(1991) Androgen increases androgen receptor protein while decreasing receptor mRNA in LNCaP cells. *Mol. Cell Endocrinol.* 76 (1-3) 79-88

Kumar, S., Tomooka, Y. & Noda, M. (1992) Identification of a set of genes with developmentally down-regulated expression in the mouse brain. *Biochem. Biophys. Res. Commun.* 185 (3) 1155-1161

Lackovic, J., Howitt, J., Callaway, J.K., Silke, J., Bartlett, P. & Tan, S.S. (2012) Differential regulation of Nedd4 ubiquitin ligases and their adaptor protein Ndfip1 in a rat model of ischemic stroke. *Exp. Neurol.* 235 (1) 326-335

Laemmli, U.K. (1970) Cleavage of structural proteins during the assembly of the head of bacteriophage T4. *Nature* 227 (5259) 680-685

Lamb, A.D., Massie, C.E. & Neal, D.E. (2014) The transcriptional programme of the androgen receptor (AR) in prostate cancer. *BJU Int.* 113 (3) 358-366

Lee, D. (2003) High androgen receptor levels are predictive of decreased survival in prostate cancer. *Clin. Prostate Cancer* 2 (1) 13-14

Lévy, F., Muehlethaler, K., Salvi, S., Peitreguin, A.L., Lindholm, C.K., Cerottini, J.C. & Rimoldi, D. (2005) Ubiquitylation of a melanosomal protein by HECT-E3 ligases serves as sorting signal for lysosomal degradation. *Mol. Biol. Cell.* 16 (4) 1777-1787

Lewis, W.H. Srinivasan, P.E. Stokoe, N. & Siminovitch, L. (1980) Parameters governing the transfer of the genes for thymidine kinase and dihydrofolate reductase into mouse cells using metaphase chromosomes or DNA. *Somatic Cell Genet.* 6 (3) 333-347

Li, H. Xu, L.L. Masuda, K. Raymundo, E. McLeod, D.G. Dobi, A. & Srivastava, S. (2008) A feedback loop between the androgen receptor and a NEDD4-binding protein, PMEPA1, in prostate cancer cells. *J. Biol. Chem.* 283 (43) 28988-28995

Li, H., Dobi, A. & Srivastava, S. (2012) Androgen receptor (AR) degradation is controlled by the co-operation of PMEPA1 and the E3 ubiquitin ligase NEDD4-1. *Cancer Res.* 74: Supplement A4

Lin, H.K., Wang, L., Hu, Y.C., Altuwaijri, S. & Chang, C. (2002) Phosphorylation-dependent ubitylation and degradation of androgen receptor by Akt require Mdm2 E3 ligase. *EMBO J.* 21 (15) 4037-4048

Linja, M.J., Savinainen, K.J., Saramäki, O.R., Tammela, T.L., Vessella, R.L. & Visakorpi, T. (2001) Amplification and overexpression of androgen receptor gene in hormone-refractory prostate cancer. *Cancer Res.* 61 (9) 3550-3555

Liu, X.F. & Culotta, V.C. (1999) Post-translational control of Nramp metal transport in yeast. Role of metal ions and the BSD2 gene. *J. Biol. Chem.* 274 (8) 4863-4868

Liu, H.M., Loo, Y.M., Horner, S.M., Zornetzer, G.A., Katze, M.G. & Gale, M. Jr. (2012) The mitochondrial targeting chaperone 14-3-3ε regulates a RIG-I translocon that mediates membrane association and innate antiviral immunity. *Cell Hosy Microbe* 11(5) 528-537

Liu, H. & Stone, S.L. (2013) Cytoplasmic degradation of the Arabidopsis transcription factor abscisic acid insensitive 5 is mediated by the RING-type E3 ligase KEEP ON GOING. *J. Biol. Chem.* 288 (28) 20267-20279

Loew, R. Heinz, N. Hampf, M. Bujard, H. & Gossen, M. (2010) Improved Tet-responsive promoters with minimized background expression. *BMC Biotechnol.* 10 (81) http://www.biomedcentral.com/1472-6750/10/81

Lorick, K.L., Jensen, J.P., Fang, S., Ong, A.M., Hatekeyama S. & Weissman, A.M. (1999) RING fingers mediate ubiquitin-conjugating enzyme (E2)-dependent ubiquitination. *Proc. Natl. Acad. Sci. USA* 96 (20) 11364-11369

Lott, J.S., Coddington-Lawson, S.J., Teesdale-Spittle, P.H. & McDonald, F.J. (2002) A single WW domain is the predominant mediator of the interaction between the human ubiquitin-protein ligase Nedd4 and the human epithelial sodium channel. *Biochem. J.* 361 (pt. 3) 481-488

Lu, C., Pribanic, S., Debonneville, A., Jiang, C. & Rotin, D. (2007) The PY motif of ENaC, mutated in Liddle syndrome, regulates channel internalization, sorting and mobilization from subapical pool. *Traffic* 8 (9) 1246-1264

Lu, P.J., Zhou, X.Z., Shen, M. & Lu, K.P. (1999) Function of WW domains as phosphoserine or phosphothreonine binding modules. *Science* 283 (5406) 1325-1328

Lu, K., Li, P., Zhang, M., Xing, G., Li, X., Zhou, W., Bartlam, M., Zhang, L., Rao, Z. & He, F. (2011) Pivotal role of the C2 domain of the Smurf1 ubiquitin ligase in substrate selection. *J. Biol. Chem.* 286 (19) 16861-16870

Luisi, B.F., Xu, W.X., Otwinowski, Z., Freedman, L.P., Yamamoto, K.R. & Sigler, P.B. (1991) Crystallographic analysis of the interaction of the glucocorticoid receptor with DNA. *Nature* 352 (6335) 497-505

Luo, W.J. & Chang, A. (1997) Novel genes involved in endosomal traffic in yeast revealed by suppression of a targeting-defective plasma membrane ATPase mutant. *J. Cell Biol.* 138 (4) 731-746

Macias, M.J., Hyvönen, M., Baraldi, E., Schultz, J., Sudol, M., Saraste, M. & Oschkinat, H. (1996) Structure of the WW domain of a kinase-associated protein complexed with a proline-rich peptide. *Nature* 382 (6592) 646-649

MacLean, H.E., Warne, G.L. & Zajac, J.D. (1997) Localization of functional domains in the androgen receptor. *J. Steroid Biochem. Mol. Biol.* 62 (4) 233-242

Maggiolini, M., Statti, G., Vivacqua, A., Gabriele, S., Rago, V., Loizzo, M., Menichini, F. & Andò, S. (2002) The mutant androgen receptor T877A mediates the proliferative but not the cytotoxic dose-dependent effects of genistein and quercetin on human LNCaP prostate cancer cells. *Mol. Pharmacol.* 62 (5) 1027-1035

Mai, T., Wang, X., Zhang, Z., Xin, D., Na, Y. & Guo, Y. (2004) Androgen receptor coregulator ARA267-alpha interacts with death receptor-6 revealed by the yeast two-hybrid. *Sci. China C. Life Sci.* 47 (5) 442-448

Malakhova, O.A. & Zhang, D.E. (2008) ISG15 inhibits Nedd4 ubiquitin E3 activity and enhances the innate antiviral response. *J. Biol. Chem.* 283 (14) 8783-8787

Marcelli, M., Ittmann, M., Mariani, S., Sutherland, R., Nigam, R., Murthy, L., Zhao, Y., DiConcini, D., Puxeddu, E., Esen, A., Eastham, J., Weigel, N.L. & Lamb, D.J. (2000) Androgen receptor mutations in prostate cancer. *Cancer Res.* 60 (4) 944-949

Marsh, J.D., Lehmann, M.H., Ritchie, R.H., Gwathmey, J.K., Green, G.E. & Schiebinger, R.J. (1998) Androgen receptors mediate hypertrophy in cardiac myocytes. *Circulation* 98 (3) 256-261

Martin-Serrano, J., Eastman, S.W., Chung, W. & Bieniasz, P.D. (2005) HECT ubiquitin ligases link viral and cellular PPXY motifs to the vacuolar protein-sorting pathway. *J. Cell Biol.* 168 (1) 89-101

Martinez-Noel, G., Müller, U. & Harbers, K. (2001) Identification of molecular determinants required for interaction of ubiquitin-conjugating enzymes and RING finger proteins. *Eur. J. Biochem.* 268 (22) 5912-5919

Mathis, D.J., Oudet, P., Wasylyk, B. & Chambon, P. (1978) Effect of histone acetylation on structure and *in vitro* transcription of chromatin. *Nucleic Acids Res.* 5 (10) 3523-3547

Matias, P.M., Donner, P., Coelho R., Thomaz, M., Peixoto, C., Macedo, S., Otto, N., Joschko,S., Scholz, P., Wegg, A., Bäsler S, Schäfer, M., Egner, U. & Carrondo, M.A. (2000) Structural evidence for ligand specificity in the binding domain of the human androgen receptor. Implications for pathogenic gene mutations. *J. Biol. Chem.* 275 (34) 26164-26171

Mayor, S., Presley, J.F. & Maxfield, F.R. (1993) Sorting of membrane components from endosomes and subsequent recycling to the cell surface occurs by a bulk flow process). *J. Cell Biol.* 121 (6) 1257-1269

Mazaleyrat, S.L., Fostier, M., Wilkin, M.B., Aslam, H., Evans, D.A., Cornell, M. & Baron, M. (2003) Down-regulation of Notch target gene expression by Suppressor of deltex. *Dev. Biol.* 255 (2) 363-372

McGrath, J.P., Jentsch, S. & Varshavsky, A. (1991) Uba1: an essential yeast gene encoding ubiquitin-activating enzyme. *EMBO J.* 10 (1) 227-236

Melchert, R.B. & Welder, A.A. (1995) Cardiovascular effects of androgenic-anabolic steroids. *Med. Sci. Sports Exerc.* 27 (9) 1252-1262

Merhi, A. & André, B. (2012) Internal amino acids promote Gap1 permease ubiquitylation via TORC1/Npr1/14-3-3-dependent control of the Bul arrestin-like adaptors. *Mol. Cell Biol.* 32 (22) 4510-4522

Minimikawa, T., Sriratana, A., Williams, D.A., Bowser, D.N., Hill, J.S. & Nagley, P. (1999) Chloromethyl-X-rosamine (Mitotracker Red) photosensitises mitochondria and induces apoptosis in intact human cells. *J. Cell Sci.* 112 (Pt. 14) 2419-2430

Morris, J.R., Boutell, C., Keppler, M., Densham, R., Weekes, D., Alamshah, A., Butler, L., Galanty, Y. Pangon, L., Kiuchi, T., Ng, T. & Solomon, E. (2009) The SUMO modification pathway is involved in the BRCA1 response to genotoxic stress. 462 (7275) 886-890

Mukherjee, S., Cruz-Rodriguez, O., Bolton, E. & Iñiguez-Lluhi, J.A. (2012) The *in vivo* role of androgen receptor SUMOylation as revealed by androgen insensitivity syndrome and prostate cancer mutations targeting the proline/glycine residues of synergy conrol motifs. *J. Biol. Chem.* 287 (37) 31195-31206

Miyazaki, K., Ozaki, T., Kato, C., Hanamoto, T., Fujita, T., Irino, S., Watanabe, K., Nakagawa, T. & Nakagawara, A. (2003) A novel HECT-type E3 ubiquitin ligase, NEDL2, stabilizes p73 and enhances its transcriptional activity. *Biochem. Biophys. Res. Commun.* 308 (1) 106-113

Muhlemann, M.F., Carter, G.D., Cream, J.J. & Wise, P. (1986) Oral spironolactone: an effective treatment for acne vulgaris in women. *Br. J. Dermatol.* 115 (2) 227-232

Mund, T. & Pelham, H.R. (2009) Control of the activity of WW-HECT domain E3 ubiquitin ligases by NDFIP proteins. *EMBO Rep.* 10 (5) 501-507

Mund, T. & Pelham, H.R. (2010) Regulation of PTEN/Akt and MAP kinase signalling pathways by the ubiquitin ligase activators Ndfip1 and Ndfip 2. *Proc. Natl. Acad. Sci. USA* 107 (25) 11429-11434

Myat, A., Henry, P., McCabe, V., Flintoft, L., Rotin, D. & Tear, G. (2002) *Drosophila* Nedd4, a ubiquitin ligase, is recruited by Commissureless to control cell surface levels at the roundabout receptor. *Neuron* 35 (3) 447-459

Nakauchi, J., Matsua, K., Ochiai, I., Kawauchi, A., Mizutani, Y., Miki, T. & Kawata, M. (2007) A differential ligand-mediated response of green fluorescent protein-tagged androgen receptor in living prostate cancer and non-prostate cancer cell lines. *J. Histochem. Cytochem.* 55 (6) 535-544

Nakatsu, F., Sakuma, M., Matsuo, Y., Arase, H., Yamasaki, S., Nakamura, N., Saito, T & Ohno, H. (2000) A di-leucine signal in the ubiquitin moiety: possible involvement in ubiquitin-mediated endocytosis. *J. Biol. Chem.* 275 (34) 26213-26219

Nagasone, M.A., Livnat-Levanon, N., Glickman, M.H., Cohen, R.E. & Fushman, D. (2013) Mixed-linkage ubiquitin chains send mixed messages. *Structure* 21 (5) 727-740
Narimatsu, M., Bose, R., Pye, M., Zhang, L, Miller, B., Ching, P., Sakuma, R., Luga, V., Roncari, L., Attisano, L. & Wrana, J.L. (2009) Regulation of planar cell polarity by Smurf ubiquitin ligases. *Cell* 137 (2) 295-307

Nakamura, N., Rabouille, C., Watson, R., Nilsson, T., Hui, N., Slusarewicz, P., Kreis, T.E. & Warren, G. (1995) Characterization of a cis-Golgi matrix protein, GM130. *J. Cell Biol.* 131 (6 Pt. 2) 1715-1726

Nakano, N., Itoh, S., Watanabe, Y. Maeyama, K., Itoh, F. & Kato, M. (2010) Requirement of TCF7L2 for TGF-β-dependent transcriptional activation of the TMEPA1 gene. *J. Biol. Chem.* 285 (49) 38023-38033

Nickerson, N.N., Tosi, T., Dessen, A., Baron, B., Raynal, B., England, P. & Pugsley, A.P. (2011) Outer membrane targeting of secretin PulD protein relies of disordered domain recognition by a dedicated chaperone. *J. Biol. Chem.* 286 (45) 38833-38843

Nilsson, B. Moks, T. Jansson, B. Abrahamsén, L. Elmblad, A. Holmgren, E. Henrichson, C. Jones, TA & Uhlén, M. (1987) A synthetic IgG-binding domain based on staphylococcal protein A. *Protein Eng.* 1 (2) 107-113

Niu, Y., Altuwaijri, S., Lai, K.P., Wu, C.T., Ricke, W.A., Messing, E.M., Yao, J., Yeh, S. & Chang, C. (2008) Androgen receptor is a tumor suppressor and proliferator in prostate cancer. *Proc. Natl. Acad. Sci. USA* 105 (34) 12182-12187

Novoselova, T.V., Zahira, K., Rose, R.S. & Sullivan, J.A. (2012) Bul proteins, a nonredundant, antagonistic family of ubiquitin ligase regulatory proteins. *Eukaryot. Cell* 11 (4) 463-470

Novoselova, T.V., Rose, R.S., Marks, H.M. & Sullivan, J.A. (2013) SUMOylation regulates the homologous to E6-AP carboxyl terminus (HECT) ubiquitin ligase Rsp5p. *J. Biol. Chem.* 228 (15) 10308-10317

Nwosu, V., Carpten, J., Trent, J.M. & Sheridan, R. (2001) Heterogeneity of genetic alterations in prostate cancer: evidence of the complex nature of the disease. *Hum. Mol. Genet.* 10 (20) 2313-2318

Oefelein, M.G., Agarwal, P.K. & Resnick, M.I. (2004) Survival of patients with hormone refractory prostate cancer in the prostate specific antigen era. *J. Urol.* 171 (4) 1525-1528

Ohta, T., Michel, J.J., Schottelius, A.J. & Xiong, Y. (1999) ROC1, a homolog of APC11, represents a family of cullin partners with an associated ubiquitin ligase activity. *Mol. Cell* 3 (4) 535-541

Ohtake, F., Fujii-Kuriyama, Y., Kawajiri, K. & Kato, S. (2011) Cross-talk of dioxin and estrogen receptor signals through the ubiquitin system. *J. Steroid Biochem. Mol. Biol.* 127 (1-2) 102-107

Oliver, P.M., Cao, X., Worthen, G.S., Shi, P., Briones, N., MacLeod, M., White, J., Kirby, P., Kappler, J., Marrack, P. & Yang, B. (2006) Ndfip1 protein promotes the function of itch ubiquitin ligase to prevent T cell activation and T helper 2 cell-mediated inflammation. *Immunity* 25 (6) 929-940

Olsen, S.K., Capili, A.D., Lu, X., Tan, D.S. & Lima, C.D. (2010) Active site remodelling accompanies thioester bond formation in the SUMO E1. *Nature* 463 (7283) 906-912

Olsen, S.K. & Lima, C.D. (2013) Structure of a ubiquitin E1-E2 complex: insights to E1-E2 thioester transfer. *Mol. Cell* 49 (5) 884-896

Orino, E., Tanaka, K., Tamura, T., Sone, S., Ogura, T. & Ichihara, A. (1991) ATP-dependent reversible association of proteasomes with multiple protein components to form 26S complexes that degrade ubiquitinated proteins in human HL-60 cells. *FEBS Lett.* 284 (2) 206-210

Orlicky, S., Tang, X., Willems, A., Tyers, M. & Sicheri, F. (2003) Structural basis for phosphodependent substrate selection and orientation by the SCFCdc4 ubiquitin ligase. *Cell* 112 (2) 243-256

Osmundson, E.C., Ray, D., Moore, F.E., Gao, Q., Thomsen, G.H. & Kiyokawa, H. (2008) The HECT E3 ligase Smurf2 is required for Mad2-dependent spindle assembly checkpoint. *J. Cell Biol.* 183 (2) 267-277

Palazzolo, I., Gliozzi, A., Rusmini, P., Sau, D., Crippa, V., Simonini, F., Onesto, E., Bolzoni, E. & Poletti, A. (2008) The role of the polyglutamine tract in androgen receptor. *J. Steroid Biochem. Mol. Biol.* 108 (3-5) 245-253

Pan, M.R., Peng, G., Hung, W.C. & Lin, S.Y. (2011) Monoubiquitination of H2AX protein regulates DNA damage response signalling. *J. Biol. Chem.* 286 (32) 28599-28607

Patnaik, A., Chau, V. & Wills, J.W. (2000) Ubiquitin is part of the retrovirus budding machinery. *Proc. Natl. Acad. Sci. USA* 97 (24) 13069-13074

Patrie, K.M. (2005) Identification and characterization of a novel tight junction-associated family of proteins that interacts with a WW domain of MAGI-1. *Biochim. Biophys. Acta.* 1745 (1) 131-144

Pelzer, C., Kassner, I., Matentzoglu, K., Singh, R.K., Wollscheid, H.P., Scheffner, M., Schmidtke, G. & Groettrup, M. (2007) 282 (32) 23010-23014

Peng, T., Zintsmaster, J.S., Namanja, A.T. & Peng, J.W. (2007) Sequence-specific dynamics modulate recognition specificity in WW domains. *Nat. Struct. Mol. Biol.* 14 (4) 325-331

Pereira de Jesus-Tran, K., Côté, P.L., Cantin, L., Blanchet, J., Labrie, F. & Breton, R. (2006) Comparison of crystal structures of human androgen receptor ligand-binding domain complexed with various agonists reveals molecular determinants responsible for binding affinity. *Protein Sci.* 15 (5) 987-999

Perets, R., Kaplan, T., Stein, I., Hidas, G., Tayeb, S., Avraham, E., Ben-Neriah, Y., Simon, I. & Pikarsky, E. (2012) Genome-wide analysis of androgen receptor targets reveals COUP-TF1 as a novel player in human prostate cancer. *PLoS One* 7 (10)

Perry, W.L., Hustad, C.M., Swing, D.A., O'Sullivan, T.N., Jenkins, N.A. & Copeland, N.G. (1998) The itchy locus encodes a novel ubiquitin protein ligase that is disrupted in a18H mice. *Nat. Genet.* 18 (2) 143-146

Persaud, A., Alberts, P., Amsen, E.M., Xiong, X., Wasmuth, J., Saadon, Z., Fladd, C., Parkinson, J. & Rotin, D. (2009) Comparison of substrate specificity of the ubiquitin ligases Nedd4 and Nedd4-2 using proteome arrays. *Mol. Syst. Biol.* 5; 333

Persaud, A., Alberts, P., Hayes, M., Guettler, S., Clarke, I., Sicheri, F., Dirks, P., Ciruna, B. & Rotin, D. (2011) Nedd4-1 binds and ubiquitylates activated FGFR1 to control its endocytosis and function. *EMBO J.* 30 (16) 3259-3273

Pham, A.D. & Sauer, F. (2000) Ubiquitin-activating/conjugating activity of TAFII250, a mediator of activation of gene expression in *Drosophila*. *Science* 289 (5488) 2357-2360

Pickart, C.M. (2001) Mechanisms underlying ubiquitination. *Annu. Rev. Biochem.* 70; 503-533

Pirozzi, G., McConnell, S.J., Uveges, A.J., Carter, J.M., Sparks, A.B., Kay, B.K. & Fowlkes, D.M. (1997) Identification of novel human WW domain-containing proteins by cloning of ligand targets. *J. Biol. Chem.* 272 (23) 14611-14616

Plant, P.J., Correa, J., Goldenberg, N., Bain, J. & Batt, J. (2009) The inositol phosphatise MTMR4 is a novel target of the ubiquitin ligase Nedd4. *Biochem. J.* 419 (1) 57-63

Platta, H.W., Abrahamsen, H., Thoresen, S.B., Stenmark, H. (2012) Nedd4-dependent lysine 11-linked polyubiquitination of the tumour suppressor Beclin 1. *Biochem. J.* 441 (1) 399-406

Plechanovová, A., Jaffray, E.G., Tatham, M.H., Naismith, J.H. & Hay, R.T. (2012) Structure of a RING E3 ligase and ubiquitin-loaded E2 primed for catalysis. *Nature* 489 (7414) 115-120

Podos, S.D., Hanson, K.K., Wang, Y.C. & Ferguson, E.L. (2001) The DSmurf ubiquitin-protein ligase restricts BMP signalling spatially and temporally during *Drosophila* embryogenesis. *Dev. Cell* 1 (4) 567-578

Prazeres, D.M.F. Schluep T. & Cooney C. (1998) Preparative purification of supercoiled plasmid DNA using anion-exchange chromatography. *J. Chroma. A* 806 (1) 31-45

Qi, J., Tripathi, M., Mishra, R., Sahgal, N., Fazli, L., Ettinger, S., Placzek, W.J., Claps, G., Chung, L.W., Bowtell, D., Gleaves, M., Bhowmich, N. & Ronai, Z.A. (2013) The E3 ubiquitin ligase Siah2 contributes to castration resistant prostate cancer by regulation of androgen receptor transcriptional activity. *Cancer Cell* 23 (3) 332-346

Rae, F.K., Hooper, J.D., Nicol, D.L. & Clements, J.A. (2001) Characterization of a novel gene, STAG/PMEPA1, upregulated in renal cell carcinoma and other solid tumors. *Mol. Carcinog.* 32 (1) 44-53

Rahighi, S., Ikeda, F., Kawasaki, M., Akutsu, M., Suzuki, N., Kato, R., Kensche, T., Uejima, T., Bloor, S., Komander, D., Randow, F., Wakatsuki, S. & Dikic, I. (2009) Specific recognition of linear ubiquitin chains by NEMO is important for NF-kappaB activation. *Cell* 136 (6) 1098-1109

Reggiori, F. & Pelham, H.R. (2001) Sorting of proteins into multivesicular bodies: ubiquitin-dependent and –independent targeting. *EMBO J.* 20 (18) 5176-5186

Robbins, J., Dilworth, S.M., Laskey, R.A. & Dingwall, C. (1991) Two interdependent basic domains in nucleoplasmin nuclear targeting sequence: identification of a class of bipartite nuclear targeting sequence. *Cell* 64 (3) 615-623

Robzyk, K., Recht, J. & Osley, M.A. (2000) Rad6-dependent ubiquitination of histone H2B in yeast. *Science* 287 (5452) 501-504

Rodriguez, M.S., Dargemont, C. & Hay, R.T. (2001) SUMO-1 conjugation *in vivo* requires both a consensus modification motif and nuclear targeting. *J. Biol. Chem.* 276 (16) 12654-12659

Rougier, J.S., Albesa, M., Abriel, H. & Viard, P. (2011) Neuronal precursor cell-expressed developmentally down-regulated 4-1 (NEDD4-1) controls the sorting of newly synthesized Ca(V)1.2 calcium channels. *J. Biol. Chem.* 286 (11) 8829-8838

Ruizeveld de Winter, J.A., Trapman, J., Vermey, M., Mulder, E., Zegers, N.D. & van der Kwast, T.H. (1991) Androgen receptor expression in human tissues: an immunohistochemical study. *J. Histochem. Cytochem.* 39 (7) 927-936

Rytinki, M., Kaikkonen, S., Sutinen, P., Paakinaho, V., Rahkama, V. & Palvimo, J.J. (2012) Dynamic SUMOylation is linked to the activity cycles of androgen receptor in the cell nucleus. *Mol. Cell Biol.* 32 (20) 4195-4205

Sack, J.S., Kish, K.F., Wang, C., Attar, R.M., Kiefer, S.E., An, Y., Wu, G.Y., Scheffler, J.E., Salvati, M.E., Krystek, S.R. Jr., Weinmann, R. & Einspahr, H.M. (2001) Crystallographic structures of the ligand-binding domains of the androgen receptor and its T877A mutant complexed with the natural agonist dihydrotestosterone. *Proc. Natl. Acad. Sci. USA* 98 (9) 4904-4909

Saporita, A.J., Zhang, Q., Navai, N., Dincer, Z., Hahn, J., Cai, X. & Wang, Z. (2003) Identification and characterization of a ligand-regulated nuclear export signal in androgen receptor. *J. Biol. Chem.* 278 (43) 41998-42005

Sasaki, T. & Takagi, H. (2013) Phosphorylation of a conserved Thr357 in yeast Nedd4-like ubiquitin ligase Rsp5 is involved in down-regulation of the general amino acid permease Gap1. *Genes Cells* 18 (6) 459-475

Savory, J.G., Hsu, B., Laquian, I.R., Giffin, W., Reich, T., Haché, R.J. & Lerebvre, Y.A. (1999) Discrimination between NL1- and NL2-mediated nuclear localization of the glucocorticoid receptor. *Mol. Cell Biol.* 19 (2) 1025-1037

Schaufele, F., Carbonell, X., Guerbadot, M., Borngraeber, S., Chapman, M.S., Ma, A.A., Miner, J.N. & Diamond, M.I. (2005) The structural basis of androgen receptor activation: intramolecular and intermolecular amino-carboxy interactions. *Proc. Natl. Acad. Sci. USA* 102 (28) 9802-9807

Scheffner, M., Nuber, U. & Huibregtse, J.M. (1995) Protein ubiquitination involving an E1-E2-E3 enzyme ubiquitination thioester cascade. *Nature* 373 (6509) 81-83

Scher, H.I., Zhang, Z.F., Nanus, D. & Kelly, W.K. (1996) Hormone and antihormone withdrawal: implications for the management of androgen-independent prostate cancer. *Urology* 47 (1A Suppl.) 61-69

Scherer, W.F. Syverton, J.T. & Gey, G.O. (1953) Studies on the propagation in vitro of poliomyelitis viruses. IV. Viral multiplication in a stable strain of human malignant epithelial cells (strain HeLa) derived from an epidermoid carcinoma of the cervix. *J. Exp. Med.* 97 (5) 695-710

Scheuring, D., Künzi, F., Viotti, C., Yan, M.S., Jiang, L., Schellman, S., Robinson, D.G. & Pimpl, P. (2012) Ubiquitin initiates sorting of Golgi and plasma membrane proteins into the vacuolar degradation pathway. *BMC Plant Biol.* 12; 164

Schild, L., Canessa, C.M., Shimkets, R.A., Gautschi, I., Lifton, R.P. & Rossier, B.C. (1995) A mutation in the epithelial sodium channel causing Liddle disease increases channel activity in the *Xenopus laevis* oocyte expression system. *Proc. Natl .Acad. Sci. USA* 92 (12) 5699-5703

Schild, L., Lu, Y., Gautschi, I., Schneeberger, E., Lifton, R.P. & Rossier, B.C. (1996) Identification of a PY motif in the epithelial Na channel subunits as a target sequence for mutations causing channel activation found in Liddle syndrome. *EMBO J.* 15 (10) 2381-2387

Schlesinger, D.H., Goldstein, G. & Niall, H.D. (1975) The complete amino acid sequence of ubiquitin, an adenylate cyclise stimulating polypeptide probably universal in living cells. *Biochemistry* 14 (10) 2214-2218

Schlesinger, D.H. & Goldstein, G. (1975) Molecular conservation of 74 amino acid sequence of ubiquitin between cattle and man. *Nature* 255 (5507) 423-424

Schweizer, A., Fransen, J.A., Bächi, T., Ginsel, L. & Hauri, H.P. (1988) Identification, by a monoclonal antibody, of a 53-kD protein associated with a tubulo-vascular compartment at the cis-side of the Golgi apparatus. *J. Cell Biol.* 107 (5) 1643-1653

Schwert, G.W. (1975) Recovery of native bovine serum albumin after precipitation with trichloroacetic acid and solution in organic solvents. *J. Am. Chem. Soc.* 79 139-141

Scott, P.M., Bioldeau, P.S., Zhdankina, O., Winistorfer, S.C., Haugland, M.J., Allaman, M.M., Kearney, W.R., Robertson, A.D., Boman, A.L. & Piper, R.C. (2004) GGA proteins bind ubiquitin to facilitate sorting at the trans-Golgi network. *Nat. Cell Biol.* 6 (3) 252-259

Sehat, B., Andersson, S., Girnita, L. & Larsson, O. (2008) Identification of c-Cbl as a new ligase for insulin-like growth factor-I receptor with distinct roles from Mdm2 in receptor ubiquitination and endocytosis. *Cancer Res.* 68 (14) 5669-5677

Seifert, W., Kühnisch, J., Maritzen, T., Horn, D., Haucke, V. & Hennies, H.C. (2011) Cohen syndrome-associated protein, COH1, is a novel, giant Golgi matrix protein required for Golgi integrity. *J. Biol. Chem.* 286 (43) 37665-37475

Seo, M.D., Park, S.J., Kim, H.J. & Lee, B.J. (2007) Identification of the WW domain-interaction sites in the unstructured N-terminal domain of EBV LMP 2A. *FEBS Lett.* 581 (1) 65-70

Sharma, N.L., Massie, C.E., Ramos-Montoya, A., Zecchini, V., Scott, H.E., Lamb, A.D., MacArthur, S., Stark, R., Warren, A.Y., Mills, I.G. & Neal, D.E. (2013) The androgen receptor induces a distinct transcriptional program in castration-resistant prostate cancer in man. *Cancer Cell* 23 (1) 35-47

Shcherbik, N., Zoladek, T., Nickels, J.T. & Haines, D.S. (2003) Rsp5p is required for ER bound Mga2p120 polyubiquitination and release of the processed/tethered transactivator Mga2p90. *Current Biol.* 13 (14) 1227-1233

Shearwin-Wyatt, L.M., Brown, D.L., Wylie, F.G., Stow, J.L. & Kumar, S. (2004) N4WBP5A (Ndfip2), a Nedd4-interacting protein, localizes to multivesicular bodies and the Golgi, and has a potential role in protein trafficking. *J. Cell Sci.* 117 (Pt. 16) 3679-3689

Shembade, N., Harhaj, N.S., Parvatiyar, K., Copeland, N.G., Jenkins, N.A., Matesic, L.E. & Harhaj, E.W. (2008) The E3 ligase Itch negatively regulates inflammatory signalling pathways by controlling the function of the ubiquitin-editing enzyme A20. *Nat. Immunol.* 9 (3) 254-262

Sherr, C.J. (1996) Cancer cell cycles. *Science* 274 (5293) 1672-1677

Shi, S., Notenboom, S., Dumont, M.E. & Ballatori, N. (2010) Identification of human gene products containing Pro-Pro-x-Tyr (PY) motifs that enhance glutathione and endocystic marker uptake in yeast. *Cell Physiol. Biochem.* 25 (2-3) 293-306

Shih, S., Sloper-Mould, K.E. & Hicke, L. (2000) Monoubiquitin carries a novel internalization signal that is appended to activated receptors. *EMBO J.* 19 (2) 187-198

Shimkets, R.A., Warnock, D.G., Bositis, C.M., Nelson-Williams, C., Hansson, J.H., Schambelan, M., Gill, J.R. Jr., Ulick, S., Milora, R.V. & Findling J.W. (1994) Liddle's syndrome: heritable human hypertension caused by mutations in the beta subunit of the epithelial sodium channel. *Cell* 79 (3) 407-414

Simental, J.A., Sar, M., Lane, M.V., French, F.S. & Wilson, E.M. (1991) Transcriptional activation and nuclear targeting signals of the human androgen receptor. *J. Biol. Chem.* 266 (1) 510-518

Simpson, M.V. (1953) The release of labelled amino acids from the proteins of rat liver slices. *J. Biol. Chem.* 201 (1) 143-154

Singer, A.U., Rohde, J.R., Lam, R., Skarina, T., Kagan, O., Dileo, R., Chirgadze, N.Y., Cuff, M.E., Joachimiak, A., Tyers, M., Sansonetti, P.J., Parsot, C. & Savchenko, A. (2008) Structure of the Shigella T3SS effector IpaH defines a new class of E3 ubiquitin ligases. *Nat. Struct. Mol. Biol.* 15 (12) 1293-1301

Singha, P.K., Yeh, I.T., Venkatachalam, M.A. & Saikumar, P. (2010) Transforming growth factor-beta (TGF-beta)-inducible gene TMEPAI converts TGF-beta from a tumor suppressor to a tumor promoter in breast cancer. *Cancer Res.* 70 (15) 6377-6383

Slamon, D.J., Godolphin, W., Jones, L.A., Holt, J.A., Wong, S.G., Keith, D.E., Levin, W.J., Stuart, S.G., Udove, J. & Ullrich, A. (1989) Studies of the HER-2/neu proto-oncogene in human breast and ovarian cancer. *Science* 244 (4905) 707-712

Springael, J.Y. & André, B. (1998) Nitrogen-regulated ubiquitination of the Gap1 permease of *Saccharomyces cerevisiae*. *Mol. Biol. Cell* 9 (6) 1253-1263

Stan, S.D. & Singh, S.V. (2009) Transcriptional repression and inhibition of nuclear translocation of androgen receptor by diallyl trisulfide in human prostate cancer cells. *Clin. Cancer Res.* 15 (15) 4895-4903

Staub, O., Dho, S., Henry, P., Correa, J., Ishikawa, T., McGlade, J. & Rotin, D. (1996) WW domains of Nedd4 bind to the proline-rich PY motifs in the epithelial Na+ channel deleted in Liddle's syndrome. *EMBO J.* 15 (10) 2371-2380

Stielow, B., Sapetschnig, A., Wink, C., Krüger, I. & Suske, G. (2008) SUMO-modified Sp3 represses transcription by provoking local heterochromatic gene silencing. *EMBO Rep.* 9 (9) 899-906

Sudol, M., Chen, H.I., Bougeret, C., Einbond, A. & Bork, P. (1995) Characterization of a novel protein-binding module – the WW domain. *FEBS Lett.* 369 (1) 67-71

Sugita, S., Kawashima, H., Tanaka, T., Kurisu, T., Sugimura, K. & Nakatani, T. (2004) Effect of type I growth factor receptor tyrosine kinase inhibitors on phosphorylation and transactivation activity of the androgen receptor in prostate cancer cells: Ligand-independent activation of the N-terminal domain of the androgen receptor. *Oncol. Rep.* 11 (6) 1273-1279

Sullivan, J.A., Lewis, M.J., Nikko, E. & Pelham, H.R. (2007) Multiple interactions drive adaptor-mediated recruitment of the ubiquitin ligase rsp5 to membrane proteins *in vivo* and *in vitro*. *Mol. Biol. Cell.* 18 (7) 2429-2440

Sun, C., Shi, Y., Xu, L.L., Nageswararao, C., Davis, L.D., Segawa, T., Dobi, A., McLeod, D.G. & Srivastava, S. (2006) Androgen receptor mutation (T877A) promotes prostate cancer cell growth and cell survival. *Oncogene* 25 (28) 3905-3913

Terrell, J., Shih, S., Dunn, R., Hicke, L. (1998) A function for monoubiquitination in the internalization of a G protein-coupled receptor. *Mol. Cell* 1 (2) 193-202

Thrower, J.S., Hoffman, L., Rechsteiner, M. & Pickart, C.M. (2000) Recognition of the polyubiquitin proteolytic signal. *EMBO J.* 19 (1) 94-102

Tofaris, G.K., Kim, H.T., Hourez, R., Jung, J.W., Kim, K.P. & Goldberg, A.L. (2011) Ubiquitin ligase Nedd4 promotes alpha-synucleain degradation by the endosomal-lysosomal pathway. *Proc. Natl. Acad. Sci. USA* 108 (41) 17004-17009

Ugai, S., Tamura, T., Tanahashi, N., Takai, S., Komi, N., Chung, C.H., Tanaka, K. & Ichihara, A. (1993) Purification and characterization of the 26S proteasome complex catalysing ATP-dependent breakdown of ubiquitin-ligated proteins from rat liver. *J. Biochem.* 113 (6) 754-768

Urlinger, S. Baron, U. Thellmann, M. Hasan, M.T. Bujard, H. & Hillen, W. (2000) Exploring the sequence space for tetracycline-dependent transcriptional activators: novel mutations yield expanded range and sensitivity. *Proc. Natl. Acad. Sci. USA* 97 (14) 7963-7968

Van Laar, J.H., Berrevoets, C.A., Trapman, J., Zegers, N.D. & Brinkmann, A.O. (1991) Hormone-dependent androgen receptor phosphorylation is accompanied by receptor transformation in human lymph node carcinoma of the prostate cells. *J. Biol. Chem.* 266 (6) 3734-3738

Van Wijk, S.J. & Timmers, H.T. (2010) The family of ubiquitin-conjugating enzymes (E2s): deciding between life and death of proteins. *FASEB J.* 24 (4) 981-983

Van Royen, M.E., Cunha, S.M., Brink, M.C., Mattern, K.A., Nigg, A.L., Dubbink. H.J., Verschure, P.J., Trapman, J. & Houtsmuller, A.B. (2007) Compartmentalization of androgen receptor protein-protein interactions in living cells. *J. Cell Biol.* 177 (1) 63-72

Varadan, R., Walker, O., Pickart, C. & Fushman, D. (2002) Structural properties of polyubiquitin chains in solution. *J. Mol. Biol.* 324 (4) 637-647

Veldscholte, J., Ris-Stalpers, C., Kuiper, G.G., Jenster, G., Berrevoets, C., Claassen, E., van Rooji, H.C., Trapman, J., Brinkmann, A.O. & Mulder, E. (1990) A mutation in the ligand binding domain of the androgen receptor of human LNCaP cells affects steroid binding characteristics and response to anti-androgens. *Biochem. Biophys. Res. Commun.* 173 (2) 534-540

Verdecia, M.A., Bowman, M.E., Lu, K.P., Hunter, T. & Noel, J.P. (2000) Structural basis for phosphoserine-proline recognition by group IV WW domains. *Nat. Struct. Biol.* 7 (8) 639-643

Verdecia, M.A., Joazeiro, C.A., Wells, N.J., Ferrer, J.L., Bowman, M.E., Hunter, T. & Noel, J.P. (2003) Conformational flexibility underlies ligation mediated by the WWP1 HECT domain E3 ligase. *Mol. Cell* 11 (1) 249-259

Vijay-Kumar, S., Bugg, C.E., Wilkinson, K.D. & Cook, W.J. (1985) Three-dimensional structure of ubiquitin at 2.8 Ä resolution. *Proc. Natl. Acad. Sci. USA* 82 (11) 3582-3585

Vijay-Kumar, S., Bugg, C.E. & Cook, W.J. (1987) Structure of ubiquitin refined at 1.8 Ä resolution. *J. Mol. Biol.* 194 (3) 531-544

Vina-Vilaseca, A., Bender-Sigel, J.,Sorkina, T., Closs, E.I. & Sorkin, A. (2011) Protein kinase C-dependent ubiquitination and clathrin-mediated endocytosis of the cationic amino acid transporter CAT-1. *J. Biol. Chem.* 286 (10) 8697-8706

Virdee, S., Ye, Y., Nguyen, D.P., Komander, D. & Chin, J.W. (2010) Engineered diubiquitin synthesis reveals Lys29-isopeptide specificity of an OTU deubiquitinase. *Nat. Chem. Biol.* 6 (10) 750-757

Wagstaff, K.M., Sivakumaran, H., Heaton, S.M., Harrich, D. & Jans, D.A. (2012) Ivermectin is a specific inhibitor of importin α/β-mediated nuclear import able to inhibit replication of HIV-1 and dengue virus. *Biochem. J.* 443 (3) 851-856

Walsh, C. (2006) Posttranslational modification of proteins: expanding nature's inventory. *Roberts & Co. Publishers*

Wang, X., Trotman, L.C., Koppie, T., Alimonti, A., Chen, Z., Gao, Z., Wang, J., Erdjument-Bromage, H., Tempst, P., Cordon-Cardo, C., Pandolfi, P.P. & Jiang, X. (2007) NEDD4-1 is a proto-oncogenic ubiquitin ligase for PTEN. *Cell* 128 (1) 129-139

Wang, Q., Li, W., Zhang, Y., Yuan, X., Xu, K., Yu, J., Chen, Z., Beroukhim, R., Wang, H., Lupien, M., Wu, T., Regan, M.M., Meyer, C.A., Carroll, J.S., Manrai, A.K., Jänne, O.A., Balk, S.P., Mehra, R., Han, B., Chinnaiyan, A.M., Rubin, M.A., True, L., Fiorentino, M., Fiore, C., Loda, M., Kantoff, P.W., Liu, X.S. & Brown, M. (2009) Androgen receptor regulates a distinct transcription program in androgen-independent prostate cancer. *Cell* 138 (2) 245-256

Watanabe, Y., Itoh, S., Goto, T., Ohnishi, E., Inamitsu, M., Itoh, F., Satoh, K., Wiercinska, E., Yang, W., Shi, L., Tanaka, A., Nakano, N., Mommas, A.M., Shibuya, H., Ten Dijke, P. & Kato, M. (2010) TMEPA1, a transmembrane TGF-beta-inducible protein, sequesters Smad proteins from active participation in TGF-beta signalling. *Mol. Cell* 37 (1) 123-134

Watson, D.C., Levy, W.B. & Dixon, G.H. (1978) Free ubiquitin is a non-histone protein of trout testis chromatin. *Nature* 276 (5684) 196-198

Waxman, L., Fagan, J.M. & Goldberg, A.L. (1987) Demonstration of two distinct high molecular weight proteases in rabbit reticulocytes, one of which degrades ubiquitin conjugates. *J. Biol. Chem.* 262 (6) 2451-2457

Wenzel, D.M., Lissounov, A., Brzovic, P.S. & Klevit, R.E. (2011) UBCH7 reactivity profile reveals parkin and HHARI to be RING/HECT hybrids. *Nature* 474 (7349) 105-108

Wetherill, Y.B., Petre, C.E., Monk, K.R., Puga, A. & Knudsen, K.E. (2002) The xenoestrogen bisphenol A induces inappropriate androgen receptor activation and mitogenesis in prostatic adenocarcinoma cells. *Mol. Cancer Ther.* 1 (7) 515-524

Wiemuth, D., Lott, J.S., Ly, K., Ke, Y., Teesdale-Spittle, P., Snyder, P.M. & McDonald, F.J. (2010) Interaction of serum- and glucocorticoid-regulated kinase 1 (SGK1) with the WW domains of Nedd4-2 is required for epithelial sodium channel regulation. *PLoS One* 5 (8) e12163

Wienken, C.J., Baaske, P., Rothbauer, U., Braun, D. & Duhr, S. (2010) Protein-binding assays in biological liquids using microscale thermophoresis. *Nat. Commun.* 1: 100

Wigler, M. Silverstein, S. Lee, L., Pellicer, A. Cheng, Y. & Axel, R. (1977) Transfer of purified herpes virus thymidine kinase gene to cultured mouse cells. *Cell* 11 (1) 223-232

Wiesner, S., Ogunjimi, A.A., Wang, H.R., Rotin, D., Sicheri, F., Wrana, J.L. & Forman-Kay, J.D. (2007) Autoinhibition of the HECT-type ubiquitin ligase Smurf2 through its C2 domain. *Cell* 130 (4) 651-662

Wilkinson, K.D., Urban, M.K. & Haas, A.L. (1980) Ubiquitin is the ATP-dependent proteolysis factor I of rabbit reticulocytes. *J. Biol. Chem.* 255 (16) 7529-7532

Wilkinson, K.D. & Audhya, T.K. (1981) Stimulation of ATP-dependent proteolysis requires ubiquitin with the COOH-terminal sequence Arg-Gly-Gly. *J. Biol. Chem.* 256 (17) 9235-9241

Wilson, E.M. & French, F.S. (1976) Binding properties of androgen receptors. Evidence for identical receptors in rat testis, epididymis, and prostate. *J. Biol. Chem.* 251 (18) 5620-5629

Wilson, J.D., Griffin, J.E., George, F.W. & Leshin, M. (1983) The endocrine control of male phenotypic development. *Aust. J. Biol. Sci.* 36 (2) 101-128

Xhou, Z.X., Lane, M.V., Kemppainen, J.A., French, F.S. & Wilson, E.M. (1995) Specificity of ligand-dependent androgen receptor stabilization: receptor domain interactions influence ligand dissociation and receptor stability. *Mol. Endocrinol.* 9 (2) 208-218

Xu, L.L., Shanmugam, N., Segawa, T., Sesterhenn, I.A., McLeod, D.G., Moul, J.W. & Srivastava, S. (2000) A novel androgen-regulated gene, PMEPA1, located on chromosome 20q13 exhibits high level expression in prostate. *Genomics* 66 (3) 257-263

Xu, L.L., Shi, Y., Petrovics, G., Sun, C., Makarem, M., Zhang, W., Sesterhenn, I.A., McLeod, D.G., Sun, L., Moul, J.W. & Srivastava, S. (2003) PMEPA1, an androgen-regulated NEDD4-binding protein, exhibits cell growth inhibitory function and decreased expression during prostate cancer progression. *Cancer Res.* 63 (15) 4299-4304

Xu, Q., Farah, M., Webster, J.M. & Wojcikiewicz, R.J. (2004) Bortezomib rapidly suppresses ubiquitin thioesterification to ubiquitin-conjugating enzymes and inhibits ubiquitination of histones and type I inositol 1,4,5-triphosphate receptor. *Mol. Cancer Ther.* 3 (10) 1263-1269

Xu, K., Shimelis, H., Linn, D.E., Jiang, R., Yang, X., Sun, F., Guo, Z., Chen, H., Li, W., Chen, H., Kong, X., Melamed, J., Fang, S., Xiao, Z., Veenstra, T.D. & Qiu, Y. (2009) Regulation of androgen receptor transcriptional activity and specificity by RNF6-induced ubiquitination. *Cancer Cell* 15 (4) 270-282

Xu, P., Duong, D.M., Seyfried, N.T., Cheng, D., Xie. Y., Robert, J., Rush, J., Hoochstrasser, M., Finley, D. & Peng, J. (2009) Quantitative proteomics reveals the function of unconventional ubiquitin chains in proteasomal degradation. *Cell* 137 (1) 133-145

Xu, D., Lin, T.H., Zhang, C., Tsai, Y.C., Li, S., Zhang, J., Yin, M., Yeh, S. & Chang, C. (2012) The selective inhibitory effect of a synthesis tanshinone derivative on prostate cancer cells. *Prostate* 72 (7) 803-816

Yang, L. & Liu, Z.R. (2004) Bacterially expressed recombinant p68 RNA helicase is phosphorylated on serine, threonine and tyrosine residues. *Protein Expr. Purif.* 35 (2) 327, 333

Yang, C.S., Xin, H.W., Kelley, J.B., Spencer, A., Brautigan, D.L. & Paschal, B.M. (2007) Ligand binding to the androgen receptor induces conformational changes that regulate phosphatase interaction. *Mol. Cell Biol.* 27 (9) 3390-3404

Yeap, B.B., Kruger, R.G. & Leedman, P.J. (1999) Differential posttranscriptional regulation of androgen receptor gene expression by androgen in prostate and breast cancer cells. *Endocrinology* 140 (7) 3282-3291

Yeh, S., Lin, H.K., Kang, H.Y., Thin, T.H., Lin, M.F. & Chang, C. (1999) From HER2/Neu signal cascade to androgen receptor and its coactivators: a novel pathway by induction of androgen target genes through MAP kinase in prostate cancer cell. *Proc. Natl. Acad. Sci. USA* 96 (10) 5458-5463

Yeh, S., Tsai, M.Y., Xu, Q., Mu, X.M., Lardy, H., Huang, K.E., Lin, H., Yeh, S.D., Altuwaijri, S., Zhou, X., Xing, L., Boyce, B.F., Hung, M.C., Zhang, S., Gan, L. & Chang, C. (2002) Generation and characterization of androgen receptor knockout (ARKO) mice: an *in vivo* model for the study of androgen functions in selective tissues. *Proc. Natl. Acad. Sci. USA* 99 (21) 13498-13503

You, J. & Pickart, C.M. (2001) A HECT domain E3 enzyme assembles novel polyubiquitin chains. *J.Biol. Chem.* 276 (23) 19871-19878

Yu, H., Chen, J.K., Feng, S., Dalgarno, D.C., Brauer, A.W. & Schreiber, S.L. (1994) Structural basis for the binding of proline-rich peptides to SH3 domains. *Cell* 76 (5) 933-945

Yu, C.S., Chen, Y.C., Lu, C.H. & Hwang, J.K. (2006) Prediction of protein subcellular localization. *Prot. Struct. Funct. & Bioinformatic.* 64 (643-651)

Zarrinpar, A. & Lim, W.A. (2000) Converging on proline: the mechanism of WW domain peptide recognition. *Nat. Struct. Biol.* 7 (8) 611-613

Zhen, M., Huang, X., Bamber, B. & Jin, Y. (2000) Regulation of presynaptic terminal organization by *C. Elegans* RPM-1, a putative guanine nucleotide exchanger with a RING-H2 finger domain. *Neuron* 26 (2) 331-343

Zitzmann, M. Depenbusch, M., Gromoll, J. & Nieschlag, E. (2003) Prostate volume and growth in testosterone-substituted hypogonadal men are dependent on the CAG repeat polymorphism of the androgen receptor gene: a longitudinal pharmacogenetic study. *J. Clin. Endocrinol. Metab.* 88 (5) 2049-2054

Zhou, R., Patel, S.V. & Snyder, P.M. (2007) Nedd4-2 catalyzes ubiquitination and degradation of cell surface ENaC. *J.Biol. Chem.* 282 (28) 20207-20212

Zhou, W., Zhu, P., Wang, J., Pascual, G., Ohgi, K.A., Lozach, J., Glass, C.K. & Rosenfield, M.G. (2008) Histone H2A monoubiquitination represses transcription by inhibiting RNA polymerase II transcriptional elongation. *Mol. Cell* 29 (1) 69-80.

Zhu, Y., Li, H., Hu, L., Wang, J., Zhou, Y., Pang, Z., Liu, L. & Shao, F. (2008) Structure of a *Shigella* effector reveals a new class of ubiquitin ligases. *Nat. Struct. Mol. Biol.* 15 (12) 1302-1308